TECHNISCHE UNIVERSITÄT
CAROLO-WILHELMINA
ZU BRAUNSCHWEIG

HELMHOLTZ
ZENTRUM FÜR
INFEKTIONSFORSCHUNG

International Graduate School
for Infection Research

Multifaceted contributions of airway epithelial cells and alveolar macrophages to homeostasis surveillance in chronic respiratory disease

Von der Fakultät für Lebenswissenschaften

der Technischen Universität Carolo-Wilhelmina zu Braunschweig

zur Erlangung des Grades einer

Doktorin der Naturwissenschaften

(Dr. rer. nat.)

genehmigte

D i s s e r t a t i o n

von Julia Désirée Boehme
aus Peine

1. Referent:	Professor Dr. Michael Steinert
2. Referentin:	Professorin Dr. Dunja Bruder
3. Referent:	Professor Dr. Mathias Hornef
eingereicht am:	19.10.2015
mündliche Prüfung (Disputation) am:	26.02.2016

Druckjahr 2016

Vorveröffentlichungen der Dissertation

Teilergebnisse aus dieser Arbeit wurden mit Genehmigung der Fakultät für Lebenswissenschaften, vertreten durch den Mentor der Arbeit, in folgenden Beiträgen vorab veröffentlicht:

Publikationen

Boehme, J.D., Pietkiewicz, S., Lavrik, I.N., Jeron, A. & Bruder, D. Morphological and functional alterations of alveolar macrophages in a murine model of chronic inflammatory lung disease. Lung (2015). DOI: 10.1007/s00408-015-9797-4

Boehme, J.D., Stegemann-Koniszewski, S., Autengruber, A., Peters, N., Wissing, J., Jänsch, L., Jeron, A. & Bruder, D. Chronic lung inflammation primes pIgR/SIg mechanisms and augments humoral immunity to *Streptococcus pneumoniae*. Mucosal Immunology (In Revision).

Tagungsbeiträge

Vorträge

Jeron, A., Boehme, J., Stegemann-Koniszewski, S., Wissing, J., Jänsch, L., Bruder, D. Chronic lung inflammation enhances humoral immunity to *Streptococcus pneumoniae* via the pIgR/sIg axis. (Talk held by Andreas Jeron) 4th European Congress of Immunology (ECI) Vienna (September 2015).

Boehme, J., Stegemann-Koniszewski, S., Autengruber, A., Peters, N., Wissing, J., Jänsch, L., Jeron, A. & Bruder, D. Alveolar Overexpression of the Polymeric Immunoglobulin Receptor in the Inflamed Lung as a Novel Mechanism for Antibody-mediated Immune Exclusion of Bacterial Pathogens. (Talk held by Dunja Bruder) 17th International Congress of Mucosal Immunology (ICMI 2015), Berlin (July 2015).

Boehme, J., Weller, M., Kasnitz, N. & Parzmair, G. Innate immune regulation and infection. HZI Graduate School Annual Retreat, Hahnenklee (2014).

Boehme, J., Rogge, K. Mucosal inflammation: impact on secondary immune responses. HZI Graduate School Annual Retreat, Hahnenklee (2013).

Boehme, J. Impact of chronic autoimmune-mediated pulmonary inflammation on pneumococcal pneumonia. 36th Symposium of the North-German Immunologists, Borstel (2013).

Posterbeiträge

Boehme, J., Jeron, A., Stegemann-Koniszewski, S., Bruder, D.: Alveolar epithelial regulation of pIgR-expression in chronic lung disease: A compensatory mechanism to prevent fatal pneumococcal invasion? 44. Jahrestagung der Deutschen Gesellschaft für Immunologie, Bonn (2014).

Boehme, J., Jeron, A., Stegemann-Koniszewski, S., Gereke, M. & Bruder, D.: Impact of chronic autoimmune-mediated lung inflammation on *Streptococcus pneumoniae* infection. 43. Jahrestagung der Deutschen Gesellschaft für Immunologie, Mainz (2013).

Für Daniel, Mama und Papa

Scientists have one thing in common with children: curiosity. To be a good scientist you must have kept this trait of childhood, and perhaps it is not easy to retain just one trait. A scientist has to be curious like a child; perhaps one can understand that there are other childish features he hasn't grown out of.

OTTO ROBERT FRISCH (1904 – 1979), Austrian-British physicist

Table of contents

1 Abstract

Experimental and epidemiologic evidence points to substantially altered immunity towards airborne pathogens in individuals with chronic respiratory disease (CRD). The identification of immunologic factors underlying this phenomenon would help to better understand infectious disease pathogenesis and to improve anti-infectious therapies for this cohort. Thus, the first part of this thesis aimed to elucidate the impact of chronic pulmonary inflammation on infection with the common respiratory pathogen *Streptococcus pneumoniae*. To this end, the SPC-HAxTCR-HA transgenic mouse model which is based on the recognition of a pulmonary self-antigen by self-antigen specific T cells, finally leading to chronic pulmonary inflammation associated with several pathologic features of human CRD, was utilized. Unexpectedly, *in vivo* infection experiments revealed increased antipneumococcal resistance of pre-diseased SPC-HAxTCR-HA mice, indicative of inflammation-induced protective mechanisms. As the alveolar macrophage (AM) phagocytic capacity was similar between healthy and pre-diseased mice, two different strategies for unbiased analyses were pursued to examine the protective microenvironment in SPC-HAxTCR-HA lungs: gene expression as well as the bronchoalveolar lavage fluid (BALF) proteome was compared between healthy and pre-diseased mice by using whole-genome microarray and LC-MS/MS technology. Both analyses pointed to an induction of the polymeric immunoglobulin receptor (pIgR)/secretory immunoglobulin (SIg) axis in SPC-HAxTCR-HA lungs, which was in high accordance with elevated airway SIg levels and airway epithelial pIgR-expression in this group. Finally, by using *in vitro* pneumococcal binding assays an increased opsonizing activity of SPC-HAxTCR-HA BALF - and thus a protective contribution of the inflammation-primed airway epithelium to SIg-mediated reinforcement of the lung mucosa against bacterial adhesion and tissue penetration – could be confirmed.

In the SPC-HAxTCR-HA model chronic inflammation has previously been shown to encompass profound molecular as well as phenotypic changes of alveolar type II (ATII) cells and the self-antigen specific T cell compartment. Though AMs are known to be able to communicate with both cell types, a comprehensive investigation of these cells has so far not been addressed. The second part of this thesis therefore aimed to examine the phenotype of AMs as well as their immunoregulatory potential in hosts with CRD. Cytometric, transcriptional and functional evaluation of these cells uncovered a markedly altered, activated phenotype and a blunted pro-inflammatory immune response to pneumococcal ligands, suggesting a partial impairment of these cells during respiratory infection. Furthermore, extensive *in vivo* clodronate liposome-depletion studies revealed that this cell type is essential for preventing the development of bronchopneumonia in SPC-HAxTCR-HA lungs. Here, no or only minor roles of AMs as pulmonary scavengers and controllers of self-antigen specific T cells could be found in SPC-HAxTCR-HA lungs. Interestingly and in high accordance with the neutrophil-dominated disease phenotype in AM-depleted SPC-HAxTCR-HA lungs, ATII-specific gene expression of IL-8 analogues was highly up-regulated in this group, revealing so far unrecognized immunoregulatory cooperativity between AMs and ATII in CRD.

Taken together, the present work identified inflammation-primed pulmonary epithelial cells as effective mucosal safeguards against respiratory infection with *Streptococcus pneumoniae*. Moreover, the AM/ATII axis was identified to be an element presumably involved in surveilling pulmonary homeostasis in CRD.

2 Introduction

Respiration is a process crucial for survival but at the same time challenges the individual with a plethora of demanding immunological tasks. Owed to its primary function the lung is continuously exposed to the outside environment harboring a wide array of harmless substances but also toxic gases and particles as well as infectious threats. The accurate discrimination between self vs. non-self as well as innocuous vs. dangerous antigens is critical for preserving organ function. On the one hand, autoimmunity or allergy and the resulting pathology can lead to severe tissue damage, on the other hand improper recognition and elimination of pathogens leaves the host vulnerable to microbial spread. It is therefore of utmost interest how pulmonary immunity manages these balancing acts during homeostasis but particularly in individuals with pre-existing respiratory ailments.

Regardless of our increasing knowledge about the underlying principles and the development of alleviating therapies during the past decades, non-communicable chronic respiratory diseases (CRDs) affect hundreds of millions of people worldwide with increasing prevalence. For instance, chronic obstructive pulmonary disease (COPD) is projected to be the fourth leading cause of death by 2030 (Mathers et al. 2006). Here the pathogenesis is generally considered to be a product of complex and continuous physiologic reactions in the lung that start long before the disease phenotype manifests and becomes clinically apparent. Despite different etiologies, chronic respiratory disorders typically involve inflammation-induced macroscopic adaptations (i.e. airway remodeling, cellular infiltrations) and - more importantly - complex changes in the lung microenvironment including substantially altered immune cell function, regulatory networks and composition of soluble mediators. Details of the physiological implications of these alterations for immune regulation and host defense are still not fully understood.

The following introductory chapters deal with principles of pulmonary immunity, with a focus on airway epithelial cells and alveolar macrophages, chronic respiratory disease, as well as the respiratory pathogen *Streptococcus pneumoniae* and pneumococcal pneumonia.

2.1 Structure of the respiratory tract

The human respiratory tract comprises a surface area of approximately 70m^2 and utilizes a versatile set of physical (cough, cilial beating), chemical (mucus, antimicrobial molecules) and cellular (phagocytes) mechanisms to maintain homeostasis (Holt et al. 2008). Basically, the airway anatomic compartment can be subdivided into the upper respiratory tract (nasopharynx down to larynx) and the lower respiratory tract (from the portion of the larynx below the voice box down to the alveoli). The nasopharynx represents the first line of defense by working as a size-exclusion mechanism against penetration of airborne antigens bigger than 2-3µm into the lower respiratory tract. Moreover, mucus secretion as well cilial beating by distinct epithelial cell types that line the upper and lower (excluding alveoli) respiratory tract constantly mediates the transport of particles from the terminal bronchioles back to the trachea, this cooperative mechanism is known as ‘mucociliary clearance’. Yet, in some chronic respiratory diseases this instrument is defective due to structural modifications of epithelial cells (chronic bronchitis) or an altered composition of the mucus (cystic fibrosis; Nicod 1999).

In addition, airway mucosal DCs (AMDCs) that reside within and beneath the epithelial layer sample airborne antigen and can initiate the onset of an adaptive immune response in the local draining lymph nodes. Moreover, the submucosal space of the conducting airways harbors macrophages, T cells and plasma cells (mainly producing dimeric IgA; Holt, Strickland et al. 2008, Figure 1).

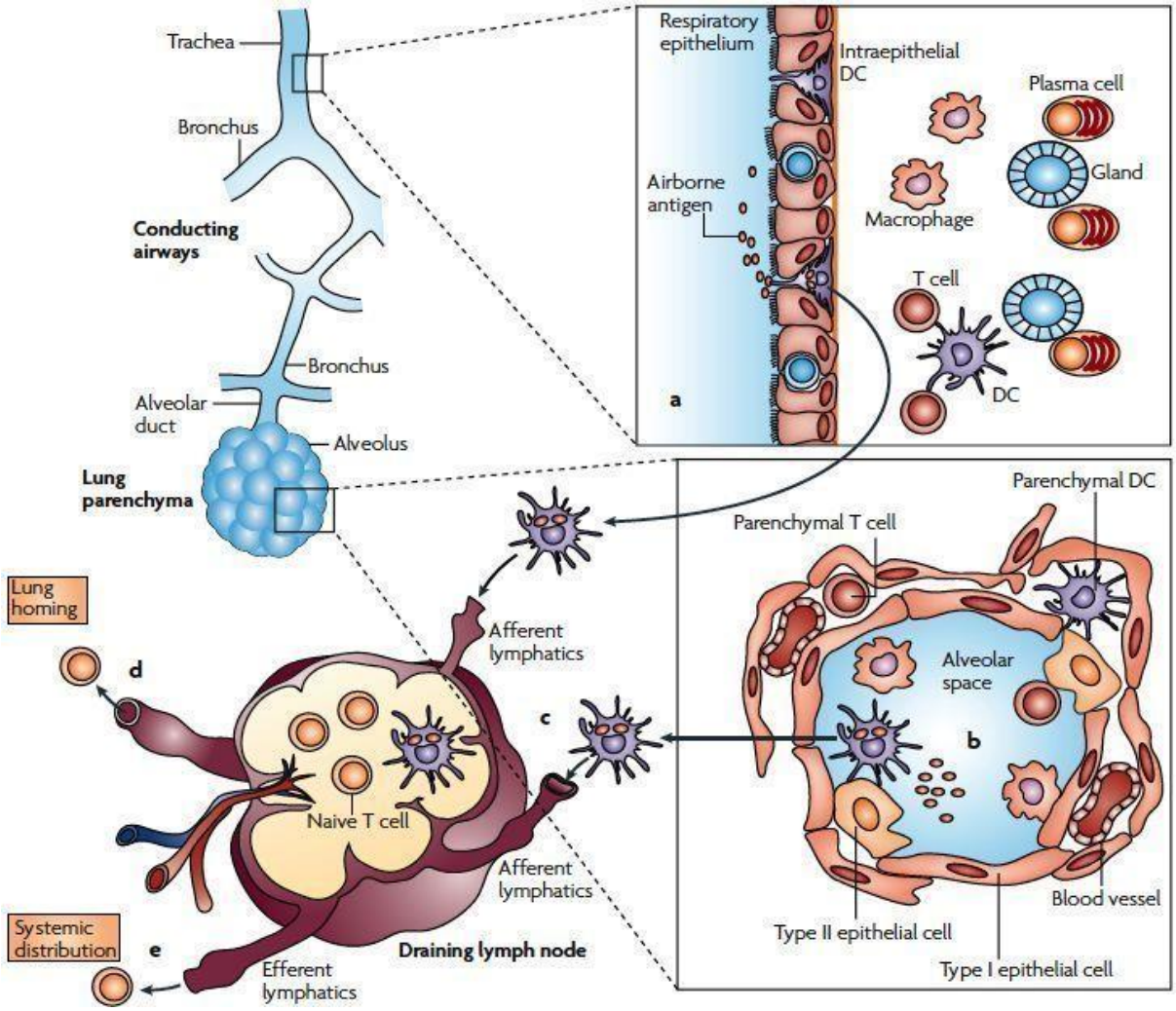

Figure 1: Structure and cellular composition of the lower respiratory tract.
Inhaled air passes through trachea, bronchi, alveolar ducts (bronchioles) into alveoli. Each compartment of the lower respiratory tract is lined with ciliated and/or secretory epithelial cell types. Local antigen is sampled by alveolar macrophages and/or dendritic cells (DCs, see **a** and **b**). Antigen-bearing respiratory DCs migrate via afferent lymphatics **(c)** into the local draining lymph nodes and activate antigen-specific naive T cells which proliferate upon priming. Proliferated effector T cells migrate into the lung parenchyma **(d)** and spread systemically via efferent lymphatics **(e)**. Figure taken from Holt, Strickland et al. 2008.

2.1.1 Epithelial cell types in the lower respiratory tract

The mucosal surface of the lower respiratory tract (from trachea down to the bronchioles) contains a pseudostratified epithelium dominated by ciliated cells and interspersed with submucosal glands (Figure 2). Basal cells which are located underneath the epithelial surface set up the progenitor pool for both ciliated and secretory cells which need to be reconstituted e.g. following lung injury. Besides ciliated cells a number of secretory cells

(serous, Clara, neuroendocrine and goblet cells) are found in the respiratory epithelium. The conducting airways and submucosal glands synthesize and secrete a plethora of molecules that unspecifically mediate aggregation, entrapment and killing of microbes (Whitsett et al. 2015). Gas exchange takes place in the alveoli, where epithelial cells are in close proximity to the pulmonary capillaries. Only two epithelial cell types are found in the alveolus: squamous alveolar type I epithelial cells (ATI cells) cover approximately 90% of the alveolar surface in the human lung and closely interact with the endothelial cells during respiration. Cuboidal alveolar type II epithelial cells (ATII cells) are critically involved in surfactant homeostasis by producing surfactant proteins (SP-A, SP-B, SP-C and SP-D; Whitsett et al. 2010). These proteins – together with surfactant lipids – are crucial for preserving surface tension and proper ventilation of the alveoli. Moreover, surfactant proteins A and D (collectins) have antimicrobial activity (Wright 2005). Importantly, ATII cells are self-renewing cells and serve as ATI-precursors (Barkauskas et al. 2013).

Airway epithelial cells (AECs) form a tight barrier against exogenous substances and microorganisms by expressing intercellular connective proteins (claudins, connexins, paranexins, adhesions and zonula occludins) that deliver structural integrity to the respiratory mucosal barrier (Whitsett and Alenghat 2015). Disruption of tight junction protein complexes was shown to increase epithelial permeability (LaFemina et al. 2014) and inflammation (Georas et al. 2014, Grainge et al. 2013) thereby contributing to lung injury.

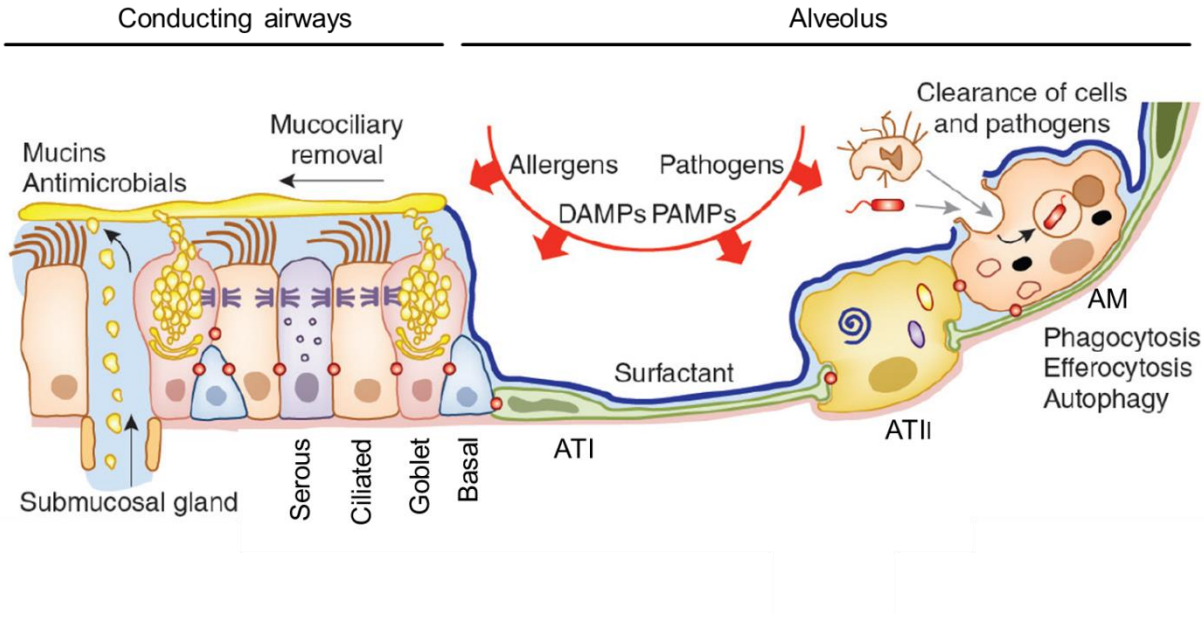

Figure 2: Epithelial and macrophage immunological mechanisms in the lower respiratory tract.
Airway epithelial cells (AECs) and alveolar macrophages (AMs) are exposed to allergens, pathogen-derived molecular patterns (PAMPs) and molecules derived from cell stress and/or death (danger-associated molecular patterns, DAMPs). These are continuously removed by mucociliary clearance and alveolar macrophage-associated mechanisms, but are also recognized by pattern-recognition receptors (PRRs) expressed by AECs & AMs. Adapted from Whitsett and Alenghat 2015.

Their multifaceted roles as pulmonary gatekeepers make AECs critical elements of the respiratory innate immune system. Importantly, they also have been shown to participate in the initiation and regulation of adaptive immune responses. For instance, by nitric oxide (NO) production AECs can interfere with functional activation of Th1 and Th2 cells (Eriksson et al. 2005) and by release of B-cell activating factor, they modulate airway B cell accumulation and/or activation (Kato et al. 2006).

2.2 Mechanisms of respiratory humoral immunity

2.2.1 AEC-derived mediators

AECs secrete a plethora of soluble factors with broad direct and indirect antimicrobial functions and thereby actively reinforce the mucosal surface against bacterial, viral and fungal invaders. For example, by producing small cationic antimicrobial peptides of the β-Defensin family AECs are believed to be involved in the clearance of pathogens (e.g. *Haemophilus influenzae*) from the lung (Moser et al. 2002) but also orchestrate chemoattraction of T cells, dendritic cells and macrophages (Beisswenger et al. 2005). Moreover, lysozyme, one of the most abundant antimicrobial proteins in the lung which is also secreted by AECs, was shown to critically enhance bacterial clearance *in vivo* after infection with *Pseudomonas* and *Streptococcus* species (Akinbi et al. 2000). Other AEC-secreted substances directly or indirectly implicated in immunity towards infectious agents are mucins, surfactant proteins A and D (collectins), serum amyloid A, complement components and other antimicrobial peptides (e.g. cathelicidins, histatins, lactoferrin; Bals 2000, Cleaver et al. 2014, Holt, Strickland et al. 2008, Strunk et al. 1988). Interestingly, epithelial antimicrobial production is regulated by exposure to inflammatory stimuli (e.g. pathogens, cytokines; Harder et al. 2000, O'Neil et al. 1999, Singh et al. 1998).

2.2.2 Secretory antibodies and AECs: cooperativity mediates protection

Similar to what has been reported for the gastro-intestinal and the genitourinary tract innate mucosal immunity in the respiratory tract critically depends on secretory immunoglobulins (SIgs). While submucosal plasma cells locally produce natural, mostly dimeric, IgA (Strugnell et al. 2010) it is still a matter of debate which B cell subsets contribute to local and systemic natural IgM levels (Ehrenstein et al. 2010). Both immunoglobulin subtypes are characterized by a common structure: the joining chain (J chain), which has an important role in the process of antibody transport onto the mucosal surface.

By directed cooperation with the humoral immune system AECs provide broad, unspecific protection of the pulmonary mucosa against a multitude of respiratory pathogens. Upon binding of the J chain by the polymeric immunoglobulin receptor (pIgR), which is expressed by AECs, active endosome-mediated transcytosis of the pIgR-antibody complex through the epithelium is initiated. After proteolytic cleavage IgA and IgM are released into the pulmonary lumen, bound to a small pIgR-subunit, the secretory component (SC).

A considerable portion of SIgA is polyreactive, i.e. it binds a plethora of antigens such as commensal bacteria and autoantigens and is thus also known as ‘natural IgA’ (Shroff, Meslin et al. 1995, Bos, Jiang et al. 2001, Notkins 2004). By binding to microbial surfaces natural IgA, which is the predominant immunoglobulin found in mucosal secretions, sterically inhibits pathogen adhesion and invasion of epithelial cells – this mechanism is known as ‘immune exclusion’ (Strugnell and Wijburg 2010, Figure 3). Moreover, SIgA/pIgR complexes have functions in intracellular virus neutralization as well as antigen excretion from subepithelial compartments back to the mucosal lumen (Strugnell and Wijburg 2010).

Furthermore, early control of infection is mediated by concerted actions of IgM and complement component C1q (Brown et al. 2002). These are constituents of the classical complement pathway which has previously been shown to be the dominant complement activation pathway required for antipneumococcal defense. Several *in vivo* studies evidence crucial roles for pIgR and SIgs in host immunity towards pathogenic bacteria and viruses (Blutt et al. 2012, Brown, Hussell et al. 2002, Sun et al. 2004, Tjarnlund et al. 2006).

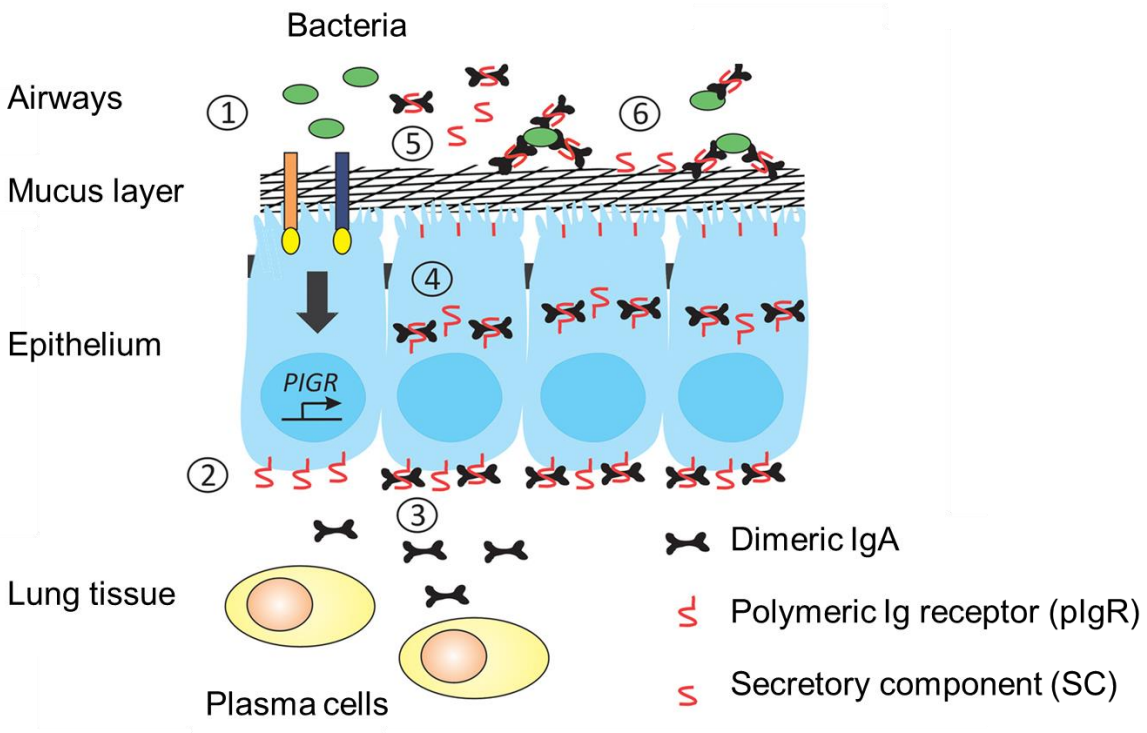

Figure 3: Principle of SIg transport in the lung.
(1) Stimulation with endogenous or exogenous ligands activates pathways that trigger *PIGR* gene expression. **(2)** Newly synthesized pIgR molecules are transported to the basolateral site of airway epithelial cells. **(3)** Dimeric IgA (dIgA), locally produced by plasma cells, binds to pIgR and initiates transepithelial transport cascades. **(4)** dIgA-coupled and unoccupied pIgR are transcytosed through epithelial cells. **(5)** Proteolytic cleavage of pIgR at the apical surface releases secretory IgA (SIgA) and secretory component (SC). **(6)** Binding of SIgA (and SC) to bacteria prevents their adhesion and invasion. The illustrated mechanism also applies to transepithelial transport of IgM onto the mucosal surface. Adapted from Johansen et al. 2011.

Identification of the factors that regulate pIgR-expression – and consequently the rate of mucosal SIg transcytosis - revealed a multitude of endogenous as well as exogenous modulators involved in this transport mechanism. These are summarized in Table 1.

Table 1: Regulators of pIgR-expression.
Adapted from Kaetzel 2005.

Stimuli		Nature of regulation (↑up, ↓down), tissue
Cytokines		
IFN-γ	↑	human intestinal epithelial cell line (Sollid et al. 1987)
TNF-α	↑	mouse intestinal epithelium (Moon et al. 2014)
IL-1β	↑	mouse intestinal epithelium (Moon, VanDussen et al. 2014)
IL-4	↑	human intestinal epithelial line (Schjerven et al. 2000)
IL-17	↑	mouse intestinal & pulmonary epithelium (Jaffar et al. 2009, Moon, VanDussen et al. 2014)
TGFβ	↓	human lung epithelial cells (Gohy et al. 2014)
Hormones		
Estradiol	↑	rat endometrium (Kaushic et al. 1995)
Progesterone	↓	rat endometrium (Kaushic, Richardson et al. 1995)
Glucocorticoids	↑	rat intestinal epithelial cell line, rat intestine (Li et al. 1999)
	↓	rabbit mammary gland (Rosato et al. 1995)
Prolactin	↑	rabbit mammary gland (Rosato, Jammes et al. 1995)
Dietary factors		
Retinoic acid	↑	human intestinal epithelial cell line, in concert with IL-4, IFN-γ, TNF-α (Sarkar et al. 1998)
Microbial factors		
Butyrate	↑	human intestinal epithelial cell line (Kvale et al. 1995)
LPS	↑	mouse intestinal epithelium (Moon, VanDussen et al. 2014)
B. thetaiotaomicron	↑	intestinal epithelium (during colonization of germ-free mice) (Hooper et al. 2001)
dsRNA	↑	human intestinal epithelial cell line (Schneeman et al. 2005)
Reovirus	↑	human intestinal epithelial cell line (Pal et al. 2005)
S. boulardii	↑	rat intestinal epithelium (Buts et al. 1990)

2.3 Chronic respiratory disease (CRD)

The term *chronic respiratory diseases (CRDs)* comprises a series of non-communicable lung disorders with different etiopathologies and clinical pictures. Being the most prevalent CRDs with globally increasing incidence (Mannino et al. 2007, Pearce et al. 2007), asthma and COPD are addressed in this paragraph.

Both diseases generally manifest in airway obstruction, yet this process is reversible in asthma while found to be progressive and mostly irreversible in COPD (Barnes 2008).

The majority of asthmatic patients are diagnosed with atopy, i.e. the presence of immunological hypersensitivity towards environmental antigens such as pollen or animal danders (Barnes 2008). In contrast, the predominant cause for COPD pathogenesis is exposure to noxious substances such as tobacco smoke and the associated direct as well as indirect inflammatory cascades triggered by these particles (Brusselle et al. 2011). Interestingly, COPD is also discussed to involve an autoimmune etiology (Agusti et al. 2003).

Both diseases are characterized by lung inflammation, which can massively increase during phases of acute exacerbation. While inflammatory processes in asthma mostly occur in the large conducting airways (bronchi), COPD manifests in small airway and parenchymal inflammation (Barnes 2000, Jeffery 2000). The immunological mechanisms orchestrating both diseases are partly mirrored in their histopathologic appearances. Bronchial biopsies taken from asthmatic individuals show eosinophilic infiltration, activated mucosal mast cells and T cells. Moreover, basement-membrane thickening (subepithelial collagen deposition) is a characteristic hallmark of this disease (Benayoun et al. 2003). In COPD lungs increased infiltrations of T cells and neutrophils are observed (Hogg 2004). In large contrast to asthmatic lungs emphysema (a major cause for airflow limitation) - as a result of enhanced proteolytic degradation of alveolar wall components - is a salient feature of COPD pathology (Ohnishi et al. 1998).

The clinical symptoms associated with asthma as well as COPD significantly deteriorate during acute exacerbations; the latter are a major cause for severe disease complications and hospitalization (Celli et al. 2007, Wark et al. 2006). Infections with airborne pathogens pose a huge risk for acute asthma and COPD disease exacerbations. While viral pathogens (e.g. rhinoviruses) usually trigger asthma deterioration, viruses as well as bacteria (e.g. *Haemophilus* species, *Streptococcus pneumoniae*) are found in exacerbating COPD patients (Barnes 2008. Sethi et al. 2008). In both CRDs exacerbations are intimately linked to increased lung inflammation, increased leukocyte infiltration and higher amounts of pro-inflammatory molecules compared to those conditions found in the steady state (Barnes 2008).

2.4 *Streptococcus pneumoniae* and pneumococcal pneumonia

The Gram-positive, lancet-shaped bacterium *Streptococcus pneumoniae* (also referred to as ‘the pneumococcus’) belongs to the group of α-streptococci. It is an encapsulated diplococcus which grows in pairs or chains and is a facultative anaerobic microorganism. Pneumococci are the most prevalent bacterial respiratory pathogens worldwide and etiologic agents of sepsis, bacterial meningitis, otitis media and pneumonia (van der Poll et al. 2009).

They frequently colonize the upper respiratory tract where they reside asymptomatically on the nasopharyngeal epithelium, however – depending on predisposing factors on the host site and bacterial virulence factors – bacterial microaspiration into the lower airways can proceed into pneumonia and eventually into invasive pneumococcal disease (IPD). Pneumococcal disease incidence is particularly high in infants, the elderly and patients who have immunodeficiencies or undergo immunosuppressive therapies, respectively. In this regard, complications of respiratory pneumococcal infections are frequently found in individuals with pre-existing impaired pulmonary conditions, such as antecedent influenza virus infection or chronic lung disease (van der Poll and Opal 2009).

2.4.1 Pneumococcal virulence factors

Pneumococcal virulence greatly varies among the 93 known serotypes (Calix et al. 2010). Here the composition and thickness of the polysaccharide capsule is a major determinant (Figure 4), as this constituent prevents entrapment in the mucus layer and neutrophil extracellular traps (NETs) and counteracts opsonophagocytosis (Hyams et al. 2010, Nelson et al. 2007, Wartha et al. 2007). Moreover, most pneumococcal strains display a remarkable plasticity: via phase variation they are able to modify their capsular composition (opaque vs. transparent colony morphology) which allows for the rapid adaptation in response to environmental cues present in the particular host tissue (van der Poll and Opal 2009).

The pneumococcal exotoxin pneumolysin (Figure 4), a cholesterol-dependent cytolysin that effects pore formation in cholesterol-containing membranes and thus host cell lysis, is found in almost all invasive pneumococcal isolates (van der Poll and Opal 2009). Reported activities of this constituent include inhibition of cilial beating on respiratory epithelial cells (Feldman et al. 1990), disruption of tight junctions of the epithelial layer (Rayner et al. 1995), inhibition of phagocyte respiratory burst (Paton et al. 1983) as well as induction of cytokine synthesis (Cockeran et al. 2002). Accumulating evidence suggests a pivotal role for pneumolysin in the development of pneumonia as well as IPD (Kadioglu et al. 2008). Interestingly, a recent *in vivo* study identified pneumolysin to induce AEC apoptosis and to block release of antifibrogenic prostaglandin E2 thereby causing disease progression in a model of lung fibrosis exacerbation. With fibrosis being a chronic respiratory disease, this mechanism highlights the importance of pneumococcal infection as comorbidity of individuals with underlying chronic pulmonary conditions (Knippenberg et al. 2015).

In addition, a number of pathogenicity factors, that mediate bacterial adhesion to epithelial or extracellular matrix components, have been identified, such as ChoP, CbpA or PavA (Kadioglu, Weiser et al. 2008, Figure 4). Effective evasion of host humoral immunity is also mediated by PspA, which prevents binding of complement component C3 onto the bacterial surface but also protects pneumococci from the antimicrobial activities of lactoferrin (Shaper et al. 2004, Tu et al. 1999). In addition to these factors, secretion of a zinc metalloproteinase cleaving human IgA1 (which accounts for 90% of the IgA in the human airways) is considered to be a factor counteracting humoral immunity (Kadioglu, Weiser et al. 2008, Figure 4). However, given the predominant function of IgA as mediator of immune exclusion it remains a matter of debate whether the residual cleaved Fab fragments on the bacterial surface might be similarly potent in preventing attachment of pneumococci to the mucosal surface.

Pneumococcal virulence and survival critically depends of nutrient availability. Consequently several bacterial virulence factors associated with microelement supply have evolved. For example, pneumococcal iron acquisition and uptake are mediated by PiaA and PiuA systems (Kadioglu, Weiser et al. 2008). Moreover, structural analyses of the lipoprotein PsaA revealed a divalent metal-ion-binding site that can bind zinc or manganese ions, and PsaA mutants were shown to require manganese supplementation (Dintilhac et al. 1997, Lawrence et al. 1998, Figure 4).

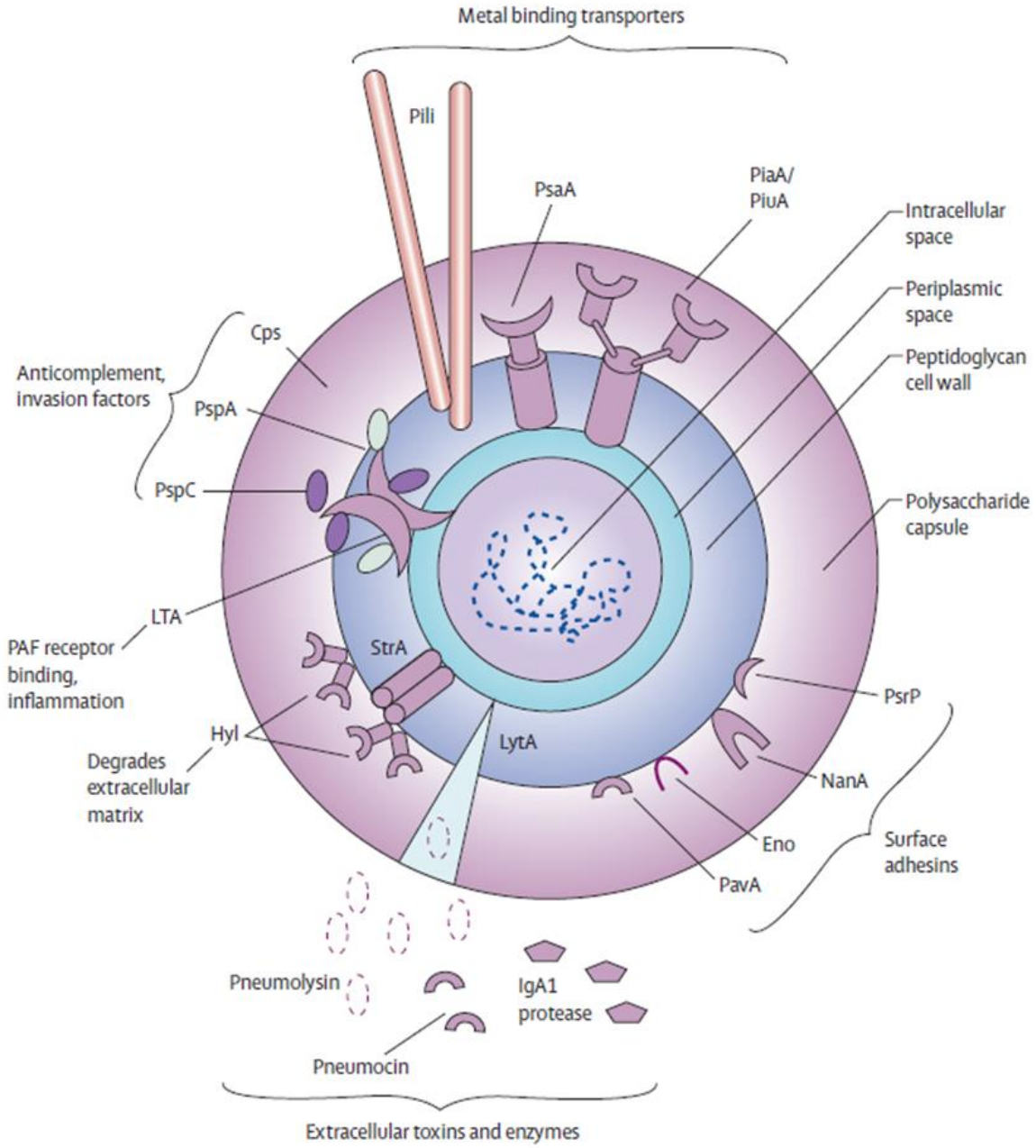

Figure 4: Virulence factors of *Streptococcus pneumoniae*.
PsaA=pneumocoocal surface antigenA. PiaA/PiuA=pneumocoocal iron acquisition and uptake. PsrP= pneumocoocal serine-rich repeat protein. NanA=neuraminidase. Eno=enolase. PavA=pneumocoocal adhesion and virulence. LytA=autolysin. StrA=sortase A. Hyl=hyluronate lyase. LTA=lipoteichoic acid. PspC= pneumococcal surface protein C. PspA=pneumocoocal surface protein A. Cps=polysaccharide capsule.
Figure taken from van der Poll and Opal 2009.

2.4.2 Role of pattern recognition for host defense against *Streptococcus pneumoniae*

The presence of receptors recognizing conserved pathogen-associated molecular patterns (PAMPs) is a central element in rapid host immunity towards *S. pneumoniae* and other pathogens. Pattern recognition receptors on alveolar macrophages (AMs) and AECs which are important for antibacterial defense include Toll-like receptors (TLRs) and NOD-like receptors (NODs). In addition to lipopolysaccharide (LPS) TLR4 recognizes pneumolysin (Malley et al. 2003). Moreover, heterodimerization of TLR2 with either TLR1 or TLR6 enables recognition of a broad range of bacterial lipopeptides and lipoteichoic acid. The intracellular receptor TLR9 recognizes unmethylated CpG dinucleotides, mainly present in prokaryotic DNA. While the loss of TLR1, TLR2, TLR4 and TLR6 has been shown to only marginally affect susceptibility during infection with *Streptococcus pneumoniae*, TLR9 was reported to have a crucial role in antipneumococcal host defense in the lower respiratory tract; mainly by governing MyD88-dependent phagocytosis and intracellular killing by AMs (Albiger et al. 2007). In this regard the adaptor molecule MyD88 (myeloid differentiation factor 88), which signals downstream of all TLR pathways (except TLR3), was previously shown to be crucial for antipneumococcal host defense (Albiger et al. 2005). In addition to TLR-dependent mechanisms intracellular sensing of *S. pneumoniae* is achieved by NOD-like receptors. Here NOD2, recognizing a conserved bacterial muramyldipeptide, was shown to be activated during pneumococcal infection and identified to be critical for NF-κB activation by *S. pneumoniae (*Opitz et al. 2004).

In addition to a versatile TLR repertoire AMs possess scavenger receptors, such as MARCO and CD36, which initiate phagocytic uptake of unopsonized particles. Both of these molecules were shown to be critical for innate host defense during pneumococcal pneumonia (Arredouani et al. 2004, Sharif et al. 2013, Figure 5).

Upon PRR-mediated sensing of bacterial, viral or fungal pathogens AMs as well as AECs secrete a wide range of pro-inflammatory cytokines and chemokines in an IRF- or NF-κB-dependent manner (Figure 5). By cell-specific interruption of NF-κB signaling it was demonstrated that AECs are predominant producers of CXCL5, GM-CSF and CCL20 whereas the lung net TNF-α, IL-1α, IL1-β, CXCL1 and CXCL2 response during early pneumococcal pneumonia is shaped by AMs (Pittet et al. 2011, Yamamoto et al. 2014). Here TNF-α is of particular interest as absence of this cytokine is linked to increased susceptibility to bacterial infection (Laichalk et al. 1996, van der Poll, Keogh, Buurman, et al. 1997). Actions of TNF-α include regulation of neutrophil-attracting chemokines, expression of neutrophil-endothelial cell-adhesion molecules but also directly increase of activity of phagocytic cells (Fan et al. 1991, Mukhopadhyay et al. 2006, Tessier et al. 1997). Moreover, AECs as well as AMs can produce IL-6 in response to microbial ligands and this cytokine is suspected to orchestrate activation of vital agonist as well antagonist mediators during bacterial pneumonia (van der Poll, Keogh, Guirao, et al. 1997).

An important hallmark of pulmonary bacterial infection is neutrophil extravasation into the lung (Figure 5). This is generally a result of a lung-blood chemokine gradient and several ligand-receptor interactions between activated neutrophils, endothelial and epithelial cells. CXCL1, CXCL2 and CXCL5, belonging to the ELR^+ CXC-chemokine family and ligands of CXCR2 on the neutrophil surface, have been described to substantially contribute to neutrophil mobilization into the airways during early pneumonia (Gibbs et al. 2014, Mehrad et al. 1999, Strieter et al. 2002).

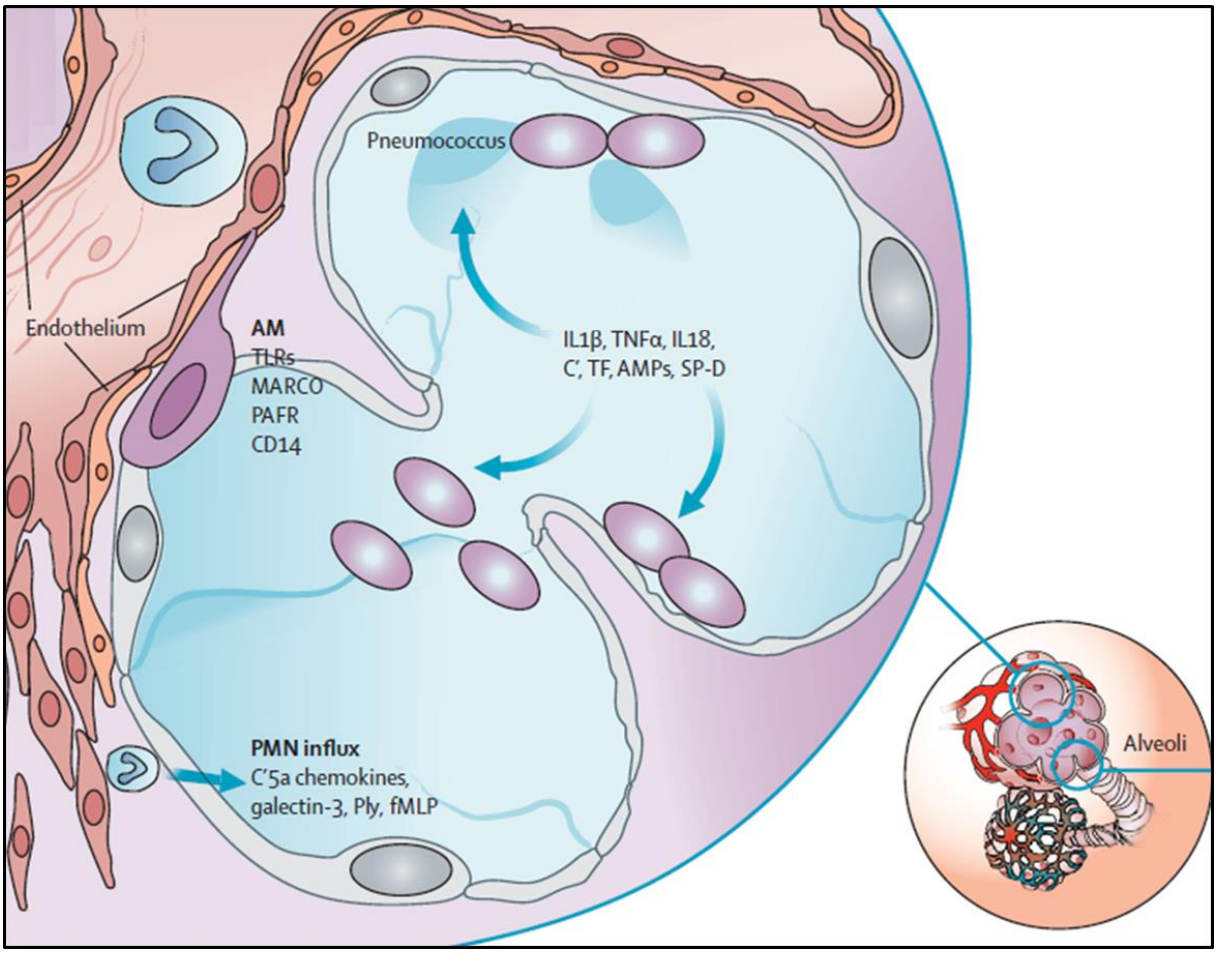

Figure 5: Host defense during pneumococcal pneumonia.
Pneumococci that enter the lower airways are recognized by pattern recognition receptors: TLRs on AECs and alveolar macrophages (AM) and AM-receptors, such as *macrophage receptor with collagenous structure* (MARCO). At low infectious doses AECs and AM clear infection without help from recruited neutrophils (PMNs), by release of pro-inflammatory cytokines, complement products (C'), tissue factor (TF), antimicrobial peptides (AMPs) and surfactant protein-D (SP-D). At high infectious doses PMN recruitment through endothelial layers is mediated by C'5a, neutrophil-attracting chemokines, galectin-3, pneumolysin (Ply) and pneumococcal-derived N-formyl-methionyl-leucyl-phenylalanine (fMLP). PAFR=platelet-activating factor receptor. Adapted from van der Poll and Opal 2009.

2.5 Macrophage phenotypes and functions

Besides their pivotal roles in mediating antimicrobial innate host defense, macrophages orchestrate pleiotropic physiological reactions involved in homeostasis, inflammation, metabolism and tissue remodeling. Consequently, a salient hallmark of the macrophage lineage is their great diversity and plasticity, enabling these cells to rapidly and dynamically adapt in response to a plethora of environmental signals in the respective tissue (Figure 6).

In analogy to the Th1/Th2 dichotomy, which is applied for T lymphocytes, rough classification into M1/M2 phenotypes is also common for the macrophage lineage. However, Mosser and Edwards proposed a nomenclature, in which macrophages are classified by their pre-dominant functions in the maintenance of homeostasis: host defense, wound healing and immune regulation (Mosser et al. 2008).

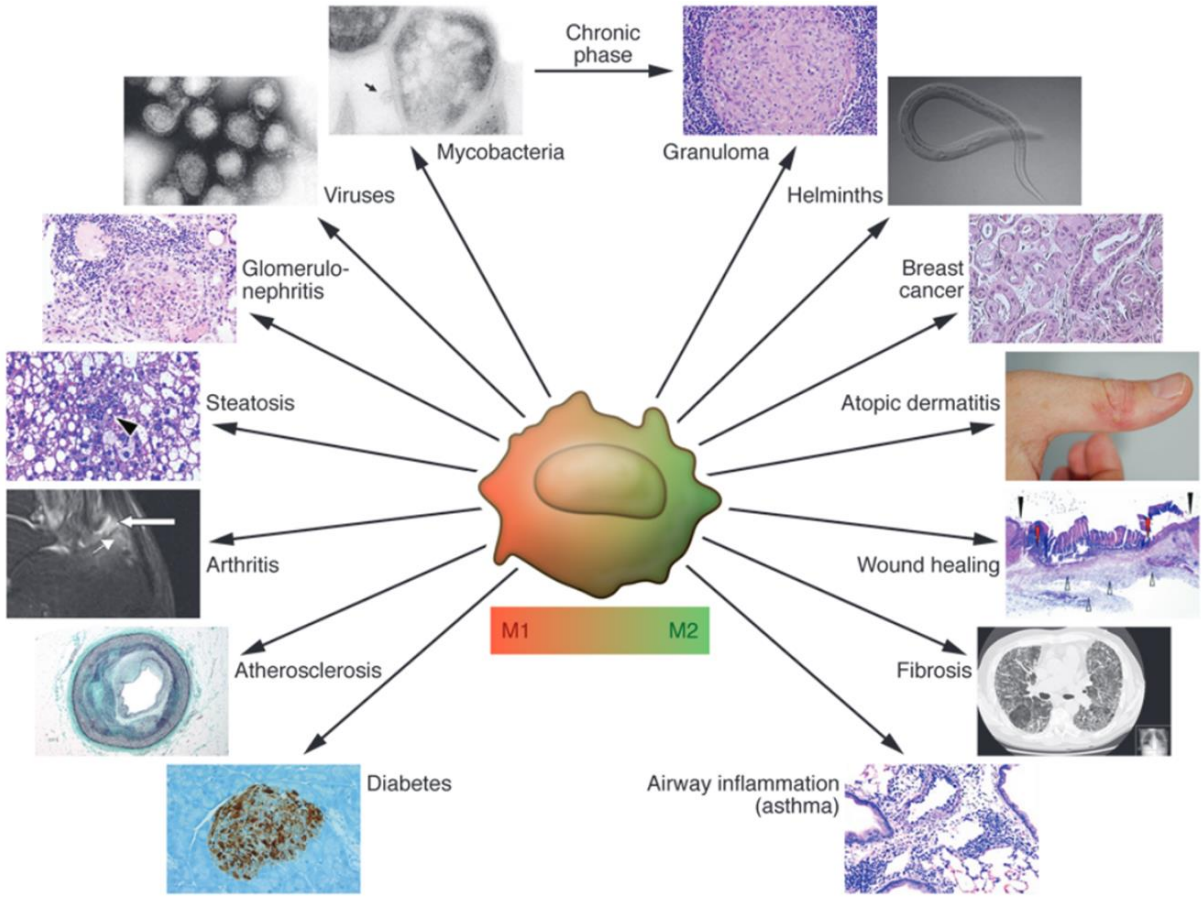

Figure 6: Macrophage polarization in pathology.
Dynamic changes of macrophage polarization patterns may occur during evolution of pathology, e.g. during transition from acute to chronic infection. Mixed phenotypes can however coexist. Figure taken from Sica et al. 2012.

Classically activated (M1) macrophages are characterized by high expression of pro-inflammatory cytokines (e.g. IL-12, IL-23 IL-1β and TNF-α), high production of reactive nitrogen and oxygen species, promotion of Th1/Th17 responses and powerful antimicrobial and anti-tumorigenic activities. M1 polarization occurs in response to LPS, TNF-α or IFN-γ, and results in enhanced antigen-presenting and phagocytic capacity, enhanced production of matrix metalloproteinases (MMPs) 7 and 9 and up-regulation of the transcription factor IRF5 (Boorsma et al. 2013, Mosser and Edwards 2008).

Alternatively activated (M2) macrophages are induced by IL-4 and IL-13, under the influence of the transcription factor IRF4, and produce the anti-inflammatory cytokine IL-10. Moreover, typical genes associated with M2-polarization are resistin-like alpha (*Retlna*, *Fizz1*) and chitinase-like 3 protein (*Chi3l3*, *Ym1*). M2 macrophages participate in anti-helminth immunity, wound healing and tumor progression. They are characterized by efficient phagocytic activity, high expression of scavenger, mannose and galactose receptors and the production of ornithine and polyamine through the arginase pathway (Boorsma, Draijer et al. 2013, Mosser and Edwards 2008, Sica and Mantovani 2012). Of note, macrophage polarization was shown to be associated with different iron recycling capabilities of M1 vs. M2 cells. In this regard, M2 cells were demonstrated to have an iron-deficient phenotype, including a

large, yet labile, intracellular iron pool, spontaneous iron release and limited storage capacity (Corna et al. 2010).

A third macrophage subgroup is termed M2-like or also 'regulatory' macrophages. This group shares some features with M2 macrophages (e.g. high expression of mannose and scavenger receptors) but has a distinct chemokine profile. Activating stimuli include IL-10, TGFβ, antibody immune complexes, apoptotic cells glucocorticoids and PGE_2. Yet, these stimuli have to be associated with a second (stronger) stimulus, such as TLR ligation, to induce IL-10 production. Transcriptional regulation of this subset is believed to involve the nuclear receptor PPARγ (Lawrence et al. 2011). Unlike M2 macrophages, regulatory macrophages are not involved in extracellular matrix repair, and can express high levels of the co-stimulatory molecules CD80 and CD86 (Boorsma, Draijer et al. 2013, Mosser and Edwards 2008, Figure 7).

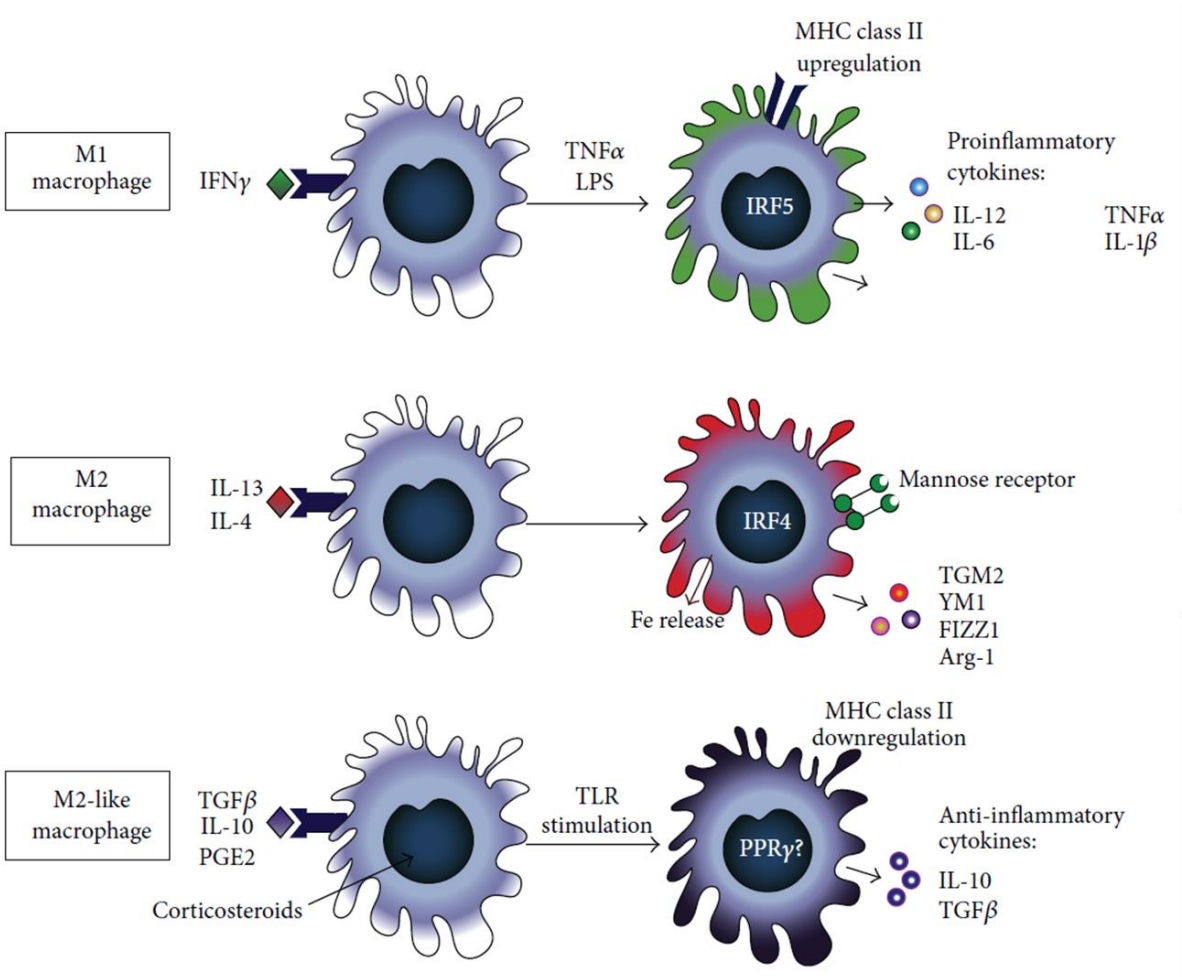

Figure 7: Macrophage subsets and their characteristics.
TGM2=transglutaminase 2; YM1=chitinase-like protein-3; FIZZ1/Retlna=resistin-like alpha; Arg-1=arginase-1; PGE_2=prostaglandin E2; PPRγ=peroxisome proliferator-activated receptor gamma (also: PPARγ). Adapted from Boorsma, Draijer et al. 2013.

2.6 Pleiotropic roles of alveolar macrophages in homeostasis and disease

Alveolar macrophages (AMs) are the most abundant cells in the airways; they constitute up to 95% of the leukocyte populations recovered by bronchoalveolar lavage (Holt 1986).

Alveolar macrophages are derived from a fetal monocyte population that colonizes the airways during the first days after birth (Guilliams et al. 2013). Interestingly, it was previously shown that alveolar macrophages have a remarkable capacity for self-renewal and that this is the predominant mechanism by which replenishment of this population is achieved during homeostasis and following influenza-induced depletion (Hashimoto et al. 2013). Moreover, alveolar macrophages are long-lived cells, with a turnover rate of only 40% in 1 year (Maus et al. 2006).

Most studies do not distinguish between airway macrophages that reside in the mucus layer of the bronchus and the bronchioles and those located in the alveoli (Figure 8). Due to the experimental procedure (bronchoalveolar lavage) required for isolation of airway macrophages, a mixture of these cells is obtained and unique markers classifying either one or the other cell type are not known thus querying the existence of distinct populations (Hussell et al. 2014). In accordance with other *in vivo* studies the airway macrophages analyzed in this study are also referred to as ‘alveolar macrophages (AMs)’.

2.6.1 Role of the AM/T cell axis in pulmonary immunity

T cell-mediated pulmonary immunity is a double-edged sword as it is known to be vital for the clearance of inhaled pathogen. At the same time, excessive, uncontrolled T cell responses are implicated in various disease settings, such as asthma and autoimmune disorders (Ohashi 2002, Robinson 2010). The suppression of T cell responses is therefore a key element of pulmonary immune regulation.

Human and rodent alveolar macrophages were shown to actively suppress T cell proliferation. One molecule likely to be involved in this process is nitric oxide (NO). This molecule was demonstrated to be constitutively expressed in rat AMs and it regulates T cell activation by interfering with the Jak3/STAT5 signaling pathway (Bingisser et al. 1998). Moreover, AMs can secrete PGE_2 (Roth et al. 1993). PGE_2 induces among others differentiation of $Foxp3^+$ T cells, inhibits T cell proliferation and induces T cell anergy.

In addition, AM-derived retinoic acid and $TGF\beta_1$ were shown to play a role in the conversion of naive $CD4^+$ T cells into IL-10 secreting $Foxp3^+$ T cells (Coleman et al. 2013), although lung-resident tissue macrophages can secrete these molecules, too (Soroosh et al. 2013). Similar to PGE_2 $TGF\beta_1$ is known to suppress T lymphocyte activation (Roth and Golub 1993, Figure 9).

Murine AMs are poor antigen-presenting cells (Lipscomb et al. 1986, Lyons et al. 1986, Toews et al. 1984), yet they are capable of transporting antigen to the lung–draining lymph nodes (Kirby et al. 2009). AMs from humans are believed to promote T cell anergy as a consequence of reduced antigen-presenting capacity and a lack of expression of the co-stimulatory molecule CD86 (Blumenthal et al. 2001).

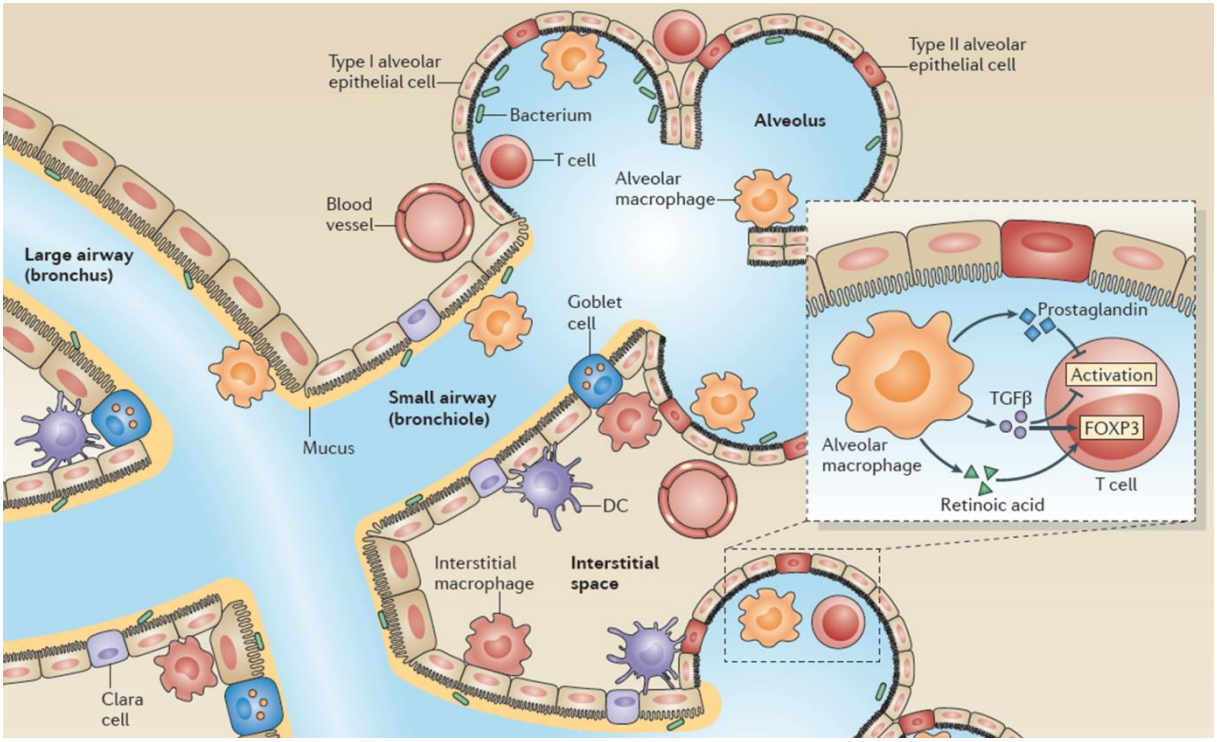

Figure 8: Cellular interactions in the lung.
Alveolar macrophages reside in the alveoli, next to alveolar type I and II epithelial cells. Macrophages in the large and small airways are in contact with the mucus layer (produced by goblet cells in the bronchi & bronchioles) and secretory Clara cells (mostly in bronchioles, nowadays referred to as 'club cells'). Commensal (and pathogenic) bacteria can be found in all compartments. Alveolar macrophages can induce forkhead box P3 (FOXP3) expression in naive and activated $CD4^+$ T cells via secretion of TGFβ and retinoic acid. Moreover, TGFβ and prostaglandins suppress T cell activation. Adapted from Hussell and Bell 2014.

2.6.2 Role of the AM/AEC axis in pulmonary immunity

Considering the fact that AECs and AMs are directly juxtaposed, it is not surprising that a number of AM/AEC communication strategies have so far been discovered. Nevertheless, while the role of the AECs as regulators of AM activation (e.g. via SP-A, TGFβ, CD200, IL-10) is widely appreciated (Hussell and Bell 2014), little knowledge exists about the reverse communication.

It was previously demonstrated that AM-derived pro-inflammatory cytokines (e.g. TNF-α) can activate alveolar epithelial and endothelial signaling cascades, which consequently facilitates neutrophil extravasation into the airspaces (Kuebler et al. 2000). Moreover, AM-released mediators (HB-EGF and PDGF-, IGF-1 and FGF-1-like molecules) were shown to exert stimulatory effects on AEC proliferation (Leslie et al. 1997, Melloni et al. 1996). To date, only a few studies however have addressed the immunosuppressive potential of AMs on AECs. Being dedicated pulmonary scavengers, AMs indirectly exhibit immunosuppressive functions by the overall reduction of microbial factors, allergens, cellular debris and apoptotic cells, thus antagonizing the initiation of a pro-inflammatory immune response by AECs (Figure 2). In this regard, AMs were shown to have an essential anti-inflammatory role during murine pneumococcal pneumonia, possibly by engulfment of apoptotic neutrophils (Knapp et al. 2003).

A recent report identified connexin43 (a protein involved in gap junction channel formation) on ATII cells and AMs to be a critical element responsible for down-regulating LPS–induced secretion of epithelial-specific (CXCL5) as well as AM-specific (MIP1-α) pro-inflammatory mediators. This study suggested alveolus-attached AMs to intercommunicate immunosuppressive signals to the epithelium, thereby reducing PAMP–induced pulmonary inflammation orchestrated by both cellular players (Westphalen et al. 2014).

Moreover, Bourdonnay and colleagues demonstrated that AM-derived suppressor of cytokine signaling (SOCS) proteins 1 and 3, which are transcellularly delivered to AECs via exosomes and microparticles, inhibit STAT1 and STAT3 activation and thus interfere with pro-inflammatory signaling pathways in these cells (Bourdonnay et al. 2015).

2.6.3 Role of AMs in termination and resolution of inflammation

Manifold physiological processes are involved in the termination of inflammation and re-establishment of tissue homeostasis in the lung. These include among others inhibition of intra-alveolar leukocyte influx, phagocytosis of apoptotic PMNs and initiation of alveolar repair mechanisms (Figure 9). Accumulating evidence suggests crucial roles for AMs in these mechanisms.

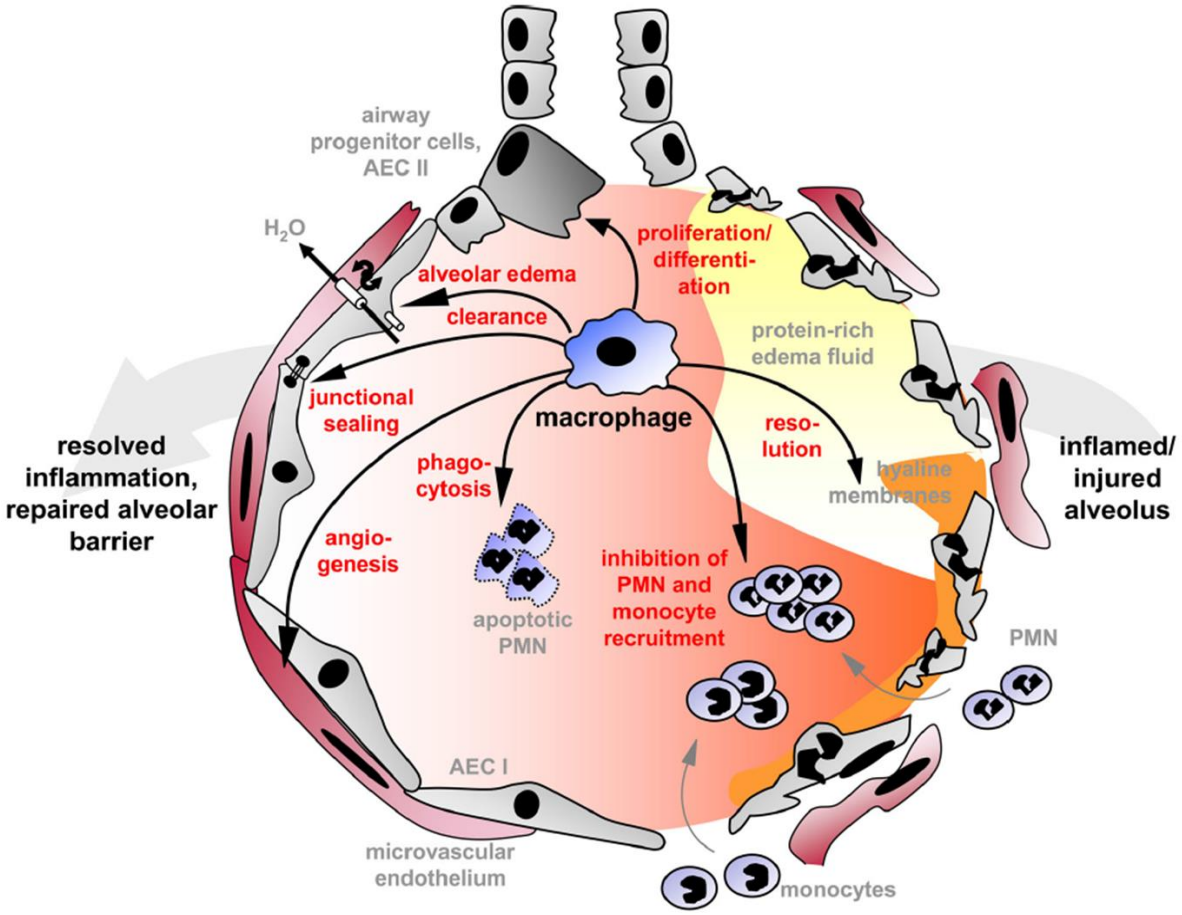

Figure 9: Alveolar macrophage-orchestrated processes for termination and resolution of alveolar inflammation.
Figure taken from Herold, Mayer, et al. 2011.

AMs produce e.g. a series of lipid-related mediators (Balter et al. 1988, Beck-Speier et al. 2005), which participate in the resolution of inflammation in the lungs by directly interfering with neutrophil functions. For example, the prostaglandins PGE_2 and PGD_2, which are synthesized in a cyclooxygenase-dependent manner, promote in an auto- and paracrine fashion the synthesis of lipoxins by AMs but also other leukocytes. Lipoxins are lipoxygenase-derived double oxygenated eicosanoids, ultimately inhibiting recruitment of neutrophils as well as their pro-inflammatory functions at sites of inflammation (Chiang et al. 2006). Interestingly, cyclooxygenases and lipoxygenases are prominent pharmaceutical targets enabling to interfere with inflammatory immune responses. Other examples of pro-resolving lipid mediators are resolvins, protectins and maresin1, derived from omega-3 polyunsaturated fatty acid, eicosapentaenoic acid and docosahexaenoic acid, respectively. Resolvin E_1 attenuates NF-κB activation (Arita et al. 2005) and antagonizes the pro-inflammatory leukotriene B_4 receptor BLT1 on leukocytes, thereby exerting anti-inflammatory functions, e.g. by dampening neutrophil migratory capacities (Arita et al. 2007). Moreover, the molecule *macrophage mediator in resolving inflammation 1* (maresin1) was also found to antagonize pathologic neutrophil functions by promoting their apoptosis in a caspase-dependent fashion (Gong et al. 2015).

Another strategy by which macrophages can antagonize immunopathology is the interference with key elements of epithelial and endothelial leukocyte recruitment cascades. For instance, via the blockade of the IL-1β signaling pathway on alveolar epithelial cells, downregulation of CXCL2 secretion and ICAM-1 expression pathologic intra-alveolar neutrophil influx and subsequent lung pathology was shown to be down-regulated during acute lung inflammation (Herold, Tabar, et al. 2011). In this regard, by using a model of LPS-induced lung injury Dean and colleagues demonstrated that MMP-12, a known product of macrophages, is able to cleave CXC-chemokines at the ELR motif, thus inhibiting binding of these mediators to their respective receptors and interfering with e.g. neutrophil chemotaxis (Dean et al. 2008).

A number of molecules, produced by wound-healing macrophage subsets, are implicated in the reestablishment of the epithelial and endothelial barrier function. Tissue repair and proliferation mechanisms are promoted by macrophage-derived fibronectin 1, TGFβ-induced matrix associated protein and insulin-like growth factor 1 (Herold, Mayer et al. 2011). In addition, it was demonstrated that AMs release the epithelial growth factors platelet-derived growth factor, fibroblast growth factors, heparin-binding EGF-like growth factor, TGFβ and vascular endothelial growth factor (Granata et al. 2010, Leslie, McCormick-Shannon et al. 1997, Medeiros et al. 2009, Melloni, Lesur et al. 1996). Moreover, ATII express CD74, which upon interaction with *macrophage migration inhibitory factor* (MIF) is involved in MIF-induced ATII–proliferation (Marsh et al. 2009). Besides, macrophage-derived growth factors might be involved in the reinforcing tight junctions in airway epithelial monolayers (Terakado et al. 2011). Lastly, uptake of apoptotic cells by macrophages effects secretion of vascular endothelial growth factor (VEGF) and macrophage-derived VEGF is believed to be involved in regulation of the endothelial barrier after lung injury (Golpon et al. 2004, Granata, Frattini et al. 2010).

2.7 Macrophage phenotypes in COPD

Exposure to smoke or other noxious particles and the resulting pulmonary inflammation are the main risk factors in people susceptible for the development of COPD. Alveolar wall destruction (emphysema), which is one hallmark of this disease, is thought to be a product of inflammatory macrophage and neutrophil recruitment, which ends up in the release of elastolytic enzymes (e.g. MMPs or neutrophil elastase; Brusselle, Joos et al. 2011). Concordantly, increased numbers of inflammatory macrophages and neutrophils are found in airways and/or lung parenchyma of COPD patients (Finkelstein et al. 1995, Lacoste et al. 1993). The role of AMs in this context becomes evident by AM-depletion e.g. in rodent models of cigarette-smoke or elastase-induced emphysema. Here, a superior role of AMs in perpetuating lung pathology was demonstrated (Ofulue et al. 1999, Ueno et al. 2015).

There are several lines of evidence describing the involvement of both M1 and M2 alveolar macrophages in COPD pathogenesis.

Increased iNOS (an inducible isoform of nitric oxide synthase; associated with M1 macrophages) expression in AMs was found in COPD patients (Ichinose et al. 2000). Expression of these molecules generates reactive oxygen species (ROS) and nitric oxide (NO); both being effectors of oxidative stress, which participates in COPD pathogenesis (Ito et al. 2009). Moreover, cytotoxic $CD8^+$ T cells (Tc1 cells) that infiltrate the lungs in COPD are important producers of IFN-γ, an M1-polarizing cytokine (O'Shaughnessy et al. 1997, Saetta et al. 1999). Accordingly, constitutive pulmonary IFN-γ expression in mice is associated with emphysema (Wang et al. 2000). Breakdown of extracellular matrix in COPD is thought to involve MMPs and pulmonary macrophages from COPD patients produce higher amounts of the M1-marker MMP-9 (Russell et al. 2002).

In contrast, the matrix metalloprotease MMP-12 which also induces emphysema in mice (Hautamaki et al. 1997) is a hallmark of M2-polarized macrophages (Kahnert et al. 2006). MMP-12 is used as a marker for alternative activation of alveolar macrophages in smokers (Woodruff et al. 2005). However, given the anti-inflammatory role of MMP-12 (i.e. antagonizing neutrophil chemoattraction, see section 2.6.3) its general role in COPD pathogenesis is so far not fully understood. M2 macrophages in mice were also found to secrete chitinase and chitinase-like proteins such as Ym1 (also known as chitinase-like 3 or CHI3L3) and Ym2 (chitinase-like 4), which can bind to extracellular matrix structures and are associated with matrix reorganization and wound healing (Lee et al. 2011, Mosser and Edwards 2008). Expression of Ym1 and Ym2 in M2 alveolar macrophages is interesting in view of the fact that elevated chitinase levels and chitinase-positive macrophages are also found in BAL from smokers with COPD (Letuve et al. 2008) thereby linking the M2 macrophage subset to COPD.

2.8 The SPC-HAxTCR-HA mouse model for CRD

In order to dissect the impact of chronic respiratory disease and the associated microenvironmental and cellular adaptations on different aspects of pulmonary immunity the SPC-HAxTCR-HA mouse model was previously established in our lab (Bruder et al. 2004).

SPC-HA mice express a model antigen (the influenza/A/PR8/34 hemagglutinin; HA) under the control of the surfactant protein C (SP-C) promotor, which is exclusively active in alveolar type II epithelial cells (ATII). Breeding of SPC-HA mice with T cell receptor (TCR) transgenic (6.5) mice expressing a major histocompatibility complex (MHC) class II-restricted HA-specific TCR (Kirberg et al. 1994) generates double transgenic SPC-HAxTCR-HA mice. In newborn SPC-HAxTCR-HA mice recognition of alveolar self-antigen by self-antigen specific T cells effects the development of severe $CD4^+$ T cell-mediated lung inflammation (Bruder, Westendorf et al. 2004). In histopathologic analyses these lungs display massive multifocal interstitial, perivascular and peribronchial lymphocytic and plasmacytic infiltrations. Moreover, the destruction of alveolar architecture (emphysema) as well as hemosiderosis are two hallmarks found to be associated with lung disease in the SPC-HAxTCR-HA model. Despite the rapid and massive onset of $CD4^+$ mediated immunepathology in neonates, lung disease does not proceed into fatal tissue destruction or death in older mice. In this regard several immunologic mechanisms leading to self-tolerance and thus the establishment chronic, yet controlled, lung disease in adult SPC-HAxTCR-HA mice have previously been identified. These include T cell anergy, associated with decreased pro-inflammatory cytokine response of self-specific $CD4^+$ T cells and reduced proliferative capacity (Bruder, Westendorf et al. 2004). Moreover, the conversion of naive $CD4^+$ T cells into $Foxp3^+$ regulatory T cells (Tregs) by means of ATII-derived TGFβ was demonstrated to be another immunoregulatory element in lungs of adult SPC-HAxTCR-HA mice (Gereke et al. 2009).

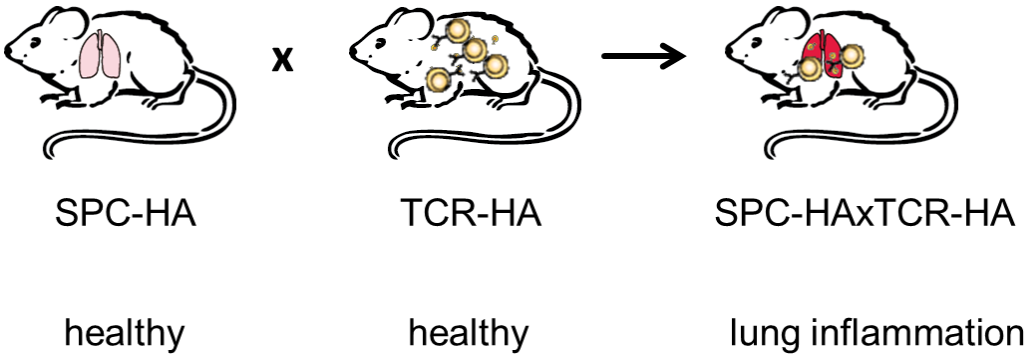

Figure 10: Scheme of the double transgenic SPC-HAxTCR-HA mouse model.

3 Aim of the study

In the context of this work two aspects were addressed.

In the first part mechanisms underlying altered pulmonary immunity against respiratory tract infections in hosts with chronic respiratory disease (CRD) were to be elucidated. To this end SPC-HAxTCR-HA mice, intrinsically developing autoimmune-mediated lung inflammation, were utilized in a bacterial infection model using the common respiratory pathogen *Streptococcus pneumoniae*. In order to identify possible cellular pathways and molecules involved in altered antipneumococcal defense, comparative transcriptomic, proteomic and histological analyses of healthy SPC-HA and pre-diseased SPC-HAxTCR-HA lungs were to be performed. The protective capacities of lung-resident cells (alveolar macrophages, airway epithelial cells) as well as humoral mediators in SPC-HA and SPC-HAxTCR-HA mice were to be compared between both mouse groups.

The second part of this work focused on the immunoregulatory roles of alveolar macrophages (AMs) in CRD. The latter has previously been described to involve complex immune responses of alveolar epithelial as well as T effector cells. Yet knowledge on the role of AMs, which are in intimate contact with both cell types, is so far incomplete. Therefore, the phenotype and function of AMs in CRD was to be elucidated using the SPC-HAxTCR-HA mouse model. In order to determine the impact of chronic inflammatory priming on the AM phenotype, comparative morphologic, transcriptional and functional analyses were to be performed. Moreover, the *in vivo* role of AMs in healthy SPC-HA and pre-diseased SPC-HAxTCR-HA mice was to be assessed using depletion experiments. In order to estimate the immunologic function of AMs in chronic respiratory disease, the autoreactive T cell phenotype as well as alveolar epithelial phenotype was to be compared in AM-depleted and AM-sufficient SPC-HA and SPC-HAxTCR-HA mice.

4 Materials and Methods

4.1 Materials

4.1.1 Buffers, solutions and media

ACK buffer

0.15mM NH_4Cl, 1mM $KHCO_3$, 0.1mM EDTA pH8.0, pH 7.2 - 7.4

Blocking buffer

5% nonfat dry milk in Blotting buffer, pH 7.4

Blotting buffer

25mM Tris pH 7.4, 150 mM NaCl, 0.1% (v/v) Tween-20

ELISA (SIgA) assay diluent

PBS, 1% (w/v) BSA, 1% (v/v) Tween-20

ELISA (SIgA) coating buffer

100mM $NaHCO_3$, 33mM Na_2CO_3, pH 9.5

ELISA (SIgA) wash buffer

PBS, 0.05% (v/v) Tween-20

ELISA (SIgA) stop solution

2N H_2SO_4

Lung digestion medium

IMDM GlutaMAX (Gibco), 5% (v/v) FBS, Collagenase D (c: 0.2mg/mL, Roche), DNase (c: 10µg/mL, Sigma)

PBS

PBS tablets (without Ca/Mg) were purchased (Life technologies) and PBS solution was made according to manufacturer's instructions.

RIPA buffer

25mM TrisHCl pH 7.6, 150mM NaCl, 1% (v/v) IGEPAL CA-630, 1% (w/v) sodium deoxycholate, 0.1% (w/v) SDS

FACS buffer

PBS, 2mM EDTA pH 8.0, 2% FBS (v/v)

Columbia Agar

Columbia Agar supplemented with 5% sheep blood was purchased from BD (Heidelberg, Germany).

Todd Hewitt – yeast (THY) medium

3.7g Todd Hewitt broth (Sigma-Aldrich), 1g Bacto-Yeast extract (BD) ad 100 mL MilliQ water

SDS running buffer (10x)

25mM Tris, 192mM Glycine, 0.1% (w/v) SDS, pH 8.3

SDS transfer buffer

25mM Tris, 192mM Glycine, 20% Methanol (v/v), 0.1% SDS, pH 8.4

TBS (10x)

1.4M NaCl, 200mM Tris, pH 7.4

TBS-T

TBS (1x), 0.1% (v/v) Tween-20

4.1.2 Bacteria

Streptococcus pneumoniae TIGR4 is an encapsulated serotype 4 strain isolated from the blood of a 30-year-old male patient in Kongsvinger, Norway (Tettelin et al. 2001). TIGR4 has been previously shown to cause invasive pneumococcal disease in mice (Sandgren et al. 2005). This strain is available at the American Type Culture Collection (ATCC® BAA-334™).

4.1.3 Mice

SPC-HA mice expressing the influenza A/PR8/34 hemagglutinin (HA) under the transcriptional control of the human surfactant protein C (SP-C) promoter exclusively in ATII have been described elsewhere (Bruder, Westendorf et al. 2004). TCR-HA transgenic mice expressing a TCR αβ specific for the I-E^d-restricted HA-peptide 110–120 from A/PR8/34 HA have been described previously (Kirberg, Baron et al. 1994). In SPC-HAxTCR-HA mice the concomitant expression of HA as neo self-antigen and generation of HA-specific $CD4^+$ T cells establishes an autoimmune milieu (Bruder, Westendorf et al. 2004). Mice were bred in the animal facility at the Helmholtz Centre for Infection Research and were kept under specific-pathogen-free (SPF) conditions. All animal experiments were performed according to national guidelines and were approved by local government institutions (Niedersächsisches Landesamt für Verbraucherschutz und Lebensmittelsicherheit, file no. 33.14-42505-04-14/1715). In all experiments SPC-HA and SPC-HAxTCR-HA mice were used between 12 to 24 weeks of age. Mice were euthanized by either CO_2 inhalation or cervical dislocation.

4.1.4 Antibodies

Flow cytometric analyses, sorting of bacterial cells or lung single cell suspensions were performed using the following antibodies:

Table 2: Utilized antibodies and conjugates for FACS.

Specificity	Clone	Label/conjugate	Manufacturer
F4-80	BM8	biotinylated, APC	BioLegend
CD11b	M1/70	PE, Pacific blue	BioLegend
Ly6G	1A8	PE-Cy7	BioLegend
CD3ε	145-2C11	FITC	BioLegend
TCR-HA	6.5	Alexa647	own production
CD43	1B11	PE	BioLegend
CD11c	N418	APC, FITC	BioLegend
IgA	C10-3	FITC	BD Pharmingen
IgM	DS-1	PE	BD Pharmingen
CD16/32 (AT2 sorting)	2.4G2	none	BD Pharmingen
CD16/32 (blocking)	93	none	BioLegend
CD19	6D5	PE	BioLegend
CD45	30-F11	none	BioLegend
rat IgG	polyclonal	PE	BD Pharmingen
Streptavidin		PE-Cy7	BioLegend

For histological analyses of lung tissue, western blot analyses and secretory immunoglobulin ELISA following antibodies were used:

Table 3: Utilized antibodies for immunoblot, immunohistochemistry and ELISA.

Specificity	Clone	Label/conjugate	Manufacturer
pIgR	polyclonal	none	R&D Systems
IgA	11-44-2	biotinylated	SouthernBiotech
goat IgG (H+L)	polyclonal	HRPO	Jackson ImmunoResearch
GAPDH	14C10		Cell Signaling

4.1.5 Oligonucleotide sequences

Table 4: Primers used for quantitative real-time RT-PCR analyses.

Gene	Sequence forward primer (5'->3')	Sequence reverse primer (5'->3')
Actb	CTTCTTTGCAGCTCCTTCGT	TCCTTCTGACCCATTCCCAC
Clca3	CAGGCACGGCTAAGGTTG	GGAGGTGACAGTCAAGGTGAG
Cxcl1	GCCACACTCAAGAATGGTCG	TTACTTGGGGACACCTTTTAGC
Cxcl2	AGATACTGAACAAAGGCAAGGCT	CGAGGCACATCAGGTACGAT
Cxcl5	CCTACGGTGGAAGTCATAGC	AGCTTTCTTTTTGTCACTGCC
Cxcl9	GAGTTCGAGGAACCCTAGTG	GGGATTTGTAGTGGATCGTG
Retlna	ACGAGTAAGCACAGGCAGTT	TGCCAATCCAGCTAACTATCCC
Glycam1	AGCCCACAGATGCCATTC	GAAGGCTCCTTGGAAAGGTC
Igj	GCATGTGTACCCGAGTTACC	TTCAAAGGGACAACAATTCGG
Msr1	GGAATAAGAGGTATTCCAGGTG	TTTGTCCTTTAGGTCCAGGAG
Pigr	GTGCCCGAAACTGGATCACC	TGGAGACCCCTGAAAAGACAGT
Ptgs2	CATCCCCTTCCTGCGAAGTT	CTCCTTATTTCCCTTCACACCCA
Raldh2	TAAGAGGCCGAGGCTGAAGAGCAC	TGGGGTTCATTGGAAGGCAGAAAG
Rps9	CTGGACGAGGGCAAGATGAAGC	TGACGTTGGCGGATGAGCACA
Tgfb	ACCGCAACAACGCCATCTAT	GTAACGCCAGGAATTGTTGC

4.2 Methods

4.2.1 Pneumococcal infections

Pneumococci were grown overnight on Columbia blood agar plates at 37°C and 5% CO_2, single colonies were resuspended and cultured in THY medium to mid-logarithmic phase (OD_{600nm} 0.3-0.5), washed, and diluted in PBS to the desired concentration. True CFU were determined by growing serial dilutions of the inoculums on blood agar plates. Bacterial suspensions were administered to mice via oropharyngeal aspiration. Mice were anesthetized by intraperitoneal injection of ketamine/xylazine and a total of 20-50µL of bacterial inoculum was continuously applied to the oropharynx and inhaled by the mouse.

For preparation of ethanol-killed pneumococcal extracts *S. pneumoniae* TIGR4 was grown to mid-logarithmic phase as described above. Serial inoculums of the bacterial suspension were plated to determine CFU. 2mL of bacterial suspension was spun down (17900xg, 3min, RT), the supernatant was removed, and the bacterial pellet was resuspended in ice-cold ethanol (70% v/v) and incubated at 4°C for 1h. The bacterial suspension was again spun down and the pellet was resuspended in 1mL sterile PBS/Glycerol solution (25% v/v). Plating

after ethanol-treatment was carried out to verify effective bacterial killing. Ethanol-killed bacterial suspensions were stored at -70°C. In order to assess the *in vivo* inflammatory response to pneumococcal ligands, mice were oropharyngeally administered with 20µL ethanol-killed bacterial suspension (equivalent to 10^6 CFU).

4.2.2 Determination of bacterial load

During the first 3 days following pneumococcal infection mice were monitored every day for the development of invasive pneumococcal disease. To this end, 5µL of peripheral blood was recovered by puncturing the tail vein with a sterile cannula (0.45mm diameter). To determine bacterial burden in the airways, the trachea was cannulated and bronchoalveolar lavage (BAL) was performed by flushing the lungs with 1mL ice-cold PBS. Typically a volume between 0.7 - 0.9mL could be retrieved. Lungs and trachea were aseptically removed, placed in sterile tubes with 1mL ice-cold PBS and mechanically homogenized using a Polytron PT 1300 D homogenizer (KINEMATICA AG, Luzern, Switzerland). Serial dilutions of tissue homogenates, BAL fluid (BALF) and blood were plated onto Columbia blood agar plates and bacterial inoculums were counted after 16-24h incubation at 37°C at 5% CO_2.

4.2.3 *In vivo* phagocytosis assay

S.pneumoniae TIGR4 was grown to mid-logarithmic phase as described before. 3mL of bacterial suspension was washed twice with PBS, again resuspended in PBS with 5µM Cell Proliferation Dye eFluor®670 (eBioscience) and incubated for 10min at 37°C in the dark. Staining reaction was stopped by adding PBS/1% BSA (w/v) and incubating another 5min on ice. Bacterial cells were washed three times with PBS/1% BSA (w/v) and resuspended in PBS. Serial dilutions of bacterial suspensions were performed to determine CFU. Mice were oropharyngeally administered with 0.5-1x10^7 CFU in 50µL, sacrificed 90min post administration and BAL was performed twice with a total volume of 1.5mL PBS. Obtained cells were erythrocyte-depleted by treatment with ACK buffer, Fcγ-receptors were blocked with anti-CD16/CD32, cells were stained with anti-F4-80 and phagocytosis was analyzed using FACS. Alveolar macrophages (AMs) were identified as F4-80^+, autofluorescence^{high} and side scatter^{high} cells. Relative phagocytic capacity of each sample was determined by calculating: median fluorescence intensity (MFI) of e670-positive AMs over the mean of all MFIs of e670-positive AMs of the control group (SPC-HA mice).

4.2.4 Isolation of mouse leukocytes

Mice were sacrificed by CO_2 inhalation or cervical dislocation. Bronchoalveolar lavage was performed by flushing the lungs with 1mL ice-cold PBS. Typically a volume between 0.7- 0.9 mL could be retrieved. Bronchoalveolar lavage fluid (BALF) was spun down (420xg, 10min, 4°C), BALF supernatants were removed and cell pellet was depleted of erythrocytes by treatment with hypotonic ACK buffer. Obtained cells were then further processed for *e.g.* RNA isolation or cytometric analyses.

For isolation of lung tissue leukocytes the thorax was opened, the lung was removed and thoroughly minced with scissors. Lung tissue pieces were then transferred into a 15mL tube containing 3mL pre-warmed digestion media, followed by enzymatic digestion at 37°C for 45min. To improve tissue disintegration, the lung digestion mix was sheared every 5min using a transfer pipette. After 30min of enzymatic digestion another 2mL digestion medium

were added to every tube. To stop enzymatic activity 5mM EDTA was added to the reaction mix, followed by incubation for another 5min. Lung cell suspension was passed through a 100µM cell strainer and washed with IMDM. Cells were pelleted by centrifugation (420xg, 15min, 4°C) and cells were erythrocyte-depleted by treatment with ACK buffer. Reaction was stopped by addition of FACS buffer, cells were again spun down and resuspended in 4mL IMDM. Lymphocytes were enriched by differential density-centrifugation, i.e. 4mL of lung cell suspension was carefully overlayed to 4mL Ficoll (Ficoll-Paque^{TM} Plus, GE Healthcare) and centrifuged (780xg, 20min, 20°C). Lymphocytes were harvested from the interphase, washed and FACS staining protocol was applied.

4.2.5 Flow cytometry

Antibody-stainings of murine single cell suspensions as well as pneumococcal cells were performed in 96-well microplates (U-shaped wells). Cell suspensions were prepared in FACS buffer (murine cells) and cells were pelleted by centrifugation (420xg, 10min, 4°C). For surface staining, cells were incubated with the indicated antibodies (diluted in FACS buffer, 100µL/well) for 10min at 4°C in the dark. Cells were then washed with FACS buffer (100µL/well), resuspended in 150-250µL FACS buffer and subsequently analyzed using either a Fortessa or LSRII FACS instrument (BD, New Jersey, USA).

4.2.6 *In vivo* antibiotics (ABX) treatment

For antibiotic *in vivo* treatment sucrose (2% w/v), ampicillin sodium salt (1.33 g/L, equivalent of 1.25 g/L ampicillin) and chloramphenicol (0.29g/L) were dissolved in autoclaved tap water. Solutions were then sterilized by filtration (0.22µM) and mice were supplied with ABX-water *ad libitum*. Control groups received sucrose-water. Drinking water was changed biweekly.

4.2.7 Depletion of alveolar macrophages

In order to deplete alveolar macrophages, mice were oropharyngeally administered 50µL clodronate liposomes (=250µg encapsulated clodronate, purchased from ClodLip BV, Amsterdam, The Netherlands). Control mice received 50µL sterile PBS or –where indicated- 50µL PBS Liposomes (ClodLip BV).

4.2.8 Isolation and purification of alveolar macrophages

BAL cells were erythrocyte-depleted and incubated in DMEM (Gibco, supplemented with 10% fetal bovine serum and antibiotics) for 90min at 37°C, 5% CO_2 in bacteriological plastic petri dishes. Non-adherent-cells were then removed by extensively rinsing the surface with PBS. To verify effective purification, adherent cells were detached by treatment with 0.05% Trypsin/EDTA (Gibco), stained with antibodies against F4-80 and CD11c and analyzed by flow cytometry. For RNA analysis, adherent cells were directly lysed on the plastic surface by treatment with RLT buffer (Qiagen, supplemented with 1% mercaptoethanol) and RNA extraction protocol was applied. RNA was extracted and purified using RNeasy Mini and RNase free DNase kit (both Qiagen) according to the manufacturer's instructions.

4.2.9 Pulse oximetry

Arterial blood oxygen saturation in untreated mice was monitored using the MouseOx system (Starr Life Sciences Corp., Oakmont, PA). Measurements were performed on non-anesthetized mice. Data from constant measuring periods (>30sec) were analyzed.

4.2.10 Enzyme-linked immunosorbent assay (ELISA)

ELISA kits for mouse IgA and IgM (eBioscience, Frankfurt am Main, Germany), mouse IL-6 and TNF-α (BioLegend, London, United Kingdom) and mouse Albumin (Bethyl Laboratories,Inc., Montgomery) were used according to the manufacturer's instructions and using recommended buffer formulations.

4.2.10.1 SIgA-ELISA

For SIgA-detection Nunc MaxiSorp plates were coated overnight with 100µL monoclonal rat anti-mouse IgA (SouthernBiotech, Birmingham, 2µg/mL, diluted in ELISA coating buffer). Plates were washed and blocked with 200µL/well ELISA assay diluent (1h, RT, shaking). Plates were washed again and incubated with 100µL of serial dilutions of BALF samples (2h, RT, shaking). Plates were washed again and incubated for 1h with 100µL secondary antibody solution (polyclonal goat anti-mouse pIgR; R&D Systems, Minneapolis, MN, 1µg/mL) followed by polyclonal donkey anti-goat-HRP for 30min (Jackson ImmunoResearch, West Grove, PA, 0.16µg/mL) and TMB substrate. Plates were read at 450 and 570nm. Due to the lack of a SIgA protein standard, relative quantification was performed. Results are expressed as the OD at 450nm (wavelength- and blank-corrected) at indicated dilutions.

4.2.11 Immunoblot

Lungs were mechanically homogenized in 5mL ice-cold RIPA lysis buffer. Cell debris was removed by centrifugation (15min, 5250xg, 4°C) and supernatants were stored at -70°C. Protein concentrations of the samples were measured using the BCA Protein Assay Kit (Life Technologies) according to the manufacturer's protocol. Equal amounts of protein were separated by SDS-PAGE (8%) in an electrophoresis chamber with SDS running buffer and subsequently transferred to a PVDF membrane using an electroblot chamber. Membrane was blocked with 5% (w/v) nonfat dry milk in TBS-T buffer for 1h and subsequently washed in TBS-T buffer. Target was identified using anti-pIgR antibody (0.2µg/mL) in TBS-T buffer with, reference protein was identified using anti-GAPDH (Cell Signaling Technology, Inc., Beverly, MA). For detection standard horseradish peroxidase conjugated polyclonal secondary antibodies were used together with ECL western blotting substrate (Life Technologies, Darmstadt, Germany).

4.2.12 Bacterial binding assay.

BAL was performed as described using 1mL PBS. Cells were separated by centrifugation (420xg, 10min, 4°C) and BALF supernatants were stored at -70°C. 96-well microplates were incubated with 1% (w/v) BSA/PBS. Freshly grown pneumococci were washed twice with blocking buffer, seeded into microwells (1-4x10^6 CFU) and incubated (45min, 4°C) with undiluted BAL supernatants. Bacteria were washed once with PBS and stained using anti-mouse IgA or anti-mouse IgM. Immunoglobulin binding was quantified by flow cytometry.

4.2.13 Sample Preparation for LC-MS/MS analysis

Proteins were purified by chloroform/methanol precipitation. Protein pellets from each sample were reduced with 10mM DTT, alkylated with 20mM jodoacetamide and digested with sequencing grade modified trypsin (Promega) as recommended in a ratio of 1:50 at 37°C overnight. The peptide solutions were vacuum-dried, and peptides were resolved in 0.2% TFA in water; desalted on self-packed LiChroprep RP-18 (Merck) SPE columns; eluted with 0.2% TFA, 60% ACN in water; and again vacuum-dried.

4.2.14 Mass spectrometry and data analysis

LC-MS/MS analyses of desalted samples were performed on an Acquity ultraperformance LC system (Waters Corp., Milford, MA) connected to a LTQ Orbitrap XL mass spectrometer (Thermo Finnigan Corp., San Jose, CA). Peptides were flushed onto a C18 precolumn (5µm Symmetry C18, 180µm × 20mm, Waters Corp.) with a flow rate of 15µL/min and washed at constant flow for 3min. Peptides were separated on an analytical column (1.7µm BEH130, 75µm × 150mm, Waters Corp.) with UPLC buffer A (0.1% formic acid in water) and UPLC buffer B (0.1% formic acid in acetonitrile) via linear 120min gradients at a flow rate of 300 nL/min controlled with Acquity UPLC software V1.22. Eluting peptides were ionized using PicoTip emitter needles (New Objective Inc., Woburn, MA), voltages of 1.7kV and a capillary temperature of 200°C. Data-dependent acquisition of MS and MS/MS data was under control of XCalibur software V2.1 (Thermo Finnigan). Survey Scans were acquired in the Orbitrap mass analyzer with a resolution of 60.000 at m/z 400. For full scans 5x10^5 ions were accumulated within a maximum injection time of 500ms and detected in the Orbitrap analyzer. Sequential isolation of the five most intense ions with charge states ≥ 2 was set to a target value of 5x10^4 (signal threshold: 2x10^4, isolation width: 4.0Da) with a maximum injection time of 500ms. CID mode was used for detection of produced fragment ions. Database searches were performed using Proteome Discoverer (1.4; Thermofisher) connected to a Mascot Server (2.4.06) in the UniProtKB/Swiss-Prot database (2015_01 taxonomy, Mus musculus with 16,702 sequences). Proteins were accepted as identified when at least one unique, search engine rank 1 and high confident peptide showed an individual score above 30, which indicates identity or extensive homology ($p < 0.05$) based on the search parameter settings used (enzyme, trypsin; maximum missed cleavages, 1; fixed modification: methylthio (Cys; variable modifications, phosphorylation (Ser, Thr, Tyr) and oxidation (Met); peptide tolerance, 10ppm; MS/MS tolerance, 0.4Da). Sample preparation and mass spectrometry acquisition was performed by Josef Wissing (HZI).

4.2.15 Microarray

RNA from whole lung tissue was isolated and purified using RNeasy Midi and RNase free DNase kit (both Qiagen, Hilden, Germany). Samples were amplified, labeled, fragmented and hybridized to GeneChip® Mouse Gene 1.0 ST arrays (Affymetrix) and treated according to manufacturer's instructions. Microarray scanning was performed using an Affymetrix GCS 3000 scanner and GCOSv1.1 software. Data analyses were conducted using GeneSpring GX software (Agilent technologies). The data were summarized, $\log_2$ transformed and normalized with the Robust Multi-array Analysis (RMA) algorithm. Cluster analyses were performed with Genesis software 1.7.6, applying a z-score transformation. Gene-ontology analyses were performed using Cytoscape software 3.2.0 and ClueGo plugin. Microarray data are deposited at Gene Expression Omnibus (http://www.ncbi.nlm.nih.gov/geo/) under accession ID: GSE66531.

4.2.16 Quantitative real-time RT-PCR

RNA from whole lung homogenates was transcribed into cDNA using M-MLV RT polymerase (Invitrogen, Carlsbad, CA) according to the manufacturer's instructions. Quantitative PCR (qPCR) was conducted using the LightCycler 480 SYBR Green I Mastermix and LightCycler 480 instrument (both Roche, Mannheim, Germany). Transcript levels were normalized to the housekeeping gene *Rps9*. For gene expression analyses of alveolar macrophages and alveolar epithelial cells, RNA was isolated and purified using RNeasy Mini and RNase free DNase kit (both Qiagen). RNA was analyzed using the SensiFAST™ SYBR® No-ROX One-Step Kit (Bioline, Luckenwalde, Germany) according to the manufacturer's instructions. Transcript levels were normalized to the housekeeping gene *Actb*.

4.2.17 Histology

For histopathological evaluation lungs were perfused with 10mL PBS, fixed in 4% paraformaldehyde and embedded in paraffin. 4µM sections were stained with hematoxylin & eosin. Histology was performed by Prof. Achim D. Gruber and Dr. Olivia Kershaw (Department of Veterinary Pathology, Freie Universität Berlin). For pIgR-localization perfused lungs were frozen in Tissue-Tek O.C.T. (Sakura Finetek GmbH, Staufen, Germany). 6µm acetone-fixed cryosections were blocked with anti-CD16/CD32, incubated with goat anti-pIgR primary antibody, blocked with 5% (v/v) donkey serum and incubated with FITC-conjugated donkey anti-goat secondary antibody (Jackson ImmunoResearch). Alveoli were identified by DAPI nuclear counterstain. Fixed tissue sections were analyzed by fluorescence microscopy, using the inverted Eclipse Ti-U, NIS-Elements imaging software (Nikon, Tokyo, Japan) and ImageJ software.

4.2.18 Imaging flow cytometry

Samples were analyzed with the imaging flow cytometer FlowSight® (Amnis®, part of EMD Millipore). The 405nm, 488nm, 642nm, 785nm lasers were used for excitation. Debris and doublets were gated out. Channel 1 (435 - 505nm), Channel 6 (SSC, 745 - 800nm) Channel 3 (560 - 595nm), Channel 5 (642 - 745nm), Channel 7 (435 - 505nm), Channel 11 (642 - 745nm) were measured and at least 10,000 events of single cells per sample were collected. Color compensation was necessary due to overlapping emission spectra. For analysis the IDEAS version 6.0 was used. Gating strategy was the following: First, focused single cells are identified (using 'gradient root mean square' of the bright field image then bright field area and aspect ratio, respectively). Alveolar macrophages were identified as F4-80$^+$ and CD11c$^+$. To exclude T cells from morphological analyses in imaging flow cytometry, cell suspensions were additionally stained with antibody against CD3. Alveolar macrophages were analyzed by applying the image-based features intensity, area, and bright detail intensity on the SSC-channel.

4.2.19 Panoptic staining: Pappenheim method

For analyses of alveolar macrophage phenotype, bronchoalveolar lavage cells from naive SPC-HA and SPC-HAxTCR-HA mice were isolated and erythrocyte-depleted by treatment with ACK buffer. Cells were spun (800rpm, 15min, RT) onto SuperFrost® glass slides (Thermo Scientific, Schwerte, Germany), air-dried and stained with May-Grünwald-reagent (Merck, Darmstadt, Germany). After 3min neutral water pH 7.2 was added and stained for 1min. Staining solution was removed and cells were stained with Giemsa-reagent (Merck, 1:10 diluted in ddH_2O) for 15min. Slides were then washed, air-dried and samples were covered with Neo-Mount (Merck) reagent and sealed by glass cover slips. Images were captured at 63x oil immersion objective using an Axio Imager Z2 microscope equipped with AxioCam MRc5 and ZEN software (both Carl Zeiss Microscopy GmbH).

4.2.20 Fluorescence-activated cell sorting of ATII cells

Isolation and purification of murine ATII cells was performed using a previously described protocol which had been established in our lab. Mice were euthanized by CO_2 inhalation and lungs were perfused as described above. 2mL dispase (37°C) followed by 0.5mL 1% low-melt agarose (45° C) was intratracheally instilled into the lungs via an indwelling canula. In order to solidify the agarose, lungs were covered with a paper towel and ice for 2min. Whole lungs were then excised, heart and thymus were removed. Lungs were digested for 45min in 2mL of pre-warmed (37°C) dispase, minced in 7mL DMEM (supplemented with 100µL DNase and anti-CD16/32 antibody) and incubated for 10min at RT. Lung cell suspensions were filtered through 100µm, 48µm and 30µm nylon gauze and spun down (15min, 900rpm, 4°C). Following erythrocyte-depletion by ACK buffer, cells were stained with fluorescence-labelled antibodies against F4-80, CD11c, CD45, CD11b and CD19, followed by a secondary staining step with PE-labelled goat anti-rat IgG. FACS was performed by Lothar Gröbe (HZI) using BD FACSAria and Beckman Coulter MoFlo cell sorters. ATII cells were sorted by negative selection as depicted in Figure 11.

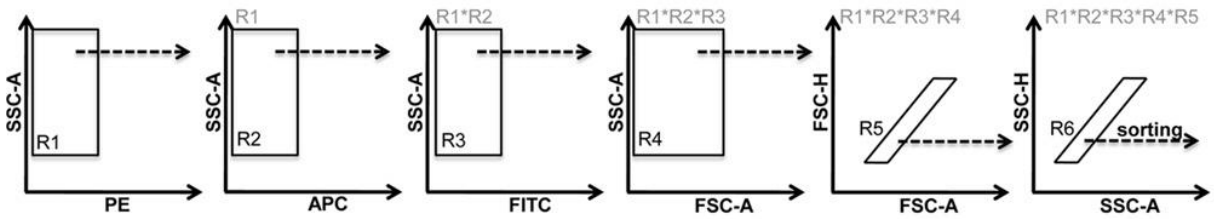

Figure 11: Gating strategy for isolation of murine ATII cells from lung cell suspensions using FACS. Lineage-positive (PE, APC and FITC-positive) cells were excluded by negative selection (R1-R3). Granular (SSC^{high}), single cells were selected and sorted (R4-R6). Adapted from Gereke et al. 2012.

4.2.21 Statistical analyses

Statistical evaluation was performed using Graph Pad Prism Software (Graph Pad Software, La Jolla). Unpaired, two-tailed Mann-Whitney-test was chosen to compare two groups, if not otherwise stated. For comparison of multiple groups one-way or two-way ANOVA followed by Bonferroni post-test was applied.

5 Results

5.1 Impact of chronic lung inflammation on pulmonary immunity to respiratory pneumococcal infection

5.1.1 Airway pathology and increased lung permeability in SPC-HAxTCR-HA mice

It is well-known that chronic respiratory diseases (CRDs) alter host immunity towards airborne pathogens in humans and mice. However, the underlying immunological mechanisms are incompletely understood. The first part of this thesis aimed to elucidate factors of CRD involved in altered antimicrobial immunity towards respiratory infection. To this end SPC-HAxTCR-HA transgenic mice that intrinsically develop autoimmune-mediated inflammation were utilized in an infection model with the common respiratory pathogen *Streptococcus pneumoniae*.

In order to initially characterize the extent of chronic, autoimmune-mediated pulmonary inflammation histopathological as well as functional examinations of lungs from healthy SPC-HA control mice and pre-diseased SPC-HAxTCR-HA mice were conducted. In line with previous observations (Bruder, Westendorf et al. 2004) lung histology of the SPC-HAxTCR-HA mice showed peribronchiolar and perivascular lymphocytic cuffings, hemosiderosis and alveolar emphysema (Figure 12a). These histopathological findings mirror the lymphocyte-driven disease etiology in SPC-HAxTCR-HA mice, suggesting lymphocyte recruitment and/or local proliferation within the lung parenchyma. The presence of hemosiderosis furthermore indicates pulmonary hemorrhage, i.e. the leak of blood components into the airspaces, finally leading to hemosiderin-laden airway macrophages in SPC-HAxTCR-HA mice. Moreover, the finding of emphysema demonstrates airway remodeling, possibly impairing effective ventilation in SPC-HAxTCR-HA mice. In order, to test whether the observed structural alterations in SPC-HAxTCR-HA mice would manifest in reduced physiological organ function and thus insufficient oxygen supply in this group, pulse oximetry analyses were performed. These however revealed similar arterial blood oxygen saturation levels in SPC-HA and SPC-HAxTCR-HA mice (Figure 12b), indicating an unaffected respiratory capacity and thus excluding severe injury of the respiratory epithelium in this group.

As the presence of hemosiderosis suggested a decreased mucosal barrier function in SPC-HAxTCR-HA lungs, the extent of pulmonary leakage was tested. To this end, serum albumin levels in bronchoalveolar lavage fluid (BALF) were determined by ELISA. Albumin usually is a serum component, which upon injury and/or activation of pulmonary capillaries and epithelial cells can passively diffuse into the airspaces, and BALF albumin levels are typically used as readout for pulmonary injury. Indeed, BALF from SPC-HAxTCR-HA mice contained about 35.6% more serum albumin compared to SPC-HA control samples (Figure 12c), indicating an increased pulmonary leak in SPC-HAxTCR-HA mice while at the same time linking chronic lung inflammation to impaired epithelial and/or endothelial barrier function.

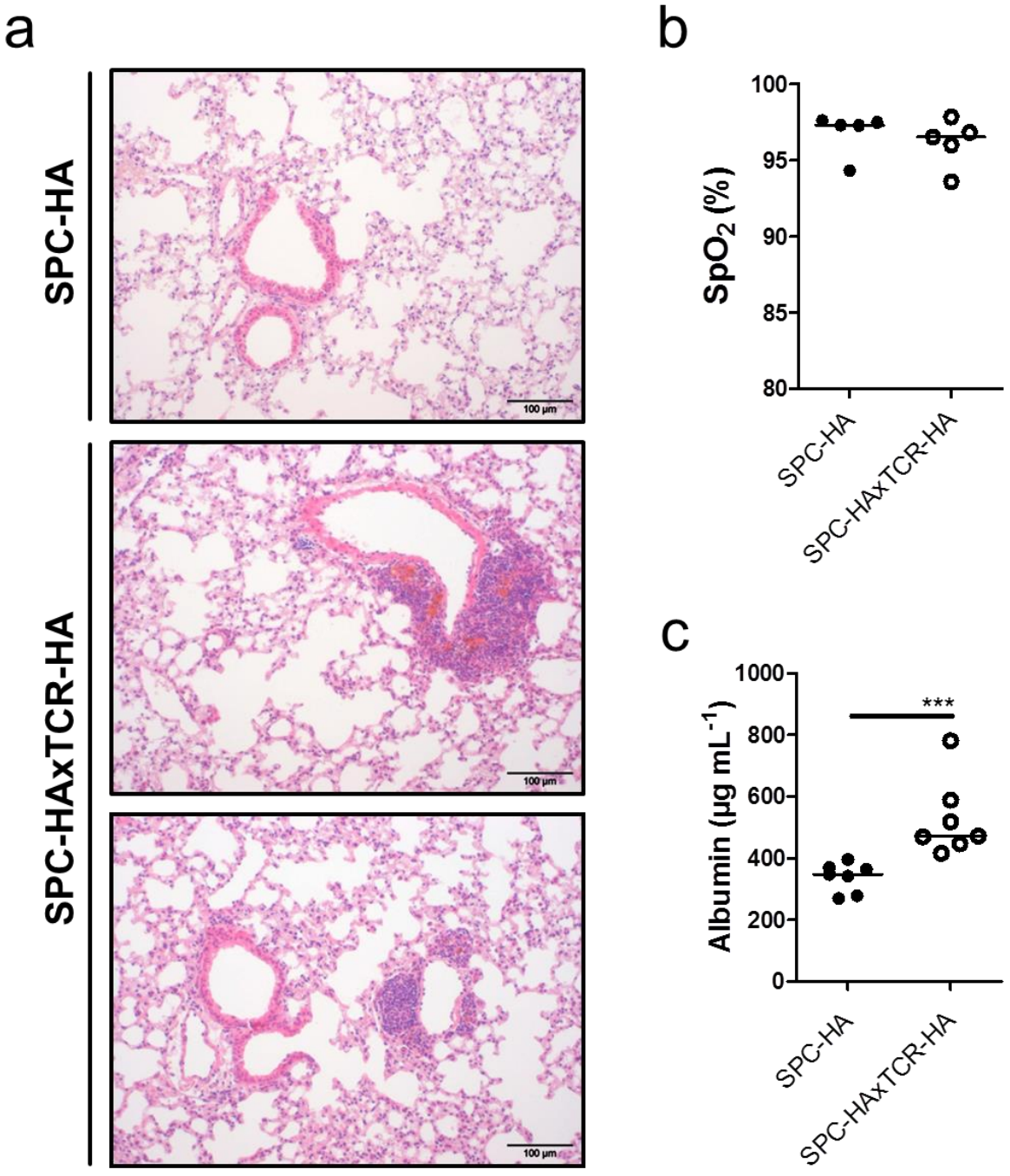

Figure 12: Lung pathology in a model of chronic autoimmune-mediated lung inflammation.
(a) Hematoxylin and eosin stained lung tissue sections of SPC-HA and SPC-HAxTCR-HA mice (representative of n=3/group; scale bar =100µm) **(b)** Blood oxygen saturation (SpO_2) **(c)** Albumin concentration in bronchoalveolar lavage fluid (BALF) ***p<0.001 Black scale bars: 100µm, magnification: 10x

5.1.2 SPC-HAxTCR-HA mice display enhanced immunity to respiratory infection with *Streptococcus pneumoniae*

In numerous infectious (Habibzay et al. 2013) and non-infectious (Sethi, Wrona et al. 2008, Talbot et al. 2005) etiologies, lung inflammation correlates with an increased susceptibility to infections and lung permeability enhances bacterial tissue penetration (LeMessurier et al. 2013). In order to determine how the above described chronic airway inflammation would affect the efficacy of local antibacterial mechanisms an encapsulated serotype 4 strain (TIGR4) of *Streptococcus pneumoniae* was chosen for infection experiments in healthy SPC-HA control mice and pre-diseased SPC-HAxTCR-HA mice. In this model, death from infection is typically preceded by pneumococcal invasion into pulmonary tissue and the subsequent development of bacteremia. As lungs of SPC-HAxTCR-HA mice displayed increased permeability, it seemed likely to detect enhanced pneumococcal invasion in these mice. To test this, SPC-HA and SPC-HAxTCR-HA mice were oropharyngeally inoculated with *S.pneumoniae* and the number of pneumococci residing in the airways (BALF) and the lung tissue at 4h and 24h following infection was determined. To exclude contaminations with bloodstream-derived pneumococci a sub-lethal infection dose ($1.5x10^4$ CFU), which typically does not cause bacteremia within 24h, was chosen.

Already at 4h post infection BALF of SPC-HAxTCR-HA mice contained significantly decreased bacterial numbers compared to SPC-HA control mice. At 24h no pneumococci were detectable in nearly 50% of the SPC-HAxTCR-HA BALF samples (compared to only 25% of SPC-HA samples). Furthermore, the median bacterial burden in the BALF did not increase over the first 24h following infection in SPC-HAxTCR-HA mice whereas there was an almost 9-fold increase in SPC-HA mice at this time point (Figure 13a). Consistent with reduced CFU in BALF, reduced proportions of lungs were invaded by *S.pneumoniae* in SPC-HAxTCR-HA mice at 4h (25% vs. 87.5%) and 24h after pneumococcal infection (22.2 % vs. 62.5%; Figure 13b).

In order to assess whether the observed reduction in the early bacterial burden would affect the ultimate outcome of infection, survival following inoculation with a lethal pneumococcal dose ($1.5x10^6$ CFU) was monitored. Here 60% mortality within 3 days in SPC-HA mice was observed compared to only 27% mortality in SPC-HAxTCR-HA mice. Seven days post infection, all infected SPC-HA mice had succumbed whereas 20% of the SPC-HAxTCR-HA mice survived (Figure 13b). These data indicate that endogenous pulmonary inflammation as displayed by SPC-HAxTCR-HA mice gives rise to a milieu that improves early innate resistance mechanisms towards respiratory *S. pneumoniae* infection leading to a significant advantage in pathogen clearance and survival and thus surprisingly contradicts the initial expectation of enhanced bacteremia as a consequence of the increased pulmonary leak as observed in Figure 12c.

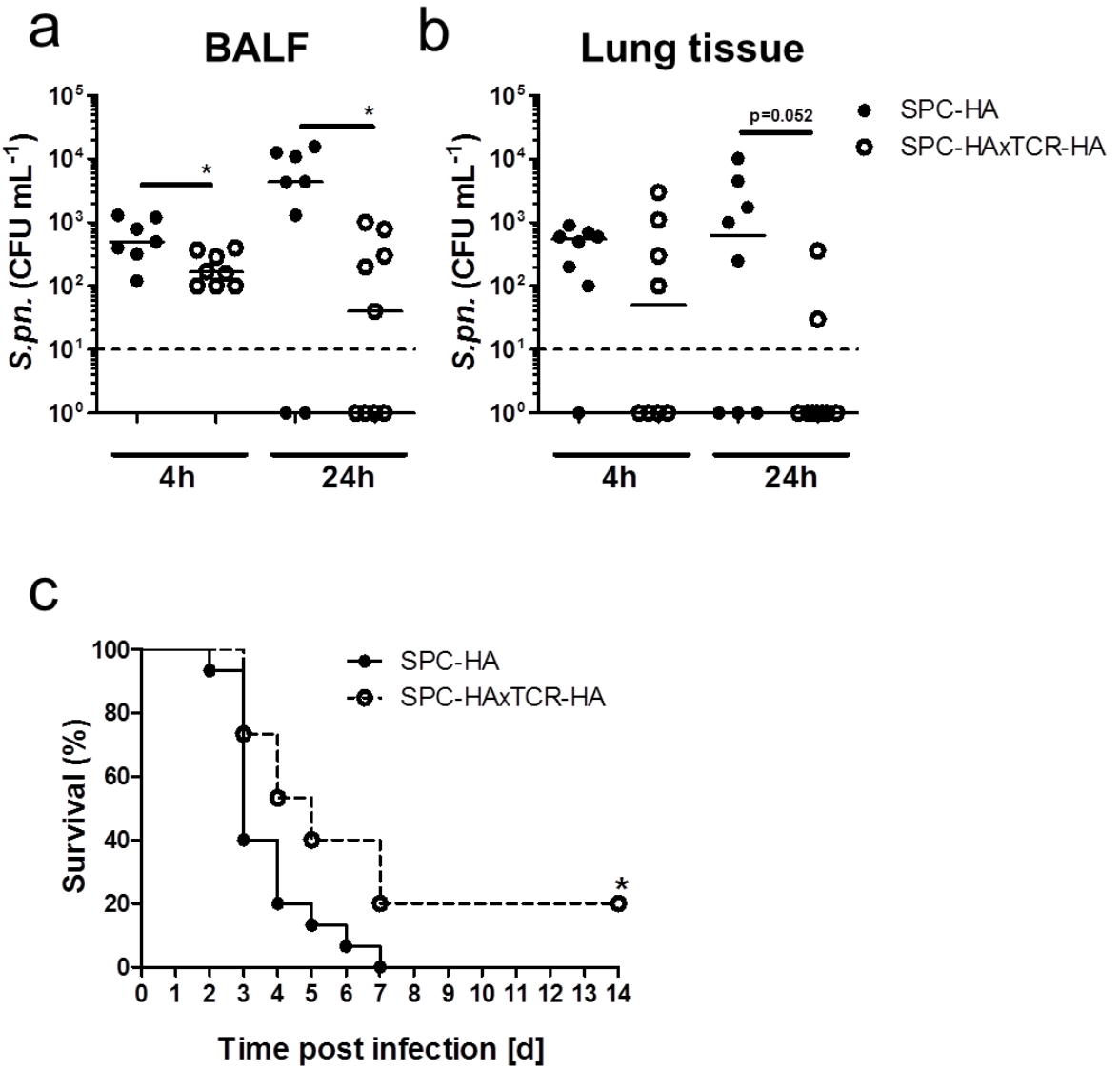

Figure 13: Improved antipneumococcal resistance of SPC-HAxTCR-HA mice.
Mice were oropharyngeally inoculated with ~1.5x10^4 CFU *S.pneumoniae* TIGR4 and were sacrificed at the indicated time points. The bacterial burden in **(a)** bronchoalveolar lavage fluid (BALF) and **(b)** lung tissue homogenates was determined. Data are shown for individual animals pooled from 2 independent experiments. Dashed lines indicate the detection limit. *p<0.05. **(c)** Mice were oropharyngeally inoculated with ~1.5x10^6 CFU *S.pneumoniae* TIGR4 and survival was followed over a period of 14 days. Statistical significance was determined using the Log-rank test, *p<0.05 (n=15/group, 2 independent experiments)

5.1.3 Similar phagocytic capacity of SPC-HA *vs.* SPC-HAxTCR-HA-derived alveolar macrophages

Alveolar macrophages (AMs) have pleiotropic protective functions during pulmonary infection including early phagocytic uptake and killing of airborne pathogens. Given the finding of significantly decreased airway CFU counts already 4h after pneumococcal infection it seemed likely that enhanced macrophage phagocytosis could be a mechanism involved in the improved disease outcome in SPC-HAxTCR-HA mice. To test this hypothesis, mice were oropharyngeally inoculated with fluorescently labelled pneumococci and bacterial uptake by AMs was quantified at 90min post infection by flow cytometric analyses. Macrophages were

identified as F4-80^{+}SSC^{high}autofluorescence^{high} cells. However, no significant differences became apparent between SPC-HA and SPC-HAxTCR-HA mice regarding the proportions of AMs that had taken up pneumococci as well as the individual phagocytic capacity (Figure 14a,b). To rule out the possibility that different AM numbers and hence an altered a priori pathogen/phagocyte ratio would mask potential differences in phagocytosis, absolute macrophage numbers in BALF of in SPC-HA and SPC-HAxTCR-HA mice were determined. Again, no significant differences between both mouse groups were observed (Figure 14c). Likewise, BALF neutrophil numbers were similar between non-infected SPC-HA and SPC-HAxTCR-HA mice and these phagocytes were virtually absent in both groups (data not shown). Therefore the amended disease outcome in SPC-HAxTCR-HA mice was probably not a consequence of enhanced early phagocytic bacterial uptake.

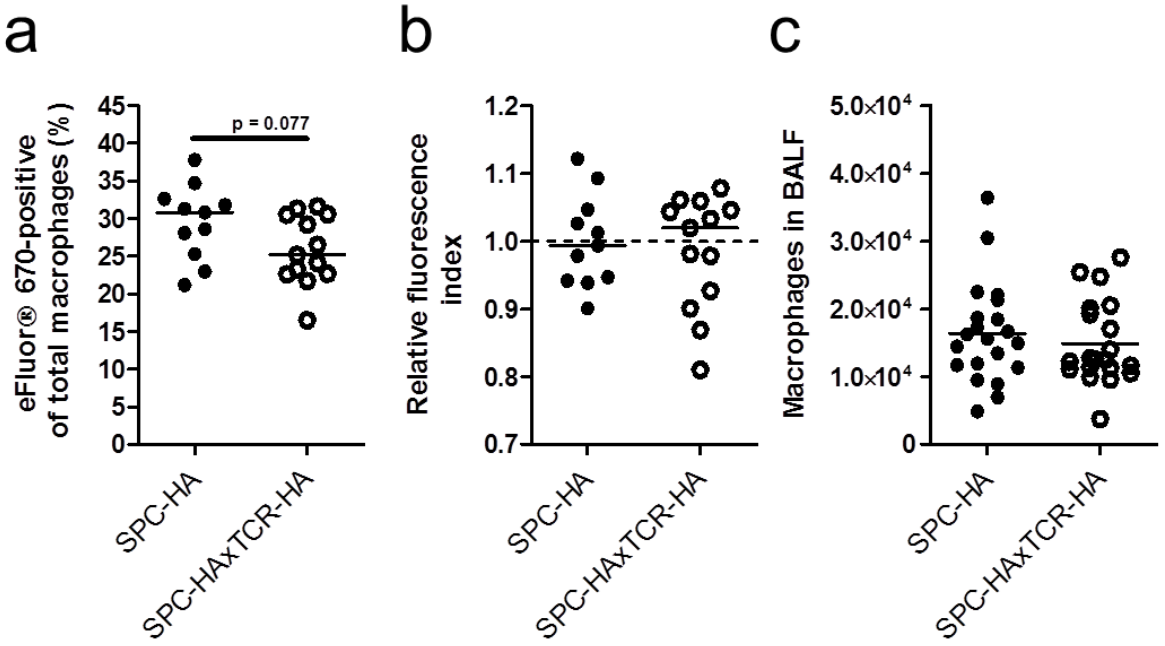

Figure 14: Similar phagocytic activity of SPC-HA and SPC-HAxTCR-HA alveolar macrophages.
Mice were oropharyngeally inoculated with ~5x10^{6} CFU eFluor®670-stained *S.pneumoniae* TIGR4. Bronchoalveolar lavage cells were isolated 90min post infection and analyzed by flow cytometry to **(a)** quantify the portion of eFluor®670^{+} alveolar macrophages out of all recovered alveolar macrophages. **(b)** The relative fluorescence index of eFluor®670^{+} macrophages of each mouse was determined as the ratio of the median fluorescence intensity (MFI) of eFluor®670+ macrophages over the mean MFI of the SPC-HA control group samples. **(c)** Absolute macrophage numbers in BALF were determined by cell counting and flow cytometric analyses. Data are pooled from at least 2 independent experiments with similar results.

5.1.4 Chronic lung inflammation in SPC-HAxTCR-HA mice does not involve an IL-6 / TNF-α cytokine milieu

Based on the previous findings of improved antipneumococcal immunity in the SPC-HAxTCR-HA group it became obvious that inflammatory priming favors the generation of a protective environment in these mice. In several studies respiratory priming with PAMP-receptor agonists was linked to improved immunity to secondary infection with airborne pathogens (Errea et al. 2010, Evans et al. 2010, Tritto et al. 2007, Tuvim et al. 2009). In these reports protective immune stimulation involved among others the induction of local as well as systemic IL-6 and TNF-α cytokine responses. In order to test a possible role of these

pro-inflammatory mediators in the SPC-HAxTCR-HA mouse model, BALF and serum samples from uninfected SPC-HA and SPC-HAxTCR-HA mice were analyzed by ELISA. However, no significant differences in the local (BALF) and systemic (serum) cytokine milieu were found - both TNF-α as well as IL-6 were almost not detectable in the two mouse groups and compartments (Figure 15). This suggested other immunological mechanisms to be involved in the generation of the protective microenvironment of SPC-HAxTCR-HA lungs.

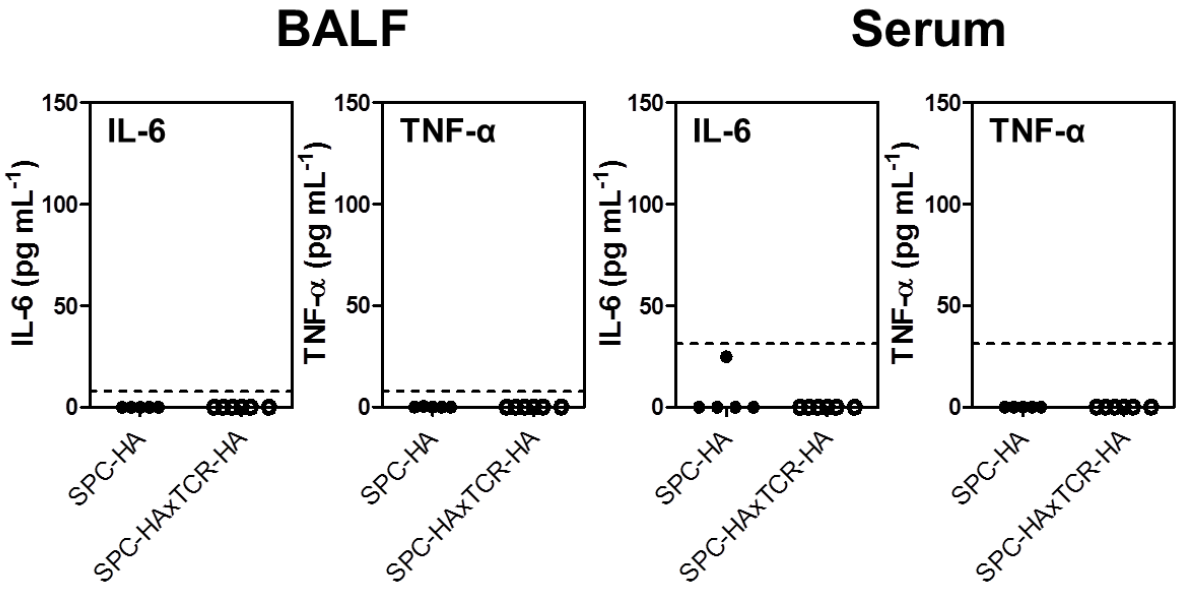

Figure 15: Chronic pulmonary inflammation is not associated with increased local nor systemic IL-6 and TNF-α levels.
Bronchoalveolar lavage fluid (BALF) and serum samples from uninfected SPC-HA and SPC-HAxTCR-HA mice (n=5-6/group) were analyzed by ELISA. Dashed line indicates limit of detection.

5.1.5 Transcriptional signature in SPC-HAxTCR-HA lungs points to an induction of humoral immunity

To identify molecular mechanisms possibly contributing to the improved antipneumococcal resistance in the inflamed lung genome-wide comparative transcriptome analyses of lung tissue from naive SPC-HA and SPC-HAxTCR-HA mice were performed using triplicate microarray analysis. Based on the comparison of the mean signal intensities of the microarray triplicates from SPC-HAxTCR-HA vs. SPC-HA lung samples and applying a fold change threshold of ± 2 a total of 378 transcripts were found to be differentially expressed in SPC-HAxTCR-HA lungs, of which 326 were up-regulated and 52 down-regulated (Figure 16).

For better visualization the individual normalized $\log_2$ transformed signal intensities of the 378 differentially expressed transcripts were z-score transformed and hierarchically clustered using a k-means cluster algorithm resulting in 5 different clusters containing 200, 25, 38, 63 and 52 transcripts, respectively (Figure 16a). Clusters 1, 2, 3 and 4 contain transcripts which are up-regulated (fold change ≥ 2) and cluster 5 contains transcripts which are down-regulated (fold change ≤ -2) in SPC-HAxTCR-HA vs. SPC-HA lungs. Annotated transcripts from cluster 1-5 are indicated in Figure 17 and Figure 18a-d, respectively. Table 5 shows the top20 up-regulated genes and their respective fold changes.

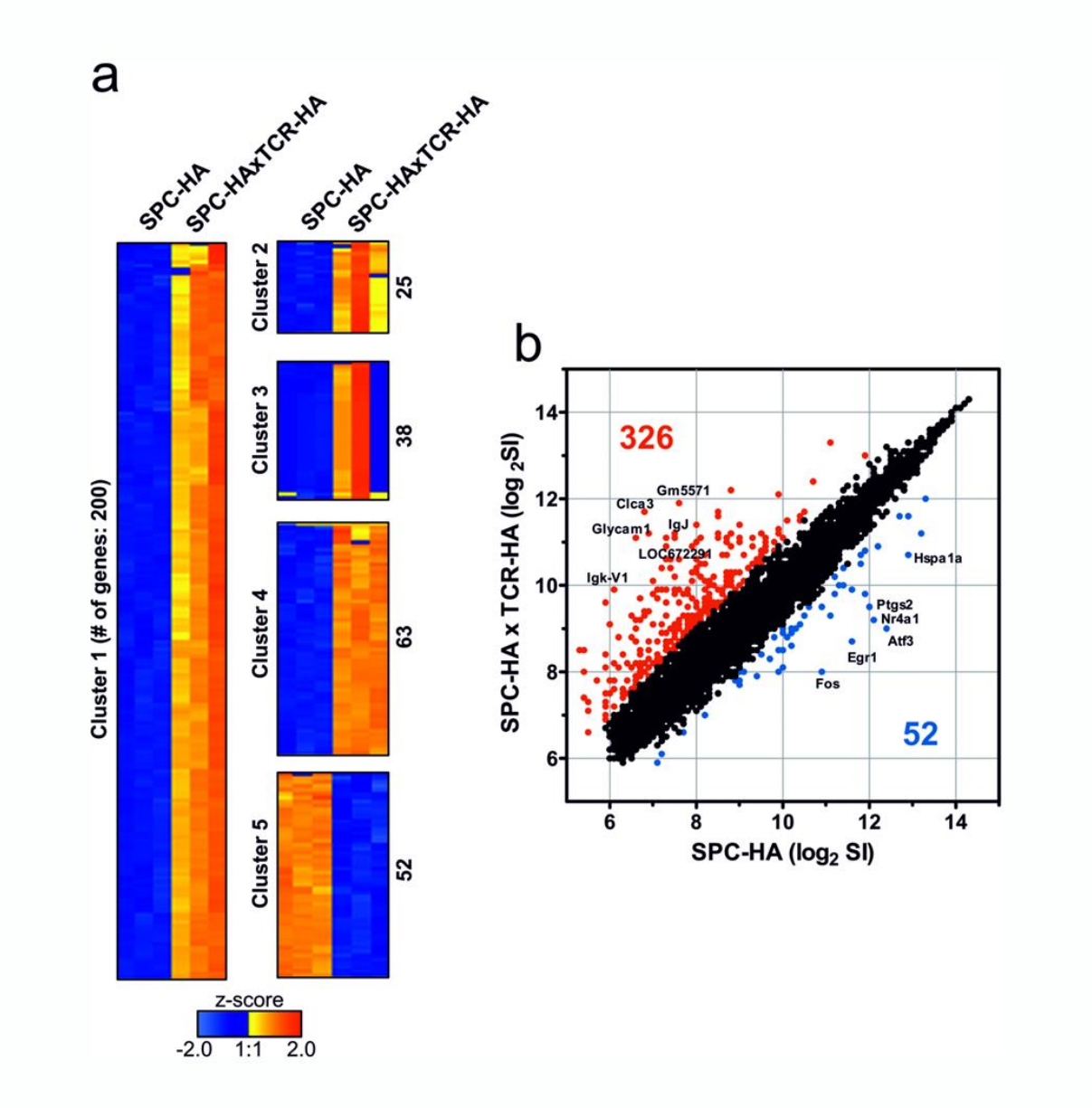

Figure 16: Transcriptional profile of whole lung tissue from SPC-HA vs. SPC-HAxTCR-HA mice.
RNA from lung tissue of SPC-HA and SPC-HAxTCR-HA mice (n=3/group) was isolated and samples were analyzed on whole transcriptome microarrays. **(a)** Expression data of 378 regulated transcripts in SPC-HA and SPC-HAxTCR-mice were clustered according to expression profile similarities (k-means clustering followed by hierarchical clustering of transcripts within clusters). Color code represents z-score; red=transcript induction, blue=transcript repression. **(b)** Scatter plot of all normalized $\log_2$ transformed signal intensities (SI). Red dots represent transcripts with a fold change ≥ 2 (up-regulated); blue dots represent transcripts with a fold change ≤ -2 (down-regulated). Black dots represent transcripts not considered regulated (fold change between -2 and 2). Gene symbols of the top6 up-/down-regulated genes are indicated as well.

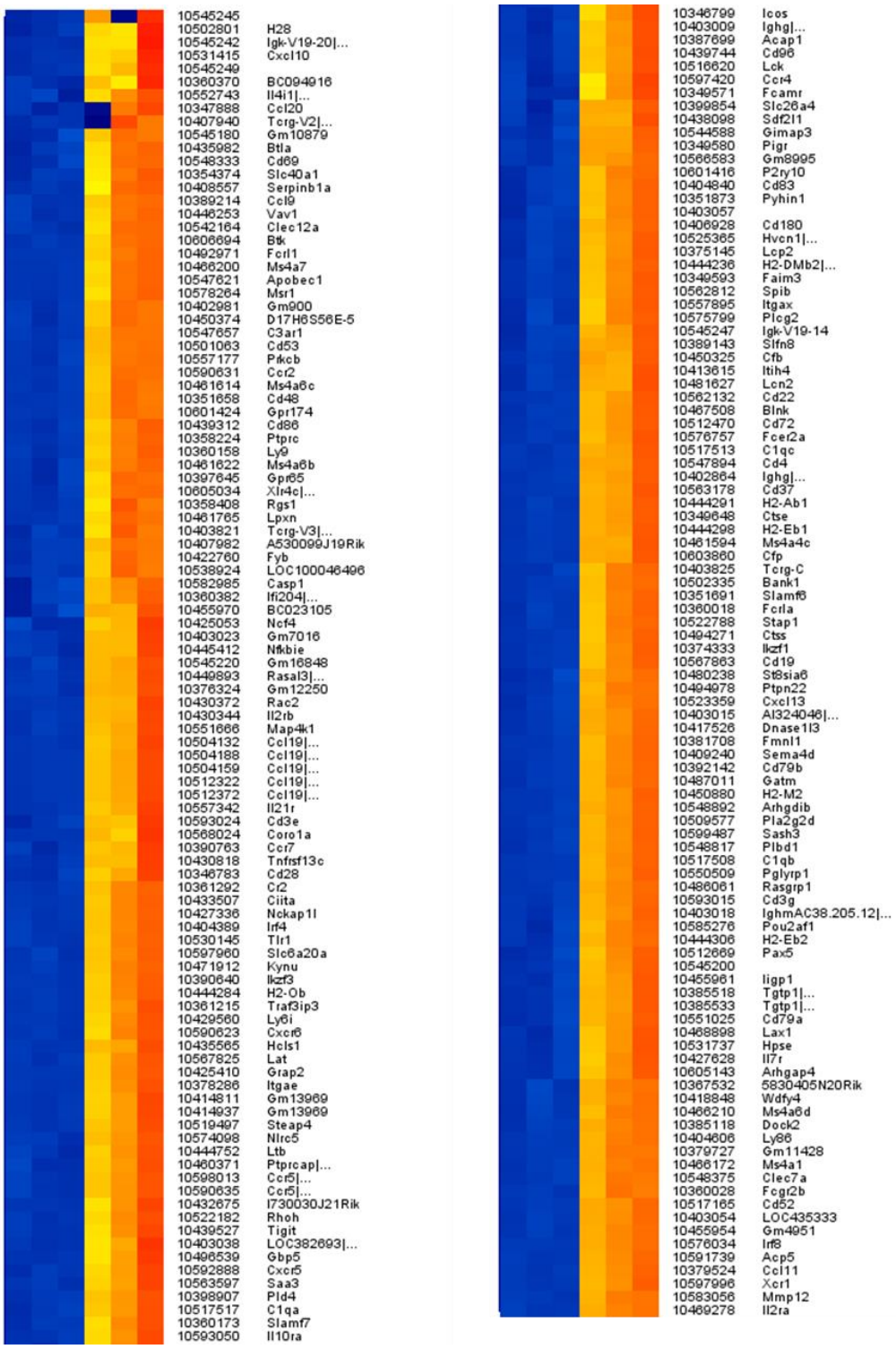

Figure 17: Expression data of genes in k-means cluster 1 (see Figure 16a).

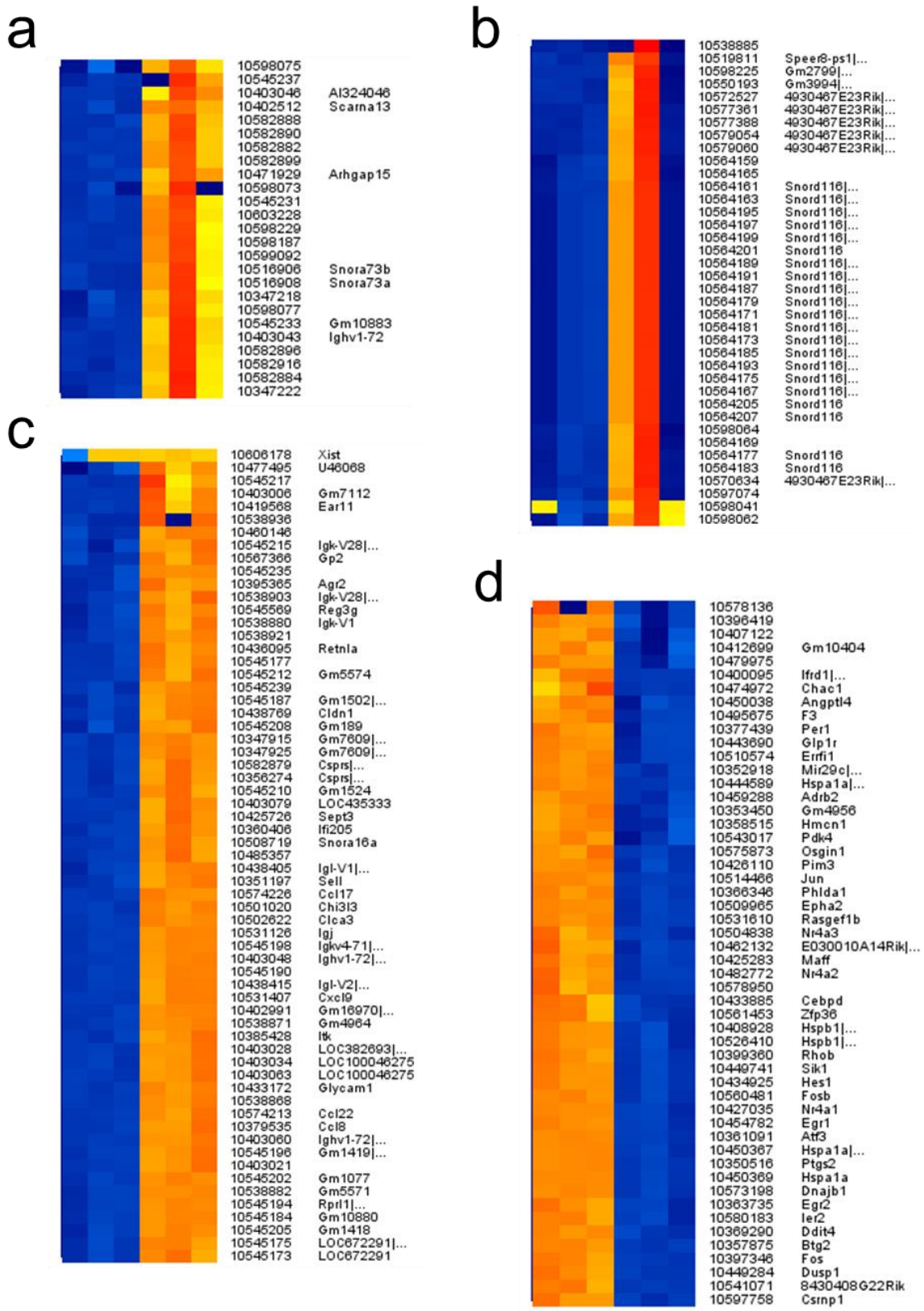

Figure 18: Expression data of genes in k-means cluster 2 (a), 3 (b), 4 (c) and 5(d); (see Figure 16a).

The differential expression of chosen candidate transcripts (Clca3, Glycam1, Igj, Cxcl9) was confirmed by qRT-PCR (Figure 19). The microarray analyses revealed Clca3 (FC Array 29.4, FC qRT-PCR 262.8), encoding for an epithelial chloride channel protein associated with mucus production in respiratory epithelial cells to be most up-regulated gene (Figure 19, Table 5). In a murine asthma model Clca3 was associated with goblet cell metaplasia and is discussed to be a probable target for intervention of hypersecretory lung diseases (Nakanishi et al. 2001). Moreover, Glycam1 (FC Array 23.1, FC qRT-PCR 194.8), encoding for an addressin found in high endothelial venules, was found to be highly up-regulated in SPC-HAxTCR-HA lungs (Figure 19, Table 5). The Cxcl9 transcript (FC Array 12, FC qRT-PCR 69.6, Figure 19, Table 5) encodes for the T cell-attracting chemokine CXCL9. CXCL9, which is also known as *monokine induced by gamma interferon* (MIG), is induced as a response to IFN-γ. Increased levels of CXCL9 were found in induced sputum from patients with COPD (Costa et al. 2008) and this cytokine is discussed to potentially perpetuate COPD by attracting Th1 and Tc1 cells into the lung which in turn are a major source of CXCL9-inducing IFN-γ (Barnes 2008). Also the eosinophil-associated RNase (Ear) 11 was found to be induced (FC Array 8.6, Table 5). Ear11 is expressed as response to Th2 cytokines, IL-33 stimulation and after bacterial priming of the respiratory mucosa. This RNase also possesses chemotactic activity for tissue macrophages (Yamada et al. 2015).

Table 5: List of top20 most up-regulated transcripts in SPC-HAxTCR-HA lungs.
Data represent mean ± SD of log_2 normalized signal intensities (SI) of triplicate microarray analyses. Expressional fold change (FC) in SPC-HAxTCR-HA lung samples was calculated in reference to the SPC-HA lung samples.

Annotation	Description	SPC-HA [log2 SI ±SD]	SPC-HAxTCR-HA [log2 SI ±SD]	FC
Clca3	calcium-activated chloride channel, expressed in mucus-producing cells	6,8 ± 0,2	11,7 ± 0,2	29,4
Glycam1	ligand for L-selectin, expressed in high endothelial venules	6,6 ± 0,2	11,1 ± 0,3	23,1
Gm5571	immunoglobulin kappa chain variable 9-120	7,6 ± 0,5	11,9 ± 0,1	19,3
Igk-V1	immunoglobulin kappa chain variable 1	6,1 ± 0,6	9,9 ± 0,6	14,2
LOC672291	similar to Ig kappa chain V-V region MOPC 173	7,3 ± 0,5	11,1 ± 0,5	14,2
Igj	immunoglobulin joining chain	7,5 ± 0,2	11,2 ± 0,2	13,6
Cxcl9	chemokine, induced by interferon-gamma	7,3 ± 0,1	10,9 ± 0,4	12
LOC672291|Igk-J1	similar to Ig kappa chain V-V region MOPC 173|immunoglobulin kappa joining 1	7,5 ± 0,5	11,1 ± 0,3	11,8
Igk-V19-14	immunoglobulin kappa variable 6-14	7,5 ± 0,4	11,1 ± 0,8	11,6
Gm4964	immunoglobulin kappa variable 1-135	7,3 ± 0,2	10,6 ± 0,1	9,6
Gm1502|Gm8760|Igkv4-71	immunoglobulin kappa chain variable 4-70| immunoglobulin kappa variable 4-59| immunoglobulin kappa chain variable 4-71	7,4 ± 0,4	10,6 ± 0,3	9,4
LOC100046496	similar to Ig kappa V-region 24B	7,2 ± 0,2	10,4 ± 0,8	8,8
Igl-V1|Igl-V2|LOC433053	immunoglobulin lambda chain, variable 1|immunoglobulin lambda chain, variable 2|similar to Ig lambda-1 chain C region	8,5 ± 0,5	11,7 ± 0,3	8,7
Ear11	eosinophil-associated, ribonuclease A family, member 11	6,0 ± 0,1	9,1 ± 0,8	8,6
Igkv4-71|Gm8760|Gm1499	immunoglobulin kappa chain variable 4-71|immunoglobulin kappa variable 4-59|immunoglobulin kappa chain variable 4-72	8,5 ± 0,2	11,6 ± 0,1	8,6
Dnase1l3	deoxyribonuclease 1-like 3	7,0 ± 0,2	10,1 ± 0,5	8,5
Gm16848	immunoglobulin kappa chain variable 12-41	6,7 ± 0,3	9,7 ± 0,8	8,1
Igl-V2|Igl-C2	immunoglobulin lambda chain variable 2 | immunoglobulin lambda chain constant region 2	7,4 ± 0,1	10,4 ± 0,3	8
Gm10880	immunoglobulin kappa variable 4-74	8,0 ± 0,3	11,0 ± 0,1	7,8
Gm16970|Igh-VX24	immunoglobulin heavy variable 2-2| immunoglobulin heavy chain (X24 family)	8,1 ± 0,2	11,1 ± 0,1	7,7

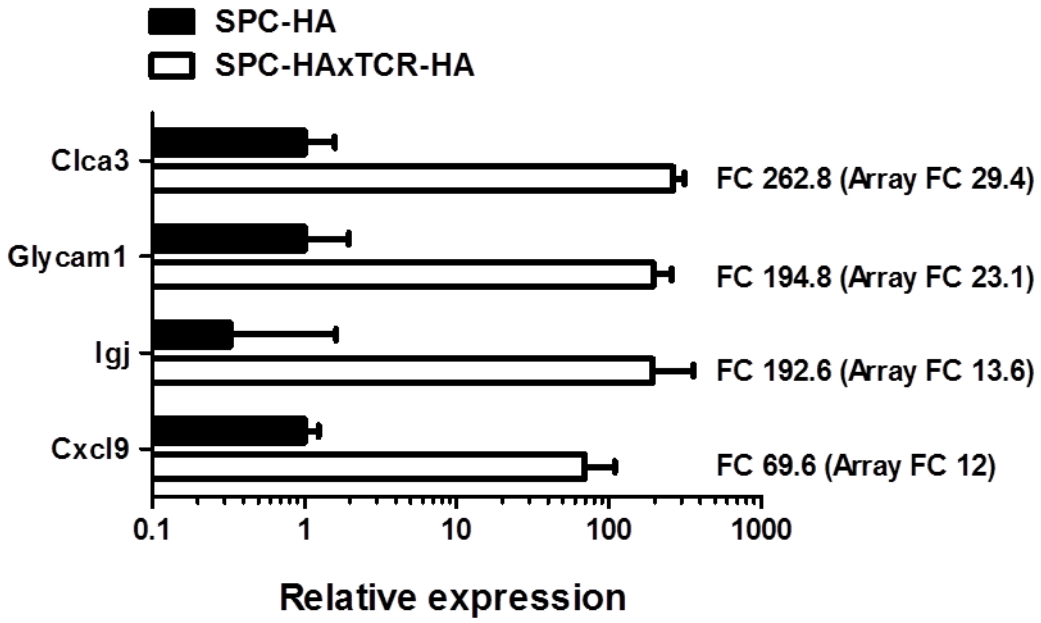

Figure 19: Validation of genes found to be up-regulated (FC>2) in SPC-HAxTCR-HA lungs by qRT-PCR. Total lung RNA from SPC-HA and SPC-HAxTCR-HA mice (n=3/group) was isolated and reversely transcribed into cDNA. Samples were analyzed by SYBR Green-based qRT-PCR analyses using the ΔΔCt algorithm. Relative expression of indicated transcripts was normalized to the expression of *rps9* housekeeping gene. Data represent mean ± SD. The expressional fold change of SPC-HAxTCR-HA vs. SPC-HA is indicated.

In order to elucidate the functional meaning of the observed differential gene expression in SPC-HAxTCR-HA lungs Gene Ontology (GO) enrichment analyses using Kyoto Encyclopedia of Genes and Genomes (KEGG) pathway annotation terms was performed. GO analyses of the differentially regulated set of genes revealed highly significant over-representation of genes associated with the KEGG terms *B cell receptor signaling pathway* (19.2% associated genes, Figure 20) and *Intestinal immune network for IgA production* (19.0% associated genes, Figure 20). Moreover, KEGG terms like *T cell receptor signaling pathway*, *Chemokine signaling pathway* and *Cytokine-cytokine receptor interaction* were also significantly overrepresented (Table 6) suggesting possible involvement of other functional gene groups apart from the abovementioned two.

Remarkably, among the 20 most intensely up-regulated genes 15 (75%) were immunoglobulin-specific (Table 5), including Igj (FC Array 13.6, FC qRT-PCR 192.6, Figure 19, Table 5), which encodes for the J chain. Taken together, the differential gene expression observed in the microarray analyses could be confirmed by the results obtained by qRT-PCR.

Table 6: KEGG pathway enrichment analyses of genes found to be up-regulated (fold change≥2) in SPC-HAxTCR-HA lungs.

KEGG ID	GO term	% associated genes	Term p-value corrected with Bonferroni
4662	**B cell receptor signaling pathway**	19,2	1,20E-11
4672	**Intestinal immune network for IgA production**	19	1,70E-06
4640	**Hematopoietic cell lineage**	14	3,10E-08
4660	**T cell receptor signaling pathway**	13,3	2,10E-09
4062	**Chemokine signaling pathway**	10,2	2,10E-11
4664	**Fc epsilon RI signaling pathway**	10	1,00E-03
4666	**Fc gamma R-mediated phagocytosis**	9,1	5,60E-04
4514	**Cell adhesion molecules (CAMs)**	8,8	5,90E-07
4612	**Antigen processing and presentation**	8,6	2,60E-03
4060	**Cytokine-cytokine receptor interaction**	8,3	8,00E-11
4064	**NF-kappa B signaling pathway**	7,9	1,50E-03
4610	**Complement and coagulation cascades**	7,8	1,50E-02
4650	**Natural killer cell mediated cytotoxicity**	6,7	4,90E-03
4670	**Leukocyte transendothelial migration**	6,6	5,50E-03
4145	**Phagosome**	5,7	2,80E-03

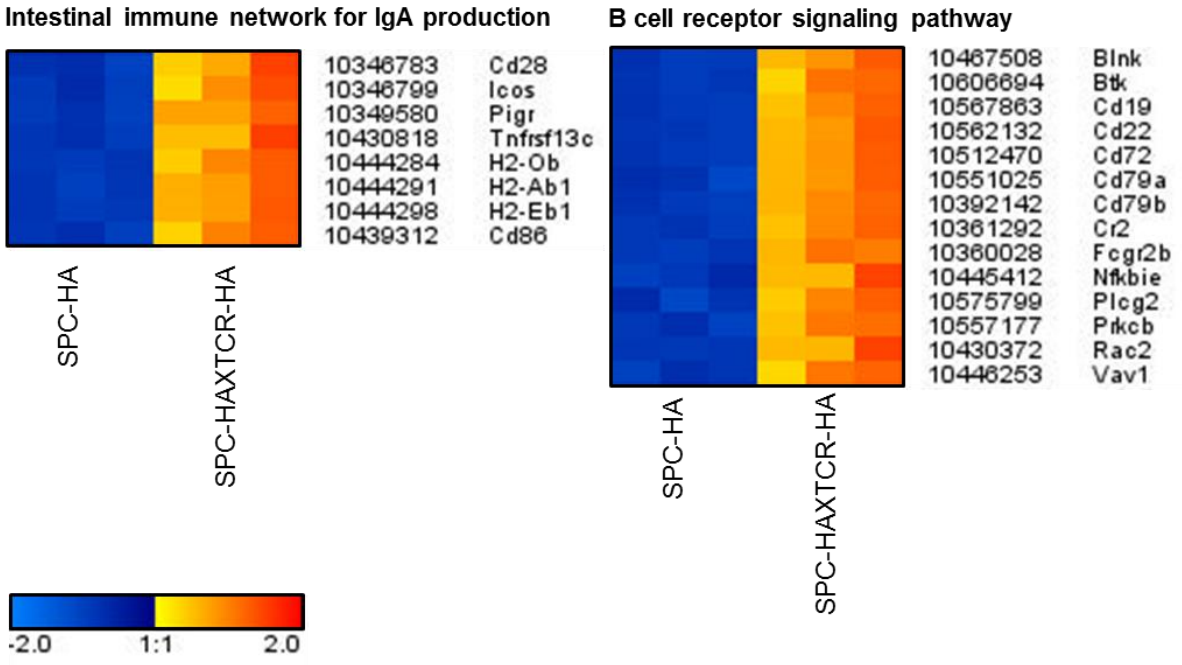

Figure 20: Expression data of transcripts from indicated GO terms in SPC-HA and SPC-HAxTCR-HA mice. Color code represents z-score, red=transcript induction, blue=transcript repression.

Altogether, these findings reveal that local chronic inflammatory imprinting encompasses substantial alterations in the lung tissue transcriptome. These most likely reflect disease-driven alterations in cytokine-orchestrated recruitment of leukocytes as well as their intercellular communication pathways. This suggests a markedly changed pulmonary cellular composition in SPC-HAxTCR-HA mice - which is well in line with e.g. the lymphocytic infiltrates previously observed in this group (Bruder, Westendorf et al. 2004, Figure 12a). Particularly correlating with this finding is the great dominance of B-lymphocyte specific transcripts among the top20 up-regulated transcripts (Table 5). The latter in combination with the general enrichment of transcripts with roles in B cell- and IgA-specific immune networks, respectively (Figure 20, Table 6); also suggests a possible role for humoral immunity in antimicrobial host defense in SPC-HAxTCR-HA lungs.

5.1.6 Altered BALF proteome composition in SPC-HAxTCR-HA mice

The finding that bacterial transmigration was blunted in SPC-HAxTCR-HA mice despite unaltered phagocyte function suggested an altered composition of soluble factors (e.g. secreted proteins) lining the airway mucosal surface in these mice. Well in line with this, the microarray analyses indicated an induction of several soluble mediators with hypothetical contributions to humoral immunity in SPC-HAxTCR-HA lungs. In a next step, it should thus be determined whether the proteins present in the airways differ between both mouse groups.

To this end BALF proteome (BALFome) analyses were performed using LC-MS/MS technology. BALF represents a highly diluted form of the lung mucosal fluid and besides leukocytes contains proteins with broad antimicrobial functions. The analysis of BALF samples pooled from 5 mice per group revealed a total of 602 proteins of which 372 (~60%) were present in BALF of both groups. 129 proteins were exclusively present in SPC-HA BALF whereas 101 proteins were only present in SPC-HAxTCR-HA BALF (Figure 21a). To identify the major biological pathways represented by the identified proteins, gene ontology (GO) analyses of the complete BALFome of SPC-HA mice (501 proteins) and SPC-HAxTCR-HA mice (473 proteins) were performed using KEGG pathway annotation terms. This yielded similar coverages of associated factors of the top5 terms (*Proteasome, Pyruvate metabolism, Glutathione metabolism, Pentose phosphate pathway, Glycolysis/Gluconeogenesis*) that are involved in protein degradation and carbohydrate metabolism in SPC-HA and SPC-HAxTCR-HA BALF. These analyses also yielded GO terms uniquely detected in BALFomes of SPC-HA (e.g. *valine, leucine and isoleucine degradation*) or SPC-HAxTCR-HA mice (*regulation of actin cytoskeleton*, see section 7.1.2, Table 15) indicating that inflammatory priming encompasses distinct proteomic adaptions affecting metabolic and cytoskeletal cellular activities on the mucosal surface.

Interestingly, the comparison of all up-regulated and annotated transcripts from SPC-HAxTCR-HA lungs (251 identified genes) with the proteins (identified by protein accession ID) exclusively detected in SPC-HAxTCR-HA BALF yielded an overlap of 10 proteins (Figure 21b). Among those were macrophage metalloelastase (*Mmp12,* FC Array 5.2, see section 7.1.1, Table 10) and cathepsin S (*Ctss*, FC Array 2.4, see section 7.1.1, Table 10), which has been shown to be expressed by AMs and AECs (Shi et al. 1992, Storm van's Gravesande et al. 2002). These proteases have elastolytic activity and are associated with the development

of alveolar emphysema (Zheng et al. 2000). Moreover, chitinase-like 3 protein (*Chil3*, FC Array 4.0, see section 7.1.1, Table 10) and resistin-like alpha (*Retnla*, FC Array 6.6, see section 7.1.1, Table 10) were also uniquely detected in the SPC-HAxTCR-HA BALFome. Both proteins are produced by airway macrophages and AECs and are found in settings of sterile pulmonary inflammation (Dasgupta et al. 2011). Interestingly, and in line with the transcriptome data, 3 proteins associated with secretory antibody-mediated immunity were identified: the immunoglobulin alpha chain C region (*Igh-VJ558*, FC Array 3.9, see section 7.1.1, Table 10), the immunoglobulin J chain (*Igj*, Table 5, Figure 19) and the polymeric immunoglobulin receptor (*Pigr*, FC Array 3.4, see section 7.1.1, Table 10). In summary, these proteome analyses complemented the previous transcriptome analyses and strengthened the hypothesis of an enhancement of humoral immunity in SPC-HAxTCR-HA mice.

a

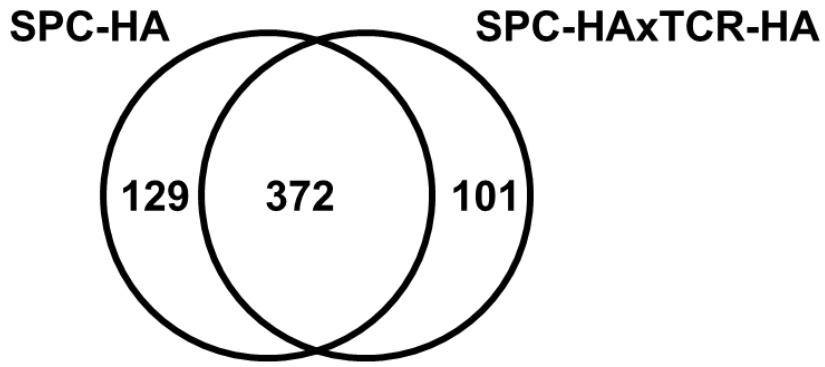

b

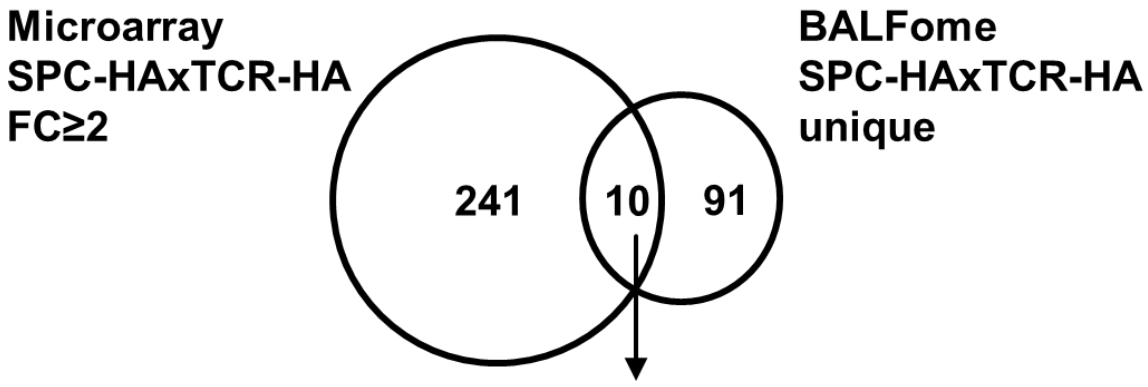

Gene symbol	Protein
Arhgdib	Rho GDP-dissociation inhibitor 2
Chil3	Chitinase-like protein 3
Coro1a	Coronin-1A
Ctss	Cathepsin S
Igh-VJ558	Immunoglobulin alpha chain C region
Igj	Immunoglobulin J chain
Iigp1	Interferon-inducible GTPase 1
Mmp12	Macrophage metalloelastase
Pigr	Polymeric immunoglobulin receptor
Retnla	Resistin-like alpha

Figure 21: Comparison of BALF proteome from SPC-HA vs. SPC-HAxTCR-HA mice.
(a) Venn diagram comparing LC-MS/MS-identified proteins from bronchoalveolar lavage fluid (BALF) of SPC-HA and SPC-HAxTCR-HA mice. Samples were pooled from 5 mice/group. **(b)** Venn diagram comparing the presence of transcripts with a fold change (FC) ≥ 2 in lungs of SPC-HAxTCR-HA mice vs. the presence of proteins uniquely detected in BALF from SPC-HAxTCR-HA mice.

5.1.7 Elevated secretory antibody levels in the airways of SPC-HAxTCR-HA mice

Based on the previous findings the absolute levels of BALF immunoglobulins (Igs) in healthy and chronically inflamed lungs were compared by ELISA. This revealed an >11-fold increase in IgA levels in BALF of SPC-HAxTCR-HA mice compared to SPC-HA mice. Likewise, BALF IgM levels were elevated to an equal extent (Figure 22a). Interestingly, serum IgA and IgM levels were similar between both groups (Figure 22b), suggesting that elevated BALF IgA and IgM levels arise from increased Ig transport from the lung tissue into the lung lumen in SPC-HAxTCR-HA mice. However, since SPC-HAxTCR-HA BALF also contained increased albumin levels (Figure 12c), it had to be tested whether the increase in airway IgA and IgM is due to active pIgR-mediated transcytosis through the epithelial barrier rather than to passive diffusion of serum components. To this end, the abundance of secretory IgA (SIgA) in BALF was compared by ELISA using an anti-IgA capture antibody and a specific anti-pIgR detection antibody. By doing so, the specific abundance of pIgR-associated and thus transcytosed SIgA – but no monomeric or conventional dimeric IgA molecules - was quantified. Indeed, significantly higher mean ODs (>6-fold at 1:10 BALF dilution) were detected in BALF samples from SPC-HAxTCR-HA mice (Figure 22c), confirming that the increase in airway IgA levels arose from amplified mucosal transport rather than passive transepithelial diffusion. This is likely to hold true also for SIgM since both molecules share the same transport mechanism (Strugnell and Wijburg 2010).

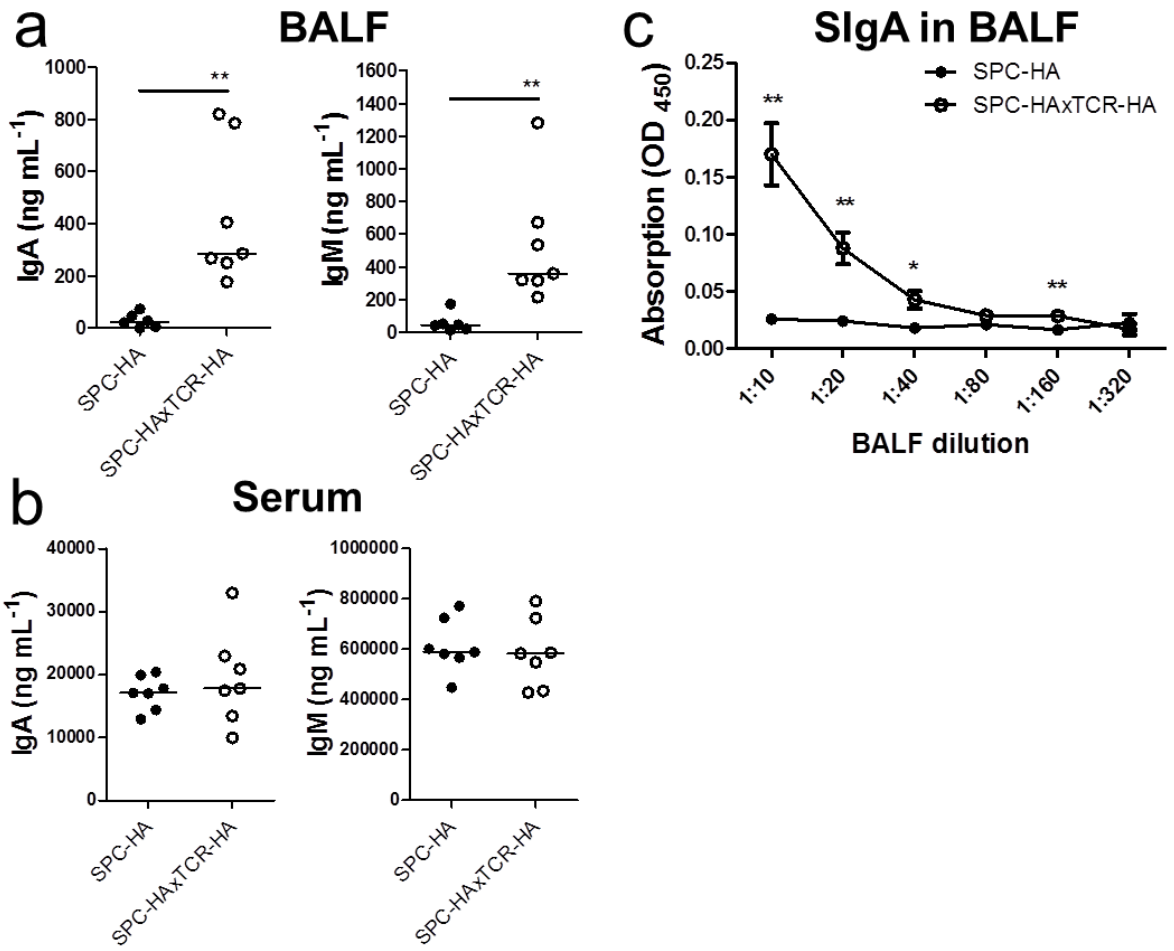

Figure 22: Secretory antibody levels in SPC-HA vs. SPC-HAxTCR-HA mice.
Absolute IgA and IgM levels in **(a)** bronchoalveolar lavage fluid and **(b)** serum of SPC-HA and SPC-HAxTCR-HA mice were determined by ELISA. **(c)** Relative secretory IgA concentrations in serial dilutions of BALF samples were determined by ELISA. Results are expressed as the mean optical density (OD) at 450nm ± SEM, *p< 0.05, ** p<0.01 (n=6-7 mice/group).

Previous studies reported inflammatory stimuli to lead to increased pIgR levels and an up-regulation of SIg transport by mucosal epithelial cells (Cao et al. 2012, Jaffar, Ferrini et al. 2009). Taking the elevated BALF SIgA protein levels in the SPC-HAxTCR-HA group into account (Figure 22c), elevated pulmonary *Pigr* gene expression was expected, as the pIgR/SIgA binding & transport mechanism involves a 1:1 stoichiometry (Kaetzel et al. 1991). In line with this, the microarray analyses already revealed *Pigr* up-regulation in SPC-HAxTCR-HA lungs (see section 7.1.1, Table 10). For this reason pIgR abundance in the respiratory tract of SPC-HAxTCR-HA and SPC-HA mice was probed in more detail. Initially, *Pigr* gene expression was probed by qRT-PCR using total RNA from whole lung homogenates of SPC-HA and SPC-HAxTCR-HA mice (n=3/group). *Pigr* gene expression was confirmed to be up-regulated 3.3-fold in SPC-HAxTCR-HA vs. SPC-HA lungs (Figure 23a). Next, using whole lung homogenates from both mouse groups (n=4/group) pIgR protein abundance was analyzed by Western Blot. High pIgR levels were found in the SPC-HAxTCR-HA group whereas this protein was almost not detectable in the SPC-HA group (Figure 23b). Given the rather modest increase in transcript levels this suggests pIgR protein levels to be regulated at a translational (or post-translational) rather than at the transcriptional level. In order to examine the spatial distribution of pIgR expression in more

detail immunofluorescence analyses of lung tissue sections from SPC-HA and SPC-HAxTCR-HA mice were conducted. Briefly, 6µm acetone-fixed lung cryosections were blocked and incubated with an anti-pIgR primary antibody as well as FITC-labelled secondary antibody. Additionally, in order to better identify the respective pulmonary microstructures, DAPI nuclear counterstain was performed. Interestingly, localization analyses revealed increased pIgR protein expression in the alveoli of SPC-HAxTCR-HA mice, where it was restricted to single, cuboidal epithelial cells; likely to be ATII (Figure 23c). Taken together, these data closely link chronic endogenous airway inflammation to the boost of epithelial-governed pIgR-dependent transport of mucosal antibodies which may improve immunity to *Streptococcus pneumoniae*.

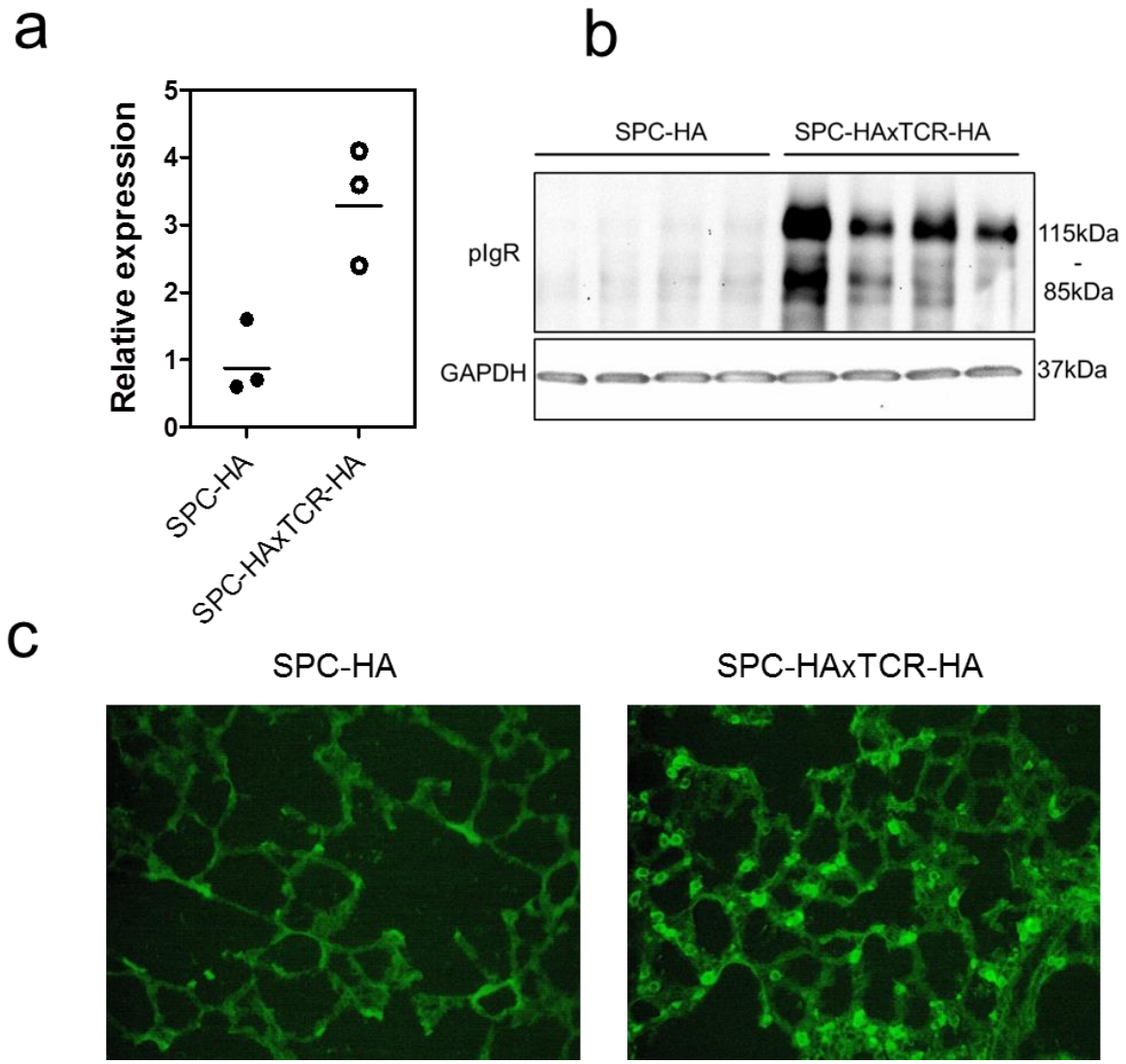

Figure 23: Increased pIgR-expression in SPC-HAxTCR-HA lungs.
(a) *Pigr* gene expression was quantified by qRT-PCR. Results are depicted as relative expression values normalized to *Actb* housekeeping gene expression. **(b)** anti-pIgR immunoblot of whole lung homogenates of SPC-HA and SPC-HAxTCR-HA mice**. (c)** Lung tissue sections were stained with goat anti-pIgR and detected by secondary anti-goat FITC-labeled antibody (green), depicted are representative alveolar structures from n=3/group from one of two independent experiments with similar outcome. Magnification: 20x

5.1.8 BALF from SPC-HAxTCR-HA mice has an increased pneumococcal binding capacity

SIgA and SIgM are key components of the mucosal barrier towards viral and bacterial pathogens and SIg deficiency is associated with increased susceptibility to respiratory infections in mice (Brown, Hussell et al. 2002, Sun, Johansen et al. 2004) and humans (Latiff et al. 2007, Louis et al. 2014). To test a possible link between elevated SIg levels in the BALF (Figure 22c) and enhanced antipneumococcal resistance (Figure 13) in SPC-HAxTCR-HA mice flow cytometry-based bacterial binding assays were performed (see section 4.2.12 for further details). Briefly, pneumococci were incubated with BALF supernatants from SPC-HA and SPC-HAxTCR-HA mice and opsonized bacteria were identified by surface staining against IgA or IgM, respectively. Pneumococci were subsequently analyzed by FACS for the percentage of positively stained bacterial cells and their respective fluorescence intensities. As controls unopsonized pneumococci were incubated with the respective anti-IgA or anti-IgM antibodies (see Figure 24a and d). Despite increased SIgA concentrations in SPC-HAxTCR-HA BALF (Figure 22c), similar fractions of IgA-positive pneumococci following incubation with both SPC-HAxTCR-HA as well as SPC-HA BALF (5.7% vs. 6.6%) were detected (Figure 24b). Quantification of relative fluorescence however indicated a significantly higher IgA deposition on pneumococci that were incubated with BALF from SPC-HAxTCR-HA mice (median index 1.16 vs. 1.01, Figure 24c). Moreover, incubation with BALF from SPC-HAxTCR-HA mice yielded increased portions of IgM-positive pneumococci (Figure 24e) as well as enhanced IgM deposition when compared to incubation with BALF from SPC-HA mice (Figure 24f).

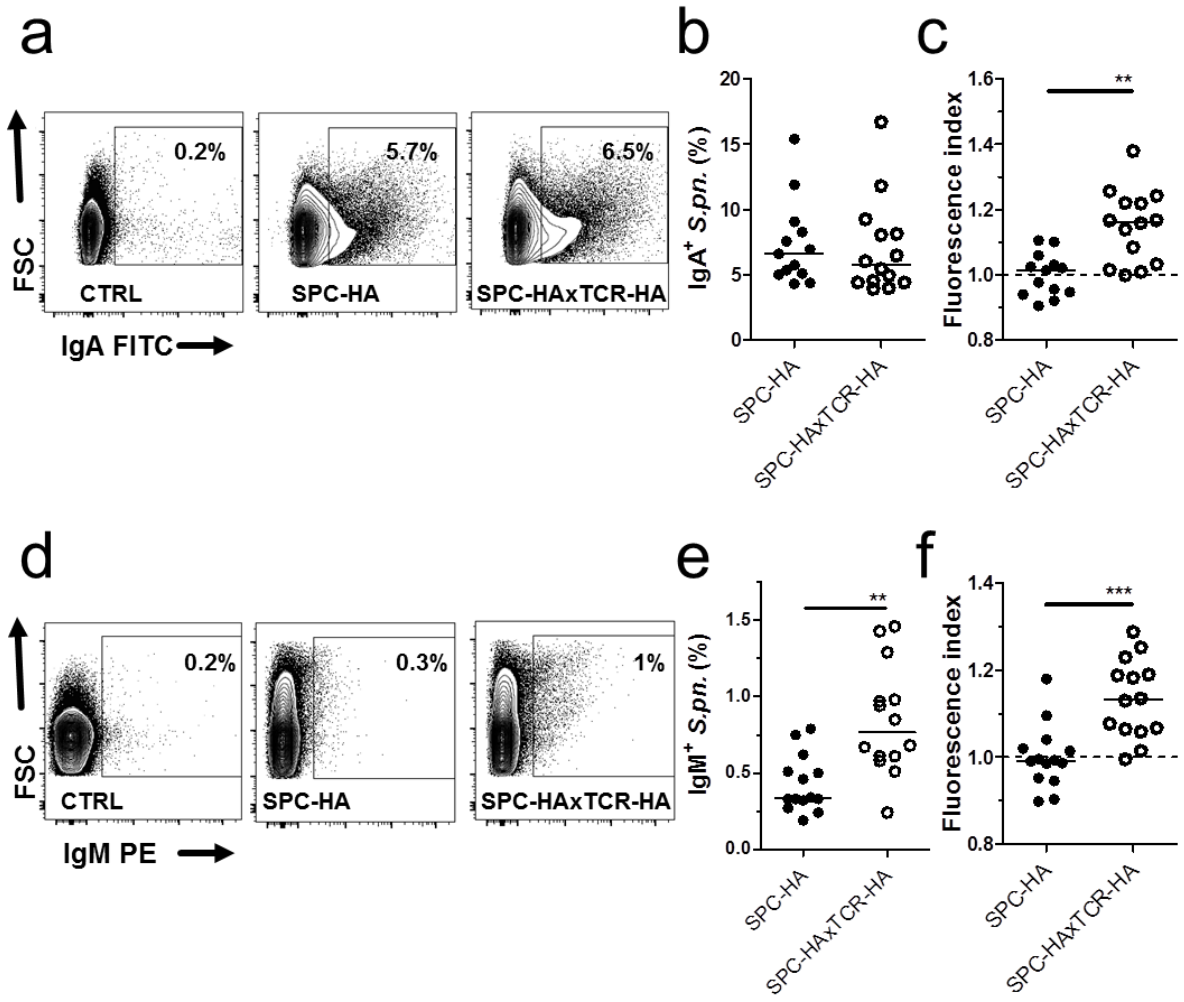

Figure 24: Increased pneumococcal binding capacities by lung mucosal fluid of SPC-HAxTCR-HA mice. *S.pneumoniae* TIGR4 were inoculated with bronchoalveolar lavage fluid (BALF) supernatants from SPC-HA and SPC-HAxTCR-HA mice. Bacteria were stained with anti-mouse IgA or anti-mouse IgM antibodies and analyzed by flow cytometry. **(a)** Representative FACS plots of IgA^+ pneumococci incubated with BALF from SPC-HA or SPC-HAxTCR-mice; control samples (CTRL) were stained with anti-IgA without prior incubation with BALF **(b)** Percentages of IgA^+ pneumococci and **(c)** relative fluorescence intensities of IgA^+ pneumococci. **(d)** Representative FACS plots of IgM^+ pneumococci incubated with BALF from SPC-HA or SPC-HAxTCR-mice; control samples (CTRL) were stained with anti-IgM without prior incubation with BALF. **(e)** Percentages of IgM^+ pneumococci and **(f)** relative fluorescence intensities of IgM^+ pneumococci. Relative fluorescence intensities are calculated by the ratio of the MFI of each individual sample over the mean MFI of the SPC-HA control group. Data are pooled from 2 independent experiments with similar results. *p<0.05 **p<0.01, ***p<0.001

In conclusion, by using the SPC-HAxTCR-HA transgenic model for CRD it was demonstrated in the first part of this thesis that chronic inflammatory imprinting in the lung is associated with marked changes in the transcriptomic and proteomic pulmonary profile indicating inflammation-induced milieu adaptations. Microarray and mass spectrometric analyses pointed towards a beneficial enhancement of the SIg axis in inflamed lungs and suggested a possible involvement of the pulmonary epithelium therein. Finally, increased pIgR-mediated SIg transepithelial transport led to augmented pneumococcal binding by IgA and IgM. These findings point towards a fundamental role of inflammation-primed airway epithelial cells in

humoral antimicrobial immunity by reinforcing the mucosal barrier and thereby counteracting pneumococcal adhesion and tissue penetration.

5.2 Phenotype and function of alveolar macrophages (AMs) in chronic endogenous lung inflammation

5.2.1 AMs from SPC-HAxTCR-HA mice show an altered phenotype

While the first part of this work focussed on the immunological implications of CRD on pulmonary antibacterial defense, the second part specifically addressed the contributions of AMs to immune regulation and inflammation within the chronically diseased lung.

Endogenous lung inflammation as displayed by SPC-HAxTCR-HA mice has previously been shown to involve a complex network of autoreactive and immunoregulatory mechanisms that are associated with substantial molecular and phenotypic alterations in the self-reactive T cell pool as well as in alveolar epithelial type II cells (Bruder, Westendorf et al. 2004, Gereke et al. 2007). Of note, it was previously demonstrated by others that alveolar macrophages are able to communicate with both ATII and effector T cells (Bingisser, Tilbrook et al. 1998, Blumenthal, Campbell et al. 2001, Bourdonnay, Zaslona et al. 2015, Westphalen, Gusarova et al. 2014). Yet, the role of AMs in chronic, pulmonary inflammation is not completely understood. Despite the unaltered numbers and phagocytosis rates of AMs in SPC-HAxTCR-HA mice it is conceivable that the inflammatory milieu and/or immunoregulatory mechanisms might affect the phenotype and immunologic functions of these cells. Therefore, the second part of this work aimed to examine the AM phenotype in the SPC-HAxTCR-HA model.

For a primary characterization of the AM phenotype in chronic lung inflammation, these cells were recovered from SPC-HA and SPC-HAxTCR-HA mice by BAL and were subjected to morphologic analyses by conventional flow cytometry (FACS) as well as imaging flow cytometry. In FACS analyses AMs were identified as $FSC^{high}SSC^{high}F4\text{-}80^{+}autofluorescence^{high}$ cells. FACS analyses revealed AMs from diseased SPC-HAxTCR-HA mice to have significantly smaller size compared to AMs from healthy SPC-HA control mice - indicated by reduced forward scatter (FSC) properties. Moreover, quantification of autofluorescence – an intrinsic AM-characteristic generally caused by electron-dense molecules – resulted in significantly reduced indices for AMs from SPC-HAxTCR-HA mice (Figure 25a).

In imaging flow cytometry, AMs were identified as $F4\text{-}80^{+}CD11c^{+}CD3^{-}$ cells. These analyses yielded altered cytoplasmic signals in AMs from SPC-HAxTCR-HA mice reflected by alterations of side scatter (SSC) characteristics (area, general intensity and bright detail intensity, Figure 25b), indicating a markedly changed cellular texture of alveolar macrophages in a persistent inflammatory pulmonary environment. In summary these results evidence chronic lung disease as displayed by SPC-HAxTCR-HA mice to manifest in distinct modifications affecting natural cellular fluorescence as well as refractive properties of AMs, thereby suggesting substantial qualitative and/or quantitative alterations in the intracellular molecular composition.

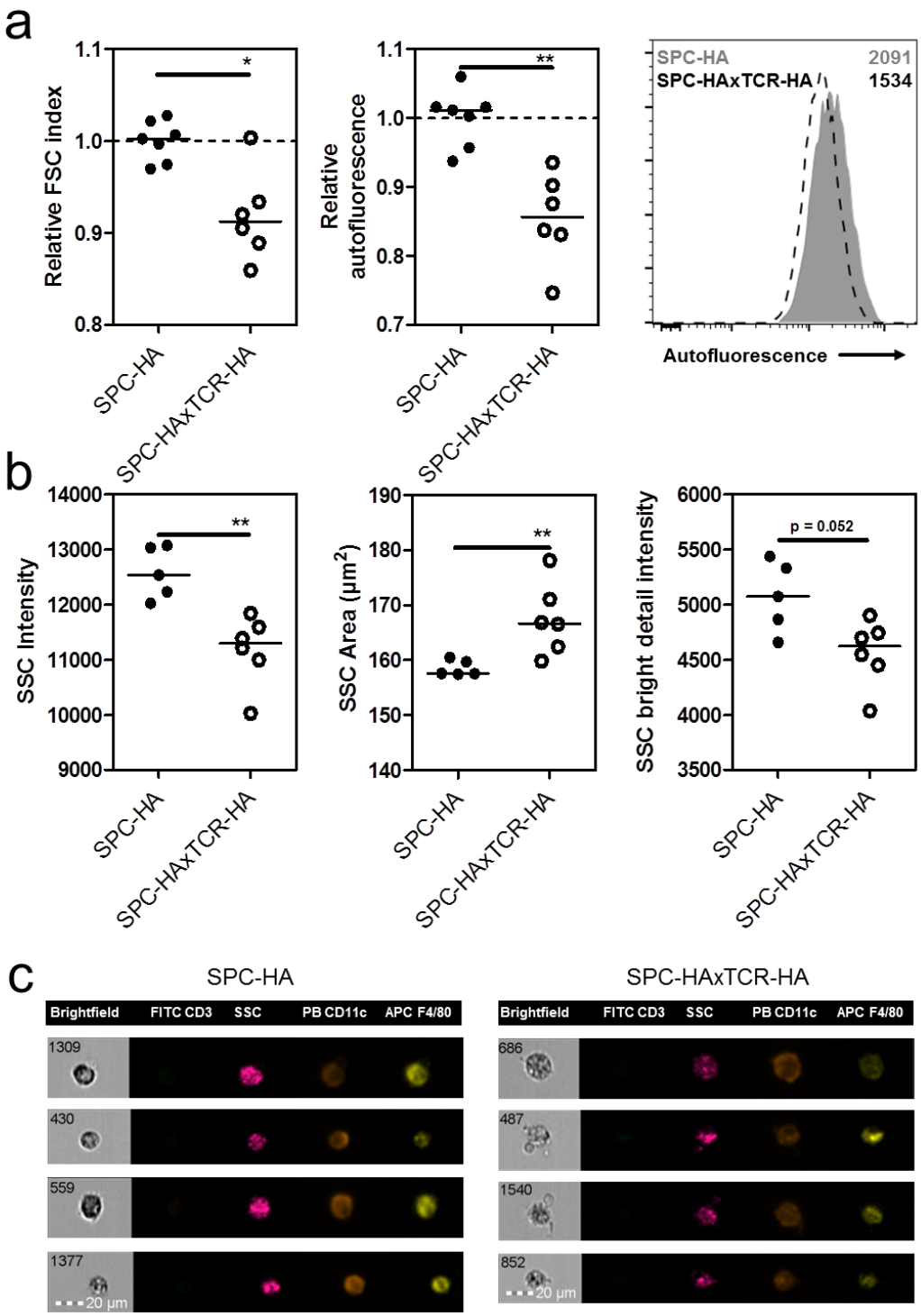

Figure 25: Flow cytometric analyses of AM morphology in SPC-HA vs. SPC-HAxTCR-HA lungs.
(a) BAL cells from SPC-HA (n=6) and SPC-HAxTCR-HA (n=6) mice were analyzed by FACS; AMs were identified as $FSC^{high}SSC^{high}F4\text{-}80^{+}autofluorescence^{high}$ cells. Relative FSC and autofluorescence was calculated by: median fluorescence intensity (MFI) of individual sample over the mean MFI of the SPC-HA (healthy) control group. Representative histogram depicts autofluorescent signal intensities of AMs from SPC-HA (grey shaded) vs. SPC-HAxTCR-HA (dashed line) mice and their respective MFI (see numbers). **(b)** BAL cells from SPC-HA (n=5) and SPC-HAxTCR-HA (n=6) mice were analyzed by imaging flow cytometry (analyzed SSC-parameters: intensity, area, bright detail intensity); AMs were identified as $F4\text{-}80^{+}CD11c^{+}CD3^{-}$ cells. Statistical analyses were performed by using unpaired, two-tailed Mann-Whitney-test. * $p<0.05$, ** $p<0.01$ **(c)** Representative images from imaging flow cytometer FlowSight® of alveolar macrophages from SPC-HA and SPC-HAxTCR-HA mice, PB: pacific blue

5.2.2 AMs from SPC-HAxTCR-HA mice display an activated phenotype

Further comparative morphologic analyses of alveolar macrophages were conducted using Pappenheim-stained cytospin samples of bronchoalveolar lavage fluid cells from SPC-HA and SPC-HAxTCR-HA mice. Microscopic evaluation demonstrated AMs from diseased SPC-HAxTCR-HA mice to display an activated phenotype, specified by increased formations of membrane protrusions (see black arrows in Figure 26).

Together, the observed morphologic alterations provide further evidence for an impact of chronic pulmonary inflammation on cellular properties of alveolar macrophages and establish a basis for extended investigations regarding functional alterations of AMs in murine lung disease.

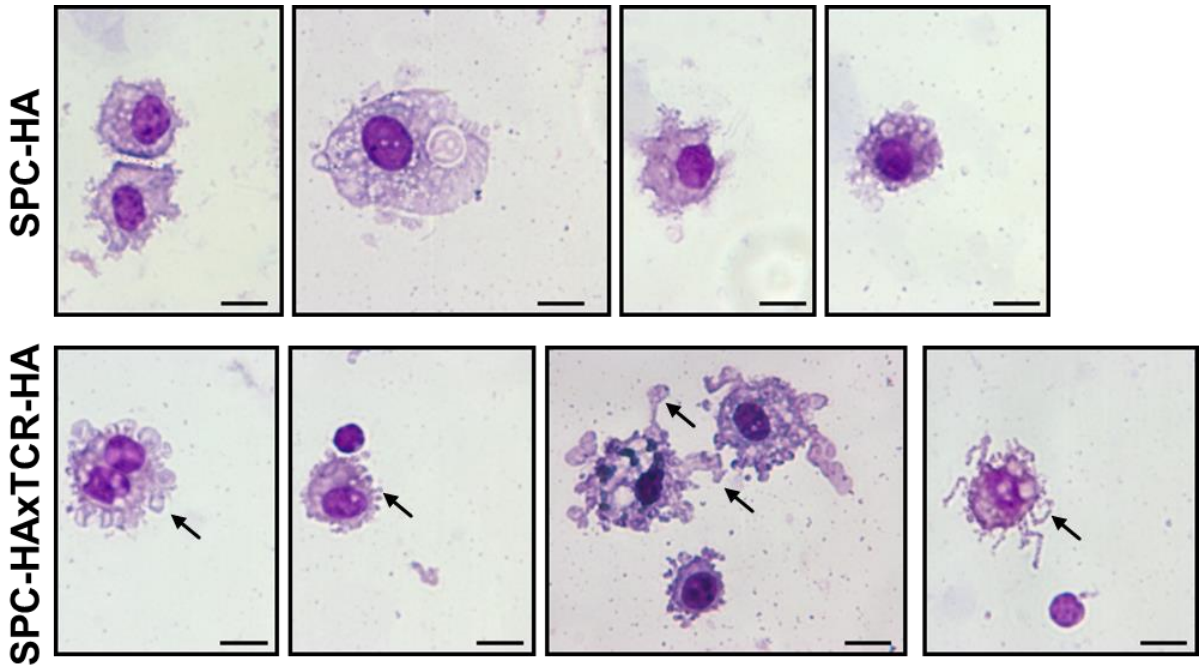

Figure 26: Analyses of AM morphology by light microscopy.
Cytospins from BAL samples from SPC-HA and SPC-HAxTCR-HA were stained with May-Grünwald and Giemsa reagent (Pappenheim method) and cell morphology was analyzed by light microscopy. Depicted are representative images of alveolar macrophages from n=4 mice/group at 63x magnification. Scale bar: 10µm. Black arrows indicate membrane protrusions.

5.2.3 M2 signature of AMs from SPC-HAxTCR-HA mice

Inflammatory conditions in multiple infectious as well as non-infectious disease settings are intimately linked to macrophage polarization into classically activated M1 or alternatively activated M2 phenotypes (see sections 2.5 and 2.7). Briefly, M1 macrophages are considered to play roles in the initiation and maintenance of inflammation (e.g. acute infection, immunologic inflammatory disorders) whereas M2 phenotypes are implicated in resolution of inflammation and wound healing but also in several settings of chronic inflammation and infection (Sica and Mantovani 2012). Previous results from whole lung microarray and BALFome analyses yielded the following proteins to be specifically induced and overrepresented in SPC-HAxTCR-HA lungs: Chitinase-like 3 protein (also known as Ym1) and resistin-like alpha as well as macrophage metalloelastase 12 (Figure 21b).

Noteworthy, these 3 factors are typical M2-markers (Kahnert, Seiler et al. 2006, Raes et al. 2002) which are associated with the breakdown and reorganization of extracellular matrix (Mosser and Edwards 2008) and the development of pulmonary emphysema in COPD patients (Molet et al. 2005), respectively. Based on these observations it seemed likely to discover M2-polarized AMs in SPC-HAxTCR-HA mice. In order to test this hypothesis, BALF cells from SPC-HA and SPC-HAxTCR-HA mice were isolated and AMs were purified by adhesion (see section 4.2.8). This method allowed for the fast and efficient isolation of highly pure (~95%) alveolar macrophages as illustrated in Figure 27.

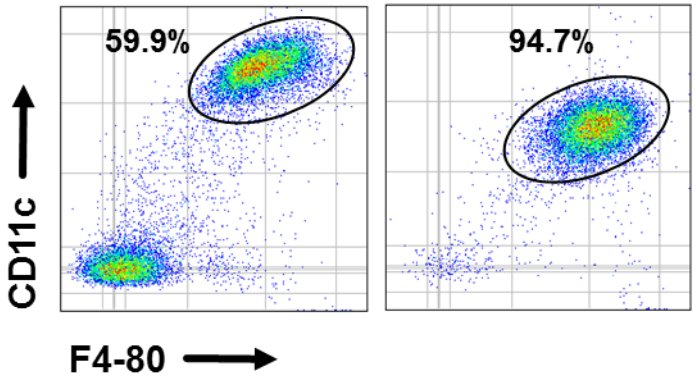

Figure 27: Purification of AMs by adhesion.
Alveolar macrophages (AMs) from erythrocyte-depleted BALF cell suspensions were purified by adhesion (90min, 37°C) on bacteriological plastic, detached by trypsin-EDTA treatment and purity was verified by FACS analysis. Left square depicts percentages of AMs ($CD11c^{high}$, $F4\text{-}80^{+}$) of analyzed singlets in non-purified BALF samples from SPC-HAxTCR-HA mice. Right square depicts AM percentages of BALF cells from SPC-HAxTCR-HA mice after purification. Note the decreased abundance of the surface molecule CD11c on AMs after trypsin-EDTA detachment.

Next, comparative gene expression analyses of total RNA isolated from purified, pooled AM samples (n=3-5 mice/group) from SPC-HA vs. SPC-HAxTCR-HA mice were conducted by quantitative real-time RT-PCR. Here, up-regulation of the genes encoding for the secreted protein resistin-like alpha (*Retlna*, fold change 16.1) and also the extracellular receptor macrophage scavenger receptor 1 (*Msr1*, fold change 5.5, Figure 28). Expression of macrophage scavenger receptor 1, also known as scavenger receptor A1 or CD204, is increased in M2 macrophages and contributes to increased uptake of low-densitity lipoprotein, but also of apoptotic cell material by these cells (Canton et al. 2013).

Collectively, these results support the hypothesis of an M2 AM-phenotype – associated with increased expression of specific surface molecules and secreted products - in SPC-HAxTCR-HA lungs and moreover suggest these cells likely to be the cellular source of the M2-proteins found in the BALF from this group.

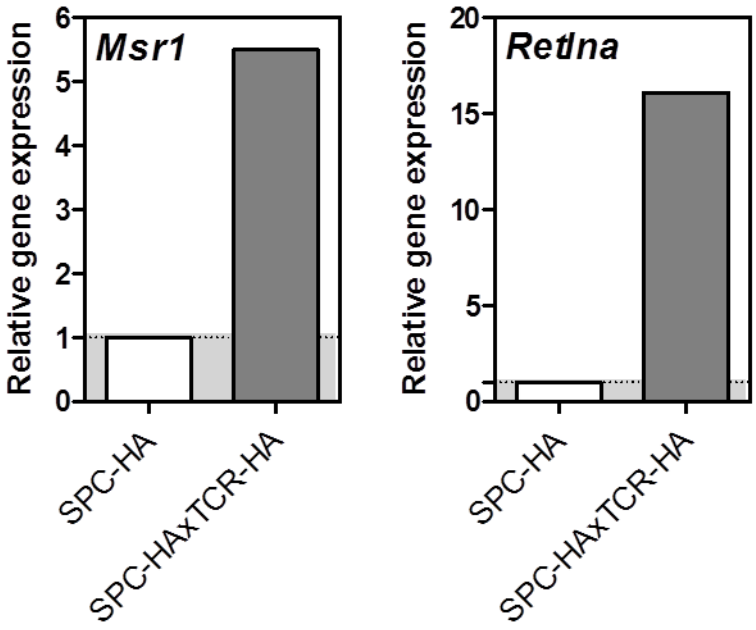

Figure 28: AMs from SPC-HAxTCR-HA mice display an M2-signature.
Purified alveolar macrophages from SPC-HA and SPC-HAxTCR-HA mice were pooled (n=3-5 mice/group), RNA was extracted and relative expression of indicated transcripts (normalized to *Actb* housekeeping gene) was determined by one-step qRT-PCR. Relative gene expression was normalized to the SPC-HA control group.

5.2.4 AMs from SPC-HAxTCR-HA mice are hyporesponsive to stimulation with pneumococcal ligands

Following recognition of respiratory pathogens alveolar macrophages mount a pro-inflammatory immune response by secreting (among other mediators) TNF-α (Schabbauer et al. 2010). This step is critical for the rapid elimination of microbial threats but on the other hand involves the risk to develop immune pathology at the expense of lung tissue integrity. In order to test the influence of chronic lung inflammation on the AM-mediated pro-inflammatory response following pathogen recognition, SPC-HAxTCR-HA mice and SPC-HA control mice were oropharyngeally inoculated with ethanol-killed *Streptococcus pneumoniae* TIGR4. Here, application of inactivated pneumococci allowed to study the very early innate recognition-triggered cytokine response while at the same time excluding confounding effects (e.g. from differential bacterial replication and invasion rates) to be detected. The early airway inflammatory response was quantified by assessing TNF-α levels in BALF at 4h following inoculation by ELISA. As expected, bacterial recognition led to an early and robust cytokine response in the airways of healthy SPC-HA mice. Strikingly, TNF-α levels were ~60% decreased in the pre-diseased SPC-HAxTCR-HA group (Figure 29, left panel).

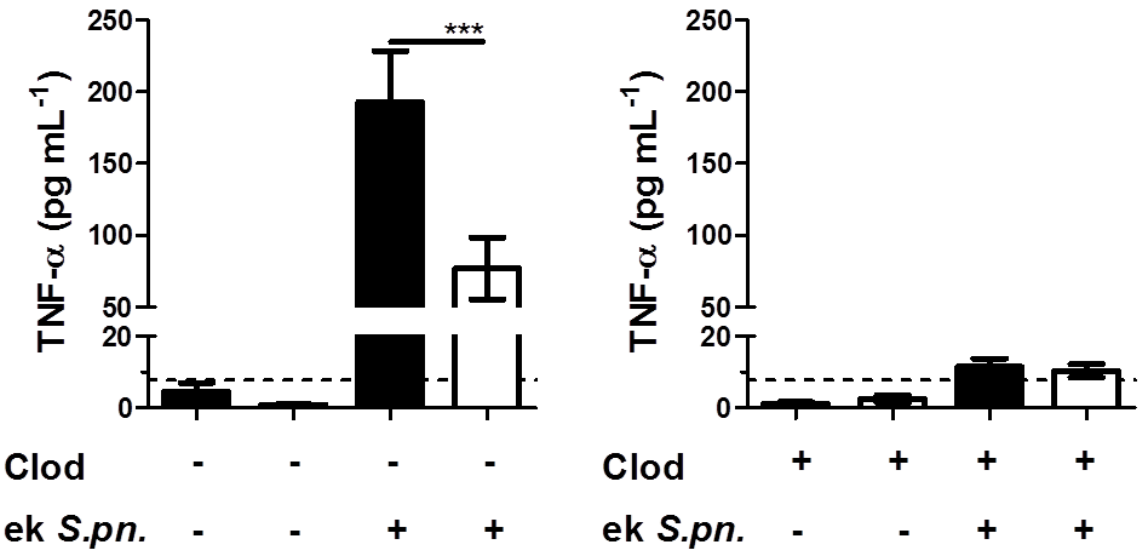

Figure 29: Blunted inflammatory response towards bacterial ligands in SPC-HAxTCR-HA mice is AM-dependent.

Mice were oropharyngeallly inoculated with 50µL clodronate liposomes on d0, control mice received PBS. At d3 mice were administered 10^6 CFU ethanol-killed *S. pneumoniae* TIGR4 (ek S.pn.) or PBS, respectively. 4h after bacterial inoculation, mice were sacrificed and TNF-α levels in bronchoalveolar lavage fluid was determined by ELISA. Depicted are mean results ± SEM of pooled samples from 2 independent experiments. (n=6-10/group). Statistical significance was calculated using two-way ANOVA followed by Bonferroni post-test. *** p<0.001.

In order to verify that this blunted inflammatory response was mediated by alveolar macrophages, these cells were depleted by oropharyngeal administration of clodronate liposomes (Clod) 3 days prior bacterial stimulation. Clodronate treatment lead to a 75% reduction of viable AM numbers in the BALF (Mean ± SEM AM counts of PBS-group vs. Clod group: 25383±6040 vs. 6330±1536) within 3 days, whereas the single administration of control liposomes (PBS-Lip) or carrier solution (PBS) had no effect on alveolar macrophage numbers (Figure 30, upper panel). Moreover, quantitative analyses of macrophage subsets in the lung tissue 3 days post treatment revealed that the reduction of alveolar macrophages was restricted to bronchoalveolar spaces whereas the percentages of lung-tissue resident alveolar macrophages (AMs) and interstitial macrophages (IMs) remained unaffected (Figure 30, lower panel). These findings confirmed that the chosen clodronate-depletion strategy is an adequate tool to specifically study the function of alveolar macrophages within the airways *in vivo*. Notably, TNF-α levels following bacterial stimulation in AM-depleted mice were substantially reduced and close to detection limit in both mouse groups (Figure 29, right panel). Taken together, this validates AMs to be the main early airway TNF-α source following pneumococcal stimulation and, more importantly, suggests a functional adaptation of these cells in chronic lung disease.

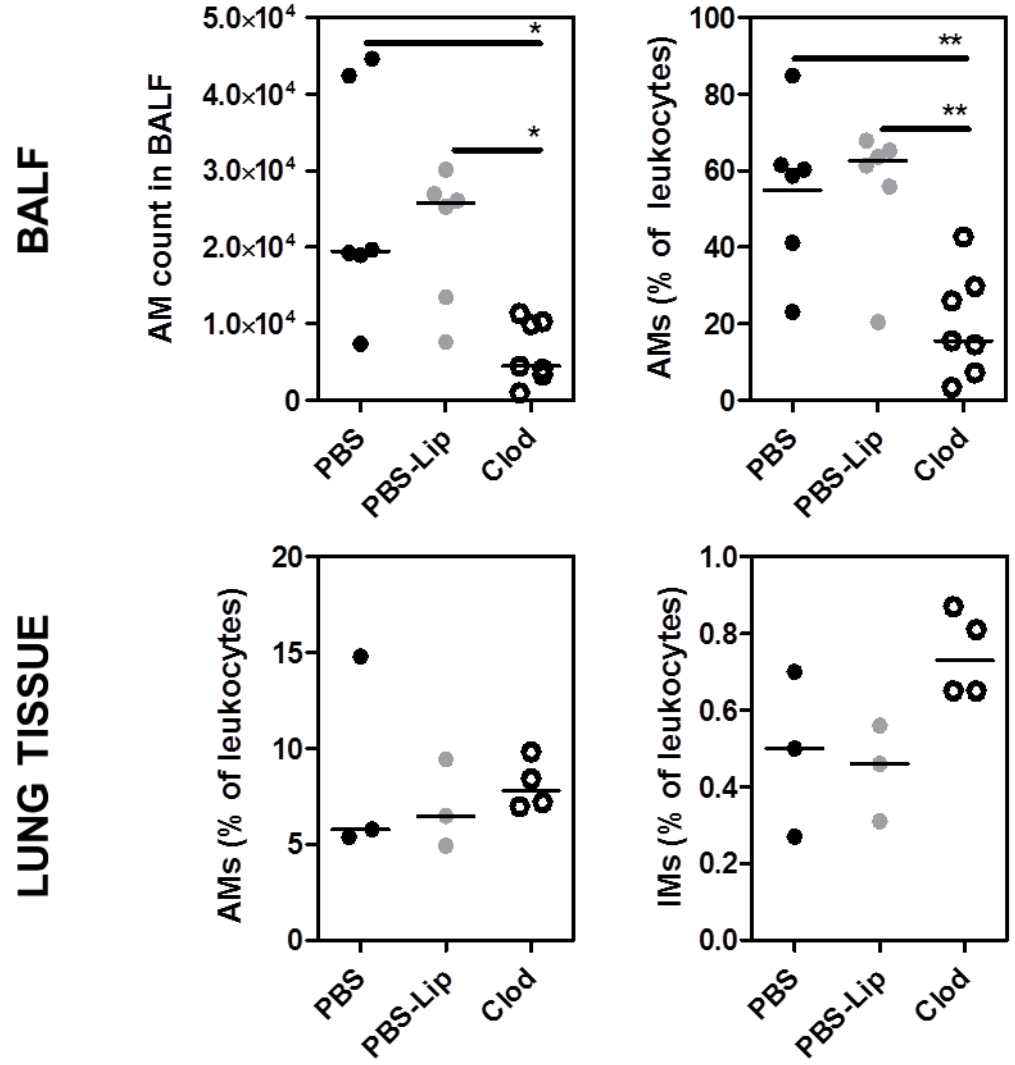

Figure 30: Oropharyngeal clodronate treatment selectively depletes macrophages in bronchoalveolar spaces.

SPC-HA mice were oropharyngeally inoculated with 50µL Clodronate-Liposomes (Clod), PBS-Liposomes (PBS-Lip) or PBS only. At d3 post administration mice were sacrificed, alveolar macrophages ($CD11c^{high}F4\text{-}80^{+}autofluorescence^{high}$) in BALF and lung tissue ($CD11c^{high}$ $CD11b^{dim}$ $F4\text{-}80^{+}$) and interstitial macrophages (IMs, $CD11c^{high}$ $CD11b^{high}$ $F4\text{-}80^{+}$) in lung tissue were quantified by flow cytometry. Data from BALF analyses were pooled from two independent experiments with similar outcomes. Statistical significance was calculated using one-way ANOVA followed by Bonferroni post-test. * $p<0.05$; ** $p<0.01$.

5.2.5 Absence of AMs aggravates disease pathology and establishes bronchopneumonia in SPC-HAxTCR-HA mice

So far, the obtained data have revealed a substantially different alveolar macrophage phenotype and function in SPC-HAxTCR-HA mice. In a next step, the immunological role of these cells in the context of chronic lung inflammation was to be further explored by *in vivo* clodronate-depletion experiments. In order to consider possible effects of short-term as well as medium-term macrophage depletion, analyses were performed either at d3 or at d10 (the

latter included two additional successive clodronate administrations at d5 and d8) post primary clodronate treatment, respectively (n=6-8/group, see Figure 31). Lungs from clodronate-treated as well as PBS–treated control mice were removed either on d3 or d10 post treatment and histopathological evaluation of lung tissue sections were performed; the latter especially under the aspect of lung infiltrating lymphocytes. Here, a scoring ranging from 1 to 4 was applied in which 1 means minimal, 2 means moderate, 3 is profound and 4 indicates severe lymphocytic infiltrations.

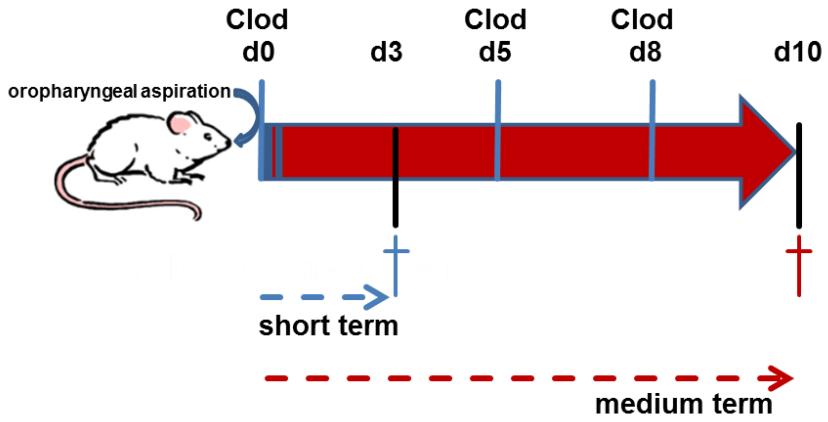

Figure 31: Experimental strategy of clodronate-mediated alveolar macrophage-depletion.

As described in section 5.1.1 lung pathology in SPC-HAxTCR-HA mice is generally characterized by mild to moderate multifocal, peribronchiolar and perivascular lymphocytic infiltrations. Interestingly, already at d3 after macrophage depletion one third of SPC-HAxTCR-HA mice displayed severe lymphocytic infiltrations and at d10 post primary depletion even 50% of SPC-HAxTCR-HA lungs are affected by severe lymphocytic infiltrations. In large contrast, alveolar macrophage depletion in SPC-HA mice is neither associated with lymphocytic infiltrations nor other histopathological manifestations (Figure 32).

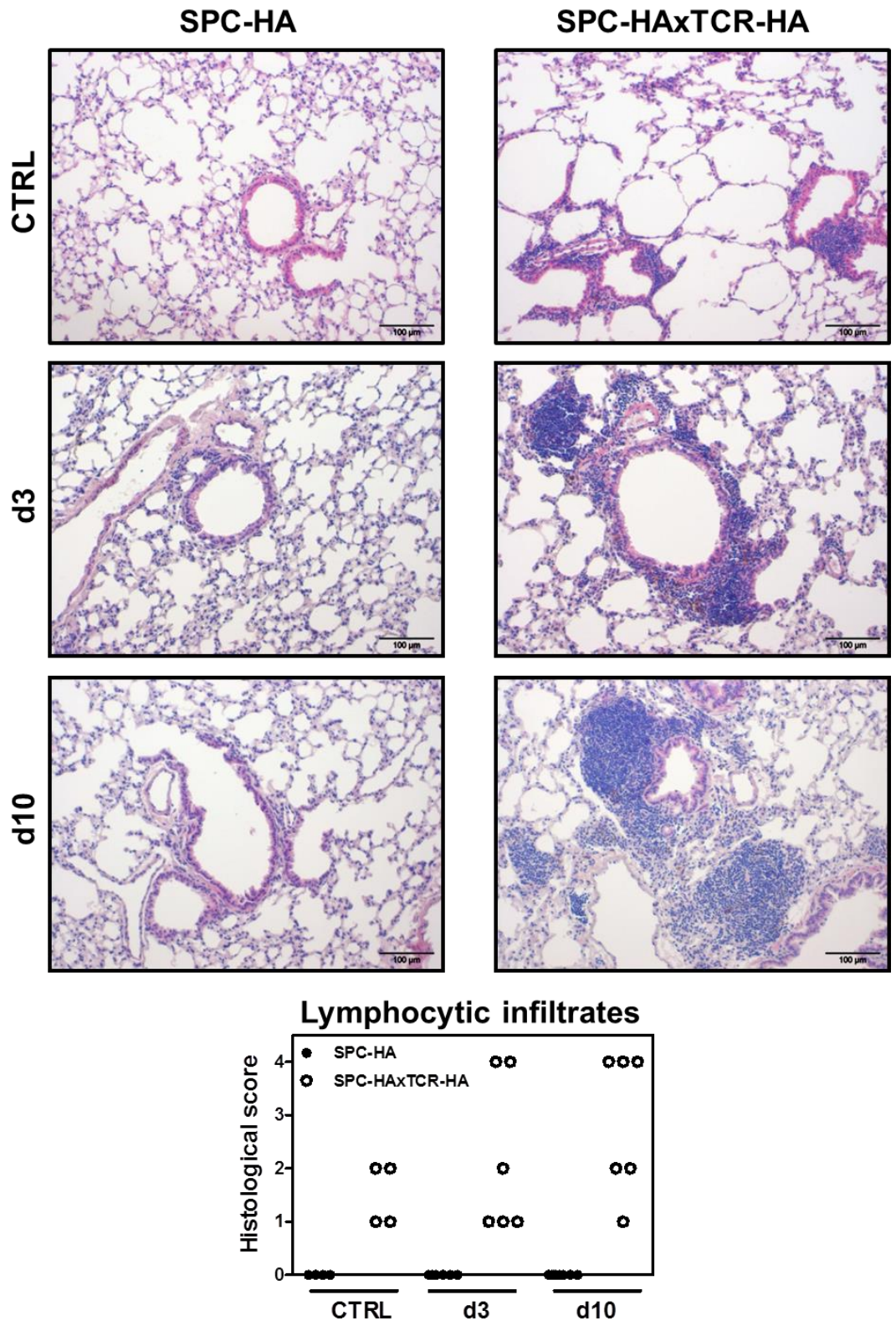

Figure 32: Absence of AMs increases lung pathology in SPC-HAxTCR-HA mice.
SPC-HA and SPC-HAxTCR-HA mice were inoculated with clodronate liposomes according to the scheme in Figure 31. Control mice were inoculated with PBS. At indicated time points post primary clodronate treatment, mice were sacrificed and lung pathology was evaluated by hematoxylin and eosin (H&E) staining. Depicted are representative microscopy images and histological scores indicating the degree of lymphocytic infiltration (1=minimal, 2=moderate, 3=profound, 4=severe) from two independent experiments with similar results.

(n=6-8/group) Black scale bar: 100µm, magnification: 10x

Of note, histopathological analyses also revealed the development of mild to severe multifocal, catarrhal-ulcerous and necrotizing bronchopneumonia at d10 post depletion in SPC-HAxTCR-HA mice, i.e. the presence of mucous and leukocyte - especially neutrophilic granulocytes - exudates as well as tissue necrosis (Figure 33).

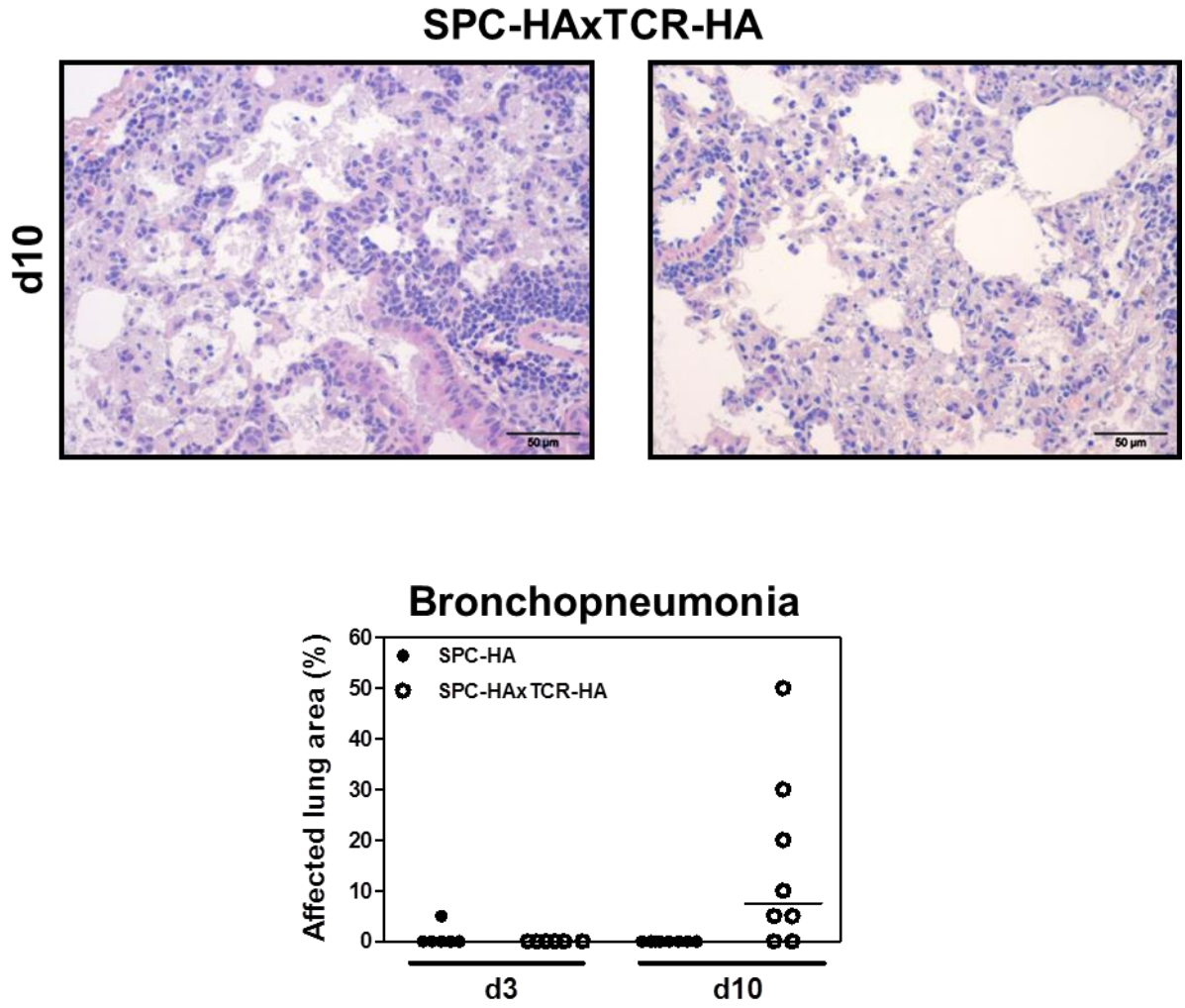

Figure 33: Absence of AMs provokes bronchopneumonia in SPC-HAxTCR-HA mice.
SPC-HA and SPC-HAxTCR-HA mice were inoculated with clodronate liposomes according to the scheme in Figure 31. At d10 post primary clodronate treatment, mice were sacrificed and lung pathology was evaluated by hematoxylin and eosin (H&E) staining. Depicted are representative images and histological scores from SPC-HAxTCR-HA lungs from two independent experiments with similar results.(n=6-8/group). Black scale bar: 50µm, magnification: 20x

Well in line with this finding, flow cytometric analyses of BALF cells from SPC-HA and SPC-HAxTCR-HA mice at d10 post primary depletion revealed a pronounced infiltration of viable neutrophilic granulocytes into the airways of SPC-HAxTCR-HA mice, indicative of florid lung inflammation (Figure 34).

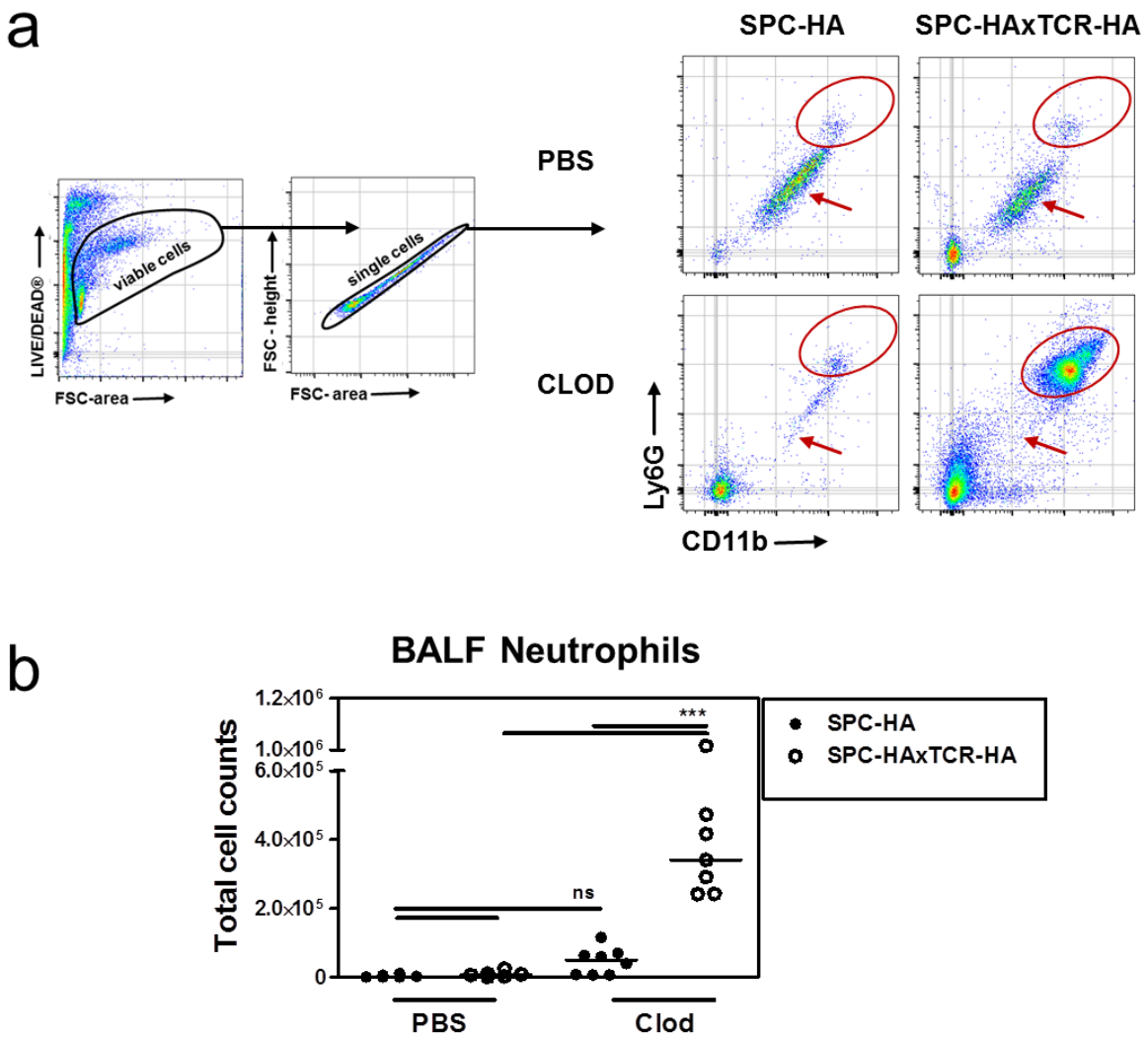

Figure 34: Pronounced neutrophilic airway infiltration in AM-depleted SPC-HAxTCR-HA mice.
SPC-HA and SPC-HAxTCR-HA mice were inoculated with clodronate liposomes according to the scheme in Figure 31. At d10 post primary clodronate treatment, mice were sacrificed and bronchoalveolar lavage cells were analyzed by FACS. Neutrophils were identified as CD11b^{high} and Ly6G^{high} cells (red oval). Alveolar macrophage populations (autofluorescence^{high}) are indicated by red arrows. **(b)** Total neutrophil counts in bronchoalveolar lavage fluid. Data are pooled from two independent experiments with similar outcomes. Statistical significance was calculated using two-way ANOVA followed by Bonferroni post-test. *** p<0.001.

In summary, these data suggest that alveolar macrophages are involved in the maintenance of disease regulation in SPC-HAxTCR-HA lungs. Consequently their absence amplifies the typical disease pattern of chronic, autoimmune-mediated lung inflammation. More importantly, the AM–dependent appearance of non-typical disease pathology (neutrophilic bronchopneumonia) in SPC-HAxTCR-HA mice clearly indicated a unique, previously unknown, regulatory role of these cells within the inflammatory framework of SPC-HAxTCR-HA lungs which needed to be further investigated.

5.2.6 No impact of AM-depletion on CD43 expression on autoreactive T cells

SPC-HAxTCR-HA mice develop severe acute lung inflammation shortly after birth which is associated with strong T cell activation and the resulting pathologic immune responses orchestrated by these cells. Yet, during adolescence immunological tolerance mechanisms are established in SPC-HAxTCR-HA mice. These include reduced proliferative capacity of auto-reactive T cells as well as their conversion into $Foxp3^+$ regulatory T cells (Tregs) and are associated with a state of chronic - but controlled - inflammation in adult SPC-HAxTCR-HA mice (Bruder, Westendorf et al. 2004, Gereke, Jung et al. 2009). Of note, macrophages are able to interfere with T cell activation as well as participate in Treg induction (see section 2.6.1)

Pulmonary macrophages can potently suppress T cell activation by TGFβ and prostaglandins (Roth and Golub 1993). Moreover, AM-derived TGFβ and retinoic acid has been associated with the induction of Tregs (Soroosh, Doherty et al. 2013). Given these macrophage-inherent mechanisms of controlling T lymphocyte immunity and the observation that AM-abolishment coincided with lymphocyte influx in SPC-HAxTCR-HA lungs it seemed conceivable to expect increased activity of the autoreactive T cell pool as a result of the loss of direct or indirect immunoregulatory mechanisms. Accordingly, the observed pathologic neutrophil infiltrations in this group would be a side effect mediated by over-exuberant T cell immune responses and the resulting tissue injury.

In order to test this hypothesis, the role of AMs in immune regulation of HA-specific T cell activation in SPC-HAxTCR-HA lungs was assessed. The number of HA-specific ($CD3^+6.5^+$) T cells in bronchoalveolar spaces (BALF) as well as the lung tissue was determined in PBS-treated and clodronate-treated (d10) SPC-HAxTCR-HA mice. Significantly increased numbers of HA-specific $CD3^+$ T cells were found in BALF from AM-depleted compared to PBS-treated SPC-HAxTCR-HA mice (Figure 35, upper left panel). This was however not accompanied with significantly increased numbers of HA-specific $CD3^+$ T cells in lung tissue from AM-depleted SPC-HAxTCR-HA mice (Figure 35, lower left panel) Moreover, the activation status of HA-specific $CD3^+$ T cells was determined by quantification of the surface marker CD43 (leukosialin). In a model of respiratory virus infection CD43 was shown to be highly expressed on activated memory $CD4^+$ T cells in the BAL fluid as well in the lung tissue (Hogan et al. 2001). Furthermore antigen-specific $CD8^+$ effector T cells have been shown to up-regulate CD43 (Harrington et al. 2000). Using CD43-expression as a readout for cellular activation of HA-specific T cells, no significant differences between T cells isolated from either AM-sufficient and AM-deficient SPC-HAxTCR-HA lungs became apparent (Figure 35, upper and lower right panel).

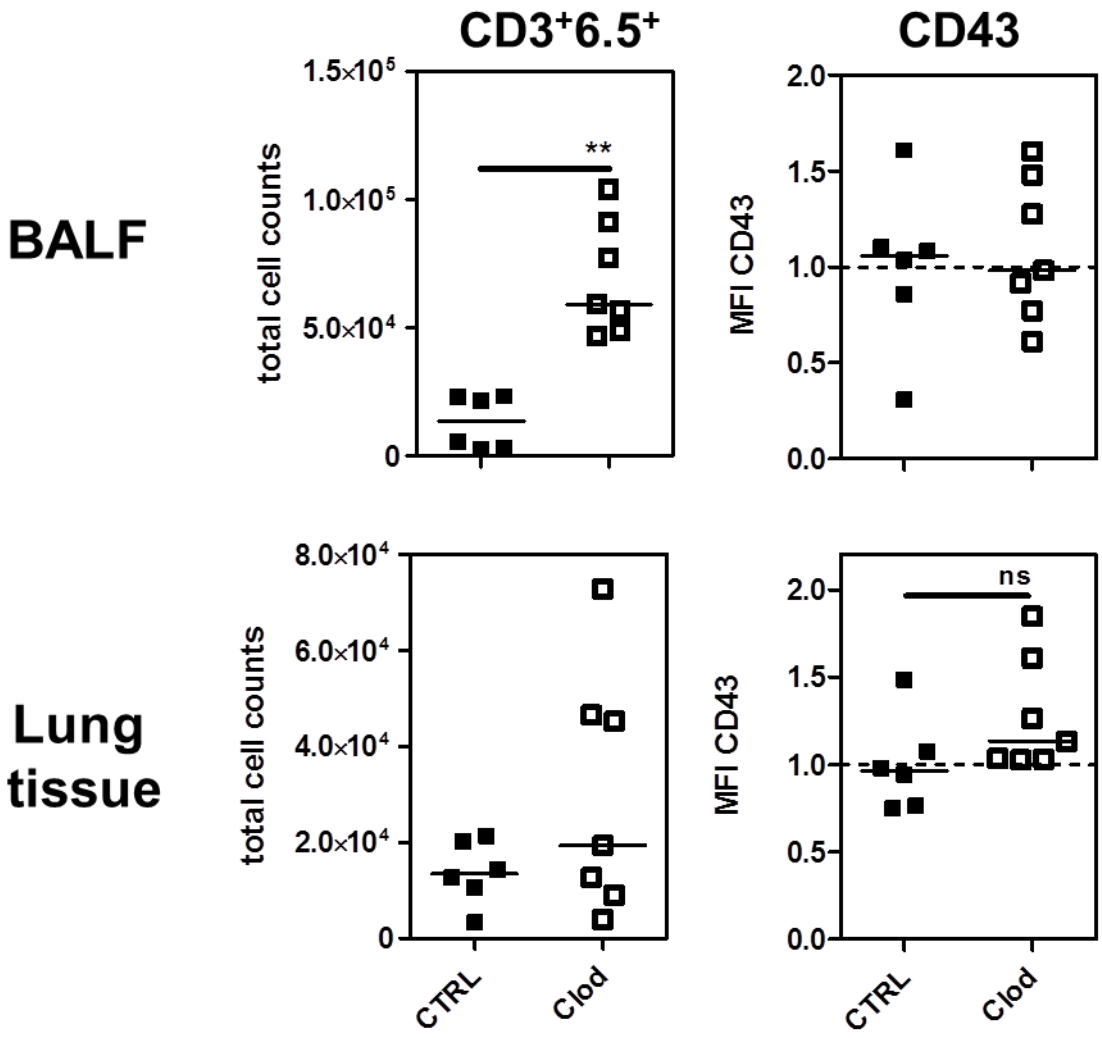

Figure 35: Bronchopneumonia induced by AM-depletion in SPC-HAxTCR-HA mice is not associated with autoreactive T cell activation.

SPC-HAxTCR-HA mice were inoculated with clodronate liposomes (Clod-group) according to the scheme in Figure 31. Control mice were inoculated with PBS (CTRL-group). At d10 post primary clodronate treatment, mice were sacrificed and the number of autoreactive T cells ($CD3^+6.5^+$) in the airways (BALF) and the lung tissue was determined by cell counting and FACS analyses. CD43 expression on $CD3^+6.5^+$ T cells was quantified by assessing CD43 median fluorescence intensity (MFI) and results are expressed as relative fluorescence indices. Depicted are pooled results from two independent experiments with similar results (n=6-7/group). Statistical analyses were performed by using unpaired, two-tailed Mann-Whitney-test. ** p≤0.01

In order to further examine the possible role of AM/T cell interaction (for details see above) in SPC-HAxTCR-HA mice, gene expression of TGFβ (*Tgfβ*), prostaglandin-endoperoxide synthase 2 (*Ptgs2,* catalyzes first conversion step from arachidonic acid to prostaglandins) and retinaldehyde dehydrogenase 2 (*Raldh2,* catalyzes synthesis of retinoid acid from retinaldehyde) in alveolar macrophages from SPC-HA control and SPC-HAxTCR-HA mice was compared. This revealed only a slight (FC<2) up-regulation of all three transcripts in AMs from SPC-HAxTCR-HA mice.

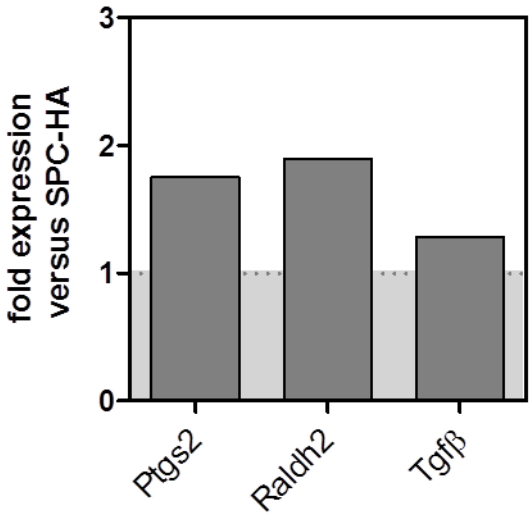

Figure 36: AMs from SPC-HAxTCR-HA mice have slightly elevated expression of genes involved in AM/T cell interaction.
Purified alveolar macrophages from naive SPC-HA and SPC-HAxTCR-HA mice were pooled (n=3-5 mice/group), RNA was extracted and relative expression of indicated transcripts was determined. Gene expression was normalized to the SPC-HA control group.

In summary, these data could not support the hypothesis of a contribution of the AM/T cell axis to immunoregulatory mechanisms in SPC-HAxTCR-HA lungs. Accordingly, pathologic immune responses of re-activated self-antigen specific T cells do not – or only partly - contribute to the histopathological findings in AM-depleted SPC-HAxTCR-HA lungs. It is however possible that AM-depletion (albeit not linked to amplified T cell activation, as shown by unchanged expression of CD43) could indirectly affect T cell mechanisms by e.g. changing the effector T cell/Treg ratio. Yet, it appears also greatly conceivable that the increased numbers of intra-alveolar HA-specific T cells could be indicative of a passive influx of lymphocytes, most likely as a result of the neutrophilic inflammation coinciding with increased epithelial and/or endothelial permeability.

5.2.7 ATII cells from SPC-HAxTCR-HA mice express increased levels of neutrophil-attractants in steady state steady state and pathological conditions

In mice the human IL-8 analogues CXCL1, CXCL2 and CXCL5 - all signal via CXCR2 on the neutrophil surface - were shown to be involved in neutrophil mobilization into the inflamed airways. This recruitment is usually a result of concerted chemokine production by myeloid and airway epithelial cells (Pittet, Quinton et al. 2011, Yamamoto, Ahyi et al. 2014). However, by the effective depletion of alveolar macrophages (Figure 30, upper panel) these cells were withdrawn from being the cellular source of these chemokines in SPC-HAxTCR-HA lungs - and consequently from actively orchestrating the development of neutrophilic bronchopneumonia. As ATII cells have previously been shown to be important producers of these molecules (Farnand et al. 2011, Bello-Irizarry et al. 2012, Gibbs, Ince et al. 2014) these cells were subjected for further investigation. To this end, SPC-HA and SPC-HAxTCR-HA mice were treated as described in Figure 31 with either PBS or clodronate liposomes and at d10 post primary treatment ATII cells were isolated by FACS using a previously described

sorting method (Gereke, Autengruber et al. 2012). Briefly, whole lung tissue homogenates were enzymatically digested and pooled samples of lung cell suspensions were fluorescently labelled with antibodies against the lineage markers CD45, CD11c, F4-80, CD11b, CD16/32 and CD19. In flow cytometric sorting ATII cells were identified by their SSC^{high} and lineage-negative profile (Figure 11). This sorting strategy yielded ATII cells with a purity between 83 and 88% (data not shown). RNA from sorted ATII samples was extracted and relative expression of the genes *Cxcl1*, *Cxcl2* and *Cxcl5* was analyzed by qRT-PCR. In Figure 37 RNA transcript levels (expressed as relative levels compared to housekeeping gene *Actb*) in ATII cells from PBS-treated and clodronate treated SPC-HA and SPC-HAxTCR-HA mice are depicted.

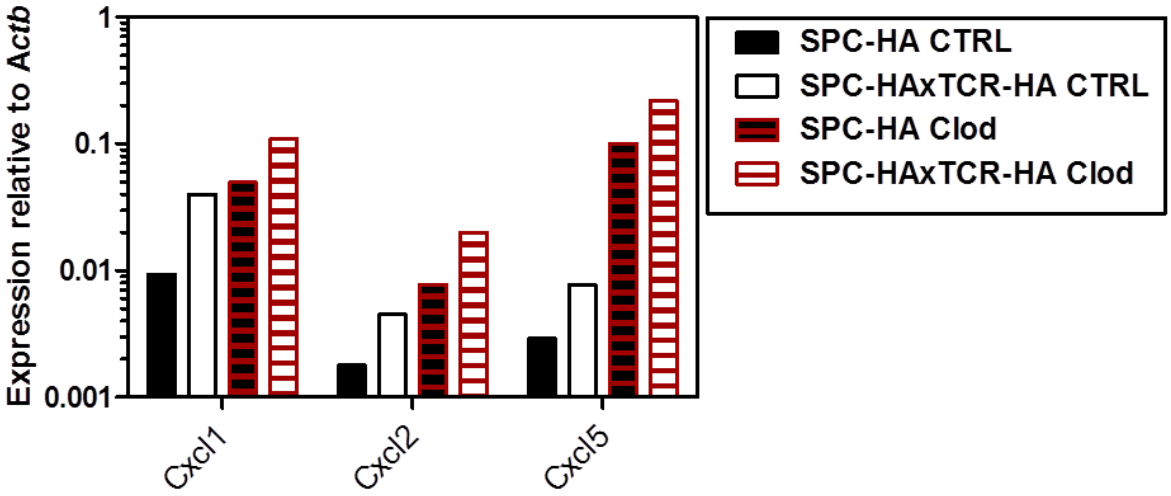

Figure 37: Increased RNA-levels of neutrophil-attracting chemokines in ATII from SPC-HA-HAxTCR-HA mice in steady state (AM-sufficient) and pathological (AM-deficient) conditions.
SPC-HA and SPC-HAxTCR-HA mice were treated according to Figure 31 with either PBS (CTRL-group) or clodronate liposomes (Clod-group). At d10 post primary clodronate treatment ATII cells were isolated by FACS, RNA of pooled samples (n= 5-6 mice/group) was extracted and transcript levels of indicated genes were quantified by qRT-PCR. Results are expressed as the ratio: gene of interest vs. the housekeeping gene beta-actin (*Actb*).

Additionally, individual fold changes between groups were calculated and are presented in Table 7, Table 8 and Table 9, respectively. Comparison of gene expression in steady state conditions (PBS-treated control groups) generally revealed increased expression of all three chemokines in ATII cells from SPC-HAxTCR-HA mice (FC *Cxcl1* 4.3; *Cxcl2* 2.5; *Cxcl5* 2.7). Interestingly, clodronate-induced AM-abolishment was intimately linked to the induction of *Cxcl1*, *Cxcl2* and *Cxcl5* in ATII cells from SPC-HA as well as SPC-HAxTCR-HA mice. Notably, especially the induction of *Cxcl5* transcripts was greatly enhanced in SPC-HA (FC over PBS-group 34.4) as well as SPC-HAxTCR-HA mice (FC over PBS-group 28.5). By comparing ATII transcript levels between AM-depleted SPC-HA and AM-depleted SPC-HAxTCR-HA groups it was found that all three chemokine transcripts were up-regulated in ATII from the SPC-HAxTCR-HA group (FC *Cxcl1* 2.2; *Cxcl2* 2.6; *Cxcl5*: 2.2, see Table 7, Table 8 and Table 9).

Table 7: List of calculated fold changes (FCs) of *Cxcl1* gene expression in ATII cells.
Individual FCs are read as the ratio: group of interest (column) vs. group of reference (row).

Cxcl1	**SPC-HA CTRL**	**SPC-HAxTCR-HA CTRL**	**SPC-HA Clod**	**SPC-HAxTCR-HA Clod**
SPC-HA CTRL	**1.0**	4.3	5.3	11.8
SPC-HAxTCR-HA CTRL		**1.0**	1.3	2.8
SPC-HA Clod			**1.0**	2.2
SPC-HAxTCR-HA Clod				**1.0**

Table 8: List of calculated fold changes (FCs) of *Cxcl2* gene expression in ATII cells.
Individual FCs are read as the ratio: group of interest (column) vs. group of reference (row).

Cxcl2	**SPC-HA CTRL**	**SPC-HAxTCR-HA CTRL**	**SPC-HA Clod**	**SPC-HAxTCR-HA Clod**
SPC-HA CTRL	**1.0**	2.5	4.4	11.2
SPC-HAxTCR-HA CTRL		**1.0**	1.7	4.5
SPC-HA Clod			**1.0**	2.6
SPC-HAxTCR-HA Clod				**1.0**

Table 9: List of calculated fold changes (FCs) of *Cxcl5* gene expression in ATII cells.
Individual FCs are read as the ratio: group of interest (column) vs. group of reference (row).

Cxcl5	**SPC-HA CTRL**	**SPC-HAxTCR-HA CTRL**	**SPC-HA Clod**	**SPC-HAxTCR-HA Clod**
SPC-HA CTRL	**1.0**	2.7	34.4	75.6
SPC-HAxTCR-HA CTRL		**1.0**	13.0	28.5
SPC-HA Clod			**1.0**	2.2
SPC-HAxTCR-HA Clod				**1.0**

In summary, these data generally imply an altered chemokine regulation of ATII cells in the chronically inflamed lung which is well in line with previously published data (Gereke, Grobe et al. 2007). Moreover, it became apparent that alveolar macrophages regulate the expression of ATII-derived neutrophil-chemoattractants – especially CXCL5 - in healthy as well as pre-diseased lungs by means of so far unclear mechanisms. Given however this universal AM-inherent immunomodulatory function, it remains elusive whether the observed differences in ATII-derived CXC-chemokine levels between AM-depleted SPC-HA and SPC-HAxTCR-HA mice are sufficient and causative for the pathologic, neutrophil airway infiltrations that are exclusively detected in SPC-HAxTCR-HA lungs.

5.2.8 Bronchopneumonia in AM-depleted SPC-HAxTCR-HA mice is not mediated by MAMP-dependent pulmonary immune responses

By the intrinsic development of a pulmonary leak in SPC-HAxTCR-HA mice (Figure 12c), increased amounts of blood components diffuse into the airways thereby inevitably providing this compartment with serum-derived nutrients and consequently potential benefits for microbial growth. Alveolar macrophages critically contribute to airway homeostasis by their function as pulmonary scavengers, i.e. they clear microbes from the lower respiratory tract and thereby antagonize microbial outgrowth in the lung. As the depletion of AMs coincided with neutrophil-dominated bronchopneumonia (Figure 33, Figure 34) - which is a typical hallmark of respiratory bacterial infection - it seemed likely that immune responses towards the increase of microbial associated molecular patterns (MAMPs) are involved in the observed histopathological manifestations. These are likely driven by airway epithelial cells, as they possess a wide array of pathogen-recognition receptors (PRRs) and were shown to produce neutrophil-attractant chemokines following PRR stimulation (Cai et al. 2010, Gibbs, Ince et al. 2014, Jeyaseelan et al. 2005). Importantly the finding of increased IL-8 analogues in ATII following clodronate treatment (Figure 37) corroborated the idea of MAMP-dependent neutrophil recruitment in SPC-HAxTCR-HA lungs. Accordingly, reducing the lower airway microbial burden would ultimately prevent or decrease neutrophil infiltrations in the lungs of AM-depleted mice. To test this hypothesis, mice were treated with broad-spectrum antibiotics (ABX) for 20 days prior to clodronate treatment and during the following 10 days post primary clodronate administration (Figure 38). As readout for antibiotic efficacy bacterial loads in the trachea and lung were determined by cultivation of tissue homogenates on Columbia Agar, incubation for 1 day (37°C, 5% CO_2) and subsequent CFU counting.

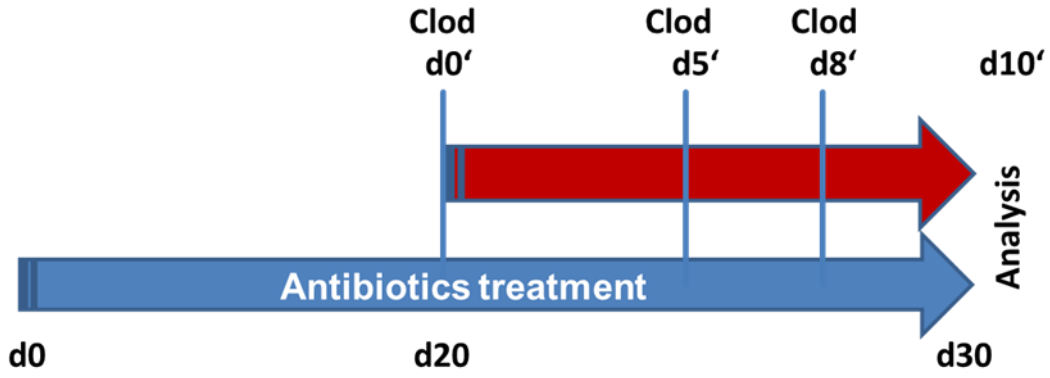

Figure 38: Experimental strategy for antibiotics-mediated airway microbiota reduction.
For oral antibiotics (ABX) treatment ampicillin and chloramphenicol and sucrose were added to the drinking water. Control (CTRL) mice received sucrose water only.

ABX-treatment clearly led to a reduction of the trachea bacterial flora (Figure 39a). In lung tissue no CFU were detectable at all times independent of ABX treatment (data not shown). Despite the clear CFU reduction, continuous ABX treatment did not reduce pronounced neutrophil airway infiltration in clodronate-treated SPC-HAxTCR-HA mice (Figure 39b) indicating neutrophil influx to be MAMP-independent.

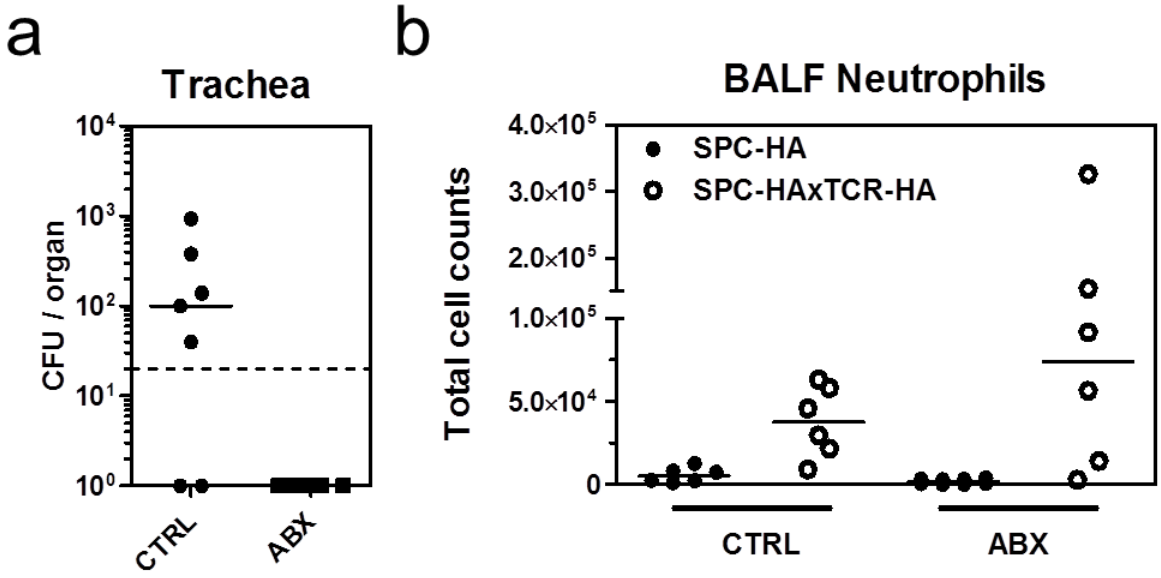

Figure 39: MAMP-driven immune responses do not contribute to bronchopneumonia in AM-depleted SPC-HAxTCR-HA lungs.
(a) SPC-HA and SPC-HAxTCR-HA mice were treated with antibiotics (ABX), control animals received sucrose water. After 10d mice were sacrificed and bacterial burden in tracheal tissue was determined by plating tissue homogenates on Columbia blood agar plates. Dashed line indicates limit of detection. **(b)** SPC-HA and SPC-HAxTCR-HA mice were treated with antibiotics (ABX) or sucrose water (CTRL) and alveolar macrophages were depleted according to scheme in Figure 38. At 10d post depletion neutrophils in the BALF were quantified by FACS and cell counting.

Collectively, these results suggest that the neutrophil-dominated disease phenotype in AM-depleted lungs of SPC-HAxTCR-HA mice is a consequence of the established T cell-induced chronic inflammatory microenvironment and more specifically the accompanied reprogramming of the lung epithelium itself which in steady state conditions may be counter-regulated by direct or indirect interactions with appropriately programmed AMs adapted to the same milieu.

6 Discussion

6.1 Chronic lung inflammation and pneumococcal infection

While it has been extensively studied and is widely accepted that viral priming of the respiratory tract manifests in a poor outcome of secondary bacterial infection (Habibzay, Weiss et al. 2013), analogous research focusing on non-viral and non-infectious settings is yielding controversial results, thus demanding a more complex view on pulmonary inflammatory networks. Airway epithelial cells (AECs) and alveolar macrophages (AMs) are key cellular components of the pulmonary network. Given their large array of receptors and effector molecules and their multifaceted roles for protective immunity during pulmonary infection (see section 2), the specific contributions of particular cell functions of AECs and AMs to antibacterial defense in hosts with chronic respiratory disease (CRD) were of special interest for this study.

In this work the SPC-HAxTCR-HA transgenic mouse model for T cell-mediated lung inflammation was utilized. In these mice the concomitant expression of a neo-self-antigen (HA) by alveolar type II epithelial cells (ATII) and the generation of self-antigen specific (HA-specific) $CD4^+$ T lymphocytes evokes the development of autoimmune pulmonary inflammation in newborn mice as well as the rapid induction of a complex set of immunoregulatory mechanisms (e.g. conversion of HA-specific $CD4^+$ T cells into $Foxp3^+$ regulatory T cells), finally leading to chronic, yet controlled, lung inflammation in adult SPC-HAxTCR-HA mice (Bruder, Westendorf et al. 2004, Gereke, Grobe et al. 2007, Gereke, Jung et al. 2009). Despite different etiologies, a participation of lymphocyte immune responses has been suggested for the pathogenesis of several chronic respiratory disorders such as COPD (Cosio et al. 2009), sarcoidosis (ATS&ERS,1999) and allergic lung inflammation (ALI; Schaller et al. 2005) and SPC-HAxTCR-HA lungs phenocopy histopathological manifestations of human CRD e.g. airway remodeling and lymphocytic infiltrations (Bruder, Westendorf et al. 2004). The well-established SPC-HAxTCR-HA model therefore represents an appropriate and valuable tool to study the impact of CRD on respiratory pneumococcal infection *in vivo*. In murine infection models the human pneumococcal isolate TIGR4 was previously shown to cause pneumonia as well as invasive pneumococcal disease (IPD; Sandgren, Albiger et al. 2005), therefore this serotype 4 strain was chosen for all experiments in this study aiming to elucidate the impact of CRD on local antibacterial defense as well as on the development of IPD.

The present study revealed sterile lung inflammation to involve marked immune pathology (Figure 12a) and a compromised pulmonary barrier, leading to increased diffusion of serum components, like albumin (Figure 12c), into the airways of SPC-HAxTCR-HA mice. Besides ubiquitous antibodies and complement proteins serum also contains a plethora of factors essential for pneumococcal survival and virulence such as glucose, amino acids and trace elements. Accordingly the “serum-enriched” airspaces of SPC-HAxTCR-HA mice can be assumed to provide a potential benefit for bacterial outgrowth. In addition, reduced barrier integrity as a consequence of low tight junction protein expression has been described to correlate with enhanced pneumococcal transmigration and invasion of lung epithelial and endothelial cells (LeMessurier, Hacker et al. 2013). Unexpectedly, infection experiments with *S. pneumoniae* TIGR4 revealed increased resistance of SPC-HAxTCR-HA mice to

pneumococcal growth and pulmonary invasion as well as to the subsequent development of IPD (Figure 13), thereby linking chronic lung inflammation to a protective microenvironment in SPC-HAxTCR-HA mice. In accordance with this finding, it was recently shown that mice with allergic lung inflammation (ALI) displayed increased protection to respiratory infection with an invasive pneumococcal serotype 3 strain which was associated with enhanced phagocytic capacity of a newly recruited population of AMs in ALI-mice (Sanfilippo et al. 2015).

Phagocytic AMs are among the first cells to encounter pathogens immediately after pulmonary infection. Of note, by using mice deficient for the phagocytic receptors MARCO (macrophage receptor with collagenous structure) or CD36 it has been shown that AM phagocytosis is a process that critically contributes to pulmonary defense following infection with *S. pneumoniae* (Arredouani, Yang et al. 2004, Sharif, Matt et al. 2013). Given the pivotal role of AM phagocytosis and the rapid decline in pulmonary bacterial burden observed in SPC-HAxTCR-HA mice, it seemed conceivable that enhanced macrophage bacterial uptake might contribute to improved antipneumococcal immunity in SPC-HAxTCR-HA mice. Probing this hypothesis with *in vivo* phagocytosis assays however revealed similar phagocytic capacities between AMs from SPC-HA and SPC-HAxTCR-HA mice. Also by quantitative analyses of AM numbers no significant differences between healthy SPC-HA and pre-diseased SPC-HAxTCR-HA mice became apparent (Figure 14), thereby ruling out numerical AM overrepresentation as a cause for enhanced early bacterial clearance in SPC-HAxTCR-HA lungs. In contrast, several human and mouse studies demonstrated however elevated macrophage numbers in the airspaces of individuals with COPD (Barnes 2004), emphysema (Finkelstein, Fraser et al. 1995) and ALI (Draijer et al. 2013, Lee et al. 2015), which is believed to be a consequence of the constant inflammatory recruitment of these cells. These opposing facts may in turn imply a lack of inflammatory intra-alveolar macrophage recruitment in SPC-HAxTCR-HA mice. Yet the fact that the aforementioned diseases underlie different etiologies and appear with varying severity, involving heterogeneous environmental factors which all shape the inflammatory milieu, makes direct comparisons of inflammatory conditions in different CRDs difficult. Moreover, this strongly emphasizes the need for better understanding and defining the inflammatory milieus in CRDs in order to appropriately interpret phenotypic or functional observations made on the cellular level.

Interestingly, the inflammatory milieu in SPC-HAxTCR-HA mice cannot be defined by typical indicators of acute inflammatory responses like IL-6 and TNF-α (Figure 15). Being innate cytokines, TNF-α and IL-6 control a series of immunological reactions during early infection e.g. acute-phase protein responses (IL-6; Kopf et al. 1994), regulation of other pro-inflammatory cytokines and control of pulmonary bacterial growth (IL-6; van der Poll, Keogh, Guirao et al. 1997) as well as control of macrophage-dependent cytotoxity (TNF-α; Fan, Fehr et al. 1991). Both molecules were shown to be required for host defense during pulmonary pneumococcal infection (van der Poll, Keogh, Buurman et al. 1997, van der Poll, Keogh, Guirao et al. 1997). As neither of these two cytokines was detectable in SPC-HA and SPC-HAxTCR-HA mice, it is likely that IL-6/TNF-α triggered mechanisms most likely are not involved in the generation of improved immunity towards *S. pneumoniae*. Still, several groups described beneficial effects of inflammatory imprinting in the lung on antimicrobial defense. Inflammatory imprinting induced by mucosal administration of LPS (Errea, Moreno et al. 2010), mutant *E.coli* enterotoxin (Tritto, Muzzi et al. 2007) or nontypeable *Haemophilus influenzae* lysate (Clement et al. 2008, Evans, Scott et al. 2010, Tuvim, Evans et al. 2009) involved among others both local (airways) and systemic (serum) increases in IL-6 and TNF-

α. A conceivable explanation for these differing findings is the type of immunologic trigger in SPC-HAxTCR-HA mice. In large contrast to the aforementioned studies inflammatory imprinting in SPC-HAxTCR-HA lungs is not generated by a singular PAMP receptor stimulation (and the resulting early immune response within several hours) but rather includes a complex network of auto-reactive and tolerogenic mechanisms and cell subsets, respectively (Bruder, Westendorf et al. 2004, Gereke, Grobe et al. 2007, Gereke, Jung et al. 2009). In summary, the absence of IL-6 and TNF-α in SPC-HAxTCR-HA mice is indicative of the non-acute quality of lung inflammation in these animals.

In order to precisely define the inflammatory milieu in SPC-HAxTCR-HA lungs and to identify molecular pathways or single molecules, respectively, that account for the protective microenvironment in SPC-HAxTCR-HA lungs comparative transcriptomic and proteomic analyses were performed. To this end gene expression in whole lung tissue from uninfected SPC-HA vs. SPC-HAxTCR-HA mice was analyzed by whole-genome microarray analyses. In addition, the protein composition of the lung mucosal fluid (BALFome) of both mouse groups was compared by using LC-MS/MS technology. These experiments generally revealed a multitude of genes (378) and proteins (473) likely to participate in the chronic inflammatory environment of SPC-HAxTCR-HA lungs (see sections 5.1.5, 5.1.6 and 7).

Remarkably, a fairly large number of proteins (129) were uniquely found in healthy SPC-HA airways (Table 13). This could be indicative of specific post-transcriptional mechanisms that control airway protein expression and/or stability in SPC-HAxTCR-HA airways. This is supported by the finding that only 52 transcripts were found by whole-lung microarray analyses to be over-represented in SPC-HA lungs as compared to SPC-HAxTCR-HA lungs (Table 11). One example of such a regulatory mechanism accounting for the divergence between gene expression and protein levels might apply to the polymeric Ig receptor (pIgR) whose modest increase in transcript numbers found by microarray analyses and qRT-PCR (Table 10, Figure 23a) was surprisingly associated with high pulmonary protein levels in the SPC-HAxTCR-HA group while being scarcely detectable in SPC-HA lungs (Figure 23b,c).

Due to the nature of the biological samples (whole lung tissue) analyzed in this study, the net differences in relative transcripts levels are influenced by numerical differences in cell types expressing a particular transcript as well as quantitative transcript differences on the single cellular level. With reference to the KEGG pathway enrichment analyses the GO terms found to be over-represented in SPC-HAxTCR-HA lungs (e.g. *T cell receptor signaling pathway*, *Chemokine signaling pathway* and *Cytokine-cytokine receptor interaction*, Table 6) can therefore be derived from an altered regulation of particular leukocyte signaling pathways but as well from the different pulmonary cellular composition found in this group (Bruder, Westendorf et al. 2004).

The antimicrobial peptides (APs) “cathelin-related antimicrobial peptide” and lactotransferrin were uniquely detected in airway mucosal lining fluid of SPC-HAxTCR-HA mice (Table 14). Lactotransferrin binds to *S. pneumoniae* (Hammerschmidt et al. 1999), however its antipneumococcal activity has been questioned and binding to lactotransferrin has been suggested as a pneumococcal iron-supply mechanism (Lee et al. 2004). Interestingly, AECs are potent producers of APs (Bals 2000) and other groups have previously shown that AECs have a key role in AP-mediated inducible host defense against pathogens (Cleaver, You et al. 2014, Evans, Scott et al. 2010). Altogether, the present study could not exclude a

potential connection between mucosal AEC-derived APs and the enhanced innate resistance towards *S. pneumoniae*. Moreover, the proteome analyses give no information on the cellular source of these molecules. It is however reasonable to assume that the substantial differences in protein composition between airway mucosal lining fluid from SPC-HA vs. SPC-HAxTCR-HA mice most likely reflect a combination of altered production rates by lung-resident cells, altered active transepithelial transport and passive transepithelial diffusion of serum or interstitial components (Figure 12c). In view of this assumption the minimal overlap of only 10 proteins between induced genes and BALF proteins uniquely identified in SPC-HAxTCR-HA mice becomes more significant (Figure 21b). These overlapping proteins found in the BALF of SPC-HAxTCR-HA mice are to be derived either from increased local production by bronchoalveolar cells (AECs or AMs) or from increased production and transport from cells from adjacent interstitial compartments.

Importantly, the extensive description of the inflammatory milieu by means of microarray and proteomics approaches allows concluding one major effect of chronic inflammatory imprinting: the development of secretory immunoglobulin-specific patterns in SPC-HAxTCR-HA lung tissue as well as in the airway mucosal lining fluid. This finding was of particular interest as secretory immunoglobulins (SIgs) as well as their exclusive transepithelial transporter, the polymeric immunoglobulin receptor (pIgR) have previously been shown to be critically involved in mucosal antibacterial defense (Blutt, Miller et al. 2012, Brown, Hussell et al. 2002, Sun, Johansen et al. 2004, Tjarnlund, Rodriguez et al. 2006). Thus, in order to estimate a possible role of pIgR and SIgs in enhanced immunity to pneumococci in SPC-HAxTCR-HA lungs, pIgR-expression in lung tissue as well as SIg levels in the airway mucosal fluid (BALF) were compared in uninfected SPC-HA and SPC-HAxTCR-HA mice.

In accordance with previous studies (Jaffar, Ferrini et al. 2009, Ohlmeier et al. 2012) lung inflammation was associated with elevated epithelial expression of pIgR in SPC-HAxTCR-HA mice (Figure 23c). Mechanistically, in SPC-HAxTCR-HA mice self-antigen recognition after birth is associated with a transient activation of autoreactive $CD4^+$ T cells leading to acute, severe pneumonitis in young mice (Bruder, Westendorf et al. 2004). Upon activation self-specific $CD4^+$ T cells secrete IFN-γ (Bruder, Westendorf et al. 2004, Huang et al. 2003), a potent inducer of pIgR-expression *in vitro* (Sollid, Kvale et al. 1987). Furthermore, transcriptomic analyses of auto-reactive $CD4^+$ T cells from SPC-HAxTCR-HA mice revealed IL-17 gene induction in these cells (Bruder, Westendorf et al. 2004). In consideration of the fact that IL-17 signaling has formerly been shown to substantially enhance pIgR-expression (and consequently SIg transcytosis through the epithelium) in airway (Jaffar, Ferrini et al. 2009) and intestinal mucosal inflammation (Cao, Yao et al. 2012), it becomes likely that IL-17 secretion by self-specific $CD4^+$ T cells might effect pIgR-mediated SIg transport onto the mucosal surface in SPC-HAxTCR-HA mice. However, given the known pleiotropic factors (cytokines, hormones, dietary factors) identified as regulators of pIgR-expression (Table 1), it remains unclear whether pIgR-induction is a consequence of the effector T cell phase in newborn SPC-HAxTCR-HA mice or rather a hallmark of immunoregulatory mechanisms that are established during their adolescence.

A correlation between inflammation and pIgR-expression was also demonstrated for human CRD by Ohlmeier and colleagues who found in a proteomics approach elevated pIgR levels in sputum, alveolar and bronchial epithelium of smokers and individuals with mild-to-moderate COPD (Ohlmeier, Mazur et al. 2012). These findings were further extended by Gohy et al. who described bronchial epithelial pIgR-downregulation to correlate with disease

severity in COPD patients and showed that $TGF\beta_1$ and possibly the epithelial reprogramming pathways orchestrated by this protein inhibit pIgR-expression in advanced COPD (Gohy, Detry et al. 2014). In this regard, it would be interesting to clarify whether a direct correlation between the levels of pulmonary pIgR-expression and the incidence of bacterial infections in the respective COPD patient cohorts exists.

Several studies addressed also a direct role of pIgR in the pathogenesis of bacterial disease in potentially promoting bacterial invasion. It was shown *in vitro* that the pneumococcal surface protein CbpA interacts with human pIgR (Zhang et al. 2000). Furthermore, CbpA protein revealed to be involved in pneumococcal transmigration of the murine blood-brain barrier (Orihuela et al. 2004) and pneumococci even co-localize with murine pIgR expressed on endothelial cells (Iovino et al. 2014). In contrast, Sun et al. described *in vivo* that abrogated mucosal SIgA transport in vaccinated pIgR knockout mice caused a loss of protection against nasopharyngeal pneumococcal colonization despite the presence of an otherwise proper vaccine-induced humoral immunity. This emphasizes the necessity of pIgR and SIgs in airway antipneumococcal immunity *in vivo* (Sun, Johansen et al. 2004).

One key reason for the abovementioned conflicting *in vitro* vs. *in vivo* findings with regard to pIgR function might be the restricted complexity of *in vitro* conditions. These poorly mimic the *in vivo* situation where increased pIgR-expression inevitably leads to a reinforcement of mucosal surfaces by SIgs (Cao, Yao et al. 2012, Jaffar, Ferrini et al. 2009) thereby compensating the fact that pIgR can in principle adhere to epithelial cells. Accordingly, by quantifying the levels of airway immunoglobulins this study confirmed that pIgR up-regulation ultimately provokes increased airway sIgA and IgM contents in SPC-HAxTCR-HA mice as compared to SPC-HA mice (Figure 22).

By using mice deficient for pIgR or its cargo molecules IgA and IgM, several groups have demonstrated a central role of the SIg axis in controlling airway pneumococcal burden and tissue invasion (Brown, Hussell et al. 2002, Sun, Johansen et al. 2004). Importantly, recurrent respiratory infections are comorbidities associated with selective IgM or IgA deficiencies in humans (Latiff and Kerr 2007, Louis and Gupta 2014). Following the hypothesis that enhanced antipneumococcal resistance in SPC-HAxTCR-HA mice directly originated from increased airway mucosal SIgA or SIgM concentrations, pneumococcal binding assays were performed. Indeed, significantly increased IgA and IgM coverage of pneumococcal surfaces as well as increased portions of IgM^+ pneumococci using SPC-HAxTCR-HA BALF could be detected. Comparison of the fractions of IgA^+ vs. IgM^+ pneumococci generally revealed that larger fractions of bacteria were IgA^+ (~4-17%) whereas IgM^+ fractions ranged only between ~0.2-1.5% (Figure 24). This finding likely resembles individual abundances of IgA and IgM in BALF (Figure 22), different binding affinities or -kinetics of IgA and IgM.

In conclusion, based on the data obtained in this part of the thesis, the following mechanism (summarized in **Figure 40**) is proposed: Alveolar self-antigen (HA) recognition by self-antigen specific CD4+ T cells effects autoimmune-mediated lung inflammation. As a result of inflammatory pathways during acute inflammatory phase and/or immunoregulatory mechanisms established during adolescence, ATII cells up-regulate pIgR-expression. Increased pIgR-expression effects increased transcytosis of natural IgA & IgM (produced locally and/or transported into the lung via the blood stream) into the alveoli, SIgA and SIgM

bind to *S. pneumoniae* and antagonize pneumococcal outgrowth and invasion by immune exclusion and complement-dependent pathways.

While lower airway colonization with bacterial pathogens such as *Streptococcus pneumoniae* has been identified to be present in 25-50% of COPD patients (Wedzicha et al. 2003), details of the causal relationship between colonization and infection, respectively, and disease exacerbations are under debate. In stable disease the airway CFU burden was found to correlate with airway inflammatory markers, and thus infection is intimately linked to inflammation (Hill et al. 2000). Also, it was demonstrated that colonization is associated with increased exacerbation frequency (Patel et al. 2002). In principle two conceivable mechanisms might underlie these observations, either as single or as concurring causes. Firstly, it is possible that bacterial infections in those patients occur as results of insufficient host defense (e.g. decreased mucociliary clearance, dysfunctional alveolar macrophages) and thus increased bacterial growth and the associated increase in PAMPs as well as bacterial cytotoxic products cause (immune) pathology. Secondly, as a consequence of a chronic inflammatory microenvironment (associated with a wide range of constant immunologic triggers) an inflammation-induced reprogramming of innate immune cells (e.g. AEC) manifests in a dysregulation of PAMP-receptor pathways (e.g. TLR expression and downstream signaling cascades) resulting in inappropriate, exuberant immune responses to microbial ligands and thus the development of an exacerbation. In this regard, by using the SPC-HAxTCR-HA model two basic cellular adaptations that in principle could promote the development of an infection-induced exacerbation were identified: the blunted AM-dependent pro-inflammatory immune response towards pneumococcal ligands as well as the inflammation-primed ATII cells, which upon loss of AMs drive the development of neutrophilic bronchopneumonia even in an environment with low or no MAMPs (see section 5.2.8, Figure 39). Despite the unexpected finding of a beneficial role of inflammation-induced microenvironmental changes (i.e. pIgR-mediated SIg transport) in the pre-diseased lung, the fashion and magnitude of an AM- and AEC-dependent pro-inflammatory immune response during the course of an actual pneumococcal infection has so far not been addressed and thus remains subject for future investigation.

The evidence of pIgR/SIg mechanisms as effectors of improved respiratory immunity is of fundamental interest for future investigations. Despite the findings of unaltered phagocytosis in the SPC-HAxTCR-HA model, patients with severe asthma and COPD are frequently diagnosed with impaired AM capacity (Berenson, Garlipp, et al. 2006, Liang et al. 2014), thus revealing insufficient myeloid-dependent host defense while at the same time underlining the important role of humoral immunity and the airway epithelium in ensuring broad protection against airborne pathogens.

Further studies are needed to explore whether prophylactic pIgR-enhancement serves as a therapeutic strategy for CRD patients with recurrent pneumococcal infections. Here, the mode of pIgR-induction would be of utmost importance as several immunologic stimuli that have been shown to enhance pIgR-expression also are considered to be key components involved in the pathogenesis of CRD. For example, the pIgR-inducing cytokine IL-17 also effects the production of neutrophil-attracting chemokines in AECs (Liu et al. 2011) and airway smooth muscle cells (Dragon et al. 2007) and is thus discussed to participate in neutrophilic lung inflammation in asthma and COPD (Barnes 2008). Moreover, pIgR-inducing IFN-γ is believed to play an important role in COPD pathogenesis, as it orchestrates the infiltrations of Th1 and Tc1 cells into the lung by upregulating chemokines as well as

chemokine receptors on these cells (Barnes 2008). Given the aforementioned two examples of pIgR-inducers, it becomes evident that therapeutic manipulation in CRD-patients with a diagnosed or suspected inflammatory disease etiology by triggers with known pro-inflammatory function would probably include severe adverse effects that might further compromise tissue integrity.

On the molecular level, within the human *PIGR* gene promoter region several regulatory motifs, which can serve as binding sites for transcription factors (TFs) e.g. USF1&2 and C/EBP, have been identified (Martin et al. 1998, Verrijdt et al. 1997). These TFs participate in various physiologic reactions, such as cellular glucose- and iron metabolism (Nicolas et al. 2001, Wang et al. 1995) and ATII-proliferation (Sugahara et al. 2001). This suggests the existence of multiple – yet unknown- molecular pathways which are possibly involved in epithelial pIgR-expression and, consequently, may be target for therapeutic manipulation of this mucosal defense mechanism. Therefore, further screenings for pathways and molecular targets involved in regulation of pIgR-expression would be of particular interest for prospective studies.

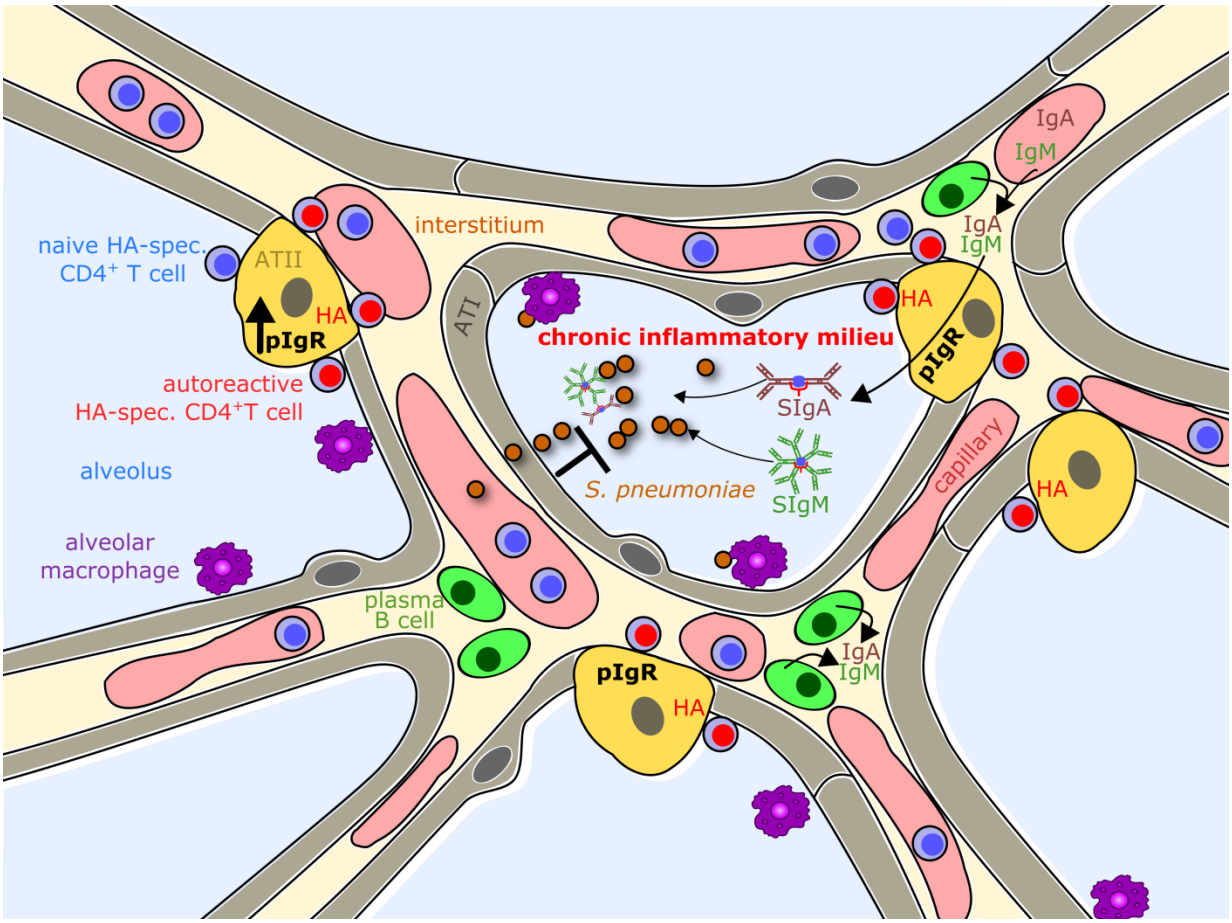

Figure 40: Proposed mechanism for enhanced pIgR-mediated antipneumocoocal defense in SPC-HAxTCR-HA lungs.

See text for details.

6.2 Phenotype and role of alveolar macrophages in chronic lung inflammation

The aim of the second part of this thesis was the elucidation of the phenotype of alveolar macrophages (AMs) as well as their contributions to immuneregulation and inflammation in CRD.

By using fluorescence-based cytometric assays several important morphological changes of AMs were detected in the SPC-HAxTCR-HA *in vivo* model. In detail, it was shown that their size, structural and intrinsic fluorescence properties are significantly affected within an inflammatory environment (Figure 25). Here, the reduced autofluorescence in the SPC-HAxTCR-HA group was of exceptional interest. Natural cellular autofluorescence is considered to be caused by electron-dense molecules such as nicotinamide adenine dinucleotide (NAD^+), riboflavins or flavin coenzymes (Aubin 1979, Benson et al. 1979). Moreover, hemosiderin, an iron-storage complex associated with the breakdown of erythrocytes, is another autofluorescent secondary metabolite present in AMs from individuals with immune alveolar hemorrhage, a feature of several chronic immunological disorders (Leatherman 1987). As pulmonary hemosiderosis (the presence of hemosiderin-laden macrophages) is a pathologic hallmark associated with lung disease in SPC-HAxTCR-HA mice (see section 5.1.1 and Bruder, Westendorf et al. 2004) it seemed conceivable to expect increased autofluorescence of AMs in this group. Given the reverse finding, which is further accompanied by their decreased size (FSC) and an altered intensity and distribution of cytoplasmic structures (SSC), it seems likely that CRD also manifests in distinct adaptations within intracellular AM-compartments probably covering various aspects of metabolic activities and products apart from hemosiderin. Here, comparative in-depth analyses of the AM-metabolome would allow expanding knowledge on molecular pathways possibly involved in the development and maintenance of an altered AM-phenotype in CRD.

Interestingly, alterations in airway macrophage side scatter and autofluorescence properties have also been reported in another study in SHIP1 (an inositol polyphosphate-5-phosphatase)-deficient mice, that spontaneously develop severe lung inflammation associated with a pathologic M2-macrophage phenotype (Duan et al. 2012).

The altered intensity and distribution of fluorescent and refractive structures might be of general interest for two reasons. First, FACS technology provides a valuable and commonly utilized tool to characterize inflammatory processes on airway mucosal surfaces. Yet the massive autofluorescence signals of airway macrophages within the FITC, PE and PerCp detectors require well-considered panel design and the utilization of additional control stainings to correctly separate large intrinsic (false) from antibody-derived (true) fluorescence signals. Since this and other studies have revealed fundamental differences of AM fluorescence properties in healthy vs. pathologic conditions, it is likely to observe similar effects in other non-infectious and infectious respiratory disease settings in which AMs are in the focus of interest. In practice, this would adversely affect accuracy of e.g. cell surface molecule quantitation on AMs. Thus, for further investigations using comparative flow cytometric analyses of airway macrophages, the aforementioned effects should definitely be considered. Second, information on parameters describing the intracellular fluorescence distribution, as derived from microscopy-based techniques - offer a simple additive tool to characterize the AM phenotype in more detail and to detect morphologic alterations that possibly hint to molecular and functional cellular adaptations. Accordingly, this study

describes a link between affected fluorescent properties and activation, polarization and functional alterations of AMs in CRD.

In this regard, the blunted AM-dependent TNF-α response towards Gram-positive bacterial ligands in SPC-HAxTCR-HA airways (Figure 29) suggests a functional impairment of these cells during infection with airborne pathogens. Functionally, TNF-α was shown to exert protective efficacy in several models of acute respiratory bacterial and fungal infection by promoting pathogen clearance (Blanchard et al. 1988, Buret et al. 1994, Chen et al. 1992, Gosselin et al. 1995). In detail, TNF-α in infection not only acts on one of its producers, the macrophages themselves, but also on neutrophils by enhancing phagocytosis of opsonized bacteria and antibody-dependent cytotoxicity (Fan, Fehr et al. 1991, Pierangeli et al. 1993). Irrespective of the influence of TNF-α on AMs, it was previously demonstrated that lung-specific overexpression of TNF-α in mice was linked to a disease phenotype mirroring hallmark features of emphysema and pulmonary fibrosis (Lundblad et al. 2005). In this context, it seems plausible that silencing of a microbial-induced TNF-α AM response has evolved as a mechanism that prevents TNF-α-driven immunopathology which might further compromise tissue integrity in the pre-diseased lung as shown by SPC-HAxTCR-HA mice. In line with this interpretation, macrophages from pre-diseased human and murine lungs were found to mount blunted cytokine responses (e.g. TNF-α, KC, IL-1β) upon stimulation with bacterial ligands like *Haemophilus* outer membrane protein or flagellin (Berenson, Wrona, et al. 2006, Didierlaurent et al. 2008). However, given the two faces of TNF-α (and other pro-inflammatory molecules) in alveolar macrophage-mediated immune responses, further studies will be needed to specifically explore their role on the shape of antibacterial host defense in the pre-diseased lung.

This however raises the question for conceivable cellular mechanisms preventing pro-inflammatory cytokine responses from AMs. Under this aspect it is noteworthy that down-regulation of TLR2 - a PRR involved in recognizing among others *S. pneumoniae* and subsequently orchestrating TNF-α immune responses - was reported for AMs from COPD patients (Droemann et al. 2005). Didierlaurent and colleagues furthermore reported that an antecedent influenza infection manifests in an inhibition of TLR-induced NF-κB signaling in AMs correlating with desensitization towards bacterial ligands (Didierlaurent, Goulding et al. 2008). Interestingly, SOCS1 which is highly up-regulated in M2 macrophages (Whyte et al. 2011) interferes with TLR4-related downstream NF-κB signaling cascades (Yoshimura et al. 2007) and SOCS1-deficient mice are hypersensitive to endotoxin challenge, i.e. they overproduce TNF-α upon LPS administration (Nakagawa et al. 2002). In summary, an altered regulation of TLR expression or altered downstream TLR signaling cascades in SPC-HAxTCR-HA AMs are probable mechanisms underlying the blunted TNF-α response following bacterial challenge.

Further molecular indications for an altered AM phenotype in SPC-HAxTCR-HA mice could be demonstrated in the present work by measuring increased M2-marker gene expression (*Msr1* and *Retlna*) in AMs from these mice (Figure 28). Furthermore, BALFome analyses revealed several proteins (MMP-12, chitinase-like protein 3 and resistin-like alpha; Figure 21b) typically produced by M2 macrophages to be exclusively present in SPC-HAxTCR-HA airways. Taken together these findings support the hypothesis of an M2-dominated milieu in the present CRD model. In line with this, M2 polarization of AMs is a known feature of other CRD-related mouse models. For instance, in a mouse parainfluenza virus (also known as

Sendai virus) infection model the special dominance of M2 pulmonary macrophages was associated with the development of postviral CRD (Wu et al. 2015). Moreover, in murine models for allergic lung inflammation the typical M2 markers resistin-like alpha (Retlna) and Ym-1 (chitinase-like protein 3) were overexpressed by lung macrophages in asthmatic mice (Draijer, Robbe et al. 2013, Moreira et al. 2010). The latter M2 markers were also found to be associated with CRD in the SPC-HAxTCR-HA model (Figure 21, Figure 28). Notably, excessive production of Retlna and Ym-1 is thought to contribute to inflammation and airway remodeling in the allergic lung (Cai et al. 2009, Dong et al. 2008). Thus, it becomes apparent that M2-polarization of AMs as found in SPC-HAxTCR-HA lungs is not a unique trait of the utilized mouse model, but rather appears to have general biological relevance in chronic inflammatory lung conditions.

Based upon the previous findings two questions arise: Firstly, which cell type constitutes the cytokine source skewing AMs into an M2 phenotype in SPC-HAxTCR-HA lungs? As stated in the introduction, the Th2 cytokines IL-4 and IL-13 typically orchestrate the induction of M2 phenotypes. Upon stimulation with self-antigen lymphocytes from SPC-HAxTCR-HA lungs were previously shown to secrete among others IL-5, another hallmark cytokine of the Th2 lineage, however no IL-4 production was found (Bruder, Westendorf et al. 2004). With regard to IL-13, it is known that apart from Th2 cells, pulmonary type 2 innate lymphoid cells (ILC2) are potent producers of this cytokine. Interestingly, an accumulation of pulmonary ILC2 is reported for murine models of allergic asthma and respiratory viral infection (Klein Wolterink et al. 2012, Monticelli et al. 2011) and increased numbers of these cells could as well be detected in SPC-HAxTCR-HA lungs (own unpublished observations). In this context, further studies dissecting lung leukocyte composition and cytokine milieu during the course of disease establishment and its regulation in SPC-HAxTCR-HA mice would be necessary in order to prove a potential role for ILC2 (and possibly IL-13)-orchestrated generation of M2 macrophages in SPC-HAxTCR-HA mice.

The second question: Is there a pathologic or beneficial role of M2-polarized alveolar macrophages in SPC-HAxTCR-HA lungs in steady state conditions? This issue was addressed in this work in several *in vivo* depletion experiments (see sections 5.2.5 - 5.2.8). By using the AM-depletion strategy it became apparent that AMs are critical cellular players that help to preserve pulmonary architecture in SPC-HAxTCR-HA lungs. Consequently, their short-term (3d) and mid-term (10d) absence was associated with an amplification of the typical disease pattern of SPC-HAxTCR-HA lungs, i.e. lymphocytic infiltrations (Figure 32). Moreover, viable polymorphonuclear neutrophils (PMNs) were found to be a major infiltrating leukocyte population in AM-depleted SPC-HAxTCR-HA lungs (Figure 34). This was of exceptional interest as this AM-dependent effect was specific for pre-diseased mice and has so far not been described in the present CRD model. It is worth mentioning that PMNs secrete a series of molecules involved in tissue destruction, such as neutrophil elastase (NE) or myeloperoxidase (MPO), whose direct or indirect actions trigger emphysema formation (Shapiro et al. 2003) and the generation of reactive oxygen species in AECs (Yang et al. 2001), respectively. Importantly, NE levels in COPD sputum samples were shown to correlate with disease severity (Paone et al. 2011) and NE concentration increased during COPD-exacerbations compared to stable disease phases (Ilumets et al. 2008). Similarly, increased sputum MPO levels are found in COPD patients as compared to healthy individuals and levels of this enzyme increase as well during exacerbations (Zhu et al. 2014). Given these examples, it becomes evident that the increased presence and activity of neutrophils is an element contributing to pathologic physiological reactions in the pre-

diseased lung. In this context, the infiltrating neutrophils observed in AM-depleted SPC-HAxTCR-HA lungs presumably are major cellular orchestrators of the necrotizing bronchopneumonia in this group. At the same time this highlights the essential immunological contribution of AMs to the prevention of neutrophil-driven pathology in the inflammatory framework of SPC-HAxTCR-HA lungs.

Thus in summary, the findings presented in this work revealed a beneficial function of AMs in the SPC-HAxTCR-HA model which opposes a number of other studies describing disease-perpetuating activities of lung macrophages. For example, in a murine emphysema model inhalation of alendronate, a nitrogen-containing bisphosphonate, evoked AM-apoptosis which correlated with disease amelioration (Ueno, Maeno et al. 2015). Moreover, Th2 and Th17 allergic lung inflammation and airway remodeling could be attenuated upon AM-depletion in mice (Lee, Jeong et al. 2015, Song et al. 2008). There are however also reports demonstrating beneficial roles for AMs in the context of sterile lung inflammation. For instance Careau and colleagues demonstrated that adoptive transfer of AMs from allergy-resistant rats into AM-depleted sensitized rats suppressed airway hyperresponsiveness following antigen challenge in the recipient group (Careau et al. 2006).

As a matter of principle, one important factor that must be taken into account when evaluating roles of pulmonary macrophages and their known subsets is the clear discrimination between resident alveolar vs. recruited macrophages. As inhaled or intratracheally administered clodronate (and other bisphosphonates) liposomes non-specifically target all airway macrophages, a clear-cut determination of the immunologic role of a particular subset is not feasible by using this strategy. Using local vs. systemic depletion strategies Zasłona and colleagues (at least partly) addressed this issue and demonstrated opposing functions of resident alveolar macrophages (suppressive) and recruited monocytes (inflammatory) in murine models of asthma (Zaslona et al. 2014). All in all, the controversial results on the immunologic roles of airway macrophage subsets in different CRDs most likely result from the different etiopathologies and thus, a more accurate discrimination between acute vs. chronic phase and resident vs. recruited macrophages would be necessary to clearly define the immunologic potential of airway macrophage populations in the pre-diseased individual. However, in the present SPC-HAxTCR-HA model it was observed that the alveolar macrophage population uniformly had a $CD11c^{high}$ $F4\text{-}80^{+}$ $autofluorescence^{high}$ profile, a hallmark of resident alveolar macrophages (Duan, Li et al. 2012, Guth et al. 2009, Hussell and Bell 2014). These were specifically depleted by the administration of clodronate without affecting the pulmonary interstitial macrophage pool (Figure 30). Also, the unaltered numbers of AMs retrieved from untreated SPC-HA vs. SPC-HAxTCR-HA mice (Figure 14) further supported a negligible role for intra-alveolar recruitment of the macrophage/monocyte lineage in chronic lung inflammation as displayed by SPC-HAxTCR-HA mice. Moreover, as the neutrophil-dominated bronchopneumonia in AM-depleted SPC-HAxTCR-HA mice was likely not a secondary effect of AM-dependent reactivation of auto-reactive T cells (Figure 35, Figure 36) the observed immunologic effects following clodronate administration could be specifically attributed to the abolition of resident AM-inherent functions in PMN containment.

In order to interpret a functional link between AM-depletion and neutrophil influx in the lungs of SPC-HAxTCR-HA mice the biology of neutrophils must be taken into account. Neutrophils are short–lived effector cells; a majority of studies using *ex vivo* labelling approaches to determine the life span of these cells under homeostatic and non-homeostatic conditions

reported half-lives of several hours up to approximately 1 day (Tak et al. 2013). The presence of viable neutrophils in the airspaces of AM-depleted SPC-HAxTCR-HA mice thus suggests a continuous recruitment of this short-lived cell population rather than a response to a singular preceding stimulus. CXCL1 (KC), CXCL2 (MIP-2α) and CXCL5 (LIX) are major factors involved in neutrophil chemoattraction to sites of inflammation (Cai, Batra et al. 2010, Driscoll et al. 1995, Mei et al. 2010). In this context, pulmonary epithelial cells were previously shown to direct pulmonary neutrophil immigration in response to infectious stimuli such as respiratory bacteria or TLR ligands (Gibbs, Ince et al. 2014, Jeyaseelan, Manzer et al. 2005, Yamamoto, Ahyi et al. 2014). In the present work increased transcription of all three chemokines in ATII isolated from AM-depleted SPC-HAxTCR-HA lungs (Figure 37,Table 7-Table 9) corroborated the hypothesis of epithelial-driven neutrophilic bronchopneumonia in this group. Moreover, this further confirms CXCL5 as a predominant neutrophil-attractant produced by alveolar epithelial cells (Jeyaseelan, Manzer et al. 2005, Nouailles et al. 2014). Importantly, the present study indicates microbiota-independent neutrophil recruitment (Figure 39) thereby describing a non-significant role of AMs as microbial scavengers and rejecting the assumption of MAMP-dependent epithelial PMN recruitment in SPC-HAxTCR-HA lungs.

Again referring to the above described effect of AM-abolishment on lung pathology in the SPC-HAxTCR-HA group, the chemokine expression results obtained by qRT-PCR analyses of ATII cells disclose two important phenomena. Firstly, an increase of chemokine transcripts as a general response of ATII cells to the loss of AMs and secondly an excess of this effect in ATII from mice with a pre-existing respiratory disorder (Figure 37,Table 7-Table 9). Here, in order to determine the functional magnitude of chemokine expression following AM-depletion in the airways, it would be of utmost importance to verify the obtained qRT-PCR results on a protein level e.g. by BALF-ELISA. Moreover, in order to estimate the specific contribution of the AM/ATII axis in pulmonary homeostasis, chemokine expression in other lung epithelial cell types (e.g. bronchial epithelial cells, Clara cells, and ATI cells) should be examined in more detail.

In this context, MMP-12, a protease secreted by M2-macrophages and found to be induced in SPC-HAxTCR-HA airways (Figure 21), might partially explain the observed effects in SPC-HAxTCR-HA lungs. Via cleavage of CXCL1, CXCL2 and CXCL5 this molecule is known to interfere with the establishment of a functional chemokine-gradient (Dean, Cox et al. 2008) and thus could antagonize neutrophil-mobilization into SPC-HAxTCR-HA airways in steady state conditions. However, upon clodronate-induced macrophage abolishment and the resulting absence of MMP-12 protease activity in SPC-HAxTCR-HA airways functional CXCL1, CXCL2 and CXCL5 can mediate chemoattraction of neutrophils from blood stream and lung tissue into the airways of SPC-HAxTCR-HA lungs and thus the development of bronchopneumonia in this group. M2 macrophage-derived MMP-12 activity might therefore provide one explanatory mechanism for the contradictory findings of neutrophil absence despite increased epithelial chemokine expression in AM-sufficient SPC-HAxTCR-HA mice. According to this hypothesis, administration of murine MMP-12 into AM-depleted SPC-HAxTCR-HA airways would ultimately prevent or decrease pathologic neutrophil influx in this group. However given the opposing roles of this enzyme in blocking neutrophil recruitment (Dean, Cox et al. 2008) and on the other hand promoting emphysema formation (Trojanek et al. 2014) it is likely that therapeutic administration could inadvertently result in tissue damage, remodeling and finally a loss in organ functionality in pre-diseased SPC-HAxTCR-HA lungs.

With regard to chemokine gene induction in ATII cells as a general response to the loss of AMs it became evident that AM/AEC crosstalk is a constitutive element in healthy as well as pre-diseased lungs (Figure 37,Table 7-Table 9). This raises the question for relevant cellular interaction interfaces between AMs and ATII cells. A possible answer to this question may be the gap junction protein Cx43 (expressed by AMs and AECs), which was recently described to be involved in a cell-cell contact dependent mechanism by which AMs communicate immunosuppressive signals to AECs (and *vice versa*) during LPS induced lung inflammation (Westphalen, Gusarova et al. 2014). However, that study also described that no AM/AEC signaling could be detected under non-inflammatory conditions thereby making Cx43-dependent mechanisms unlikely to be involved in AM-dependent chemokine transcript induction in the healthy SPC-HA control group.

Another AM/ATII interaction interface by which epithelial cytokine signaling pathways can be downmodulated may be the constitutive secretion of AM-derived SOCS-protein containing exosomes and microparticles which are subsequently taken up by AECs (Bourdonnay, Zaslona et al. 2015). SOCS1, which is up-regulated in M2 macrophages (Whyte, Bishop et al. 2011), can interfere with NF-κB signaling pathways by decreasing the stability of the NF-κB-subunit p65 in the nucleus (Strebovsky et al. 2011). In this context, it was demonstrated that he transcription of IL-8 and IL-8-related chemokines essentially requires NF-κB signaling (Kim et al. 2006). Albeit primarily proposed as a constitutive AM-to-AEC immunoregulatory signaling strategy (Bourdonnay, Zaslona et al. 2015), transcellular delivery of SOCS1 containing particles possibly is a mechanism that is up-regulated in an M2-polarized microenvironment as displayed in SPC-HAxTCR-HA lungs and thus can decrease chemokine transcripts levels in healthy as well as pre-conditioned lung epithelial cells in a varying degree. With reference to the ATII cells analyzed in this work it was found that these however produce higher levels of IL-8 analogues in steady state conditions (Figure 37,Table 7-Table 9) indicative of either irreversible inflammatory imprinting during the phase of acute lung inflammation or continuous immunologic triggers which are present in the phase of controlled, chronic lung disease.

In addition to the possible implications of soluble and membrane-bound proteins in AM/ATII immunomodulatory interactions, lipid mediators represent another group of interesting candidate components possibly involved in this regulatory axis. Lipid mediators (lipoxins, resolvins, protectins, maresins) fulfill pleiotropic anti-inflammatory and pro-resolving functions by acting on macrophages themselves as well as on other leukocytes and non-hematopoetic cells (see section 2.6.3). Lipoxins are derivates of arachidonic acid, whose release is a result of enzymatic cleavage of membrane phospholipids catalyzed by phospholipase A2 (Pla2). Of note, alveolar macrophages are able to produce several isoforms of secretory Pla2 (Kitsiouli et al. 2009) and gene expression of the Pla2-IID isoform, is indeed found to be up-regulated in SPC-HAxTCR-HA lung tissue (FC: 4.8; see section 7.1.1, Table 10). This suggests that production of arachidonate-derived anti-inflammatory lipid mediators could as well be increased in SPC-HAxTCR-HA lungs. Due to the experimental protocol applied for the LC-MS/MS BALFome analyses in this work it was not possible to detect bronchoalveolar lipid components by using this method. Yet, in order to more precisely define the pulmonary inflammatory milieu and to corroborate a role for lipid mediators in SPC-HAxTCR-HA mice, supplementary mass spectrometry analyses of the BALF lipidome would be an interesting approach.

In this regard, LipoxinA_4 is a promising candidate mediator, as this molecule was shown to reduce IL-8 production by epithelial cells (Gewirtz et al. 2002) but also to inhibit interaction of neutrophils with endothelial and epithelial cells (Fierro et al. 2003). Given the example of LipoxinA_4 it becomes evident that pathologic neutrophil infiltrations in clodronate-treated SPC-HAxTCR-HA mice might indeed be the net result from AM-dependent reactivation events in the adjacent epithelial but also parenchymal (endothelium, neutrophils) and systemic (neutrophils) compartments. As a secondary effect of increased endothelial and epithelial permeability the influx of other leukocytes would be a likely consequence following AM-depletion in the pre-diseased lung which would somewhat explain the parenchymal and intra-alveolar lymphocytic infiltrations in SPC-HAxTCR-HA mice (Figure 32, Figure 35).

In conclusion, based on the data obtained in this part of the thesis, the following mechanism (summarized in Figure 41) is proposed: Chronic autoimmune-mediated lung inflammation is associated with polarization of alveolar macrophages into an M2 phenotype as well as an induction of CXCL1, 2, 5 gene expression in ATII cells. AMs antagonize ATII-chemokine production by cell-cell-contact dependent pathways and/or by secreted factors (e.g. lipid mediators, microparticles). M2-macrophage-derived MMP-12 can proteolytically inactivate alveolar CXCL1, 2, 5 and thus prevent establishment of a functional chemokine gradient in steady state conditions. Moreover, AM-derived products may also act on adjacent epithelial (e.g. ATI) or distal (e.g. endothelial) cell types. Upon loss of AMs ATII cells produce increased amounts of CXCL1, 2, 5. Functional CXCL1, 2, 5 gradients mediate attraction and transmigration of neutrophils from local (interstitium) and/or systemic (blood stream) compartments into the alveoli.

In summary, the results obtained in this part of the thesis extend our knowledge about the cellular players orchestrating immuneregulation in the SPC-HAxTCR-HA mouse model for CRD. While ATII and HA-specific $CD4^+Foxp3^+$ T cells have been demonstrated to be critical participants during acute inflammation and subsequent tolerance induction in autoimmune-mediated lung disease (Gereke, Grobe et al. 2007, Gereke, Jung et al. 2009), respectively, the roles of AMs were so far unresolved. Based on the fact that AMs were found to acquire fundamentally changed characteristics in chronic lung disease, further elucidating the functional implications of these alterations for the pre-diseased host is of highest interest for future investigations. Here, comparative analyses of the AM transcriptome, metabolome and also secretome would help to identify elements (secreted lipids/proteins vs. cell-cell contact-dependent mechanisms) involved in immunoregulatory networks in SPC-HAxTCR-HA lungs. Given the observed prominent roles of AMs in suppressing potentially harmful pulmonary epithelial immune responses comprehensive investigation of the ATII-phenotype following macrophage depletion would probably shed light on pathways involved in AM/epithelial communication. In the future, these findings could be particularly promising for those CRD cohorts in which this communication axis is interrupted or dysfunctional due to the loss of AMs (e.g. as a consequence of myeloablative therapy, hematologic malignancies or smoke exposure) and reactivation of the inflammation-imprinted pulmonary epithelium would further compromise tissue integrity and physiological function in the pre-diseased lung.

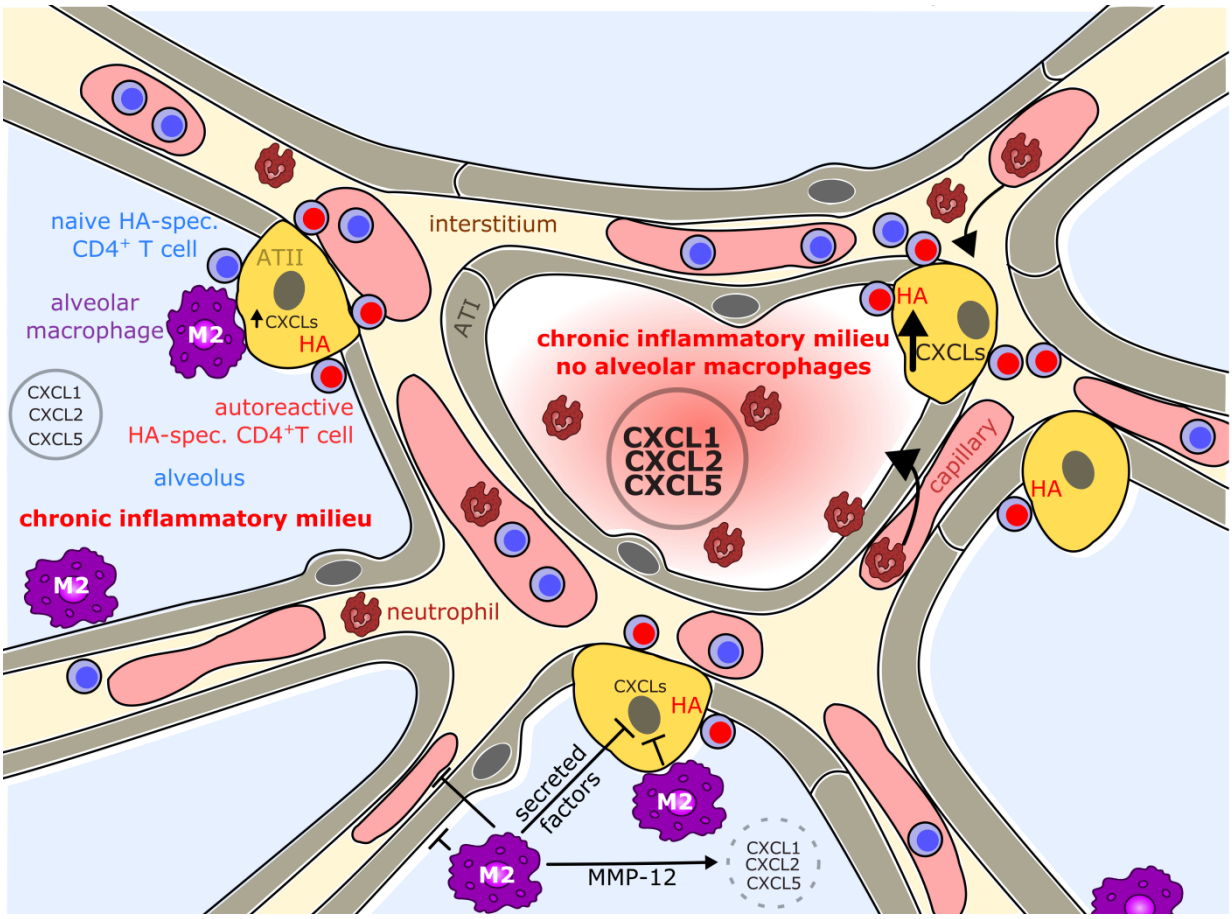

Figure 41: Proposed mechanism for AM-dependent immunoregulatory circuits in SPC-HAxTCR-HA lungs. See text for details.

7 Appendix

7.1 Supplemental tables

7.1.1 Microarray

Table 10: Genes found to be up-regulated (=fold change [FC] ≥ 2) in lungs of SPC-HAxTCR-HA mice when compared to lung tissue from SPC-HA control mice (Σ 326).

Transcript cluster ID	Gene symbol	FC
10502622	*Clca3*	29,4
10433172	*Glycam1*	23,1
10538882	*Gm5571*	19,3
10545231		18,9
10538880	*Igk-V1*	14,2
10545173	*LOC672291*	14,2
10531126	*Igj*	13,6
10545249		13,4
10531407	*Cxcl9*	12,0
10545175	*LOC672291|Igk-J1*	11,8
10545247	*Igk-V19-14*	11,6
10538921		10,3
10538868		10,1
10538871	*Gm4964*	9,6
10545187	*Gm1502|Gm8760|Igkv4-71*	9,4
10545237		9,1
10538924	*LOC100046496*	8,8
10438405	*Igl-V1|Igl-V2|LOC433053*	8,7
10419568	*Ear11*	8,6
10545198	*Igkv4-71|Gm8760|Gm1499*	8,6
10417526	*Dnase1l3*	8,5
10545190		8,5
10545220	*Gm16848*	8,1
10438415	*Igl-V2|Igl-C2*	8,0
10545177		7,9
10545184	*Gm10880*	7,8
10402991	*Gm16970|Igh-VX24*	7,7
10466172	*Ms4a1*	7,7
10545205	*Gm1418*	7,1
10403034	*LOC100046275*	6,8
10545239		6,7
10562812	*Spib*	6,7
10545202	*Gm1077*	6,7
10436095	*Retnla*	6,6
10545196	*Gm1419|Igkv4-71|Gm1524|Igk-C|Gm10880*	6,3
10379535	*Ccl8*	6,1
10545233	*Gm10883*	6,1

10403018	*IghmAC38.205.12|AI324046*	6,0
10403015	*AI324046|IghmAC38.205.12|LOC634541|LOC634206*	6,0
10545212	*Gm5574*	6,0
10403063	*LOC100046275*	5,9
10545194	*Rprl1|Gm8760|Igkv4-71*	5,8
10551025	*Cd79a*	5,7
10403021		5,6
10545180	*Gm10879*	5,6
10361292	*Cr2*	5,6
10402981	*Gm900*	5,5
10545208	*Gm189*	5,5
10545215	*Igk-V28|Igkv12-46*	5,4
10403006	*Gm7112*	5,4
10582882		5,3
10403054	*LOC435333*	5,3
10545569	*Reg3g*	5,3
10583056	*Mmp12*	5,2
10403048	*Ighv1-72|LOC631518*	5,2
10582888		5,1
10576757	*Fcer2a*	5,0
10538903	*Igk-V28|Gm7202|Igk-V21-4|Igkv6-25|Gm16939*	5,0
10512470	*Cd72*	4,9
10403060	*Ighv1-72|LOC382693|Gm16710*	4,9
10509577	*Pla2g2d*	4,8
10349593	*Faim3*	4,8
10603228		4,7
10582890		4,7
10485357		4,6
10403079	*LOC435333*	4,6
10523359	*Cxcl13*	4,5
10599092		4,5
10545235		4,4
10450880	*H2-M2*	4,4
10502335	*Bank1*	4,4
10550509	*Pglyrp1*	4,4
10545242	*Igk-V19-20|Igk-V28*	4,3
10392142	*Cd79b*	4,3
10403046	*AI324046*	4,3
10403028	*LOC382693|Gm16710*	4,2
10403009	*Ighg|LOC100045391*	4,2
10517165	*Cd52*	4,2
10582899		4,2
10593015	*Cd3g*	4,1
10563597	*Saa3*	4,1
10522788	*Stap1*	4,1
10567863	*Cd19*	4,0
10598225	*Gm2799|Gm2825|Gm2863|Gmcl1l|Gm14346*	4,0

10501020	*Chi3l3*	4,0
10538885		3,9
10379727	*Gm11428*	3,9
10402864	*Ighg|Igh-VJ558|AI324046|LOC544903|Igh-6|Igh-5|Ighg1|Igh-3|Igh-VS107|LOC380804|LOC630565|Igh-VX24|Ighv14-2|Igh-2*	3,9
10367532	*5830405N20Rik*	3,8
10547894	*Cd4*	3,8
10545200		3,8
10403057		3,7
10406928	*Cd180*	3,6
10512372	*Ccl19|LOC100043921|Gm13309|Gm2442*	3,6
10466200	*Ms4a7*	3,5
10512322	*Ccl19|LOC100043921|Gm13309|Gm2442*	3,5
10504159	*Ccl19|LOC100043921|Gm13309|Gm2442*	3,5
10585276	*Pou2af1*	3,5
10349580	*Pigr*	3,4
10347915	*Gm7609|Csprs|Gm7592*	3,4
10606178	*Xist*	3,4
10504188	*Ccl19|LOC100043921|Gm13309|Gm2442*	3,4
10545217		3,4
10598077		3,3
10598229		3,3
10598062		3,3
10403821	*Tcrg-V3|Tcrg-V2*	3,3
10486061	*Rasgrp1*	3,3
10404606	*Ly86*	3,3
10598187		3,2
10601416	*P2ry10*	3,2
10597996	*Xcr1*	3,2
10351691	*Slamf6*	3,1
10598064		3,1
10347925	*Gm7609|Csprs|Gm7592*	3,1
10545245		3,1
10403023	*Gm7016*	3,1
10504132	*Ccl19|LOC100043921|Gm13309|Gm2442*	3,1
10517513	*C1qc*	3,1
10574213	*Ccl22*	3,0
10563178	*Cd37*	3,0
10598075		3,0
10574226	*Ccl17*	3,0
10429560	*Ly6i*	3,0
10346799	*Icos*	3,0
10590623	*Cxcr6*	3,0
10582879	*Csprs|Gm7609|Gm7592*	2,9
10582916		2,9
10492971	*Fcrl1*	2,9
10461594	*Ms4a4c*	2,9
10390640	*Ikzf3*	2,9

10545210	*Gm1524*	2,9
10403825	*Tcrg-C*	2,9
10582896		2,8
10557177	*Prkcb*	2,8
10351873	*Pyhin1*	2,8
10469278	*Il2ra*	2,8
10430818	*Tnfrsf13c*	2,8
10466210	*Ms4a6d*	2,8
10356274	*Csprs|Gm7609|Gm7592*	2,8
10444236	*H2-DMb2|H2-DMb1*	2,8
10395365	*Agr2*	2,8
10347888	*Ccl20*	2,8
10467508	*Blnk*	2,8
10444284	*H2-Ob*	2,8
10517508	*C1qb*	2,8
10450325	*Cfb*	2,7
10403038	*LOC382693|Gm16710*	2,7
10547657	*C3ar1*	2,7
10530145	*Tlr1*	2,7
10349648	*Ctse*	2,7
10601424	*Gpr174*	2,7
10517517	*C1qa*	2,7
10389214	*Ccl9*	2,7
10544588	*Gimap3*	2,7
10360406	*Ifi205*	2,7
10591739	*Acp5*	2,7
10525365	*Hvcn1|Tctn1*	2,7
10460146		2,6
10455970	*BC023105*	2,6
10471912	*Kynu*	2,6
10408557	*Serpinb1a*	2,6
10531737	*Hpse*	2,6
10432675	*I730030J21Rik*	2,6
10407940	*Tcrg-V2|Tcrg-V1*	2,6
10592888	*Cxcr5*	2,6
10576034	*Irf8*	2,6
10590631	*Ccr2*	2,6
10403043	*Ighv1-72*	2,5
10564163	*Snord116|Snord116l1|Snord116l2*	2,5
10564179	*Snord116|Snord116l1|Snord116l2*	2,5
10548892	*Arhgdib*	2,5
10564181	*Snord116|Snord116l1|Snord116l2*	2,5
10564165		2,5
10407982	*A530099J19Rik*	2,5
10564205	*Snord116*	2,5
10564175	*Snord116|Snord116l1|Snord116l2*	2,5
10564207	*Snord116*	2,5

10564187	*Snord116|Snord116l1|Snord116l2*	2,5
10564167	*Snord116|Snord116l1|Snord116l2*	2,5
10564185	*Snord116|Snord116l1|Snord116l2*	2,5
10564171	*Snord116|Snord116l1|Snord116l2*	2,5
10564193	*Snord116|Snord116l1|Snord116l2*	2,5
10564201	*Snord116*	2,5
10564173	*Snord116|Snord116l1|Snord116l2*	2,5
10564197	*Snord116|Snord116l1|Snord116l2*	2,5
10564195	*Snord116|Snord116l1|Snord116l2*	2,5
10564199	*Snord116|Snord116l1|Snord116l2*	2,5
10564189	*Snord116|Snord116l1|Snord116l2*	2,5
10564191	*Snord116|Snord116l1|Snord116l2*	2,5
10414811	*Gm13969*	2,5
10564161	*Snord116|Snord116l1|Snord116l2*	2,5
10455961	*Iigp1*	2,5
10414937	*Gm13969*	2,5
10593024	*Cd3e*	2,5
10347218		2,5
10399854	*Slc26a4*	2,5
10430372	*Rac2*	2,5
10603860	*Cfp*	2,5
10385533	*Tgtp1|Tgtp2|Gm12185*	2,5
10567825	*Lat*	2,5
10444752	*Ltb*	2,5
10439312	*Cd86*	2,4
10455954	*Gm4951*	2,4
10516620	*Lck*	2,4
10519497	*Steap4*	2,4
10351658	*Cd48*	2,4
10444306	*H2-Eb2*	2,4
10461614	*Ms4a6c*	2,4
10564159		2,4
10385518	*Tgtp1|Tgtp2|Gm12185*	2,4
10360028	*Fcgr2b*	2,4
10547621	*Apobec1*	2,4
10494271	*Ctss*	2,4
10531415	*Cxcl10*	2,4
10404389	*Irf4*	2,4
10590635	*Ccr5|Ccr2*	2,4
10404840	*Cd83*	2,4
10597960	*Slc6a20a*	2,4
10598013	*Ccr5|Ccr2*	2,3
10564183	*Snord116*	2,3
10461622	*Ms4a6b*	2,3
10564169		2,3
10480238	*St8sia6*	2,3
10516906	*Snora73b*	2,3
10439744	*Cd96*	2,3

10387699	*Acap1*	2,3
10557342	*Il21r*	2,3
10599487	*Sash3*	2,3
10562132	*Cd22*	2,3
10501063	*Cd53*	2,3
10570634	*4930467E23Rik|Gm15319|Trim44|Gm7827*	2,3
10430344	*Il2rb*	2,3
10548817	*Plbd1*	2,3
10568024	*Coro1a*	2,3
10477495	*U46068*	2,3
10438769	*Cldn1*	2,3
10435982	*Btla*	2,3
10418848	*Wdfy4*	2,3
10360158	*Ly9*	2,3
10548375	*Clec7a*	2,3
10385118	*Dock2*	2,3
10516908	*Snora73a*	2,3
10389143	*Slfn8*	2,3
10444298	*H2-Eb1*	2,3
10548333	*Cd69*	2,3
10433507	*Ciita*	2,3
10398907	*Pld4*	2,2
10450374	*D17H6S56E-5*	2,2
10572527	*4930467E23Rik|Gm15319|Gm7827|Trim44*	2,2
10378286	*Itgae*	2,2
10379524	*Ccl11*	2,2
10496539	*Gbp5*	2,2
10385428	*Itk*	2,2
10567366	*Gp2*	2,2
10360018	*Fcrla*	2,2
10374333	*Ikzf1*	2,2
10439527	*Tigit*	2,2
10542164	*Clec12a*	2,2
10360173	*Slamf7*	2,2
10605034	*Xlr4c|Xlr4b|Xlr4a*	2,2
10422760	*Fyb*	2,2
10597420	*Ccr4*	2,2
10445412	*Nfkbie*	2,2
10446253	*Vav1*	2,2
10409240	*Sema4d*	2,2
10519811	*Speer8-ps1|Speer7-ps1*	2,2
10351197	*Sell*	2,2
10552743	*Il4i1|Nup62-il4i1*	2,2
10551666	*Map4k1*	2,2
10358224	*Ptprc*	2,2
10360382	*Ifi204|Mnda*	2,2
10597074		2,1

10494978	*Ptpn22*	2,1
10358408	*Rgs1*	2,1
10606694	*Btk*	2,1
10564177	*Snord116*	2,1
10512669	*Pax5*	2,1
10582884		2,1
10579054	*4930467E23Rik|Gm15319|Trim44*	2,1
10582985	*Casp1*	2,1
10502801	*H28*	2,1
10579060	*4930467E23Rik|Gm15319|Trim44*	2,1
10349571	*Fcamr*	2,1
10360370	*BC094916*	2,1
10461765	*Lpxn*	2,1
10598041		2,1
10593050	*Il10ra*	2,1
10427628	*Il7r*	2,1
10508719	*Snora16a*	2,1
10354374	*Slc40a1*	2,1
10375145	*Lcp2*	2,1
10444291	*H2-Ab1*	2,1
10427336	*Nckap1l*	2,1
10381708	*Fmnl1*	2,1
10577361	*4930467E23Rik|Gm15319|Trim44|Gm7827*	2,1
10468898	*Lax1*	2,1
10449893	*Rasal3|A530088E08Rik*	2,1
10538936		2,1
10390763	*Ccr7*	2,0
10402512	*Scarna13*	2,0
10346783	*Cd28*	2,0
10347222		2,0
10425053	*Ncf4*	2,0
10413615	*Itih4*	2,0
10397645	*Gpr65*	2,0
10574098	*Nlrc5*	2,0
10575799	*Plcg2*	2,0
10425726	*Sep 03*	2,0
10605143	*Arhgap4*	2,0
10598073		2,0
10522182	*Rhoh*	2,0
10425410	*Grap2*	2,0
10577388	*4930467E23Rik|Gm15319|Trim44|Gm7827*	2,0
10376324	*Gm12250*	2,0
10557895	*Itgax*	2,0
10471929	*Arhgap15*	2,0
10487011	*Gatm*	2,0
10481627	*Lcn2*	2,0
10435565	*Hcls1*	2,0
10438098	*Sdf2l1*	2,0

10361215	*Traf3ip3*	2,0
10460371	*Ptprcap|Rps6kb2*	2,0
10578264	*Msr1*	2,0
10550193	*Gm3994|Gm10679*	2,0
10566583	*Gm8995*	2,0

Table 11: Genes found to be down-regulated (=fold change [FC] ≤-2) in lungs of SPC-HAxTCR-HA mice when compared to lung tissue from SPC-HA control mice (Σ 52).

Transcript Cluster ID	Gene symbol	FC
10399360	Rhob	-2,0
10443690	Glp1r	-2,0
10353450	Gm4956	-2,0
10425283	Maff	-2,0
10450038	Angptl4	-2,0
10352918	Mir29c|A330023F24Rik	-2,1
10358515	Hmcn1	-2,1
10407122		-2,1
10510574	Errfi1	-2,1
10426110	Pim3	-2,1
10462132	E030010A14Rik|Pgm5	-2,2
10479975		-2,2
10396419		-2,2
10526410	Hspb1|Gm9817	-2,2
10408928	Hspb1|Gm9817	-2,2
10449741	Sik1	-2,2
10578950		-2,2
10412699	Gm10404	-2,3
10369290	Ddit4	-2,3
10400095	Ifrd1|Gm7008	-2,3
10578136		-2,4
10482772	Nr4a2	-2,4
10459288	Adrb2	-2,4
10377439	Per1	-2,4
10531610	Rasgef1b	-2,4
10575873	Osgin1	-2,5
10357875	Btg2	-2,5
10449284	Dusp1	-2,5
10509965	Epha2	-2,5
10580183	Ier2	-2,6
10495675	F3	-2,6
10514466	Jun	-2,6
10474972	Chac1	-2,6
10504838	Nr4a3	-2,7

10597758	Csrnp1	-2,7
10543017	Pdk4	-2,7
10561453	Zfp36	-2,7
10433885	Cebpd	-2,8
10541071	8430408G22Rik	-2,9
10363735	Egr2	-2,9
10434925	Hes1	-3,2
10366346	Phlda1	-3,3
10450367	Hspa1a|Hspa1b	-3,8
10444589	Hspa1a|Hspa1b	-3,8
10560481	Fosb	-3,8
10573198	Dnajb1	-4,3
10450369	Hspa1a	-4,5
10350516	Ptgs2	-5,8
10427035	Nr4a1	-7,5
10397346	Fos	-7,5
10454782	Egr1	-7,8
10361091	Atf3	-10,4

7.1.2 BALFome analyses

Table 12: List of proteins identified in BALF from SPC-HA and SPC-HAxTCR-HA mice (Σ372).

Accession ID	Protein	Gene symbol	Entrez Gene ID
Q64433	10 kDa heat shock protein, mitochondrial	*Hspe1*	15528
Q9CQV8	14-3-3 protein beta/alpha	*Ywhab*	54401
P62259	14-3-3 protein epsilon	*Ywhae*	22627
P68510	14-3-3 protein eta	*Ywhah*	22629
P61982	14-3-3 protein gamma	*Ywhag*	22628
O70456	14-3-3 protein sigma	*Sfn*	55948
P68254	14-3-3 protein theta	*Ywhaq*	22630
P63101	14-3-3 protein zeta/delta	*Ywhaz*	22631
Q99L13	3-hydroxyisobutyrate dehydrogenase, mitochondrial	*Hibadh*	58875
Q8BWT1	3-ketoacyl-CoA thiolase, mitochondrial	*Acaa2*	52538
P62858	40S ribosomal protein S28	*Rps28*	54127
P63038	60 kDa heat shock protein, mitochondrial	*Hspd1*	15510
P14869	60S acidic ribosomal protein P0	*Rplp0*	11837
P99027	60S acidic ribosomal protein P2	*Rplp2*	67186
P53026	60S ribosomal protein L10a	*Rpl10a*	19896
P35979	60S ribosomal protein L12	*Rpl12*	269261
Q9DCD0	6-phosphogluconate dehydrogenase, decarboxylating	*Pgd*	110208
Q9R1Z7	6-pyruvoyl tetrahydrobiopterin synthase	*Pts*	19286
P20029	78 kDa glucose-regulated protein	*Hspa5*	14828
Q8QZT1	Acetyl-CoA acetyltransferase, mitochondrial	*Acat1*	110446
Q99KI0	Aconitate hydratase, mitochondrial	*Aco2*	11429
P60710	Actin, cytoplasmic 1	*Actb*	11461
Q9JM76	Actin-related protein 2/3 complex subunit 3	*Arpc3*	56378
P59999	Actin-related protein 2/3 complex subunit 4	*Arpc4*	68089
Q9CPW4	Actin-related protein 2/3 complex subunit 5	*Arpc5*	67771
P11031	Activated RNA polymerase II transcriptional coactivator p15	*Sub1*	20024
O55137	Acyl-coenzyme A thioesterase 1	*Acot1*	26897
Q9QYR9	Acyl-coenzyme A thioesterase 2, mitochondrial	*Acot2*	171210
P50247	Adenosylhomocysteinase	*Ahcy*	269378
Q9WTP6	Adenylate kinase 2, mitochondrial	*Ak2*	11637
P40124	Adenylyl cyclase-associated protein 1	*Cap1*	12331
P61205	ADP-ribosylation factor 3	*Arf3*	11842
Q8QZR5	Alanine aminotransferase 1	*Gpt*	76282
Q9JII6	Alcohol dehydrogenase [NADP(+)]	*Akr1a1*	58810
O35945	Aldehyde dehydrogenase, cytosolic 1	*Aldh1a7*	26358
P47738	Aldehyde dehydrogenase, mitochondrial	*Aldh2*	11669

G3X982	Aldehyde oxidase 3	*Aox3*	71724
Q8K157	Aldose 1-epimerase	*Galm*	319625
P45376	Aldose reductase	*Akr1b1*	11677
Q8VCR7	Alpha/beta hydrolase domain-containing protein 14B	*Abhd14b*	76491
Q7TPR4	Alpha-actinin-1	*Actn1*	109711
P57780	Alpha-actinin-4	*Actn4*	60595
P17182	Alpha-enolase	*Eno1*	13806
P12023	Amyloid beta A4 protein	*App*	11820
P07356	Annexin A2	*Anxa2*	12306
Q9Z0X1	Apoptosis-inducing factor 1, mitochondrial	*Aifm1*	26926
P05201	Aspartate aminotransferase, cytoplasmic	*Got1*	14718
P05202	Aspartate aminotransferase, mitochondrial	*Got2*	14719
Q9Z2W0	Aspartyl aminopeptidase	*Dnpep*	13437
Q03265	ATP synthase subunit alpha, mitochondrial	*Atp5a1*	11946
P56480	ATP synthase subunit beta, mitochondrial	*Atp5b*	11947
Q9D3D9	ATP synthase subunit delta, mitochondrial	*Atp5d*	66043
Q91V92	ATP-citrate synthase	*Acly*	104112
Q9R069	Basal cell adhesion molecule	*Bcam*	57278
P09803	Cadherin-1	*Cdh1*	12550
P62204	Calmodulin	*Calm1*	12315
O35887	Calumenin	*Calu*	12321
P28651	Carbonic anhydrase-related protein	*Ca8*	12319
P08074	Carbonyl reductase [NADPH] 2	*Cbr2*	12409
Q8VCT4	Carboxylesterase 1D	*Ces1d*	104158
P24270	Catalase	*Cat*	12359
P26231	Catenin alpha-1	*Ctnna1*	12385
P10605	Cathepsin B	*Ctsb*	13030
P18242	Cathepsin D	*Ctsd*	13033
Q61490	CD166 antigen	*Alcam*	11658
Q61362	Chitinase-3-like protein 1	*Chi3l1*	12654
Q9Z1Q5	Chloride intracellular channel protein 1	*Clic1*	114584
Q9QYB1	Chloride intracellular channel protein 4	*Clic4*	29876
P23198	Chromobox protein homolog 3	*Cbx3*	12417
Q06890	Clusterin	*Clu*	12759
Q5XJY5	Coatomer subunit delta	*Arcn1*	213827
Q9QZE5	Coatomer subunit gamma-1	*Copg1*	54161
P18760	Cofilin-1	*Cfl1*	12631
P45591	Cofilin-2	*Cfl2*	12632
P01027	Complement C3	*C3*	12266
O35658	Complement component 1 Q subcomponent-binding protein, mitochondrial	*C1qbp*	12261
O08997	Copper transport protein ATOX1	*Atox1*	11927
Q8CCK0	Core histone macro-H2A.2	*H2afy2*	404634
P30275	Creatine kinase U-type, mitochondrial	*Ckmt1*	12716

Q6ZQ38	Cullin-associated NEDD8-dissociated protein 1	*Cand1*	71902
P21460	Cystatin-C	*Cst3*	13010
P97315	Cysteine and glycine-rich protein 1	*Csrp1*	13007
Q9DCT8	Cysteine-rich protein 2	*Crip2*	68337
P62897	Cytochrome c, somatic	*Cycs*	13063
O88487	Cytoplasmic dynein 1 intermediate chain 2	*Dync1i2*	13427
Q9CPY7	Cytosol aminopeptidase	*Lap3*	66988
Q91V12	Cytosolic acyl coenzyme A thioester hydrolase	*Acot7*	70025
Q9D1A2	Cytosolic non-specific dipeptidase	*Cndp2*	66054
O35215	D-dopachrome decarboxylase	*Ddt*	13202
P10518	Delta-aminolevulinic acid dehydratase	*Alad*	17025
Q9R0P5	Destrin	*Dstn*	56431
O08749	Dihydrolipoyl dehydrogenase, mitochondrial	*Dld*	13382
O08553	Dihydropyrimidinase-related protein 2	*Dpysl2*	12934
P97821	Dipeptidyl peptidase 1	*Ctsc*	13032
Q99KK7	Dipeptidyl peptidase 3	*Dpp3*	75221
P28843	Dipeptidyl peptidase 4	*Dpp4*	13482
Q99KJ8	Dynactin subunit 2	*Dctn2*	69654
Q9D8Y0	EF-hand domain-containing protein D2	*Efhd2*	27984
P70372	ELAV-like protein 1	*Elavl1*	15568
P10126	Elongation factor 1-alpha 1	*Eef1a1*	13627
O70251	Elongation factor 1-beta	*Eef1b*	55949
P57776	Elongation factor 1-delta	*Eef1d*	66656
Q9D8N0	Elongation factor 1-gamma	*Eef1g*	67160
P58252	Elongation factor 2	*Eef2*	13629
P57759	Endoplasmic reticulum resident protein 29	*Erp29*	67397
P08113	Endoplasmin	*Hsp90b1*	22027
P42125	Enoyl-CoA delta isomerase 1, mitochondrial	*Eci1*	13177
Q6ZWX6	Eukaryotic translation initiation factor 2 subunit 1	*Eif2s1*	13665
Q99L45	Eukaryotic translation initiation factor 2 subunit 2	*Eif2s2*	67204
Q9ERK4	Exportin-2	*Cse1l*	110750
P26040	Ezrin	*Ezr*	22350
P47754	F-actin-capping protein subunit alpha-2	*Capza2*	12343
P47757	F-actin-capping protein subunit beta	*Capzb*	12345
Q3U0V1	Far upstream element-binding protein 2	*Khsrp*	16549
Q920E5	Farnesyl pyrophosphate synthase	*Fdps*	110196
P19096	Fatty acid synthase	*Fasn*	14104
Q05816	Fatty acid-binding protein, epidermal	*Fabp5*	16592
P09528	Ferritin heavy chain	*Fth1*	14319
P29391	Ferritin light chain 1	*Ftl1*	14325
Q8BTM8	Filamin-A	*Flna*	192176
Q80X90	Filamin-B	*Flnb*	286940

P70695	Fructose-1,6-bisphosphatase isozyme 2	*Fbp2*	14120
P05064	Fructose-bisphosphate aldolase A	*Aldoa*	11674
P97807	Fumarate hydratase, mitochondrial	*Fh*	14194
P35505	Fumarylacetoacetase	*Fah*	14085
P23591	GDP-L-fucose synthase	*Tsta3*	22122
P13020	Gelsolin	*Gsn*	227753
P06745	Glucose-6-phosphate isomerase	*Gpi*	14751
O08795	Glucosidase 2 subunit beta	*Prkcsh*	19089
P26443	Glutamate dehydrogenase 1, mitochondrial	*Glud1*	14661
P97494	Glutamate--cysteine ligase catalytic subunit	*Gclc*	14629
Q9QUH0	Glutaredoxin-1	*Glrx*	93692
P11352	Glutathione peroxidase 1	*Gpx1*	14775
P47791	Glutathione reductase, mitochondrial	*Gsr*	14782
P24472	Glutathione S-transferase A4	*Gsta4*	14860
P10649	Glutathione S-transferase Mu 1	*Gstm1*	14862
P15626	Glutathione S-transferase Mu 2	*Gstm2*	14863
P19157	Glutathione S-transferase P 1	*Gstp1*	14870
P51855	Glutathione synthetase	*Gss*	14854
Q8CI94	Glycogen phosphorylase, brain form	*Pygb*	110078
Q9ET01	Glycogen phosphorylase, liver form	*Pygl*	110095
Q9CPV4	Glyoxalase domain-containing protein 4	*Glod4*	67201
Q99JX3	Golgi reassembly-stacking protein 2	*Gorasp2*	70231
Q99LP6	GrpE protein homolog 1, mitochondrial	*Grpel1*	17713
Q9WTP7	GTP:AMP phosphotransferase AK3, mitochondrial	*Ak3*	56248
P01921	H-2 class II histocompatibility antigen, A-D beta chain	*H2-Ab1*	14961
P04227	H-2 class II histocompatibility antigen, A-Q alpha chain (Fragment)	*H2-Aa*	14960
Q9CYW4	Haloacid dehalogenase-like hydrolase domain-containing protein 3	*Hdhd3*	72748
Q61696	Heat shock 70 kDa protein 1A	*Hspa1a*	193740
Q61316	Heat shock 70 kDa protein 4	*Hspa4*	15525
P63017	Heat shock cognate 71 kDa protein	*Hspa8*	15481
Q9CQN1	Heat shock protein 75 kDa, mitochondrial	*Trap1*	68015
P07901	Heat shock protein HSP 90-alpha	*Hsp90aa1*	15519
P11499	Heat shock protein HSP 90-beta	*Hsp90ab1*	15516
P17156	Heat shock-related 70 kDa protein 2	*Hspa2*	15512
P51859	Hepatoma-derived growth factor	*Hdgf*	15191
Q99020	Heterogeneous nuclear ribonucleoprotein A/B	*Hnrnpab*	15384
P49312	Heterogeneous nuclear ribonucleoprotein A1	*Hnrnpa1*	15382
Q8BG05	Heterogeneous nuclear ribonucleoprotein A3	*Hnrnpa3*	229279

Q60668	Heterogeneous nuclear ribonucleoprotein D0	*Hnrnpd*	11991
O35737	Heterogeneous nuclear ribonucleoprotein H	*Hnrnph1*	59013
P61979	Heterogeneous nuclear ribonucleoprotein K	*Hnrnpk*	15387
Q7TMK9	Heterogeneous nuclear ribonucleoprotein Q	*Syncrip*	56403
P17710	Hexokinase-1	*Hk1*	15275
O54879	High mobility group protein B3	*Hmgb3*	15354
P70349	Histidine triad nucleotide-binding protein 1	*Hint1*	15254
P15864	Histone H1.2	*Hist1h1c*	50708
P43274	Histone H1.4	*Hist1h1e*	50709
Q8CGP6	Histone H2A type 1-H	*Hist1h2ah*	319168
P0C0S6	Histone H2A.Z	*H2afz*	51788
P10853	Histone H2B type 1-F/J/L	*Hist1h2bf*	665622
P02301	Histone H3.3C	*H3f3c*	625328
P62806	Histone H4	*Hist1h4a*	320332
Q99L47	Hsc70-interacting protein	*St13*	70356
P00493	Hypoxanthine-guanine phosphoribosyltransferase	*Hprt1*	15452
Q91VM9	Inorganic pyrophosphatase 2, mitochondrial	*Ppa2*	74776
O55023	Inositol monophosphatase 1	*Impa1*	55980
O88844	Isocitrate dehydrogenase [NADP] cytoplasmic	*Idh1*	15926
P58044	Isopentenyl-diphosphate Delta-isomerase 1	*Idi1*	319554
P02535	Keratin, type I cytoskeletal 10	*Krt10*	16661
Q9Z2K1	Keratin, type I cytoskeletal 16	*Krt16*	16666
Q9QWL7	Keratin, type I cytoskeletal 17	*Krt17*	16667
P05784	Keratin, type I cytoskeletal 18	*Krt18*	16668
P19001	Keratin, type I cytoskeletal 19	*Krt19*	16669
Q6IFX2	Keratin, type I cytoskeletal 42	*Krt42*	68239
P04104	Keratin, type II cytoskeletal 1	*Krt1*	16678
Q3UV17	Keratin, type II cytoskeletal 2 oral	*Krt76*	77055
P50446	Keratin, type II cytoskeletal 6A	*Krt6a*	16687
Q9DCV7	Keratin, type II cytoskeletal 7	*Krt7*	110310
Q8VED5	Keratin, type II cytoskeletal 79	*Krt79*	223917
P11679	Keratin, type II cytoskeletal 8	*Krt8*	16691
Q9CPU0	Lactoylglutathione lyase	*Glo1*	109801
Q61029	Lamina-associated polypeptide 2, isoforms beta/delta/epsilon/gamma	*Tmpo*	21917
P14733	Lamin-B1	*Lmnb1*	16906
P21619	Lamin-B2	*Lmnb2*	16907
Q61792	LIM and SH3 domain protein 1	*Lasp1*	16796
P06151	L-lactate dehydrogenase A chain	*Ldha*	16828
P16125	L-lactate dehydrogenase B chain	*Ldhb*	16832

P51174	Long-chain specific acyl-CoA dehydrogenase, mitochondrial	*Acadl*	11363
Q91X52	L-xylulose reductase	*Dcxr*	67880
Q99MN1	Lysine--tRNA ligase	*Kars*	85305
P11438	Lysosome-associated membrane glycoprotein 1	*Lamp1*	16783
P08905	Lysozyme C-2	*Lyz2*	17105
Q9DAR7	m7GpppX diphosphatase	*Dcps*	69305
P24452	Macrophage-capping protein	*Capg*	12332
P14152	Malate dehydrogenase, cytoplasmic	*Mdh1*	17449
P08249	Malate dehydrogenase, mitochondrial	*Mdh2*	17448
Q9CXI5	Mesencephalic astrocyte-derived neurotrophic factor	*Manf*	74840
P12032	Metalloproteinase inhibitor 1	*Timp1*	21857
P26041	Moesin	*Msn*	17698
Q02496	Mucin-1	*Muc1*	17829
Q60605	Myosin light polypeptide 6	*Myl6*	17904
Q3THE2	Myosin regulatory light chain 12B	*Myl12b*	67938
Q6URW6	Myosin-14	*Myh14*	71960
Q8VDD5	Myosin-9	*Myh9*	17886
P62774	Myotrophin	*Mtpn*	14489
P70441	Na(+)/H(+) exchange regulatory cofactor NHE-RF1	*Slc9a3r1*	26941
Q8K4Z3	NAD(P)H-hydrate epimerase	*Apoa1bp*	246703
Q9D6J6	NADH dehydrogenase [ubiquinone] flavoprotein 2, mitochondrial	*Ndufv2*	72900
Q9DCN2	NADH-cytochrome b5 reductase 3	*Cyb5r3*	109754
P06801	NADP-dependent malic enzyme	*Me1*	17436
Q60817	Nascent polypeptide-associated complex subunit alpha	*Naca*	17938
Q99KQ4	Nicotinamide phosphoribosyltransferase	*Nampt*	59027
Q9CZ44	NSFL1 cofactor p47	*Nsfl1c*	386649
O35685	Nuclear migration protein nudC	*Nudc*	18221
P62960	Nuclease-sensitive element-binding protein 1	*Ybx1*	22608
P81117	Nucleobindin-2	*Nucb2*	53322
P09405	Nucleolin	*Ncl*	17975
P15532	Nucleoside diphosphate kinase A	*Nme1*	18102
P29758	Ornithine aminotransferase, mitochondrial	*Oat*	18242
Q9D0J8	Parathymosin	*Ptms*	69202
O70400	PDZ and LIM domain protein 1	*Pdlim1*	54132
P17742	Peptidyl-prolyl cis-trans isomerase A	*Ppia*	268373
P24369	Peptidyl-prolyl cis-trans isomerase B	*Ppib*	19035
P30412	Peptidyl-prolyl cis-trans isomerase C	*Ppic*	19038
P26883	Peptidyl-prolyl cis-trans isomerase FKBP1A	*Fkbp1a*	14225
P45878	Peptidyl-prolyl cis-trans isomerase FKBP2	*Fkbp2*	14227

P30416	Peptidyl-prolyl cis-trans isomerase FKBP4	*Fkbp4*	14228
P35700	Peroxiredoxin-1	*Prdx1*	18477
Q61171	Peroxiredoxin-2	*Prdx2*	21672
P99029	Peroxiredoxin-5, mitochondrial	*Prdx5*	54683
O08709	Peroxiredoxin-6	*Prdx6*	11758
P70296	Phosphatidylethanolamine-binding protein 1	*Pebp1*	23980
Q9CYR6	Phosphoacetylglucosamine mutase	*Pgm3*	109785
Q9D0F9	Phosphoglucomutase-1	*Pgm1*	72157
P09411	Phosphoglycerate kinase 1	*Pgk1*	18655
P22777	Plasminogen activator inhibitor 1	*Serpine1*	18787
Q61233	Plastin-2	*Lcp1*	18826
Q99K51	Plastin-3	*Pls3*	102866
Q08857	Platelet glycoprotein 4	*Cd36*	12491
Q9QXS1	Plectin	*Plec*	18810
Q8CG72	Poly(ADP-ribose) glycohydrolase ARH3	*Adprhl2*	100206
P60335	Poly(rC)-binding protein 1	*Pcbp1*	23983
Q61990	Poly(rC)-binding protein 2	*Pcbp2*	18521
Q3UEB3	Poly(U)-binding-splicing factor PUF60	*Puf60*	67959
P29341	Polyadenylate-binding protein 1	*Pabpc1*	18458
P0CG49	Polyubiquitin-B	*Ubb*	22187
Q03958	Prefoldin subunit 6	*Pfdn6*	14976
P48678	Prelamin-A/C	*Lmna*	16905
P62962	Profilin-1	*Pfn1*	18643
Q9WU78	Programmed cell death 6-interacting protein	*Pdcd6ip*	18571
P97371	Proteasome activator complex subunit 1	*Psme1*	19186
P97372	Proteasome activator complex subunit 2	*Psme2*	19188
Q9R1P4	Proteasome subunit alpha type-1	*Psma1*	26440
O70435	Proteasome subunit alpha type-3	*Psma3*	19167
Q9R1P0	Proteasome subunit alpha type-4	*Psma4*	26441
Q9Z2U1	Proteasome subunit alpha type-5	*Psma5*	26442
Q9QUM9	Proteasome subunit alpha type-6	*Psma6*	26443
Q9Z2U0	Proteasome subunit alpha type-7	*Psma7*	26444
O09061	Proteasome subunit beta type-1	*Psmb1*	19170
Q9R1P3	Proteasome subunit beta type-2	*Psmb2*	26445
Q9R1P1	Proteasome subunit beta type-3	*Psmb3*	26446
P99026	Proteasome subunit beta type-4	*Psmb4*	19172
Q60692	Proteasome subunit beta type-6	*Psmb6*	19175
P70195	Proteasome subunit beta type-7	*Psmb7*	19177
P28063	Proteasome subunit beta type-8	*Psmb8*	16913
O35522	Proteasome subunit beta type-9	*Psmb9*	16912
P09103	Protein disulfide-isomerase	*P4hb*	18453
P27773	Protein disulfide-isomerase A3	*Pdia3*	14827
P08003	Protein disulfide-isomerase A4	*Pdia4*	12304
Q922R8	Protein disulfide-isomerase A6	*Pdia6*	71853
Q99LX0	Protein DJ-1	*Park7*	57320
Q921M7	Protein FAM49B	*Fam49b*	223601

Q9WVE8	Protein kinase C and casein kinase substrate in neurons protein 2	*Pacsin2*	23970
P97352	Protein S100-A13	*S100a13*	20196
P97816	Protein S100-G	*S100g*	12309
Q9D1M0	Protein SEC13 homolog	*Sec13*	110379
Q9EQU5	Protein SET	*Set*	56086
P26350	Prothymosin alpha	*Ptma*	19231
P61458	Pterin-4-alpha-carbinolamine dehydratase	*Pcbd1*	13180
P50405	Pulmonary surfactant-associated protein B	*Sftpb*	20388
P21841	Pulmonary surfactant-associated protein C	*Sftpc*	20389
P50404	Pulmonary surfactant-associated protein D	*Sftpd*	20390
P23492	Purine nucleoside phosphorylase	*Pnp*	18950
Q11011	Puromycin-sensitive aminopeptidase	*Npepps*	19155
Q64G17	Putative acidic leucine-rich nuclear phosphoprotein 32 family member C	*Anp32c*	448829
P52480	Pyruvate kinase PKM	*Pkm*	18746
P50396	Rab GDP dissociation inhibitor alpha	*Gdi1*	14567
Q61598	Rab GDP dissociation inhibitor beta	*Gdi2*	14569
P26043	Radixin	*Rdx*	19684
P34022	Ran-specific GTPase-activating protein	*Ranbp1*	19385
P97855	Ras GTPase-activating protein-binding protein 1	*G3bp1*	27041
Q9JKF1	Ras GTPase-activating-like protein IQGAP1	*Iqgap1*	29875
Q9DCV4	Regulator of microtubule dynamics protein 1	*Rmdn1*	66302
P24549	Retinal dehydrogenase 1	*Aldh1a1*	11668
Q99PT1	Rho GDP-dissociation inhibitor 1	*Arhgdia*	192662
Q91VI7	Ribonuclease inhibitor	*Rnh1*	107702
Q99PL5	Ribosome-binding protein 1	*Rrbp1*	81910
Q9JI75	Ribosyldihydronicotinamide dehydrogenase [quinone]	*Nqo2*	18105
Q91VM5	RNA binding motif protein, X-linked-like-1	*Rbmxl1*	19656
Q61545	RNA-binding protein EWS	*Ewsr1*	14030
P56959	RNA-binding protein FUS	*Fus*	233908
P17563	Selenium-binding protein 1	*Selenbp1*	20341
P58389	Serine/threonine-protein phosphatase 2A activator	*Ppp2r4*	110854
Q921I1	Serotransferrin	*Tf*	22041
Q60854	Serpin B6	*Serpinb6*	20719
Q9JJU8	SH3 domain-binding glutamic acid-rich-like protein	*Sh3bgrl*	56726
Q91VW3	SH3 domain-binding glutamic acid-rich-like protein 3	*Sh3bgrl3*	73723
P62320	Small nuclear ribonucleoprotein Sm D3	*Snrpd3*	67332
P61957	Small ubiquitin-related modifier 2	*Sumo2*	170930

Q9DBP0	Sodium-dependent phosphate transport protein 2B	*Slc34a2*	20531
Q64442	Sorbitol dehydrogenase	*Sord*	20322
P16546	Spectrin alpha chain, non-erythrocytic 1	*Sptan1*	20740
Q62261	Spectrin beta chain, non-erythrocytic 1	*Sptbn1*	20742
Q9WTX5	S-phase kinase-associated protein 1	*Skp1*	21402
Q9Z1N5	Spliceosome RNA helicase Ddx39b	*Ddx39b*	53817
Q8VIJ6	Splicing factor, proline- and glutamine-rich	*Sfpq*	71514
Q60864	Stress-induced-phosphoprotein 1	*Stip1*	20867
P28862	Stromelysin-1	*Mmp3*	17392
Q9D0K2	Succinyl-CoA:3-ketoacid coenzyme A transferase 1, mitochondrial	*Oxct1*	67041
P08228	Superoxide dismutase [Cu-Zn]	*Sod1*	20655
P09671	Superoxide dismutase [Mn], mitochondrial	*Sod2*	20656
O35988	Syndecan-4	*Sdc4*	20971
P26039	Talin-1	*Tln1*	21894
P10639	Thioredoxin	*Txn*	22166
Q91W90	Thioredoxin domain-containing protein 5	*Txndc5*	105245
Q9JMH6	Thioredoxin reductase 1, cytoplasmic	*Txnrd1*	50493
P20108	Thioredoxin-dependent peroxide reductase, mitochondrial	*Prdx3*	11757
P52196	Thiosulfate sulfurtransferase	*Tst*	22117
P35441	Thrombospondin-1	*Thbs1*	21825
Q93092	Transaldolase	*Taldo1*	21351
Q9WVA4	Transgelin-2	*Tagln2*	21346
Q01853	Transitional endoplasmic reticulum ATPase	*Vcp*	269523
P40142	Transketolase	*Tkt*	21881
Q62348	Translin	*Tsn*	22099
Q9JHJ0	Tropomodulin-3	*Tmod3*	50875
P58771	Tropomyosin alpha-1 chain	*Tpm1*	22003
P21107	Tropomyosin alpha-3 chain	*Tpm3*	59069
Q6IRU2	Tropomyosin alpha-4 chain	*Tpm4*	326618
P58774	Tropomyosin beta chain	*Tpm2*	22004
P05213	Tubulin alpha-1B chain	*Tuba1b*	22143
P68373	Tubulin alpha-1C chain	*Tuba1c*	22146
P68372	Tubulin beta-4B chain	*Tubb4b*	227613
Q9CRB6	Tubulin polymerization-promoting protein family member 3	*Tppp3*	67971
P48428	Tubulin-specific chaperone A	*Tbca*	21371
Q62393	Tumor protein D52	*Tpd52*	21985
Q9CYZ2	Tumor protein D54	*Tpd52l2*	66314
P61087	Ubiquitin-conjugating enzyme E2 K	*Ube2k*	53323
P68037	Ubiquitin-conjugating enzyme E2 L3	*Ube2l3*	22195
P61089	Ubiquitin-conjugating enzyme E2 N	*Ube2n*	93765
Q9D2M8	Ubiquitin-conjugating enzyme E2 variant 2	*Ube2v2*	70620
Q9DBP5	UMP-CMP kinase	*Cmpk1*	66588

Q06318	Uteroglobin	*Scgb1a1*	22287
P54728	UV excision repair protein RAD23 homolog B	*Rad23b*	19359
Q9QY76	Vesicle-associated membrane protein-associated protein B	*Vapb*	56491
P20152	Vimentin	*Vim*	22352
Q64727	Vinculin	*Vcl*	22330
P50516	V-type proton ATPase catalytic subunit A	*Atp6v1a*	11964
P62814	V-type proton ATPase subunit B, brain isoform	*Atp6v1b2*	11966
P50518	V-type proton ATPase subunit E 1	*Atp6v1e1*	11973
Q9CR51	V-type proton ATPase subunit G 1	*Atp6v1g1*	66290
Q00519	Xanthine dehydrogenase/oxidase	*Xdh*	22436

Table 13: List of proteins only identified in BALF from SPC-HA mice (Σ129).

Accession ID	Protein	Gene symbol	Entrez Gene ID
Q3UHX2	28 kDa heat- and acid-stable phosphoprotein	*Pdap1*	231887
Q9Z0S1	3'(2'),5'-bisphosphate nucleotidase 1	*Bpnt1*	23827
Q8QZS1	3-hydroxyisobutyryl-CoA hydrolase, mitochondrial	*Hibch*	227095
Q8K010	5-oxoprolinase	*Oplah*	75475
Q9CQ60	6-phosphogluconolactonase	*Pgls*	66171
P33434	72 kDa type IV collagenase	*Mmp2*	17390
Q91XA9	Acidic mammalian chitinase	*Chia*	81600
Q9Z2N8	Actin-like protein 6A	*Actl6a*	56456
Q6P5E6	ADP-ribosylation factor-binding protein GGA2	*Gga2*	74105
P97449	Aminopeptidase N	*Anpep*	16790
G5E8K5	Ankyrin-3	*Ank3*	11735
O35639	Annexin A3	*Anxa3*	11745
O35841	Apoptosis inhibitor 5	*Api5*	11800
Q7SIG6	Arf-GAP with SH3 domain, ANK repeat and PH domain-containing protein 2	*Asap2*	211914
Q91YI0	Argininosuccinate lyase	*Asl*	109900
Q9DC29	ATP-binding cassette sub-family B member 6, mitochondrial	*Abcb6*	74104
Q9JLV1	BAG family molecular chaperone regulator 3	*Bag3*	29810
Q99NF1	Beta,beta-carotene 9',10'-oxygenase	*Bco2*	170752
P28653	Biglycan	*Bgn*	12111
Q8R016	Bleomycin hydrolase	*Blmh*	104184

O35855	Branched-chain-amino-acid aminotransferase, mitochondrial	*Bcat2*	12036
Q9DB16	Calcium-binding protein 39-like	*Cab39l*	69008
Q9D7J7	Calpain small subunit 2	*Capns2*	69543
Q08093	Calponin-2	*Cnn2*	12798
P14211	Calreticulin	*Calr*	12317
P00920	Carbonic anhydrase 2	*Ca2*	12349
Q9D7S9	Charged multivesicular body protein 5	*Chmp5*	76959
P83917	Chromobox protein homolog 1	*Cbx1*	12412
P59242	Cingulin	*Cgn*	70737
Q68FD5	Clathrin heavy chain 1	*Cltc*	67300
O08585	Clathrin light chain A	*Clta*	12757
P61924	Coatomer subunit zeta-1	*Copz1*	56447
P11087	Collagen alpha-1(I) chain	*Col1a1*	12842
Q62426	Cystatin-B	*Cstb*	13014
P99028	Cytochrome b-c1 complex subunit 6, mitochondrial	*Uqcrh*	66576
Q8R0Y6	Cytosolic 10-formyltetrahydrofolate dehydrogenase	*Aldh1l1*	107747
Q9CQJ6	Density-regulated protein	*Denr*	68184
P62627	Dynein light chain roadblock-type 1	*Dynlrb1*	67068
Q7TNG5	Echinoderm microtubule-associated protein-like 2	*Eml2*	72205
Q9DCW4	Electron transfer flavoprotein subunit beta	*Etfb*	110826
Q99K30	Epidermal growth factor receptor kinase substrate 8-like protein 2	*Eps8l2*	98845
Q9WUK2	Eukaryotic translation initiation factor 4H	*Eif4h*	22384
P63242	Eukaryotic translation initiation factor 5A-1	*Eif5a*	276770
P97447	Four and a half LIM domains protein 1	*Fhl1*	14199
Q921G8	Gamma-tubulin complex component 2	*Tubgcp2*	74237
P16406	Glutamyl aminopeptidase	*Enpep*	13809
P10648	Glutathione S-transferase A2	*Gsta2*	14858
P30115	Glutathione S-transferase A3	*Gsta3*	14859
P43081	Guanylyl cyclase-activating protein 1	*Guca1a*	14913
O88569	Heterogeneous nuclear ribonucleoproteins A2/B1	*Hnrnpa2b1*	53379
Q9Z204	Heterogeneous nuclear ribonucleoproteins C1/C2	*Hnrnpc*	15381
P63158	High mobility group protein B1	*Hmgb1*	15289
P17095	High mobility group protein HMG-I/HMG-Y	*Hmga1*	15361
Q60972	Histone-binding protein RBBP4	*Rbbp4*	19646
Q61425	Hydroxyacyl-coenzyme A dehydrogenase, mitochondrial	*Hadh*	15107
P40936	Indolethylamine N-methyltransferase	*Inmt*	21743
O88792	Junctional adhesion molecule A	*F11r*	16456
Q3TTY5	Keratin, type II cytoskeletal 2 epidermal	*Krt2*	16681

Q99KP3	Lambda-crystallin homolog	*Cryl1*	68631
P02468	Laminin subunit gamma-1	*Lamc1*	226519
P24527	Leukotriene A-4 hydrolase	*Lta4h*	16993
Q9D358	Low molecular weight phosphotyrosine protein phosphatase	*Acp1*	11431
P17047	Lysosome-associated membrane glycoprotein 2	*Lamp2*	16784
Q9EQK5	Major vault protein	*Mvp*	78388
P25785	Metalloproteinase inhibitor 2	*Timp2*	21858
Q9Z2D6	Methyl-CpG-binding protein 2	*Mecp2*	17257
Q9EQ20	Methylmalonate-semialdehyde dehydrogenase [acylating], mitochondrial	*Aldh6a1*	104776
Q9CRB9	MICOS complex subunit Mic19	*Chchd3*	66075
Q0P557	Mitochondria-eating protein	*Spata18*	73472
P62075	Mitochondrial import inner membrane translocase subunit Tim13	*Timm13*	30055
Q6PEB6	MOB-like protein phocein	*Mob4*	19070
Q69ZN7	Myoferlin	*Myof*	226101
P82343	N-acylglucosamine 2-epimerase	*Renbp*	19703
Q8BHN3	Neutral alpha-glucosidase AB	*Ganab*	14376
Q8R1F1	Niban-like protein 1	*Fam129b*	227737
P18608	Non-histone chromosomal protein HMG-14	*Hmgn1*	15312
P32020	Non-specific lipid-transfer protein	*Scp2*	20280
Q80XU3	Nuclear ubiquitous casein and cyclin-dependent kinase substrate 1	*Nucks1*	98415
Q9WV85	Nucleoside diphosphate kinase 3	*Nme3*	79059
Q62446	Peptidyl-prolyl cis-trans isomerase FKBP3	*Fkbp3*	30795
Q9CWW6	Peptidyl-prolyl cis-trans isomerase NIMA-interacting 4	*Pin4*	69713
Q9R269	Periplakin	*Ppl*	19041
Q9DBJ1	Phosphoglycerate mutase 1	*Pgam1*	18648
Q9CY58	Plasminogen activator inhibitor 1 RNA-binding protein	*Serbp1*	66870
O54724	Polymerase I and transcript release factor	*Ptrf*	19285
P17225	Polypyrimidine tract-binding protein 1	*Ptbp1*	19205
Q6NSR8	Probable aminopeptidase NPEPL1	*Npepl1*	228961
P50580	Proliferation-associated protein 2G4	*Pa2g4*	18813
Q9QUR6	Prolyl endopeptidase	*Prep*	19072
Q99MN9	Propionyl-CoA carboxylase beta chain, mitochondrial	*Pccb*	66904
P49722	Proteasome subunit alpha type-2	*Psma2*	19166
O55234	Proteasome subunit beta type-5	*Psmb5*	19173
Q9CQ89	Protein CutA	*Cuta*	67675
Q99LT0	Protein dpy-30 homolog	*Dpy30*	66310
Q62433	Protein NDRG1	*Ndrg1*	17988
Q9CQE1	Protein NipSnap homolog 3B	*Nipsnap3b*	66536

P14069	Protein S100-A6	*S100a6*	20200
Q91V41	Ras-related protein Rab-14	*Rab14*	68365
P62821	Ras-related protein Rab-1A	*Rab1A*	19324
Q8BHL4	Retinoic acid-induced protein 3	*Gprc5a*	232431
Q9CWY8	Ribonuclease H2 subunit A	*Rnaseh2a*	69724
P52760	Ribonuclease UK114	*Hrsp12*	15473
Q9CWZ3	RNA-binding protein 8A	*Rbm8a*	60365
Q8R4Y8	Rotatin	*Rttn*	246102
Q99J08	SEC14-like protein 2	*Sec14l2*	67815
Q8R0F9	SEC14-like protein 4	*Sec14l4*	103655
O55131	Septin-7	*Sept7*	235072
Q76MZ3	Serine/threonine-protein phosphatase 2A 65 kDa regulatory subunit A alpha isoform	*Ppp2r1a*	51792
P07724	Serum albumin	*Alb*	11657
P55012	Solute carrier family 12 member 2	*Slc12a2*	20496
Q9CWK8	Sorting nexin-2	*Snx2*	67804
P07214	SPARC	*Sparc*	20692
Q8K4Z5	Splicing factor 3A subunit 1	*Sf3a1*	67465
Q921M3	Splicing factor 3B subunit 3	*Sf3b3*	101943
Q9DBG9	Tax1-binding protein 3	*Tax1bp3*	76281
P80317	T-complex protein 1 subunit zeta	*Cct6a*	12466
Q9JLT4	Thioredoxin reductase 2, mitochondrial	*Txnrd2*	26462
P97493	Thioredoxin, mitochondrial	*Txn2*	56551
Q8CDN6	Thioredoxin-like protein 1	*Txnl1*	53382
P42669	Transcriptional activator protein Pur-alpha	*Pura*	19290
Q9R1Q8	Transgelin-3	*Tagln3*	56370
P17751	Triosephosphate isomerase	*Tpi1*	21991
O35900	U6 snRNA-associated Sm-like protein LSm2	*Lsm2*	27756
Q91ZJ5	UTP--glucose-1-phosphate uridylyltransferase	*Ugp2*	216558
P40336	Vacuolar protein sorting-associated protein 26A	*Vps26a*	30930
Q99KC8	von Willebrand factor A domain-containing protein 5A	*Vwa5a*	67776
Q9D1K2	V-type proton ATPase subunit F	*Atp6v1f*	66144
O88342	WD repeat-containing protein 1	Wdr1	22388
Q11136	Xaa-Pro dipeptidase	Pepd	18624

Table 14: List of proteins only identified in BALF from SPC-HAxTCR-HA mice (Σ101).

Accession ID	Protein	Gene symbol	Entrez Gene ID
P61161	Actin-related protein 2	*Actr2*	66713
P56376	Acylphosphatase-1	*Acyp1*	66204
P28474	Alcohol dehydrogenase class-3	*Adh5*	11532
P55264	Adenosine kinase	*Adk*	11534
P47739	Aldehyde dehydrogenase, dimeric NADP-preferring	*Aldh3a1*	11670
P10107	Annexin A1	*Anxa1*	16952
P22892	AP-1 complex subunit gamma-1	*Ap1g1*	11765
Q61599	Rho GDP-dissociation inhibitor 2	*Arhgdib*	11857
Q9CVB6	Actin-related protein 2/3 complex subunit 2	*Arpc2*	76709
P01887	Beta-2-microglobulin	*B2m*	12010
P51437	Cathelin-related antimicrobial peptide	*Camp*	12796
P35564	Calnexin	*Canx*	12330
O35350	Calpain-1 catalytic subunit	*Capn1*	12333
P51125	Calpastatin	*Cast*	12380
P80314	T-complex protein 1 subunit beta	*Cct2*	12461
P80318	T-complex protein 1 subunit gamma	*Cct3*	12462
P80315	T-complex protein 1 subunit delta	*Cct4*	12464
P42932	T-complex protein 1 subunit theta	*Cct8*	12469
P10810	Monocyte differentiation antigen CD14	*Cd14*	12475
O35744	Chitinase-like protein 3	*Chil3*	12655
Q04447	Creatine kinase B-type	*Ckb*	12709
Q99KN9	Clathrin interactor 1	*Clint1*	216705
Q9QXT0	Protein canopy homolog 2	*Cnpy2*	56530
O89053	Coronin-1A	*Coro1a*	12721
Q9CQI6	Coactosin-like protein	*Cotl1*	72042
Q02248	Catenin beta-1	*Ctnnb1*	12387
O70370	Cathepsin S	*Ctss*	13040
P48024	Eukaryotic translation initiation factor 1	*Eif1*	20918
Q60872	Eukaryotic translation initiation factor 1A	*Eif1a*	13664
Q3UGC7	Eukaryotic translation initiation factor 3 subunit J-A	*Eif3j1*	78655
P60843	Eukaryotic initiation factor 4A-I	*Eif4a1*	13681
O55135	Eukaryotic translation initiation factor 6	*Eif6*	16418
Q9CQ92	Mitochondrial fission 1 protein	*Fis1*	66437
P16858	Glyceraldehyde-3-phosphate dehydrogenase	*Gapdh*	14433
Q01514	Interferon-induced guanylate-binding protein 1	*Gbp1*	14468
Q9Z0E6	Interferon-induced guanylate-binding protein 2	*Gbp2*	14469
Q9R111	Guanine deaminase	*Gda*	14544

Q9CQM9	Glutaredoxin-3	*Glrx3*	30926
Q60631	Growth factor receptor-bound protein 2	*Grb2*	14784
P10922	Histone H1.0	*H1f0*	14958
P01902	H-2 class I histocompatibility antigen, K-D alpha chain	*H2-K1*	14972
P14430	H-2 class I histocompatibility antigen, Q8 alpha chain	*H2-Q8*	15019
Q61035	Histidine--tRNA ligase, cytoplasmic	*Hars*	15115
P02088	Hemoglobin subunit beta-1	*Hbb-b1*	15129
P43276	Histone H1.5	*Hist1h1b*	56702
P13597	Intercellular adhesion molecule 1	*Icam1*	15894
P01868	Ig gamma-1 chain C region secreted form	*Ighg1*	16017
P01872	Ig mu chain C region	*Ighm*	16019
P01878	Ig alpha chain C region	*Igh-VJ558*	16061
P01592	Immunoglobulin J chain	*Igj*	16069
P01837	Ig kappa chain C region	*Igkc*	16071
Q9QZ85	Interferon-inducible GTPase 1	*Iigp1*	60440
Q8CAQ8	Mitochondrial inner membrane protein	*Immt*	76614
P49442	Inositol polyphosphate 1-phosphatase	*Inpp1*	16329
O89112	LanC-like protein 1	*Lancl1*	14768
Q07797	Galectin-3-binding protein	*Lgals3bp*	19039
P08071	Lactotransferrin	*Ltf*	17002
P61327	Protein mago nashi homolog	*Magoh*	17149
P34960	Macrophage metalloelastase	*Mmp12*	17381
Q8BPB0	MOB kinase activator 1B	*Mob1b*	68473
Q922D8	C-1-tetrahydrofolate synthase, cytoplasmic	*Mthfd1*	108156
Q9JK81	UPF0160 protein MYG1, mitochondrial	*Myg1*	60315
Q6PDN3	Myosin light chain kinase, smooth muscle	*Mylk*	107589
P29595	NEDD8	*Nedd8*	18002
Q61937	Nucleophosmin	*Npm1*	18148
Q02819	Nucleobindin-1	*Nucb1*	18220
P56812	Programmed cell death protein 5	*Pdcd5*	100042424
Q62048	Astrocytic phosphoprotein PEA-15	*Pea15*	18611
O70591	Prefoldin subunit 2	*Pfdn2*	18637
Q8CHP8	Phosphoglycolate phosphatase	*Pgp*	67078
O70570	Polymeric immunoglobulin receptor	*Pigr*	18703
A3KGF7	1-phosphatidylinositol 4,5-bisphosphate phosphodiesterase beta-2	*Plcb2*	18796
Q9Z2M7	Phosphomannomutase 2	*Pmm2*	54128
Q9D819	Inorganic pyrophosphatase	*Ppa1*	67895
Q9CR16	Peptidyl-prolyl cis-trans isomerase D	*Ppid*	67738
Q61207	Prosaposin	*Psap*	19156
O35955	Proteasome subunit beta type-10	*Psmb10*	19171
Q9EPB4	Apoptosis-associated speck-like protein containing a CARD	*Pycard*	66824

Q8BND5	Sulfhydryl oxidase 1	*Qsox1*	104009
P62492	Ras-related protein Rab-11A	*Rab11a*	53869
Q9EP95	Resistin-like alpha	*Retnla*	57262
Q9CZX8	40S ribosomal protein S19	*Rps19*	20085
P62908	40S ribosomal protein S3	*Rps3*	27050
P14206	40S ribosomal protein SA	*Rpsa*	16785
Q01730	Ras suppressor protein 1	*Rsu1*	20163
P56565	Protein S100-A1	*S100a1*	20193
Q60710	Deoxynucleoside triphosphate triphosphohydrolase SAMHD1	*Samhd1*	56045
P07759	Serine protease inhibitor A3K	*Serpina3k*	20714
P97290	Plasma protease C1 inhibitor	*Serping1*	12258
P35242	Pulmonary surfactant-associated protein A	*Sftpa1*	20387
Q64105	Sepiapterin reductase	*Spr*	20751
P13609	Serglycin	*Srgn*	19073
Q62093	Serine/arginine-rich splicing factor 2	*Srsf2*	20382
P37804	Transgelin	*Tagln*	21345
P10711	Transcription elongation factor A protein 1	*Tcea1*	21399
P21981	Protein-glutamine gamma-glutamyltransferase 2	*Tgm2*	21817
Q9QZE7	Translin-associated protein X	*Tsnax*	53424
Q9Z0P5	Twinfilin-2	*Twf2*	23999
Q02053	Ubiquitin-like modifier-activating enzyme 1	*Uba1*	22201
Q9Z1Z0	General vesicular transport factor p115	*Uso1*	56041
Q9Z1Q9	Valine--tRNA ligase	*Vars*	22321

Table 15: KEGG pathway analyses of SPC-HA and SPC-HAxTCR-HA BALFomes.
n.e. = no significant enrichment

		SPC-HA		SPC-HAxTCR-HA	
KEGG ID	**GOTerm**	**% associated genes**	**Term p-value corrected with Bonferroni**	**% associated genes**	**Term p-value corrected with Bonferroni**
3050	**Proteasome**	40	3,50E-12	37,8	3,90E-11
620	**Pyruvate metabolism**	28,2	2,20E-05	30,8	1,70E-06
480	**Glutathione metabolism**	27,3	2,50E-07	20	7,00E-04
30	**Pentose phosphate pathway**	26,7	1,50E-03	23,3	1,10E-02
10	**Glycolysis / Gluconeogenesis**	24,2	4,70E-07	25,8	4,10E-08
630	**Glyoxylate and dicarboxylate metabolism**	23,1	3,50E-02	23,1	3,30E-02
280	**Valine, leucine and isoleucine degradation**	22,2	1,00E-04	n.e.	n.e.
640	**Propanoate metabolism**	22,2	4,20E-02	n.e.	n.e.
4966	**Collecting duct acid secretion**	22,2	4,20E-02	n.e.	n.e.
20	**Citrate cycle (TCA cycle)**	21,9	1,80E-02	21,9	1,60E-02
51	**Fructose and mannose metabolism**	20	3,10E-02	20	2,90E-02
270	**Cysteine and methionine metabolism**	20	1,30E-02	20	1,20E-02
40	**Pentose and glucuronate interconversions**	19,4	3,70E-02	n.e.	n.e.
520	**Amino sugar and nucleotide sugar metabolism**	19,1	7,50E-03	n.e.	n.e.
330	**Arginine and proline metabolism**	15,3	4,00E-02	15,3	3,60E-02
4141	**Protein processing in endoplasmic reticulum**	13,6	2,70E-05	13,6	1,90E-05
3040	**Spliceosome**	11,9	7,90E-03	n.e.	n.e.
4145	**Phagosome**	10,9	6,50E-03	13,2	3,10E-05
4810	**Regulation of actin cytoskeleton**	n.e.	n.e.	9,6	1,20E-02

7.2 Abbreviations

α	**alpha**
A	adenosine nucleotide
AEC	airway epithelial cell
ALI	allergic lung inflammation
ATI	alveolar type I epithelial cell
ATII	alveolar type II epithelial cell
AM	alveolar macrophage
AMDC	airway mucosal dendritic cell
APC	allophycocyanin, also: antigen-presenting cell
ATCC	American Type Culture Collection
β	**beta**
BAL	bronchoalveolar lavage
BALF	bronchoalveolar lavage fluid
BSA	bovine serum albumin
°C	**degree Celsius**
C	cytosine nucleotide
CD	cluster of differentiation
cDNA	copy DNA
CFU	colony forming unit
COPD	chronic obstructive pulmonary disease
CpG	cytosine-phosphate-guanine
CRD	chronic respiratory disease
CTRL	control
CXCL	CXC chemokine ligand
CXCR	CXC chemokine receptor
Δ	**delta**
d	day
Da	dalton
DAMP	danger-associated molecular pattern
DAPI	4',6-diamidino-2-phenylindole
DNA	deoxyribonucleic acid
ds	double-stranded
e.g.	***exempli gratia***
EDTA	ethylenediaminetetraacetic acid
ELISA	enzyme-linked immunosorbent assay
ELR	conserved sequence motif (glutamic acid-leucine-arginine) found in many chemokines
ek	ethanol-killed
et al.	*et alii*

FACS	**fluorescence-activated cell sorting**
FBS	fetal bovine serum
FC	fold change
FITC	fluorescein isothiocyanate (fluorophore)
Foxp3	forkhead box P3
FSC	forward scatter
γ	**gamma**
g	gravitational force, also : gram
G	guanine nucleotide
GO	gene ontology
h	hour(s)
H&E	hematoxylin and eosin
HA	hemagglutinin
HRP	horseradish peroxidase
HZI	Helmholtz Centre for Infection Research
ICAM	**intercellular adhesion molecule**
i.e.	*id est*
IFN	interferon
Ig	immunoglobulin
IL	interleukin
IMDM	Iscove's Modified Dulbecco's Medium
IPD	invasive pneumococcal disease
IRF	interferon regulatory factor
κ	**kappa**
KC	keratinocyte chemoattractant
kDA	kilodalton
KEGG	Kyoto Encyclopedia of Genes and Genomes
L	**liter**
LC-MS/MS	liquid chromatography-tandem mass spectrometry (MS) technique
log2	binary logarithm
LPS	lipopolysaccharide
µ	**micro**
m	milli
M	molar
MAMP	microbial-associated molecular pattern
MARCO	macrophage receptor with collagenous structure
MFI	median fluorescence intensity
MHC	major histocompatibility complex
min	minute(s)
MMP	matrix metalloproteinase

n	**number; also: nano**
n.e.	not significantly enriched
NO	nitric oxide
n.s.	not significant
OD	**optical density**
PAMP	**pathogen-associated molecular pattern**
PBS	phosphate buffered saline
PCR	polymerase chain reaction
PE	phycoerythrin (fluorophore)
PerCp	peridinin chlorophyll (fluorophore)
PGE_2	prostaglandin E_2
pH	indicates degree of acidity or basicity
pIgR	polymeric immunoglobulin receptor
PMN	polymorphonuclear neutrophil
PRR	pattern-recognition receptor
PVDF	polyvinylidene fluoride
RNA	**ribonucleic acid**
RT	reverse transcriptase
SC	**secretory component**
SD	standard deviation
SDS	sodium dodecyl sulfate
sec	second(s)
SEM	standard error of the mean
SIg	secretory immunoglobulin
SOCS	suppressor of cytokine signaling
T	**thymine nucleotide**
TCR	T cell receptor
TF	transcription factor
TGFβ	transforming growth factor beta
Th	T helper cell
TLR	Toll-like receptor
TNF-α	tumor necrosis factor alpha
Treg	regulatory T cell
v/v	**volume per volume**
vs.	*versus*
w/v	**weight per volume**

7.3 Table of figures

7.4 Table of tables

7.5 References

(1999). "Statement on sarcoidosis. Joint Statement of the American Thoracic Society (ATS), the European Respiratory Society (ERS) and the World Association of Sarcoidosis and Other Granulomatous Disorders (WASOG) adopted by the ATS Board of Directors and by the ERS Executive Committee, February 1999." Am J Respir Crit Care Med **160**(2): 736-755.

Agusti, A., W. MacNee, K. Donaldson and M. Cosio (2003). "Hypothesis: does COPD have an autoimmune component?" Thorax **58**(10): 832-834.

Akinbi, H. T., R. Epaud, H. Bhatt and T. E. Weaver (2000). "Bacterial killing is enhanced by expression of lysozyme in the lungs of transgenic mice." J Immunol **165**(10): 5760-5766.

Albiger, B., S. Dahlberg, A. Sandgren, F. Wartha, K. Beiter, H. Katsuragi, S. Akira, S. Normark and B. Henriques-Normark (2007). "Toll-like receptor 9 acts at an early stage in host defence against pneumococcal infection." Cell Microbiol **9**(3): 633-644.

Albiger, B., A. Sandgren, H. Katsuragi, U. Meyer-Hoffert, K. Beiter, F. Wartha, M. Hornef, S. Normark and B. H. Normark (2005). "Myeloid differentiation factor 88-dependent signalling controls bacterial growth during colonization and systemic pneumococcal disease in mice." Cell Microbiol **7**(11): 1603-1615.

Arita, M., F. Bianchini, J. Aliberti, A. Sher, N. Chiang, S. Hong, R. Yang, N. A. Petasis and C. N. Serhan (2005). "Stereochemical assignment, antiinflammatory properties, and receptor for the omega-3 lipid mediator resolvin E1." J Exp Med **201**(5): 713-722.

Arita, M., T. Ohira, Y. P. Sun, S. Elangovan, N. Chiang and C. N. Serhan (2007). "Resolvin E1 selectively interacts with leukotriene B4 receptor BLT1 and ChemR23 to regulate inflammation." J Immunol **178**(6): 3912-3917.

Arredouani, M., Z. Yang, Y. Ning, G. Qin, R. Soininen, K. Tryggvason and L. Kobzik (2004). "The scavenger receptor MARCO is required for lung defense against pneumococcal pneumonia and inhaled particles." J Exp Med **200**(2): 267-272.

Aubin, J. E. (1979). "Autofluorescence of viable cultured mammalian cells." J Histochem Cytochem **27**(1): 36-43.

Bals, R. (2000). "Epithelial antimicrobial peptides in host defense against infection." Respir Res **1**(3): 141-150.

Balter, M. S., W. L. Eschenbacher and M. Peters-Golden (1988). "Arachidonic acid metabolism in cultured alveolar macrophages from normal, atopic, and asthmatic subjects." Am Rev Respir Dis **138**(5): 1134-1142.

Barkauskas, C. E., M. J. Cronce, C. R. Rackley, E. J. Bowie, D. R. Keene, B. R. Stripp, S. H. Randell, P. W. Noble and B. L. Hogan (2013). "Type 2 alveolar cells are stem cells in adult lung." J Clin Invest **123**(7): 3025-3036.

Barnes, P. J. (2000). "Mechanisms in COPD: differences from asthma." Chest **117**(2 Suppl): 10S-14S.

Barnes, P. J. (2004). "Alveolar macrophages as orchestrators of COPD." COPD **1**(1): 59-70.

Barnes, P. J. (2008). "The cytokine network in asthma and chronic obstructive pulmonary disease." J Clin Invest **118**(11): 3546-3556.

Barnes, P. J. (2008). "Immunology of asthma and chronic obstructive pulmonary disease." Nat Rev Immunol **8**(3): 183-192.

Beck-Speier, I., N. Dayal, E. Karg, K. L. Maier, G. Schumann, H. Schulz, M. Semmler, S. Takenaka, K. Stettmaier, W. Bors, A. Ghio, J. M. Samet and J. Heyder (2005). "Oxidative stress and lipid mediators induced in alveolar macrophages by ultrafine particles." Free Radic Biol Med **38**(8): 1080-1092.

Beisswenger, C. and R. Bals (2005). "Antimicrobial peptides in lung inflammation." Chem Immunol Allergy **86**: 55-71.

Bello-Irizarry, S. N., J. Wang, K. Olsen, F. Gigliotti and T. W. Wright (2012). "The alveolar epithelial cell chemokine response to pneumocystis requires adaptor molecule MyD88 and interleukin-1 receptor but not toll-like receptor 2 or 4." Infect Immun **80**(11): 3912-3920.

Benayoun, L., A. Druilhe, M. C. Dombret, M. Aubier and M. Pretolani (2003). "Airway structural alterations selectively associated with severe asthma." Am J Respir Crit Care Med **167**(10): 1360-1368.

Benson, R. C., R. A. Meyer, M. E. Zaruba and G. M. McKhann (1979). "Cellular autofluorescence--is it due to flavins?" J Histochem Cytochem **27**(1): 44-48.

Berenson, C. S., M. A. Garlipp, L. J. Grove, J. Maloney and S. Sethi (2006). "Impaired phagocytosis of nontypeable Haemophilus influenzae by human alveolar macrophages in chronic obstructive pulmonary disease." J Infect Dis **194**(10): 1375-1384.

Berenson, C. S., C. T. Wrona, L. J. Grove, J. Maloney, M. A. Garlipp, P. K. Wallace, C. C. Stewart and S. Sethi (2006). "Impaired alveolar macrophage response to Haemophilus antigens in chronic obstructive lung disease." Am J Respir Crit Care Med **174**(1): 31-40.

Bingisser, R. M., P. A. Tilbrook, P. G. Holt and U. R. Kees (1998). "Macrophage-derived nitric oxide regulates T cell activation via reversible disruption of the Jak3/STAT5 signaling pathway." J Immunol **160**(12): 5729-5734.

Blanchard, D. K., J. Y. Djeu, T. W. Klein, H. Friedman and W. E. Stewart, 2nd (1988). "Protective effects of tumor necrosis factor in experimental Legionella pneumophila infections of mice via activation of PMN function." J Leukoc Biol **43**(5): 429-435.

Blumenthal, R. L., D. E. Campbell, P. Hwang, R. H. DeKruyff, L. R. Frankel and D. T. Umetsu (2001). "Human alveolar macrophages induce functional inactivation in antigen-specific CD4 T cells." J Allergy Clin Immunol **107**(2): 258-264.

Blutt, S. E., A. D. Miller, S. L. Salmon, D. W. Metzger and M. E. Conner (2012). "IgA is important for clearance and critical for protection from rotavirus infection." Mucosal Immunol **5**(6): 712-719.

Boorsma, C. E., C. Draijer and B. N. Melgert (2013). "Macrophage heterogeneity in respiratory diseases." Mediators Inflamm **2013**: 769214.

Bourdonnay, E., Z. Zaslona, L. R. Penke, J. M. Speth, D. J. Schneider, S. Przybranowski, J. A. Swanson, P. Mancuso, C. M. Freeman, J. L. Curtis and M. Peters-Golden (2015). "Transcellular delivery of vesicular SOCS proteins from macrophages to epithelial cells blunts inflammatory signaling." J Exp Med **212**(5): 729-742.

Brown, J. S., T. Hussell, S. M. Gilliland, D. W. Holden, J. C. Paton, M. R. Ehrenstein, M. J. Walport and M. Botto (2002). "The classical pathway is the dominant complement pathway required for innate immunity to Streptococcus pneumoniae infection in mice." Proc Natl Acad Sci U S A **99**(26): 16969-16974.

Bruder, D., A. M. Westendorf, R. Geffers, A. D. Gruber, M. Gereke, R. I. Enelow and J. Buer (2004). "CD4 T Lymphocyte-mediated lung disease: steady state between pathological and tolerogenic immune reactions." Am J Respir Crit Care Med **170**(11): 1145-1152.

Brusselle, G. G., G. F. Joos and K. R. Bracke (2011). "New insights into the immunology of chronic obstructive pulmonary disease." Lancet **378**(9795): 1015-1026.

Buret, A., M. L. Dunkley, G. Pang, R. L. Clancy and A. W. Cripps (1994). "Pulmonary immunity to Pseudomonas aeruginosa in intestinally immunized rats roles of alveolar macrophages, tumor necrosis factor alpha, and interleukin-1 alpha." Infect Immun **62**(12): 5335-5343.

Buts, J. P., P. Bernasconi, J. P. Vaerman and C. Dive (1990). "Stimulation of secretory IgA and secretory component of immunoglobulins in small intestine of rats treated with Saccharomyces boulardii." Dig Dis Sci **35**(2): 251-256.

Cai, S., S. Batra, S. A. Lira, J. K. Kolls and S. Jeyaseelan (2010). "CXCL1 regulates pulmonary host defense to Klebsiella Infection via CXCL2, CXCL5, NF-kappaB, and MAPKs." J Immunol **185**(10): 6214-6225.

Cai, Y., R. K. Kumar, J. Zhou, P. S. Foster and D. C. Webb (2009). "Ym1/2 promotes Th2 cytokine expression by inhibiting 12/15(S)-lipoxygenase: identification of a novel pathway for regulating allergic inflammation." J Immunol **182**(9): 5393-5399.

Calix, J. J. and M. H. Nahm (2010). "A new pneumococcal serotype, 11E, has a variably inactivated wcjE gene." J Infect Dis **202**(1): 29-38.

Canton, J., D. Neculai and S. Grinstein (2013). "Scavenger receptors in homeostasis and immunity." Nat Rev Immunol **13**(9): 621-634.

Cao, A. T., S. Yao, B. Gong, C. O. Elson and Y. Cong (2012). "Th17 cells upregulate polymeric Ig receptor and intestinal IgA and contribute to intestinal homeostasis." J Immunol **189**(9): 4666-4673.

Careau, E., L. I. Proulx, P. Pouliot, A. Spahr, V. Turmel and E. Y. Bissonnette (2006). "Antigen sensitization modulates alveolar macrophage functions in an asthma model." Am J Physiol Lung Cell Mol Physiol **290**(5): L871-879.

Celli, B. R. and P. J. Barnes (2007). "Exacerbations of chronic obstructive pulmonary disease." Eur Respir J **29**(6): 1224-1238.

Chen, W., E. A. Havell and A. G. Harmsen (1992). "Importance of endogenous tumor necrosis factor alpha and gamma interferon in host resistance against Pneumocystis carinii infection." Infect Immun **60**(4): 1279-1284.

Chiang, N., C. N. Serhan, S. E. Dahlen, J. M. Drazen, D. W. Hay, G. E. Rovati, T. Shimizu, T. Yokomizo and C. Brink (2006). "The lipoxin receptor ALX: potent ligand-specific and stereoselective actions in vivo." Pharmacol Rev **58**(3): 463-487.

Cleaver, J. O., D. You, D. R. Michaud, F. A. Pruneda, M. M. Juarez, J. Zhang, P. M. Weill, R. Adachi, L. Gong, S. J. Moghaddam, M. E. Poynter, M. J. Tuvim and S. E. Evans (2014). "Lung epithelial cells are essential effectors of inducible resistance to pneumonia." Mucosal Immunol **7**(1): 78-88.

Clement, C. G., S. E. Evans, C. M. Evans, D. Hawke, R. Kobayashi, P. R. Reynolds, S. J. Moghaddam, B. L. Scott, E. Melicoff, R. Adachi, B. F. Dickey and M. J. Tuvim (2008). "Stimulation of lung innate immunity protects against lethal pneumococcal pneumonia in mice." Am J Respir Crit Care Med **177**(12): 1322-1330.

Cockeran, R., C. Durandt, C. Feldman, T. J. Mitchell and R. Anderson (2002). "Pneumolysin activates the synthesis and release of interleukin-8 by human neutrophils in vitro." J Infect Dis **186**(4): 562-565.

Coleman, M. M., D. Ruane, B. Moran, P. J. Dunne, J. Keane and K. H. Mills (2013). "Alveolar macrophages contribute to respiratory tolerance by inducing FoxP3 expression in naive T cells." Am J Respir Cell Mol Biol **48**(6): 773-780.

Corna, G., L. Campana, E. Pignatti, A. Castiglioni, E. Tagliafico, L. Bosurgi, A. Campanella, S. Brunelli, A. A. Manfredi, P. Apostoli, L. Silvestri, C. Camaschella and P. Rovere-Querini (2010). "Polarization dictates iron handling by inflammatory and alternatively activated macrophages." Haematologica **95**(11): 1814-1822.

Cosio, M. G., M. Saetta and A. Agusti (2009). "Immunologic aspects of chronic obstructive pulmonary disease." N Engl J Med **360**(23): 2445-2454.

Costa, C., R. Rufino, S. L. Traves, E. S. J. R. Lapa, P. J. Barnes and L. E. Donnelly (2008). "CXCR3 and CCR5 chemokines in induced sputum from patients with COPD." Chest **133**(1): 26-33.

Dasgupta, P., S. P. Chapoval, E. P. Smith and A. D. Keegan (2011). "Transfer of in vivo primed transgenic T cells supports allergic lung inflammation and FIZZ1 and Ym1 production in an IL-4Ralpha and STAT6 dependent manner." BMC Immunol **12**: 60.

Dean, R. A., J. H. Cox, C. L. Bellac, A. Doucet, A. E. Starr and C. M. Overall (2008). "Macrophage-specific metalloelastase (MMP-12) truncates and inactivates ELR+ CXC chemokines and generates CCL2, -7, -8, and -13 antagonists: potential role of the macrophage in terminating polymorphonuclear leukocyte influx." Blood **112**(8): 3455-3464.

Didierlaurent, A., J. Goulding, S. Patel, R. Snelgrove, L. Low, M. Bebien, T. Lawrence, L. S. van Rijt, B. N. Lambrecht, J. C. Sirard and T. Hussell (2008). "Sustained desensitization to bacterial Toll-like receptor ligands after resolution of respiratory influenza infection." J Exp Med **205**(2): 323-329.

Dintilhac, A., G. Alloing, C. Granadel and J. P. Claverys (1997). "Competence and virulence of Streptococcus pneumoniae: Adc and PsaA mutants exhibit a requirement for Zn and Mn resulting from inactivation of putative ABC metal permeases." Mol Microbiol **25**(4): 727-739.

Dong, L., S. J. Wang, B. Camoretti-Mercado, H. J. Li, M. Chen and W. X. Bi (2008). "FIZZ1 plays a crucial role in early stage airway remodeling of OVA-induced asthma." J Asthma **45**(8): 648-653.

Dragon, S., M. S. Rahman, J. Yang, H. Unruh, A. J. Halayko and A. S. Gounni (2007). "IL-17 enhances IL-1beta-mediated CXCL-8 release from human airway smooth muscle cells." Am J Physiol Lung Cell Mol Physiol **292**(4): L1023-1029.

Draijer, C., P. Robbe, C. E. Boorsma, M. N. Hylkema and B. N. Melgert (2013). "Characterization of macrophage phenotypes in three murine models of house-dust-mite-induced asthma." Mediators Inflamm **2013**: 632049.

Driscoll, K. E., D. G. Hassenbein, B. W. Howard, R. J. Isfort, D. Cody, M. H. Tindal, M. Suchanek and J. M. Carter (1995). "Cloning, expression, and functional characterization of rat MIP-2: a neutrophil chemoattractant and epithelial cell mitogen." J Leukoc Biol **58**(3): 359-364.

Droemann, D., T. Goldmann, T. Tiedje, P. Zabel, K. Dalhoff and B. Schaaf (2005). "Toll-like receptor 2 expression is decreased on alveolar macrophages in cigarette smokers and COPD patients." Respir Res **6**: 68.

Duan, M., W. C. Li, R. Vlahos, M. J. Maxwell, G. P. Anderson and M. L. Hibbs (2012). "Distinct macrophage subpopulations characterize acute infection and chronic inflammatory lung disease." J Immunol **189**(2): 946-955.

Ehrenstein, M. R. and C. A. Notley (2010). "The importance of natural IgM: scavenger, protector and regulator." Nat Rev Immunol **10**(11): 778-786.

Eriksson, U., U. Egermann, M. P. Bihl, F. Gambazzi, M. Tamm, P. G. Holt and R. M. Bingisser (2005). "Human bronchial epithelium controls TH2 responses by TH1-induced, nitric oxide-mediated STAT5 dephosphorylation: implications for the pathogenesis of asthma." J Immunol **175**(4): 2715-2720.

Errea, A., G. Moreno, F. Sisti, J. Fernandez, M. Rumbo and D. F. Hozbor (2010). "Mucosal innate response stimulation induced by lipopolysaccharide protects against Bordetella pertussis colonization." Med Microbiol Immunol **199**(2): 103-108.

Evans, S. E., B. L. Scott, C. G. Clement, D. T. Larson, D. Kontoyiannis, R. E. Lewis, P. R. Lasala, J. Pawlik, J. W. Peterson, A. K. Chopra, G. Klimpel, G. Bowden, M. Hook, Y. Xu, M. J. Tuvim and B. F. Dickey (2010). "Stimulated innate resistance of lung epithelium protects mice broadly against bacteria and fungi." Am J Respir Cell Mol Biol **42**(1): 40-50.

Fan, S., H. G. Fehr and D. Adams (1991). "Activation of macrophages for ADCC in vitro: effects of IL-4, TNF, interferons-alpha/beta, interferon-gamma, and GM-CSF." Cell Immunol **135**(1): 78-87.

Farnand, A. W., A. J. Eastman, R. Herrero, J. F. Hanson, S. Mongovin, W. A. Altemeier and G. Matute-Bello (2011). "Fas activation in alveolar epithelial cells induces KC (CXCL1) release by a MyD88-dependent mechanism." Am J Respir Cell Mol Biol **45**(3): 650-658.

Feldman, C., T. J. Mitchell, P. W. Andrew, G. J. Boulnois, R. C. Read, H. C. Todd, P. J. Cole and R. Wilson (1990). "The effect of Streptococcus pneumoniae pneumolysin on human respiratory epithelium in vitro." Microb Pathog **9**(4): 275-284.

Fierro, I. M., S. P. Colgan, G. Bernasconi, N. A. Petasis, C. B. Clish, M. Arita and C. N. Serhan (2003). "Lipoxin A4 and aspirin-triggered 15-epi-lipoxin A4 inhibit human neutrophil migration: comparisons between synthetic 15 epimers in chemotaxis and transmigration with microvessel endothelial cells and epithelial cells." J Immunol **170**(5): 2688-2694.

Finkelstein, R., R. S. Fraser, H. Ghezzo and M. G. Cosio (1995). "Alveolar inflammation and its relation to emphysema in smokers." Am J Respir Crit Care Med **152**(5 Pt 1): 1666-1672.

Georas, S. N. and F. Rezaee (2014). "Epithelial barrier function: at the front line of asthma immunology and allergic airway inflammation." J Allergy Clin Immunol **134**(3): 509-520.

Gereke, M., A. Autengruber, L. Grobe, A. Jeron, D. Bruder and S. Stegemann-Koniszewski (2012). "Flow cytometric isolation of primary murine type II alveolar epithelial cells for functional and molecular studies." J Vis Exp(70).

Gereke, M., L. Grobe, S. Prettin, M. Kasper, S. Deppenmeier, A. D. Gruber, R. I. Enelow, J. Buer and D. Bruder (2007). "Phenotypic alterations in type II alveolar epithelial cells in CD4+ T cell mediated lung inflammation." Respir Res **8**: 47.

Gereke, M., S. Jung, J. Buer and D. Bruder (2009). "Alveolar type II epithelial cells present antigen to CD4(+) T cells and induce Foxp3(+) regulatory T cells." Am J Respir Crit Care Med **179**(5): 344-355.

Gewirtz, A. T., L. S. Collier-Hyams, A. N. Young, T. Kucharzik, W. J. Guilford, J. F. Parkinson, I. R. Williams, A. S. Neish and J. L. Madara (2002). "Lipoxin a4 analogs attenuate induction of intestinal epithelial proinflammatory gene expression and reduce the severity of dextran sodium sulfate-induced colitis." J Immunol **168**(10): 5260-5267.

Gibbs, J., L. Ince, L. Matthews, J. Mei, T. Bell, N. Yang, B. Saer, N. Begley, T. Poolman, M. Pariollaud, S. Farrow, F. DeMayo, T. Hussell, G. S. Worthen, D. Ray and A. Loudon (2014). "An epithelial circadian clock controls pulmonary inflammation and glucocorticoid action." Nat Med **20**(8): 919-926.

Gohy, S. T., B. R. Detry, M. Lecocq, C. Bouzin, B. A. Weynand, G. D. Amatngalim, Y. M. Sibille and C. Pilette (2014). "Polymeric immunoglobulin receptor down-regulation in chronic obstructive pulmonary disease. Persistence in the cultured epithelium and role of transforming growth factor-beta." Am J Respir Crit Care Med **190**(5): 509-521.

Golpon, H. A., V. A. Fadok, L. Taraseviciene-Stewart, R. Scerbavicius, C. Sauer, T. Welte, P. M. Henson and N. F. Voelkel (2004). "Life after corpse engulfment: phagocytosis of apoptotic cells leads to VEGF secretion and cell growth." FASEB J **18**(14): 1716-1718.

Gong, J., H. Liu, J. Wu, H. Qi, Z. Y. Wu, H. Q. Shu, H. B. Li, L. Chen, Y. X. Wang, B. Li, M. Tang, Y. D. Ji, S. Y. Yuan, S. L. Yao and Y. Shang (2015). "Maresin 1 Prevents Lipopolysaccharide-Induced Neutrophil Survival and Accelerates Resolution of Acute Lung Injury." Shock **44**(4): 371-380.

Gosselin, D., J. DeSanctis, M. Boule, E. Skamene, C. Matouk and D. Radzioch (1995). "Role of tumor necrosis factor alpha in innate resistance to mouse pulmonary infection with Pseudomonas aeruginosa." Infect Immun **63**(9): 3272-3278.

Grainge, C. L. and D. E. Davies (2013). "Epithelial injury and repair in airways diseases." Chest **144**(6): 1906-1912.

Granata, F., A. Frattini, S. Loffredo, R. I. Staiano, A. Petraroli, D. Ribatti, R. Oslund, M. H. Gelb, G. Lambeau, G. Marone and M. Triggiani (2010). "Production of vascular endothelial growth factors from human lung macrophages induced by group IIA and group X secreted phospholipases A2." J Immunol **184**(9): 5232-5241.

Guilliams, M., I. De Kleer, S. Henri, S. Post, L. Vanhoutte, S. De Prijck, K. Deswarte, B. Malissen, H. Hammad and B. N. Lambrecht (2013). "Alveolar macrophages develop from fetal monocytes that differentiate into long-lived cells in the first week of life via GM-CSF." J Exp Med **210**(10): 1977-1992.

Guth, A. M., W. J. Janssen, C. M. Bosio, E. C. Crouch, P. M. Henson and S. W. Dow (2009). "Lung environment determines unique phenotype of alveolar macrophages." Am J Physiol Lung Cell Mol Physiol **296**(6): L936-946.

Habibzay, M., G. Weiss and T. Hussell (2013). "Bacterial superinfection following lung inflammatory disorders." Future Microbiol **8**(2): 247-256.

Hammerschmidt, S., G. Bethe, P. H. Remane and G. S. Chhatwal (1999). "Identification of pneumococcal surface protein A as a lactoferrin-binding protein of Streptococcus pneumoniae." Infect Immun **67**(4): 1683-1687.

Harder, J., U. Meyer-Hoffert, L. M. Teran, L. Schwichtenberg, J. Bartels, S. Maune and J. M. Schroder (2000). "Mucoid Pseudomonas aeruginosa, TNF-alpha, and IL-1beta, but not IL-6, induce human beta-defensin-2 in respiratory epithelia." Am J Respir Cell Mol Biol **22**(6): 714-721.

Harrington, L. E., M. Galvan, L. G. Baum, J. D. Altman and R. Ahmed (2000). "Differentiating between memory and effector CD8 T cells by altered expression of cell surface O-glycans." J Exp Med **191**(7): 1241-1246.

Hashimoto, D., A. Chow, C. Noizat, P. Teo, M. B. Beasley, M. Leboeuf, C. D. Becker, P. See, J. Price, D. Lucas, M. Greter, A. Mortha, S. W. Boyer, E. C. Forsberg, M. Tanaka, N. van Rooijen, A. Garcia-Sastre, E. R. Stanley, F. Ginhoux, P. S. Frenette and M. Merad (2013). "Tissue-resident macrophages self-maintain locally throughout adult life with minimal contribution from circulating monocytes." Immunity **38**(4): 792-804.

Hautamaki, R. D., D. K. Kobayashi, R. M. Senior and S. D. Shapiro (1997). "Requirement for macrophage elastase for cigarette smoke-induced emphysema in mice." Science **277**(5334): 2002-2004.

Herold, S., K. Mayer and J. Lohmeyer (2011). "Acute lung injury: how macrophages orchestrate resolution of inflammation and tissue repair." Front Immunol **2**: 65.

Herold, S., T. S. Tabar, H. Janssen, K. Hoegner, M. Cabanski, P. Lewe-Schlosser, J. Albrecht, F. Driever, I. Vadasz, W. Seeger, M. Steinmueller and J. Lohmeyer (2011). "Exudate macrophages attenuate lung injury by the release of IL-1 receptor antagonist in gram-negative pneumonia." Am J Respir Crit Care Med **183**(10): 1380-1390.

Hill, A. T., E. J. Campbell, S. L. Hill, D. L. Bayley and R. A. Stockley (2000). "Association between airway bacterial load and markers of airway inflammation in patients with stable chronic bronchitis." Am J Med **109**(4): 288-295.

Hogan, R. J., W. Zhong, E. J. Usherwood, T. Cookenham, A. D. Roberts and D. L. Woodland (2001). "Protection from respiratory virus infections can be mediated by antigen-specific CD4(+) T cells that persist in the lungs." J Exp Med **193**(8): 981-986.

Hogg, J. C. (2004). "Pathophysiology of airflow limitation in chronic obstructive pulmonary disease." Lancet **364**(9435): 709-721.

Holt, P. G. (1986). "Down-regulation of immune responses in the lower respiratory tract: the role of alveolar macrophages." Clin Exp Immunol **63**(2): 261-270.

Holt, P. G., D. H. Strickland, M. E. Wikstrom and F. L. Jahnsen (2008). "Regulation of immunological homeostasis in the respiratory tract." Nat Rev Immunol **8**(2): 142-152.

Hooper, L. V., M. H. Wong, A. Thelin, L. Hansson, P. G. Falk and J. I. Gordon (2001). "Molecular analysis of commensal host-microbial relationships in the intestine." Science **291**(5505): 881-884.

Huang, C. T., D. L. Huso, Z. Lu, T. Wang, G. Zhou, E. P. Kennedy, C. G. Drake, D. J. Morgan, L. A. Sherman, A. D. Higgins, D. M. Pardoll and A. J. Adler (2003). "CD4+ T cells pass through an effector phase during the process of in vivo tolerance induction." J Immunol **170**(8): 3945-3953.

Hussell, T. and T. J. Bell (2014). "Alveolar macrophages: plasticity in a tissue-specific context." Nat Rev Immunol **14**(2): 81-93.

Hyams, C., E. Camberlein, J. M. Cohen, K. Bax and J. S. Brown (2010). "The Streptococcus pneumoniae capsule inhibits complement activity and neutrophil phagocytosis by multiple mechanisms." Infect Immun **78**(2): 704-715.

Ichinose, M., H. Sugiura, S. Yamagata, A. Koarai and K. Shirato (2000). "Increase in reactive nitrogen species production in chronic obstructive pulmonary disease airways." Am J Respir Crit Care Med **162**(2 Pt 1): 701-706.

Ilumets, H., P. H. Rytila, A. R. Sovijarvi, T. Tervahartiala, M. Myllarniemi, T. A. Sorsa and V. L. Kinnula (2008). "Transient elevation of neutrophil proteinases in induced sputum during COPD exacerbation." Scand J Clin Lab Invest **68**(7): 618-623.

Iovino, F., G. Molema and J. J. Bijlsma (2014). "Streptococcus pneumoniae Interacts with pIgR expressed by the brain microvascular endothelium but does not co-localize with PAF receptor." PLoS One **9**(5): e97914.

Ito, K. and P. J. Barnes (2009). "COPD as a disease of accelerated lung aging." Chest **135**(1): 173-180.

Jaffar, Z., M. E. Ferrini, L. A. Herritt and K. Roberts (2009). "Cutting edge: lung mucosal Th17-mediated responses induce polymeric Ig receptor expression by the airway epithelium and elevate secretory IgA levels." J Immunol **182**(8): 4507-4511.

Jeffery, P. K. (2000). "Comparison of the structural and inflammatory features of COPD and asthma. Giles F. Filley Lecture." Chest **117**(5 Suppl 1): 251S-260S.

Jeyaseelan, S., R. Manzer, S. K. Young, M. Yamamoto, S. Akira, R. J. Mason and G. S. Worthen (2005). "Induction of CXCL5 during inflammation in the rodent lung involves activation of alveolar epithelium." Am J Respir Cell Mol Biol **32**(6): 531-539.

Johansen, F. E. and C. S. Kaetzel (2011). "Regulation of the polymeric immunoglobulin receptor and IgA transport: new advances in environmental factors that stimulate pIgR expression and its role in mucosal immunity." Mucosal Immunol **4**(6): 598-602.

Kadioglu, A., J. N. Weiser, J. C. Paton and P. W. Andrew (2008). "The role of Streptococcus pneumoniae virulence factors in host respiratory colonization and disease." Nat Rev Microbiol **6**(4): 288-301.

Kaetzel, C. S. (2005). "The polymeric immunoglobulin receptor: bridging innate and adaptive immune responses at mucosal surfaces." Immunol Rev **206**: 83-99.

Kaetzel, C. S., J. K. Robinson, K. R. Chintalacharuvu, J. P. Vaerman and M. E. Lamm (1991). "The polymeric immunoglobulin receptor (secretory component) mediates transport of immune complexes across epithelial cells: a local defense function for IgA." Proc Natl Acad Sci U S A **88**(19): 8796-8800.

Kahnert, A., P. Seiler, M. Stein, S. Bandermann, K. Hahnke, H. Mollenkopf and S. H. Kaufmann (2006). "Alternative activation deprives macrophages of a coordinated defense program to Mycobacterium tuberculosis." Eur J Immunol **36**(3): 631-647.

Kato, A., A. Q. Truong-Tran, A. L. Scott, K. Matsumoto and R. P. Schleimer (2006). "Airway epithelial cells produce B cell-activating factor of TNF family by an IFN-beta-dependent mechanism." J Immunol **177**(10): 7164-7172.

Kaushic, C., J. M. Richardson and C. R. Wira (1995). "Regulation of polymeric immunoglobulin A receptor messenger ribonucleic acid expression in rodent uteri: effect of sex hormones." Endocrinology **136**(7): 2836-2844.

Kim, J. M., J. Y. Lee, Y. M. Yoon, Y. K. Oh, J. Youn and Y. J. Kim (2006). "NF-kappa B activation pathway is essential for the chemokine expression in intestinal epithelial cells stimulated with Clostridium difficile toxin A." Scand J Immunol **63**(6): 453-460.

Kirberg, J., A. Baron, S. Jakob, A. Rolink, K. Karjalainen and H. von Boehmer (1994). "Thymic selection of CD8+ single positive cells with a class II major histocompatibility complex-restricted receptor." J Exp Med **180**(1): 25-34.

Kirby, A. C., M. C. Coles and P. M. Kaye (2009). "Alveolar macrophages transport pathogens to lung draining lymph nodes." J Immunol **183**(3): 1983-1989.

Kitsiouli, E., G. Nakos and M. E. Lekka (2009). "Phospholipase A2 subclasses in acute respiratory distress syndrome." Biochim Biophys Acta **1792**(10): 941-953.

Klein Wolterink, R. G., A. Kleinjan, M. van Nimwegen, I. Bergen, M. de Bruijn, Y. Levani and R. W. Hendriks (2012). "Pulmonary innate lymphoid cells are major producers of IL-5 and IL-13 in murine models of allergic asthma." Eur J Immunol **42**(5): 1106-1116.

Knapp, S., J. C. Leemans, S. Florquin, J. Branger, N. A. Maris, J. Pater, N. van Rooijen and T. van der Poll (2003). "Alveolar macrophages have a protective antiinflammatory role during murine pneumococcal pneumonia." Am J Respir Crit Care Med **167**(2): 171-179.

Knippenberg, S., B. Ueberberg, R. Maus, J. Bohling, N. Ding, M. Tort Tarres, H. G. Hoymann, D. Jonigk, N. Izykowski, J. C. Paton, A. D. Ogunniyi, S. Lindig, M. Bauer, T. Welte, W. Seeger, A. Guenther, T. H. Sisson, J. Gauldie, M. Kolb and U. A. Maus (2015). "Streptococcus pneumoniae triggers progression of pulmonary fibrosis through pneumolysin." Thorax **70**(7): 636-646.

Kopf, M., H. Baumann, G. Freer, M. Freudenberg, M. Lamers, T. Kishimoto, R. Zinkernagel, H. Bluethmann and G. Kohler (1994). "Impaired immune and acute-phase responses in interleukin-6-deficient mice." Nature **368**(6469): 339-342.

Kuebler, W. M., K. Parthasarathi, P. M. Wang and J. Bhattacharya (2000). "A novel signaling mechanism between gas and blood compartments of the lung." J Clin Invest **105**(7): 905-913.

Kvale, D. and P. Brandtzaeg (1995). "Constitutive and cytokine induced expression of HLA molecules, secretory component, and intercellular adhesion molecule-1 is modulated by butyrate in the colonic epithelial cell line HT-29." Gut **36**(5): 737-742.

Lacoste, J. Y., J. Bousquet, P. Chanez, T. Van Vyve, J. Simony-Lafontaine, N. Lequeu, P. Vic, I. Enander, P. Godard and F. B. Michel (1993). "Eosinophilic and neutrophilic inflammation in asthma, chronic bronchitis, and chronic obstructive pulmonary disease." J Allergy Clin Immunol **92**(4): 537-548.

LaFemina, M. J., K. M. Sutherland, T. Bentley, L. W. Gonzales, L. Allen, C. J. Chapin, D. Rokkam, K. A. Sweerus, L. G. Dobbs, P. L. Ballard and J. A. Frank (2014). "Claudin-18 deficiency results in alveolar barrier dysfunction and impaired alveologenesis in mice." Am J Respir Cell Mol Biol **51**(4): 550-558.

Laichalk, L. L., S. L. Kunkel, R. M. Strieter, J. M. Danforth, M. B. Bailie and T. J. Standiford (1996). "Tumor necrosis factor mediates lung antibacterial host defense in murine Klebsiella pneumonia." Infect Immun **64**(12): 5211-5218.

Latiff, A. H. and M. A. Kerr (2007). "The clinical significance of immunoglobulin A deficiency." Ann Clin Biochem **44**(Pt 2): 131-139.

Lawrence, M. C., P. A. Pilling, V. C. Epa, A. M. Berry, A. D. Ogunniyi and J. C. Paton (1998). "The crystal structure of pneumococcal surface antigen PsaA reveals a metal-binding site and a novel structure for a putative ABC-type binding protein." Structure **6**(12): 1553-1561.

Lawrence, T. and G. Natoli (2011). "Transcriptional regulation of macrophage polarization: enabling diversity with identity." Nat Rev Immunol **11**(11): 750-761.

Leatherman, J. W. (1987). "Immune alveolar hemorrhage." Chest **91**(6): 891-897.

Lee, C. G., C. A. Da Silva, C. S. Dela Cruz, F. Ahangari, B. Ma, M. J. Kang, C. H. He, S. Takyar and J. A. Elias (2011). "Role of chitin and chitinase/chitinase-like proteins in inflammation, tissue remodeling, and injury." Annu Rev Physiol **73**: 479-501.

Lee, H. Y., A. Andalibi, P. Webster, S. K. Moon, K. Teufert, S. H. Kang, J. D. Li, M. Nagura, T. Ganz and D. J. Lim (2004). "Antimicrobial activity of innate immune molecules against Streptococcus pneumoniae, Moraxella catarrhalis and nontypeable Haemophilus influenzae." BMC Infect Dis **4**: 12.

Lee, Y. G., J. J. Jeong, S. Nyenhuis, E. Berdyshev, S. Chung, R. Ranjan, M. Karpurapu, J. Deng, F. Qian, E. A. Kelly, N. N. Jarjour, S. J. Ackerman, V. Natarajan, J. W. Christman and G. Y. Park (2015). "Recruited alveolar macrophages, in response to airway epithelial-derived monocyte chemoattractant protein 1/CCl2, regulate airway inflammation and remodeling in allergic asthma." Am J Respir Cell Mol Biol **52**(6): 772-784.

LeMessurier, K. S., H. Hacker, L. Chi, E. Tuomanen and V. Redecke (2013). "Type I interferon protects against pneumococcal invasive disease by inhibiting bacterial transmigration across the lung." PLoS Pathog **9**(11): e1003727.

Leslie, C. C., K. McCormick-Shannon, J. M. Shannon, B. Garrick, D. Damm, J. A. Abraham and R. J. Mason (1997). "Heparin-binding EGF-like growth factor is a mitogen for rat alveolar type II cells." Am J Respir Cell Mol Biol **16**(4): 379-387.

Letuve, S., A. Kozhich, N. Arouche, M. Grandsaigne, J. Reed, M. C. Dombret, P. A. Kiener, M. Aubier, A. J. Coyle and M. Pretolani (2008). "YKL-40 is elevated in patients with chronic obstructive pulmonary disease and activates alveolar macrophages." J Immunol **181**(7): 5167-5173.

Li, T. W., J. Wang, J. T. Lam, E. M. Gutierrez, R. S. Solorzano-Vargus, H. V. Tsai and M. G. Martin (1999). "Transcriptional control of the murine polymeric IgA receptor promoter by glucocorticoids." Am J Physiol **276**(6 Pt 1): G1425-1434.

Liang, Z., Q. Zhang, C. M. Thomas, K. K. Chana, D. Gibeon, P. J. Barnes, K. F. Chung, P. K. Bhavsar and L. E. Donnelly (2014). "Impaired macrophage phagocytosis of bacteria in severe asthma." Respir Res **15**: 72.

Lipscomb, M. F., C. R. Lyons, G. Nunez, E. J. Ball, P. Stastny, W. Vial, V. Lem, J. Weissler and L. M. Miller (1986). "Human alveolar macrophages: HLA-DR-positive macrophages that are poor stimulators of a primary mixed leukocyte reaction." J Immunol **136**(2): 497-504.

Liu, Y., J. Mei, L. Gonzales, G. Yang, N. Dai, P. Wang, P. Zhang, M. Favara, K. C. Malcolm, S. Guttentag and G. S. Worthen (2011). "IL-17A and TNF-alpha exert synergistic effects on expression of CXCL5 by alveolar type II cells in vivo and in vitro." J Immunol **186**(5): 3197-3205.

Louis, A. G. and S. Gupta (2014). "Primary selective IgM deficiency: an ignored immunodeficiency." Clin Rev Allergy Immunol **46**(2): 104-111.

Lundblad, L. K., J. Thompson-Figueroa, T. Leclair, M. J. Sullivan, M. E. Poynter, C. G. Irvin and J. H. Bates (2005). "Tumor necrosis factor-alpha overexpression in lung disease: a single cause behind a complex phenotype." Am J Respir Crit Care Med **171**(12): 1363-1370.

Lyons, C. R., E. J. Ball, G. B. Toews, J. C. Weissler, P. Stastny and M. F. Lipscomb (1986). "Inability of human alveolar macrophages to stimulate resting T cells correlates with decreased antigen-specific T cell-macrophage binding." J Immunol **137**(4): 1173-1180.

Malley, R., P. Henneke, S. C. Morse, M. J. Cieslewicz, M. Lipsitch, C. M. Thompson, E. Kurt-Jones, J. C. Paton, M. R. Wessels and D. T. Golenbock (2003). "Recognition of pneumolysin by Toll-like receptor 4 confers resistance to pneumococcal infection." Proc Natl Acad Sci U S A **100**(4): 1966-1971.

Mannino, D. M. and A. S. Buist (2007). "Global burden of COPD: risk factors, prevalence, and future trends." Lancet **370**(9589): 765-773.

Marsh, L. M., L. Cakarova, G. Kwapiszewska, W. von Wulffen, S. Herold, W. Seeger and J. Lohmeyer (2009). "Surface expression of CD74 by type II alveolar epithelial cells: a potential mechanism for macrophage migration inhibitory factor-induced epithelial repair." Am J Physiol Lung Cell Mol Physiol **296**(3): L442-452.

Martin, M. G., J. Wang, T. W. Li, J. T. Lam, E. M. Gutierrez, R. S. Solorzano-Vargas and A. H. Tsai (1998). "Characterization of the 5'-flanking region of the murine polymeric IgA receptor gene." Am J Physiol **275**(4 Pt 1): G778-788.

Mathers, C. D. and D. Loncar (2006). "Projections of global mortality and burden of disease from 2002 to 2030." PLoS Med **3**(11): e442.

Maus, U. A., S. Janzen, G. Wall, M. Srivastava, T. S. Blackwell, J. W. Christman, W. Seeger, T. Welte and J. Lohmeyer (2006). "Resident alveolar macrophages are replaced by recruited monocytes in response to endotoxin-induced lung inflammation." Am J Respir Cell Mol Biol **35**(2): 227-235.

Medeiros, A. I., C. H. Serezani, S. P. Lee and M. Peters-Golden (2009). "Efferocytosis impairs pulmonary macrophage and lung antibacterial function via PGE2/EP2 signaling." J Exp Med **206**(1): 61-68.

Mehrad, B. and T. J. Standiford (1999). "Role of cytokines in pulmonary antimicrobial host defense." Immunol Res **20**(1): 15-27.

Mei, J., Y. Liu, N. Dai, M. Favara, T. Greene, S. Jeyaseelan, M. Poncz, J. S. Lee and G. S. Worthen (2010). "CXCL5 regulates chemokine scavenging and pulmonary host defense to bacterial infection." Immunity **33**(1): 106-117.

Melloni, B., O. Lesur, T. Bouhadiba, A. Cantin, M. Martel and R. Begin (1996). "Effect of exposure to silica on human alveolar macrophages in supporting growth activity in type II epithelial cells." Thorax **51**(8): 781-786.

Molet, S., C. Belleguic, H. Lena, N. Germain, C. P. Bertrand, S. D. Shapiro, J. M. Planquois, P. Delaval and V. Lagente (2005). "Increase in macrophage elastase (MMP-12) in lungs from patients with chronic obstructive pulmonary disease." Inflamm Res **54**(1): 31-36.

Monticelli, L. A., G. F. Sonnenberg, M. C. Abt, T. Alenghat, C. G. Ziegler, T. A. Doering, J. M. Angelosanto, B. J. Laidlaw, C. Y. Yang, T. Sathaliyawala, M. Kubota, D. Turner, J. M. Diamond, A. W. Goldrath, D. L. Farber, R. G. Collman, E. J. Wherry and D. Artis (2011). "Innate lymphoid cells promote lung-tissue homeostasis after infection with influenza virus." Nat Immunol **12**(11): 1045-1054.

Moon, C., K. L. VanDussen, H. Miyoshi and T. S. Stappenbeck (2014). "Development of a primary mouse intestinal epithelial cell monolayer culture system to evaluate factors that modulate IgA transcytosis." Mucosal Immunol **7**(4): 818-828.

Moreira, A. P., K. A. Cavassani, R. Hullinger, R. S. Rosada, D. J. Fong, L. Murray, D. P. Hesson and C. M. Hogaboam (2010). "Serum amyloid P attenuates M2 macrophage activation and protects against fungal spore-induced allergic airway disease." J Allergy Clin Immunol **126**(4): 712-721 e717.

Moser, C., D. J. Weiner, E. Lysenko, R. Bals, J. N. Weiser and J. M. Wilson (2002). "beta-Defensin 1 contributes to pulmonary innate immunity in mice." Infect Immun **70**(6): 3068-3072.

Mosser, D. M. and J. P. Edwards (2008). "Exploring the full spectrum of macrophage activation." Nat Rev Immunol **8**(12): 958-969.

Mukhopadhyay, S., J. R. Hoidal and T. K. Mukherjee (2006). "Role of TNFalpha in pulmonary pathophysiology." Respir Res **7**: 125.

Nakagawa, R., T. Naka, H. Tsutsui, M. Fujimoto, A. Kimura, T. Abe, E. Seki, S. Sato, O. Takeuchi, K. Takeda, S. Akira, K. Yamanishi, I. Kawase, K. Nakanishi and T. Kishimoto (2002). "SOCS-1 participates in negative regulation of LPS responses." Immunity **17**(5): 677-687.

Nakanishi, A., S. Morita, H. Iwashita, Y. Sagiya, Y. Ashida, H. Shirafuji, Y. Fujisawa, O. Nishimura and M. Fujino (2001). "Role of gob-5 in mucus overproduction and airway hyperresponsiveness in asthma." Proc Natl Acad Sci U S A **98**(9): 5175-5180.

Nelson, A. L., A. M. Roche, J. M. Gould, K. Chim, A. J. Ratner and J. N. Weiser (2007). "Capsule enhances pneumococcal colonization by limiting mucus-mediated clearance." Infect Immun **75**(1): 83-90.

Nicod, L. P. (1999). "Pulmonary defence mechanisms." Respiration **66**(1): 2-11.

Nicolas, G., M. Bennoun, I. Devaux, C. Beaumont, B. Grandchamp, A. Kahn and S. Vaulont (2001). "Lack of hepcidin gene expression and severe tissue iron overload in upstream stimulatory factor 2 (USF2) knockout mice." Proc Natl Acad Sci U S A **98**(15): 8780-8785.

Nouailles, G., A. Dorhoi, M. Koch, J. Zerrahn, J. Weiner, 3rd, K. C. Fae, F. Arrey, S. Kuhlmann, S. Bandermann, D. Loewe, H. J. Mollenkopf, A. Vogelzang, C. Meyer-Schwesinger, H. W. Mittrucker, G. McEwen and S. H. Kaufmann (2014). "CXCL5-secreting pulmonary epithelial cells drive destructive neutrophilic inflammation in tuberculosis." J Clin Invest **124**(3): 1268-1282.

O'Neil, D. A., E. M. Porter, D. Elewaut, G. M. Anderson, L. Eckmann, T. Ganz and M. F. Kagnoff (1999). "Expression and regulation of the human beta-defensins hBD-1 and hBD-2 in intestinal epithelium." J Immunol **163**(12): 6718-6724.

O'Shaughnessy, T. C., T. W. Ansari, N. C. Barnes and P. K. Jeffery (1997). "Inflammation in bronchial biopsies of subjects with chronic bronchitis: inverse relationship of CD8+ T lymphocytes with FEV1." Am J Respir Crit Care Med **155**(3): 852-857.

Ofulue, A. F. and M. Ko (1999). "Effects of depletion of neutrophils or macrophages on development of cigarette smoke-induced emphysema." Am J Physiol **277**(1 Pt 1): L97-105.

Ohashi, P. S. (2002). "T-cell signalling and autoimmunity: molecular mechanisms of disease." Nat Rev Immunol **2**(6): 427-438.

Ohlmeier, S., W. Mazur, A. Linja-Aho, N. Louhelainen, M. Ronty, T. Toljamo, U. Bergmann and V. L. Kinnula (2012). "Sputum proteomics identifies elevated PIGR levels in smokers and mild-to-moderate COPD." J Proteome Res **11**(2): 599-608.

Ohnishi, K., M. Takagi, Y. Kurokawa, S. Satomi and Y. T. Konttinen (1998). "Matrix metalloproteinase-mediated extracellular matrix protein degradation in human pulmonary emphysema." Lab Invest **78**(9): 1077-1087.

Opitz, B., A. Puschel, B. Schmeck, A. C. Hocke, S. Rosseau, S. Hammerschmidt, R. R. Schumann, N. Suttorp and S. Hippenstiel (2004). "Nucleotide-binding oligomerization domain proteins are innate immune receptors for internalized Streptococcus pneumoniae." J Biol Chem **279**(35): 36426-36432.

Orihuela, C. J., G. Gao, K. P. Francis, J. Yu and E. I. Tuomanen (2004). "Tissue-specific contributions of pneumococcal virulence factors to pathogenesis." J Infect Dis **190**(9): 1661-1669.

Pal, K., C. S. Kaetzel, K. Brundage, C. A. Cunningham and C. F. Cuff (2005). "Regulation of polymeric immunoglobulin receptor expression by reovirus." J Gen Virol **86**(Pt 8): 2347-2357.

Paone, G., V. Conti, A. Vestri, A. Leone, G. Puglisi, F. Benassi, G. Brunetti, G. Schmid, I. Cammarella and C. Terzano (2011). "Analysis of sputum markers in the evaluation of lung inflammation and functional impairment in symptomatic smokers and COPD patients." Dis Markers **31**(2): 91-100.

Patel, I. S., T. A. Seemungal, M. Wilks, S. J. Lloyd-Owen, G. C. Donaldson and J. A. Wedzicha (2002). "Relationship between bacterial colonisation and the frequency, character, and severity of COPD exacerbations." Thorax **57**(9): 759-764.

Paton, J. C. and A. Ferrante (1983). "Inhibition of human polymorphonuclear leukocyte respiratory burst, bactericidal activity, and migration by pneumolysin." Infect Immun **41**(3): 1212-1216.

Pearce, N., N. Ait-Khaled, R. Beasley, J. Mallol, U. Keil, E. Mitchell, C. Robertson and I. P. T. S. Group (2007). "Worldwide trends in the prevalence of asthma symptoms: phase III of the International Study of Asthma and Allergies in Childhood (ISAAC)." Thorax **62**(9): 758-766.

Pierangeli, S. S. and G. Sonnenfeld (1993). "Treatment of murine macrophages with murine interferon-gamma and tumour necrosis factor-alpha enhances uptake and intracellular killing of Pseudomonas aeruginosa." Clin Exp Immunol **93**(2): 165-171.

Pittet, L. A., L. J. Quinton, K. Yamamoto, B. E. Robson, J. D. Ferrari, H. Algul, R. M. Schmid and J. P. Mizgerd (2011). "Earliest innate immune responses require macrophage RelA during pneumococcal pneumonia." Am J Respir Cell Mol Biol **45**(3): 573-581.

Raes, G., W. Noel, A. Beschin, L. Brys, P. de Baetselier and G. H. Hassanzadeh (2002). "FIZZ1 and Ym as tools to discriminate between differentially activated macrophages." Dev Immunol **9**(3): 151-159.

Rayner, C. F., A. D. Jackson, A. Rutman, A. Dewar, T. J. Mitchell, P. W. Andrew, P. J. Cole and R. Wilson (1995). "Interaction of pneumolysin-sufficient and -deficient isogenic variants of Streptococcus pneumoniae with human respiratory mucosa." Infect Immun **63**(2): 442-447.

Robinson, D. S. (2010). "The role of the T cell in asthma." J Allergy Clin Immunol **126**(6): 1081-1091; quiz 1092-1083.

Rosato, R., H. Jammes, L. Belair, C. Puissant, J. P. Kraehenbuhl and J. Djiane (1995). "Polymeric-Ig receptor gene expression in rabbit mammary gland during pregnancy and lactation: evolution and hormonal regulation." Mol Cell Endocrinol **110**(1-2): 81-87.

Roth, M. D. and S. H. Golub (1993). "Human pulmonary macrophages utilize prostaglandins and transforming growth factor beta 1 to suppress lymphocyte activation." J Leukoc Biol **53**(4): 366-371.

Russell, R. E., S. V. Culpitt, C. DeMatos, L. Donnelly, M. Smith, J. Wiggins and P. J. Barnes (2002). "Release and activity of matrix metalloproteinase-9 and tissue inhibitor of metalloproteinase-1 by alveolar macrophages from patients with chronic obstructive pulmonary disease." Am J Respir Cell Mol Biol **26**(5): 602-609.

Saetta, M., S. Baraldo, L. Corbino, G. Turato, F. Braccioni, F. Rea, G. Cavallesco, G. Tropeano, C. E. Mapp, P. Maestrelli, A. Ciaccia and L. M. Fabbri (1999). "CD8+ve cells in the lungs of smokers with chronic obstructive pulmonary disease." Am J Respir Crit Care Med **160**(2): 711-717.

Sandgren, A., B. Albiger, C. J. Orihuela, E. Tuomanen, S. Normark and B. Henriques-Normark (2005). "Virulence in mice of pneumococcal clonal types with known invasive disease potential in humans." J Infect Dis **192**(5): 791-800.

Sanfilippo, A. M., Y. Furuya, S. Roberts, S. L. Salmon and D. W. Metzger (2015). "Allergic Lung Inflammation Reduces Tissue Invasion and Enhances Survival from Pulmonary Pneumococcal Infection in Mice, Which Correlates with Increased Expression of Transforming Growth Factor beta1 and SiglecFlow Alveolar Macrophages." Infect Immun **83**(7): 2976-2983.

Sarkar, J., N. N. Gangopadhyay, Z. Moldoveanu, J. Mestecky and C. B. Stephensen (1998). "Vitamin A is required for regulation of polymeric immunoglobulin receptor (pIgR) expression by interleukin-4 and interferon-gamma in a human intestinal epithelial cell line." J Nutr **128**(7): 1063-1069.

Schabbauer, G., U. Matt, P. Gunzl, J. Warszawska, T. Furtner, E. Hainzl, I. Elbau, I. Mesteri, B. Doninger, B. R. Binder and S. Knapp (2010). "Myeloid PTEN promotes inflammation but impairs bactericidal activities during murine pneumococcal pneumonia." J Immunol **185**(1): 468-476.

Schaller, M. A., S. K. Lundy, G. B. Huffnagle and N. W. Lukacs (2005). "CD8+ T cell contributions to allergen induced pulmonary inflammation and airway hyperreactivity." Eur J Immunol **35**(7): 2061-2070.

Schjerven, H., P. Brandtzaeg and F. E. Johansen (2000). "Mechanism of IL-4-mediated up-regulation of the polymeric Ig receptor: role of STAT6 in cell type-specific delayed transcriptional response." J Immunol **165**(7): 3898-3906.

Schneeman, T. A., M. E. Bruno, H. Schjerven, F. E. Johansen, L. Chady and C. S. Kaetzel (2005). "Regulation of the polymeric Ig receptor by signaling through TLRs 3 and 4: linking innate and adaptive immune responses." J Immunol **175**(1): 376-384.

Sethi, S., C. Wrona, K. Eschberger, P. Lobbins, X. Cai and T. F. Murphy (2008). "Inflammatory profile of new bacterial strain exacerbations of chronic obstructive pulmonary disease." Am J Respir Crit Care Med **177**(5): 491-497.

Shaper, M., S. K. Hollingshead, W. H. Benjamin, Jr. and D. E. Briles (2004). "PspA protects Streptococcus pneumoniae from killing by apolactoferrin, and antibody to PspA enhances killing of pneumococci by apolactoferrin [corrected]." Infect Immun **72**(9): 5031-5040.

Shapiro, S. D., N. M. Goldstein, A. M. Houghton, D. K. Kobayashi, D. Kelley and A. Belaaouaj (2003). "Neutrophil elastase contributes to cigarette smoke-induced emphysema in mice." Am J Pathol **163**(6): 2329-2335.

Sharif, O., U. Matt, S. Saluzzo, K. Lakovits, I. Haslinger, T. Furtner, B. Doninger and S. Knapp (2013). "The scavenger receptor CD36 downmodulates the early inflammatory response while enhancing bacterial phagocytosis during pneumococcal pneumonia." J Immunol **190**(11): 5640-5648.

Shi, G. P., J. S. Munger, J. P. Meara, D. H. Rich and H. A. Chapman (1992). "Molecular cloning and expression of human alveolar macrophage cathepsin S, an elastinolytic cysteine protease." J Biol Chem **267**(11): 7258-7262.

Sica, A. and A. Mantovani (2012). "Macrophage plasticity and polarization: in vivo veritas." J Clin Invest **122**(3): 787-795.

Singh, P. K., H. P. Jia, K. Wiles, J. Hesselberth, L. Liu, B. A. Conway, E. P. Greenberg, E. V. Valore, M. J. Welsh, T. Ganz, B. F. Tack and P. B. McCray, Jr. (1998). "Production of beta-defensins by human airway epithelia." Proc Natl Acad Sci U S A **95**(25): 14961-14966.

Sollid, L. M., D. Kvale, P. Brandtzaeg, G. Markussen and E. Thorsby (1987). "Interferon-gamma enhances expression of secretory component, the epithelial receptor for polymeric immunoglobulins." J Immunol **138**(12): 4303-4306.

Song, C., L. Luo, Z. Lei, B. Li, Z. Liang, G. Liu, D. Li, G. Zhang, B. Huang and Z. H. Feng (2008). "IL-17-producing alveolar macrophages mediate allergic lung inflammation related to asthma." J Immunol **181**(9): 6117-6124.

Soroosh, P., T. A. Doherty, W. Duan, A. K. Mehta, H. Choi, Y. F. Adams, Z. Mikulski, N. Khorram, P. Rosenthal, D. H. Broide and M. Croft (2013). "Lung-resident tissue macrophages generate Foxp3+ regulatory T cells and promote airway tolerance." J Exp Med **210**(4): 775-788.

Storm van's Gravesande, K., M. D. Layne, Q. Ye, L. Le, R. M. Baron, M. A. Perrella, L. Santambrogio, E. S. Silverman and R. J. Riese (2002). "IFN regulatory factor-1 regulates IFN-gamma-dependent cathepsin S expression." J Immunol **168**(9): 4488-4494.

Strebovsky, J., P. Walker, R. Lang and A. H. Dalpke (2011). "Suppressor of cytokine signaling 1 (SOCS1) limits NFkappaB signaling by decreasing p65 stability within the cell nucleus." FASEB J **25**(3): 863-874.

Strieter, R. M., J. A. Belperio and M. P. Keane (2002). "Cytokines in innate host defense in the lung." J Clin Invest **109**(6): 699-705.

Strugnell, R. A. and O. L. Wijburg (2010). "The role of secretory antibodies in infection immunity." Nat Rev Microbiol **8**(9): 656-667.

Strunk, R. C., D. M. Eidlen and R. J. Mason (1988). "Pulmonary alveolar type II epithelial cells synthesize and secrete proteins of the classical and alternative complement pathways." J Clin Invest **81**(5): 1419-1426.

Sugahara, K., K. I. Iyama, T. Kimura, K. Sano, G. J. Darlington, T. Akiba and M. Takiguchi (2001). "Mice lacking CCAAt/enhancer-binding protein-alpha show hyperproliferation of alveolar type II cells and increased surfactant protein mRNAs." Cell Tissue Res **306**(1): 57-63.

Sun, K., F. E. Johansen, L. Eckmann and D. W. Metzger (2004). "An important role for polymeric Ig receptor-mediated transport of IgA in protection against Streptococcus pneumoniae nasopharyngeal carriage." J Immunol **173**(7): 4576-4581.

Tak, T., K. Tesselaar, J. Pillay, J. A. Borghans and L. Koenderman (2013). "What's your age again? Determination of human neutrophil half-lives revisited." J Leukoc Biol **94**(4): 595-601.

Talbot, T. R., T. V. Hartert, E. Mitchel, N. B. Halasa, P. G. Arbogast, K. A. Poehling, W. Schaffner, A. S. Craig and M. R. Griffin (2005). "Asthma as a risk factor for invasive pneumococcal disease." N Engl J Med **352**(20): 2082-2090.

Terakado, M., Y. Gon, A. Sekiyama, I. Takeshita, Y. Kozu, K. Matsumoto, N. Takahashi and S. Hashimoto (2011). "The Rac1/JNK pathway is critical for EGFR-dependent barrier formation in human airway epithelial cells." Am J Physiol Lung Cell Mol Physiol **300**(1): L56-63.

Tessier, P. A., P. H. Naccache, I. Clark-Lewis, R. P. Gladue, K. S. Neote and S. R. McColl (1997). "Chemokine networks in vivo: involvement of C-X-C and C-C chemokines in neutrophil extravasation in vivo in response to TNF-alpha." J Immunol **159**(7): 3595-3602.

Tettelin, H., K. E. Nelson, I. T. Paulsen, J. A. Eisen, T. D. Read, S. Peterson, J. Heidelberg, R. T. DeBoy, D. H. Haft, R. J. Dodson, A. S. Durkin, M. Gwinn, J. F. Kolonay, W. C. Nelson, J. D. Peterson, L. A. Umayam, O. White, S. L. Salzberg, M. R. Lewis, D. Radune, E. Holtzapple, H. Khouri, A. M. Wolf, T. R. Utterback, C. L. Hansen, L. A. McDonald, T. V. Feldblyum, S. Angiuoli, T. Dickinson, E. K. Hickey, I. E. Holt, B. J. Loftus, F. Yang, H. O. Smith, J. C. Venter, B. A. Dougherty, D. A. Morrison, S. K. Hollingshead and C. M. Fraser (2001). "Complete genome sequence of a virulent isolate of Streptococcus pneumoniae." Science **293**(5529): 498-506.

Tjarnlund, A., A. Rodriguez, P. J. Cardona, E. Guirado, J. Ivanyi, M. Singh, M. Troye-Blomberg and C. Fernandez (2006). "Polymeric IgR knockout mice are more susceptible to mycobacterial infections in the respiratory tract than wild-type mice." Int Immunol **18**(5): 807-816.

Toews, G. B., W. C. Vial, M. M. Dunn, P. Guzzetta, G. Nunez, P. Stastny and M. F. Lipscomb (1984). "The accessory cell function of human alveolar macrophages in specific T cell proliferation." J Immunol **132**(1): 181-186.

Tritto, E., A. Muzzi, I. Pesce, E. Monaci, S. Nuti, G. Galli, A. Wack, R. Rappuoli, T. Hussell and E. De Gregorio (2007). "The acquired immune response to the mucosal adjuvant LTK63 imprints the mouse lung with a protective signature." J Immunol **179**(8): 5346-5357.

Trojanek, J. B., A. Cobos-Correa, S. Diemer, M. Kormann, S. C. Schubert, Z. Zhou-Suckow, R. Agrawal, J. Duerr, C. J. Wagner, J. Schatterny, S. Hirtz, O. Sommerburg, D. Hartl, C. Schultz and M. A. Mall (2014). "Airway mucus obstruction triggers macrophage activation and matrix metalloproteinase 12-dependent emphysema." Am J Respir Cell Mol Biol **51**(5): 709-720.

Tu, A. H., R. L. Fulgham, M. A. McCrory, D. E. Briles and A. J. Szalai (1999). "Pneumococcal surface protein A inhibits complement activation by Streptococcus pneumoniae." Infect Immun **67**(9): 4720-4724.

Tuvim, M. J., S. E. Evans, C. G. Clement, B. F. Dickey and B. E. Gilbert (2009). "Augmented lung inflammation protects against influenza A pneumonia." PLoS One **4**(1): e4176.

Ueno, M., T. Maeno, S. Nishimura, F. Ogata, H. Masubuchi, K. Hara, K. Yamaguchi, F. Aoki, T. Suga, R. Nagai and M. Kurabayashi (2015). "Alendronate inhalation ameliorates elastase-induced pulmonary emphysema in mice by induction of apoptosis of alveolar macrophages." Nat Commun **6**: 6332.

van der Poll, T., C. V. Keogh, W. A. Buurman and S. F. Lowry (1997). "Passive immunization against tumor necrosis factor-alpha impairs host defense during pneumococcal pneumonia in mice." Am J Respir Crit Care Med **155**(2): 603-608.

van der Poll, T., C. V. Keogh, X. Guirao, W. A. Buurman, M. Kopf and S. F. Lowry (1997). "Interleukin-6 gene-deficient mice show impaired defense against pneumococcal pneumonia." J Infect Dis **176**(2): 439-444.

van der Poll, T. and S. M. Opal (2009). "Pathogenesis, treatment, and prevention of pneumococcal pneumonia." Lancet **374**(9700): 1543-1556.

Verrijdt, G., J. Swinnen, B. Peeters, G. Verhoeven, W. Rombauts and F. Claessens (1997). "Characterization of the human secretory component gene promoter." Biochim Biophys Acta **1350**(2): 147-154.

Wang, N. D., M. J. Finegold, A. Bradley, C. N. Ou, S. V. Abdelsayed, M. D. Wilde, L. R. Taylor, D. R. Wilson and G. J. Darlington (1995). "Impaired energy homeostasis in C/EBP alpha knockout mice." Science **269**(5227): 1108-1112.

Wang, Z., T. Zheng, Z. Zhu, R. J. Homer, R. J. Riese, H. A. Chapman, Jr., S. D. Shapiro and J. A. Elias (2000). "Interferon gamma induction of pulmonary emphysema in the adult murine lung." J Exp Med **192**(11): 1587-1600.

Wark, P. A. and P. G. Gibson (2006). "Asthma exacerbations . 3: Pathogenesis." Thorax **61**(10): 909-915.

Wartha, F., K. Beiter, B. Albiger, J. Fernebro, A. Zychlinsky, S. Normark and B. Henriques-Normark (2007). "Capsule and D-alanylated lipoteichoic acids protect Streptococcus pneumoniae against neutrophil extracellular traps." Cell Microbiol **9**(5): 1162-1171.

Wedzicha, J. A. and G. C. Donaldson (2003). "Exacerbations of chronic obstructive pulmonary disease." Respir Care **48**(12): 1204-1213; discussion 1213-1205.

Westphalen, K., G. A. Gusarova, M. N. Islam, M. Subramanian, T. S. Cohen, A. S. Prince and J. Bhattacharya (2014). "Sessile alveolar macrophages communicate with alveolar epithelium to modulate immunity." Nature **506**(7489): 503-506.

Whitsett, J. A. and T. Alenghat (2015). "Respiratory epithelial cells orchestrate pulmonary innate immunity." Nat Immunol **16**(1): 27-35.

Whitsett, J. A., S. E. Wert and T. E. Weaver (2010). "Alveolar surfactant homeostasis and the pathogenesis of pulmonary disease." Annu Rev Med **61**: 105-119.

Whyte, C. S., E. T. Bishop, D. Ruckerl, S. Gaspar-Pereira, R. N. Barker, J. E. Allen, A. J. Rees and H. M. Wilson (2011). "Suppressor of cytokine signaling (SOCS)1 is a key determinant of differential macrophage activation and function." J Leukoc Biol **90**(5): 845-854.

Woodruff, P. G., L. L. Koth, Y. H. Yang, M. W. Rodriguez, S. Favoreto, G. M. Dolganov, A. C. Paquet and D. J. Erle (2005). "A distinctive alveolar macrophage activation state induced by cigarette smoking." Am J Respir Crit Care Med **172**(11): 1383-1392.

Wright, J. R. (2005). "Immunoregulatory functions of surfactant proteins." Nat Rev Immunol **5**(1): 58-68.

Wu, K., D. E. Byers, X. Jin, E. Agapov, J. Alexander-Brett, A. C. Patel, M. Cella, S. Gilfilan, M. Colonna, D. L. Kober, T. J. Brett and M. J. Holtzman (2015). "TREM-2 promotes macrophage survival and lung disease after respiratory viral infection." J Exp Med **212**(5): 681-697.

Yamada, K. J., T. Barker, K. D. Dyer, T. A. Rice, C. M. Percopo, K. E. Garcia-Crespo, S. Cho, J. J. Lee, K. M. Druey and H. F. Rosenberg (2015). "Eosinophil-associated ribonuclease 11 is a macrophage chemoattractant." J Biol Chem **290**(14): 8863-8875.

Yamamoto, K., A. N. Ahyi, Z. A. Pepper-Cunningham, J. D. Ferrari, A. A. Wilson, M. R. Jones, L. J. Quinton and J. P. Mizgerd (2014). "Roles of lung epithelium in neutrophil recruitment during pneumococcal pneumonia." Am J Respir Cell Mol Biol **50**(2): 253-262.

Yang, J. J., G. A. Preston, W. F. Pendergraft, M. Segelmark, P. Heeringa, S. L. Hogan, J. C. Jennette and R. J. Falk (2001). "Internalization of proteinase 3 is concomitant with endothelial cell apoptosis and internalization of myeloperoxidase with generation of intracellular oxidants." Am J Pathol **158**(2): 581-592.

Yoshimura, A., T. Naka and M. Kubo (2007). "SOCS proteins, cytokine signalling and immune regulation." Nat Rev Immunol **7**(6): 454-465.

Zaslona, Z., S. Przybranowski, C. Wilke, N. van Rooijen, S. Teitz-Tennenbaum, J. J. Osterholzer, J. E. Wilkinson, B. B. Moore and M. Peters-Golden (2014). "Resident alveolar macrophages suppress, whereas recruited monocytes promote, allergic lung inflammation in murine models of asthma." J Immunol **193**(8): 4245-4253.

Zhang, J. R., K. E. Mostov, M. E. Lamm, M. Nanno, S. Shimida, M. Ohwaki and E. Tuomanen (2000). "The polymeric immunoglobulin receptor translocates pneumococci across human nasopharyngeal epithelial cells." Cell **102**(6): 827-837.

Zheng, T., Z. Zhu, Z. Wang, R. J. Homer, B. Ma, R. J. Riese, Jr., H. A. Chapman, Jr., S. D. Shapiro and J. A. Elias (2000). "Inducible targeting of IL-13 to the adult lung causes matrix metalloproteinase- and cathepsin-dependent emphysema." J Clin Invest **106**(9): 1081-1093.

Zhu, A., D. Ge, J. Zhang, Y. Teng, C. Yuan, M. Huang, I. M. Adcock, P. J. Barnes and X. Yao (2014). "Sputum myeloperoxidase in chronic obstructive pulmonary disease." Eur J Med Res **19**: 12.

7.6 Acknowledgments

Mein besonderer Dank gilt meiner Betreuerin Prof. Dunja Bruder, in deren Arbeitsgruppe IREG ich diese Arbeit anfertigen durfte. Danke für Dein Vertrauen, Deine Unterstützung, Deinen riesengroßen persönlichen Einsatz für jeden Deiner Mitarbeiter und die tolle Chance mein Thema noch weiterhin als ein Teil der IREGleins bearbeiten zu können!

Bedanken möchte ich mich außerdem bei meinem Mentor, Mitglied meines Thesis-Committees und Begutachter dieser Arbeit: Prof. Michael Steinert sowie bei Prof. Stefan Dübel für die Übernahme des Vorsitzes meiner Prüfungskommission. Außerdem ein großes Dankeschön an die weiteren Mitglieder meines Thesis-Committees für deren wissenschaftlichen Input: Prof. Ulrich Maus und Dr. Oliver Goldmann. Ein Dankeschön auch an Prof. Sylvia Knapp, Simona Saluzzo und Rui Martins, die mir während meines Aufenthaltes am CeMM in Wien viele Einblicke in die faszinierende Welt der Makrophagen ermöglicht haben. Außerdem danke ich Dr. Josef Wissing und Prof. Lothar Jänsch für die BALF Proteom Analysen und Dr. Lothar Gröbe für das ATII-Sorten und alles Wissenswerte rund um FACS.

An dieser Stelle möchte ich meinem Co-Betreuer Dr. Andreas Jeron ein riesengroßes Dankeschön aussprechen. Seitdem ich 2011 als “Masterette“ bei den IREGs anfing, haben wir so manches umfangreiche Projekt zusammen bearbeitet. Seitdem habe ich so vieles von Dir gelernt - auch, dass etwas Mut, ein anderer Blickwinkel und ein “Hast Du Dich schonmal gefragt…?“ oftmals der Anfang einer spannenden Geschichte sein können. Noch viel wichtiger: auf Deine ehrliche Meinung und Deine Unterstützung konnte und kann ich mich stets verlassen. Danke Ändy für Deine engagierte Betreuung, wunderbare Zusammenarbeit und die Möglichkeit neugierig sein zu dürfen!

Wissenschaft ist zum Glück keine Einzelsportart und Ihr, liebe IREGleins, wart und seid die besten Mannschaftskameraden, die ich mir vorstellen kann. Sowohl Eure tatkräftige Unterstützung im Labor und Tierhaus als auch die Gewissheit, Euch jederzeit um experimentellen, technischen, oder auch Statistik-Rat fragen zu können, haben maßgeblich zum Fortschritt dieser Projekte beigetragen. Hervorzuheben sind die guten Feen Tanja Hirsch und Silvia (P) Prettin: ohne Euren Einsatz und Durchblick sähen wir alle wirklich ganz schön alt aus. Außerdem Danke an Dr. Marcus Gereke für Dein riesengroßes Engagement für die ganze Gruppe und natürlich Deine unzähligen Insider-Tipps zu Lunge, ATII und Co. Darüber hinaus freue ich mich besonders auf: weitere unvergessliche Mitttags- und Kaffeepausen (mit ebenso unvergesslichen, schräg-absurden Gesprächen!), die kleinen und großen Feiern, Badminton, schwarzen Humor und viel Lachen mit Euch. Besonders Letzteres hat fast jeden blöden Tag oder missglückten Versuch irgendwie wieder retten können. Ein riesengroßes Dankeschön also an das IREG-Team: Dunja, Ändy, Nicole, Franzi, Sarah, P, Tanja, Marcus, Sabine, Julia, Geri, Niharika, Priya, Kathleen und Kristin. Ihr seid großartig!

Meine lieben Großeltern, Horst und Ruth Schaper, möchte ich an dieser Stelle erwähnen. In die Förderung Eurer Enkel habt Ihr Euch, seitdem ich mich erinnern kann, mit sehr großem persönlichen Einsatz eingebracht. Meinen größten Respekt und ein inniges Dankeschön dafür! Zu guter Letzt, lieber Sebastian: Danke, dass Du mein Zuhause, Partner und bester Freund bist und ich immer bedingungslos auf Dich zählen kann.